

2-P (m!x)

JPL Contract 953311

Outer Planet Entry Probe System Study

Final Report
Volume IV
Common
Saturn/Uranus
Probe Studies

January 1973

MARTIN MARIETTA

(NASA-CR-131227) OUTER PLANET ENTRY
PROBE SYSTEM STUDY. VOLUME 4: COMMON
SATURN/URANUS PROBE STUDIES Final Report
(Martin Marietta Corp.) 239 p HC \$14.00
CSCS 22A G3/31

745619101661998

N73-19883
Unclas
65371

JPL Contract 953311

Volume IV

Common
Saturn/Uranus
Probe Studies

January 1973

**OUTER PLANET
ENTRY PROBE SYSTEM
STUDY**

FINAL REPORT

Approved



R. S. Wiltshire
Program Manager

**This work was performed for the Jet Propulsion Laboratory,
California Institute of Technology, sponsored by the
National Aeronautics and Space Administration under
Contract NAS7-100.**

**MARTIN MARIETTA CORPORATION
P.O. Box 179
Denver, Colorado 80201**

Reproduced from
best available copy.



Survivable Saturn Atmosphere Probe

FOREWORD

This final report has been prepared in accordance with requirements of Contract JPL-953311, Modification No. 7, Task Order No. RD-10, (follow-on to the basic contract) to present data and conclusions drawn from a three-month study by Martin Marietta Corporation, Denver Division, for the Jet Propulsion Laboratory. The report is Volume IV; the first three volumes documented the basic contract results. The four volumes are:

Volume I - Summary

Volume II - Supporting Technical Studies

Volume III - Appendixes

Volume IV - Common Saturn/Uranus Probe Studies.

ACKNOWLEDGEMENTS

The following Martin Marietta Corporation, Denver Division, personnel participated in this study, and their efforts are greatly appreciated:

Raymond S. Wiltshire	Study Leader, Program Manager
Allen R. Barger	Science Integration
Eugene A. Berkery	Telecommunications, Data Handling, Power, and ACS, Lead
Dennis V. Byrnes	Navigation
Philip C. Carney	Mission Analysis
Patrick C. Carroll	Systems
Revis E. Compton, Jr.	Telecommunications
Robert G. Cook	Mechanical Design
W. Sidney Cook	Cloud Structures Analysis
Douglas B. Cross	Mission Analysis
Ralph F. Fearn	Propulsion
Robert B. Fischer	Mission Analysis
Thomas C. Hendricks	Mission Analysis, Lead
John W. Hungate	Systems, Lead
Carl L. Jensen	Thermal Analysis
Rufus O. Moses	Mechanical/Structural/Probe Integration, Lead
Kenneth W. Ledbetter	Science, Lead
Paula S. Lewis	Mission Analysis
John R. Mellin	Structures
Jack D. Pettus	Data Link Analysis
Robert J. Richardson	Receiver Systems
Arlen I. Reichert	Propulsion
E. Doyle Vogt	Mission Analysis
Donald E. Wainwright	Systems
Clifford M. Webb	Thermal Analysis
Charles E. Wilkerson	Data Handling

CONTENTS

	<u>Page</u>
I. INTRODUCTION	I-1 and I-2
II. SUMMARY, CONCLUSIONS AND RECOMMENDATIONS	II-1
A. Summary	II-1
B. Conclusions and Recommendations	II-21 thru II-25
III. SATURN/URANUS PARAMETRIC ANALYSIS	III-1
A. Mission Design Considerations	III-2
B. Science Investigations	III-24
C. System Integration	III-51
D. Electrical and Electronics Subsystems	III-57
E. Thermal Control Subsystem	III-97
F. Parametric Analysis Summary	III-104
G. References	III-109
IV. SATURN/URANUS PROBE SYSTEM DEFINITION WITH SCIENCE ADVISORY GROUP'S EXPLORATORY PAYLOAD	IV-1
A. Mission Definition	IV-1
B. Science Instrumentation and Performance	IV-11
C. System Design and Integration	IV-14
D. Telecommunications Subsystem	IV-21
E. Data Handling Subsystem	IV-29
F. Power and Pyrotechnic Subsystem	IV-31
G. Attitude Control	IV-33
H. Structural and Mechanical Subsystems	IV-35
I. Propulsion Subsystem	IV-48
J. Thermal Control Subsystem	IV-51
K. Probe-to-Spacecraft Integration	IV-56 thru IV-59
V. SATURN/URANUS PROBE SYSTEM DEFINITION WITH EXPANDED SCIENCE COMPLEMENT	V-1
A. Mission Definition	V-1
B. Science Instrumentation and Performance	V-1
C. System Design and Integration	V-6
D. Telecommunications Subsystem	V-11

E.	Data Handling Subsystem	V-18
F.	Power and Pyrotechnic Subsystem	V-19
G.	Attitude Control	V-21
H.	Structural and Mechanical Subsystem	V-23
I.	Propulsion Subsystem	V-29
J.	Thermal Control Subsystem	V-29
K.	Probe-to-Spacecraft Integration	V-33

Figure

I-1	Follow-On Study Task Definition and Flow Diagram	I-1
II-1	Science Instrument Locations, Expanded Science Payload	II-5
II-2	Pre-entry Measurement Performance	II-6
II-3	Science Constraints on Mission Analysis	II-8
II-4	Mission Design Configurations	II-8
II-5	Saturn (SU 80) Mission	II-9
II-6	Uranus (SU 80) Mission Design	II-9
II-7	Pictorial Sequence of Events (Task II)	II-10
II-8	Data Profile (Task II)	II-12
II-9	Power Profile (Task II)	II-12
II-10	Probe Configuration Description	II-16
II-11	General Entry Probe Configuration	II-16
II-12	Entry Probe Configuration Comparison	II-17
II-13	Descent Probe Configuration Comparison	II-17
II-14	Probe Integration with Mariner Spacecraft	II-19
II-15	Cloud Locations and End-of-Mission Limits for Various Model Atmospheres	II-20
III-1	1979 Saturn Interplanetary Trajectory	III-3
III-2	1980 Saturn/Uranus Interplanetary Trajectory	III-3
III-3	Estimated Shuttle Performance Data	III-5
III-4	Titan III/Centaur Performance Data	III-5
III-5	Saturn 1979 and Saturn/Uranus 1980 Launch Energy Contours	III-8
III-6	Saturn and Uranus Entry Velocity Variations	III-8
III-7	V_{HP} , ZAE, and ZAP Variations with Arrival Date	III-9
III-8	Navigation Uncertainties	III-10
III-9	Saturn and Uranus Look-Direction Dispersions	III-12
III-10	Saturn Entry Site Dispersions	III-13
III-11	Uranus Entry Site Dispersions	III-13
III-12	Relay Link Parameters	III-15
III-13	Deceleration to Subsonic Speeds at Saturn	III-21
III-14	Deceleration to Subsonic Speeds at Uranus	III-21
III-15	Maximum Deceleration at Saturn and Uranus vs Entry Angle	III-22

III-16	Maximum Dynamic Pressure at Saturn and Uranus vs Entry Angle	III-22
III-17	Saturn Deceleration Profile	III-23
III-18	Uranus Deceleration Profile	III-23
III-19	Pressure vs Temperature and Cloud Levels for Saturn Model Atmospheres	III-25
III-20	Pressure vs Temperature for Uranus Model Atmospheres	III-25
III-21	Pressure vs Altitude for Saturn Model Atmospheres	III-26
III-22	Pressure vs Altitude for Saturn Model Atmospheres	III-26
III-23	Ion-Retarding Potential Analyzer	III-31
III-24	Neutral-Retarding Potential Analyzer	III-33
III-25	Langmuir Probe and RPA Location	III-36
III-26	Descent Side-Looking Nephelometer	III-38
III-27	Pre-entry Velocity/Altitude Time History	III-45
III-28	Probe Velocities at Entry vs Saturn Entry Angle	III-45
III-29	Pre-entry Performance vs Saturn Entry Angle	III-47
III-30	Pre-entry Instrument Measurement Performance vs Sampling Time	III-47
III-31	Pressure Descent Profiles	III-50
III-32	Parachute Deployment Analysis, Saturn and Uranus	III-52
III-33	Data Profile for Task II Data Mode Tradeoff	III-54
III-34	Preliminary Data Profile for Saturn/Uranus Probe (Task II)	III-56
III-35	Thermal Noise Temperature of the Milky Way Galaxy	III-60
III-36	Trajectory Geometry for the Saturn/Uranus 1980 Mission	III-60
III-37	Receiving System Noise Temperature for Saturn	III-62
III-38	Receiving System Noise Temperature for Uranus	III-62
III-39	Location of Clouds That Affect Microwave Absorption	III-64
III-40	Absorption Coefficient for the Cool Jupiter Atmosphere	III-66
III-41	Zenith Absorption for Saturn Nominal Atmosphere	III-67
III-42	Zenith Absorption at Selected Pressures for the Saturn Nominal Atmosphere	III-67
III-43	Zenith Absorption for the Saturn Cool Atmosphere	III-68
III-44	Zenith Absorption at Selected Pressures for the Saturn Cool Atmosphere	III-68
III-45	Zenith Absorption for the Uranus Nominal Atmosphere	III-69

III-46	Zenith Absorption at Selected Pressures for the Uranus Nominal Atmosphere	III-69
III-47	Circularly Polarized Turnstile/Cone Probe Antenna Patterns	III-71
III-48	Probe Turnstile/Cone Antenna	III-73
III-49	Prototype Turnstile/Cone Antenna Mounted on Probe Model	III-74
III-50	Antenna Pattern Polarization Loss	III-76
III-51	Probe Aspect Angle for the Three Missions	III-82
III-52	Spacecraft Antenna Requirements for the Three Missions	III-83
III-53	Definition of Spacecraft-to-Probe Look Direction	III-85
III-54	Data Handling Subsystem Functional Diagram	III-85
III-55	Power and Pyrotechnic Subsystem Block Diagram	III-90
III-56	Probe Thermal Control Concept	III-98
III-57	Worst-Case Saturn/Uranus Atmospheric Temperature Profiles	III-100
III-58	Cruise/Coast Probe Equilibrium Temperatures Based on Thermal Coating Selection	III-100
III-59	Cloud Locations and End-of-Mission Limits for Various Model Atmospheres	III-108
IV-1	1979 Saturn Mission Definition	IV-2
IV-2	Saturn/SU 80 Mission Definition	IV-5
IV-3	Uranus/SU 80 Mission Definition	IV-9
IV-4	Sequence of Events (Task II)	IV-14
IV-5	Data Profile for Saturn/Uranus Probe (Task I)	IV-18
IV-6	Power Profile for Saturn/Uranus Probe (Task I)	IV-19
IV-7	Probe-to-Spacecraft Communications Range for the Saturn/SU 80 Mission	IV-22
IV-8	Saturn/SU 80 Mission Probe Aspect Angle	IV-23
IV-9	Probe RF Power Requirements (Task I)	IV-26
IV-10	Saturn/Uranus Common Entry Probe (Task I)	IV-37
IV-11	Saturn/Uranus Common Entry Probe Structural Breakdown	IV-41
IV-12	Attitude Control Propulsion System	IV-49
IV-13	Saturn/Uranus Probe Thermal History for Saturn Mission	IV-54
IV-14	Saturn/Uranus Probe Thermal History for Uranus Mission	IV-55
IV-15	Probe and Spacecraft Interface Arrangement	IV-57
V-1	Data Profile for Saturn/Uranus Probe (Task II)	V-10
V-2	Power Profile for Saturn/Uranus Probe (Task II)	V-10
V-3	Task II Probe RF Power Requirements	V-14
V-4	Saturn/Uranus Common Entry Probe, Task II	V-25
V-5	Saturn/Uranus Probe Thermal History for Saturn Mission (Expanded Science Payload)	V-31
V-6	Saturn/Uranus Probe Thermal History for Uranus Mission (Expanded Science Payload)	V-32

Table

II-1	Study Constraints	II-2
II-2	Science Instruments Related to Measurements	II-3
II-3	Science Instrument Characteristics	II-3
II-4	Descent Measurement Performance	II-6
II-5	Mission Design Summary	II-10
II-6	Telecommunication Summary	II-14
II-7	Power and Pyrotechnic Summary	II-14
II-8	Structural/Mechanical Summary	II-18
II-9	Weight Comparisons	II-18
II-10	Probe Comparison Summary	II-19
II-11	Compromises for Commonality	II-22
II-12	Probe Subsystem Development Status	II-23
III-1	Saturn Direct '79 Mission Launch Capability	III-4
III-2	Saturn/Uranus '80 Mission Launch Capability	III-4
III-3	Mission Launch Energy Requirements	III-4
III-4	Navigation Uncertainties at Saturn (1σ)	III-11
III-5	Entry and Communication Parameter Dispersions	III-14
III-6	Saturn Model Atmosphere Entry Parameter Definition	III-19
III-7	Uranus Model Atmosphere Entry Parameter Definition	III-19
III-8	Saturn/Uranus Modeled Cloud Locations	III-27
III-9	Instruments Related to Measurements	III-28
III-10	IRPA Characteristics	III-30
III-11	NRPA Characteristics	III-32
III-12	Langmuir Probe Characteristics	III-36
III-13	Nephelometer Characteristics	III-38
III-14	Variation of Parameters with Atmosphere	III-40
III-15	Start of Pre-entry Measurements	III-43
III-16	Latitude and Longitude Variations	III-46
III-17	Accelerometer Measurement Performance	III-48
III-18	Descent Data Rate Composition	III-50
III-19	Task II Data Mode Analysis Results	III-55
III-20	Ammonia Abundance in the Atmosphere Models	III-65
III-21	Telecommunication Subsystem Parameters for the Common Probe Development	III-78
III-22	Telecommunications Subsystem Characteristics Comparison Summary	III-80
III-23	Typical Probe Equipment Temperature Limits	III-101
III-24	Comparison of Mission Designs	III-105
III-25	Science Analysis Summary	III-105
III-26	Parachute Deployment Results	III-106
III-27	Task II Data Mode Analysis Results	III-107
III-28	Communications Parameters	III-108
IV-1	Saturn 1979 Mission Summary Data	IV-3
IV-2	Saturn/SU 80 Mission Summary Data	IV-6

IV-3	Uranus/SU 80 Mission Summary Data	IV-10
IV-4	Instrument Sampling Times and Data Rates for Common Saturn/Uranus Probe with Exploratory Payload . .	IV-12
IV-5	Saturn Descent Measurement Performance, Exploratory Payload	IV-13
IV-6	Uranus Descent Measurement Performance, Exploratory Payload	IV-13
IV-7	Saturn Sequence of Events (Task I)	IV-15
IV-8	Uranus Sequence of Events (Task I)	IV-16
IV-9	Weight Summary for Saturn/Uranus Probe with SAG Exploratory Payload	IV-20
IV-10	Probe Telemetry Link Design for the Saturn/SU 80 Mission with Task I Science	IV-27
IV-11	Telecommunications RF Subsystem for the Task I Mission	IV-28
IV-12	Baseline Common Saturn/Uranus Probe Weight Breakdown	IV-39
IV-13	Minimum and Maximum Probe Temperatures for Worst-Case Atmospheric Encounter and Arrival Uncertainties	IV-53
V-1	Instrument Characteristics	V-2
V-2	Instrument Sampling Times and Data Rates for Common Saturn/Uranus	V-3
V-3	Saturn Descent Measurement Performance, Expanded Payload	V-5
V-4	Uranus Descent Measurement Performance, Expanded Payload	V-5
V-5	Pre-entry Measurement Performance	V-6
V-6	Saturn Sequence of Events (Task II)	V-7
V-7	Uranus Sequence of Events (Task II)	V-8
V-8	Weight Summary for Saturn/Uranus Probe with Expanded Science Complement	V-11
V-9	Task II Telecommunication Subsystem Comparisons for the Saturn/SU 80 Mission	V-11
V-10	Probe Pre-entry Telemetry Link Design for Task II Mission	V-13
V-11	Probe Descent Telemetry Link Design for Task II Mission	V-16
V-12	Telecommunications RF Subsystem for Task II Mission . .	V-17
V-13	Task II Saturn/Uranus Probe Weight Breakdown (Added Science)	V-28
V-14	Minimum and Maximum Probe Temperatures for Worst-Case Atmospheric Encounters and Arrival Uncertainties	V-33

I. INTRODUCTION

The material in this volume summarizes results of a common scientific probes study to explore the atmospheres of Saturn and Uranus. This was a three-month follow-on effort to the Outer Planet Entry Probe System study. Two major tasks, shown in Figure I-1, and their relationship to other tasks in the basic study were considered. The first task established a reference definition that was used to determine the impact of the additional science complement in the second task.

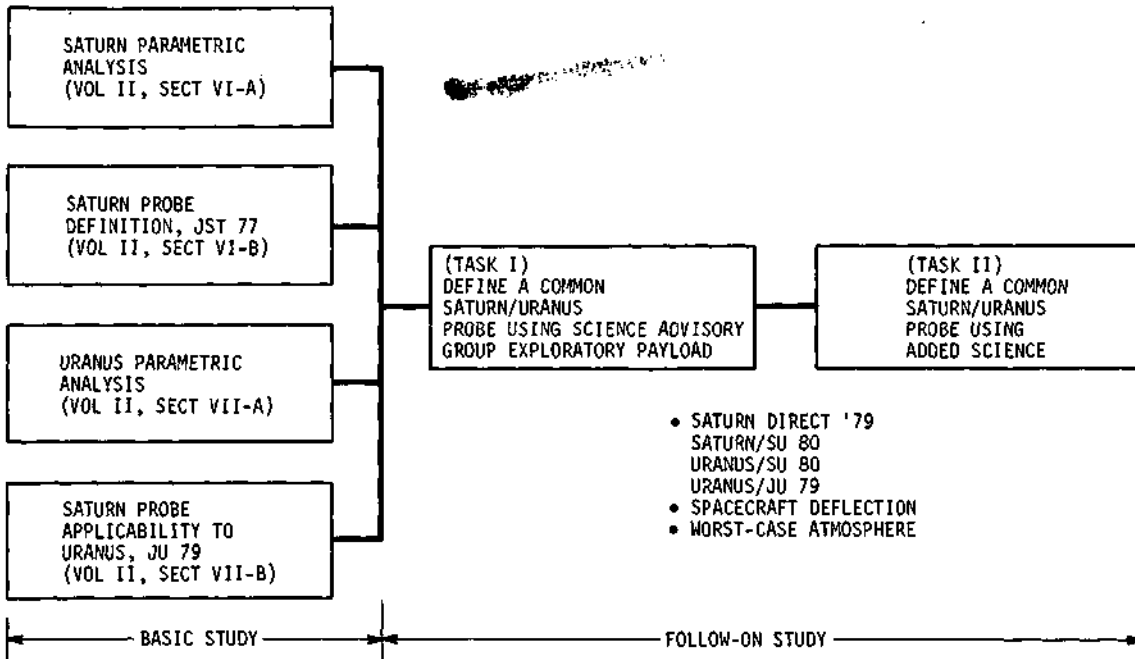


Fig. I-1 Follow-on Study Task Definition and Flow Diagram

The report is arranged to present (1) a summary, conclusions and recommendations of this study, (2) parametric analysis conducted to support the two system definitions, (3) common Saturn/Uranus probe system definition using the Science Advisory Group's (SAG) exploratory payload and, (4) common Saturn/Uranus probe system definition using an expanded science complement. Each of the probe system definitions consists of detailed discussions of the

mission, science, system and subsystems including telecommunications, data handling, power, pyrotechnics, attitude control, structures, propulsion, thermal control and probe-to-spacecraft integration. References are made to the contents of the first three volumes where it is feasible to do so.

II. SUMMARY, CONCLUSIONS AND RECOMMENDATIONS

A. SUMMARY

1. General

The study objectives consist of using configuration concepts and subsystem definition data generated in the basic study, and extending this data to define a common:

- 1) Saturn/Uranus probe using the Science Advisory Group (SAG) exploratory payload (Task I);
- 2) Saturn/Uranus probe using an expanded science payload (Task II).

The constraints for the study are shown in Table II-1. The Saturn Direct 79 and Uranus (SU 80) missions are terminal missions at the respective planets, and Saturn/SU 80 is a flyby mission. The science instruments, used for Task I, are the same ones used for the basic study and are discussed in detail in Volume II, Chapter III. The pre-entry Task II science instruments provide data to define the structure and composition of the upper atmosphere and the ionosphere. The added Task II descent instrument provides data to more precisely identify location of major cloud formations.

The spacecraft deflection mode, used for this study, provides a simpler probe definition than the probe deflection mode that was used in the basic study.

The effects of warm, nominal, and cool atmospheric models were evaluated for Saturn and Uranus and the "worst case" was used for the common probe definition. In the basic study, only the nominal atmospheric model was used.

2. Science

The basic science objectives are to:

- 1) determine the structure and composition of the bulk atmosphere;
- 2) define the density, pressure, and temperature profiles;
- 3) determine the composition of the major clouds.

Table II-1 Study Constraints

Missions: Saturn Direct '79, Saturn (SU'80) and Uranus (SU'80)

Science Instruments:

Task I (SAG Exploratory Payload)

Neutral Mass Spectrometer	}	Descent
Temperature Gage		
Pressure Gages		
Accelerometers - Entry and Descent		

Task II (Preentry Instruments)

Langmuir Probes
Ion Retarding Potential Analyzer (IRPA)
Neutral Particle Retarding Potential Analyzer (NRPA)

Task II (Descent Additional Instrument)

Nephelometer

Deflection Mode: Spacecraft

Atmospheric Models: Worst Case at Saturn and Uranus

Entry Angles, Latitude and Descent Depth: Compatible with Mission Set and Science Objectives

Secondary objectives, requiring the addition of extra instrumentation are to:

- 1) identify the location of the major cloud formations;
- 2) define the structure and composition of the upper atmosphere;
- 3) define the structure and composition of the dayside ionosphere.

The science instruments and their relationship to the measurements for the three science mission phases of pre-entry, entry, and descent are shown in Table II-2. The entry and descent instruments (except for the nephelometer) comprise the Task I science payload. At least one instrument contributes directly to all descent measurements except the atmospheric turbulence measurement. In this application, four instruments provide related data from which information is derived.

The science instrument characteristics for both study tasks are shown in Table II-3 in terms of weight, volume, power requirement, sampling times, and science data rate. Task II totals for weight, volume, and power are approximately double that for Task I. Although the science weight differs by 6.4 kg, the total entry probe weight difference is only 14 kg, and the probe diameter difference is only 5 cm.

Table II-2 Science Instruments Related to Measurements

Instruments	Temp Gage	Press Gage	Accelerometers	Neutral Mass Spec	Nephelometer	Langmuir Probes	IRPA	NRPA
<u>Preentry</u>								
Ion Concentration Profiles						D	D	N
Neutral Concentration Profiles						N	R	D
Electron Density & Temp						D	R	N
<u>Entry</u>								
Deceleration Loads			D					
<u>Descent</u>								
H/He Ratio	R	R	R	D	N			
Isotopic Ratios	N	N	N	D	N			
Minor Constituents	R	R	N	D	R			
Atmospheric Temperature	D	R	R	R	N			
Atmospheric Pressure	R	D	R	R	N			
Cloud Location/Structure	R	R	R	R	D			
Cloud Composition	R	R	R	D	R			
Atmospheric Turbulence	R	R	R	N	R			

D = Direct Measurement, R = Related Measurement, N = Little or No Relation

Table II-3 Science Instrument Characteristics

	Weight, kg	Volume, cm ³	Power, Watts	Sampling Time, sec	Science Data Rate, bps
<u>Task I, Exploratory Payload</u>					
Neutral Mass Spectrometer	5.45	5,314	14.0	50	8.7
Temperature Gage	0.45	426	1.4	4	2.6
Pressure Gages	0.68	246	1.3	4	2.6
Accelerometers: Entry	1.50	918	2.8	0.2	100*
Turbulence	Same	Same	Same	8	7.8
<u>Totals - Task I</u>	<u>8.08</u>	<u>6,904</u>	<u>19.5</u>		
<u>Task II, Expanded Payload Additions</u>					
Nephelometer (Descent)	1.14	1,312	3.0	3	3.4
<u>Preentry</u>					
Langmuir Probes	1.36	1,200	3.0	0.5	60
Ion Retarding Potential Analyzer	1.59	2,200	3.0	2.0	60
Neutral Particle RPA	2.27	2,500	5.0	3.0	93.3
<u>Totals - Task II</u>	<u>14.4</u>	<u>14,116</u>	<u>33.5</u>		

*Stored for later transmission at 3.2 bps.

The location of each instrument of the expanded science payload complement is shown in Figure II-1. The neutral retarding potential analyzer (NRPA) and ion retarding potential analyzer (IRPA) are located so that the apertures of the instruments are slightly forward of the probe apex to minimize the possibility of heat shield particles reaching the aperture. Of the two Langmuir probes, one is mounted perpendicular to the flight velocity vector and the other is parallel. The sampling port for the neutral mass spectrometer (NMS) is located at the stagnation point of the descent probe, and the analyzer, electronics, and ballast volume tank are located nearby. The accelerometers are located on the longitudinal axis aft of the NMS. The temperature gage, pressure gages, and nephelometer are all mounted on the descent probe outer wall to have access to sensing ports.

The science measurement performance for the descent and preentry instruments are shown in Table II-4 and Figure II-2, respectively. The table shows the NMS sampling duration to be 50 seconds. The high methane cloud in the Uranus warm atmosphere necessitated this NMS interval as compared with 60-second sampling time in the basic study. The warm atmospheres generally present the worst case for performance because of the large pressure and density scale heights. This means that a smaller pressure differential is detected with a given change in altitude, thus with the descent based upon pressure, there are fewer measurements per kilometer. The Saturn warm atmosphere has slightly larger scale heights than for Uranus.

The criteria denoted in the table shows that three general types of measurements are:

- 1) a specified number of measurements per scale height or per °K or per km, measured throughout descent;
- 2) a specified number of measurements within each modeled cloud;
- 3) total number of measurements.

The NMS performance, when defined to provide two measurements in the CH₄ cloud, greatly surpasses the other requirements. The accelerometer has a criteria of one measurement per kilometer. It makes 0.7 measurements in the worse case atmosphere and 2.4 in the best case atmosphere at the highest altitude. This performance increases up to a maximum of 7.2 measurements.

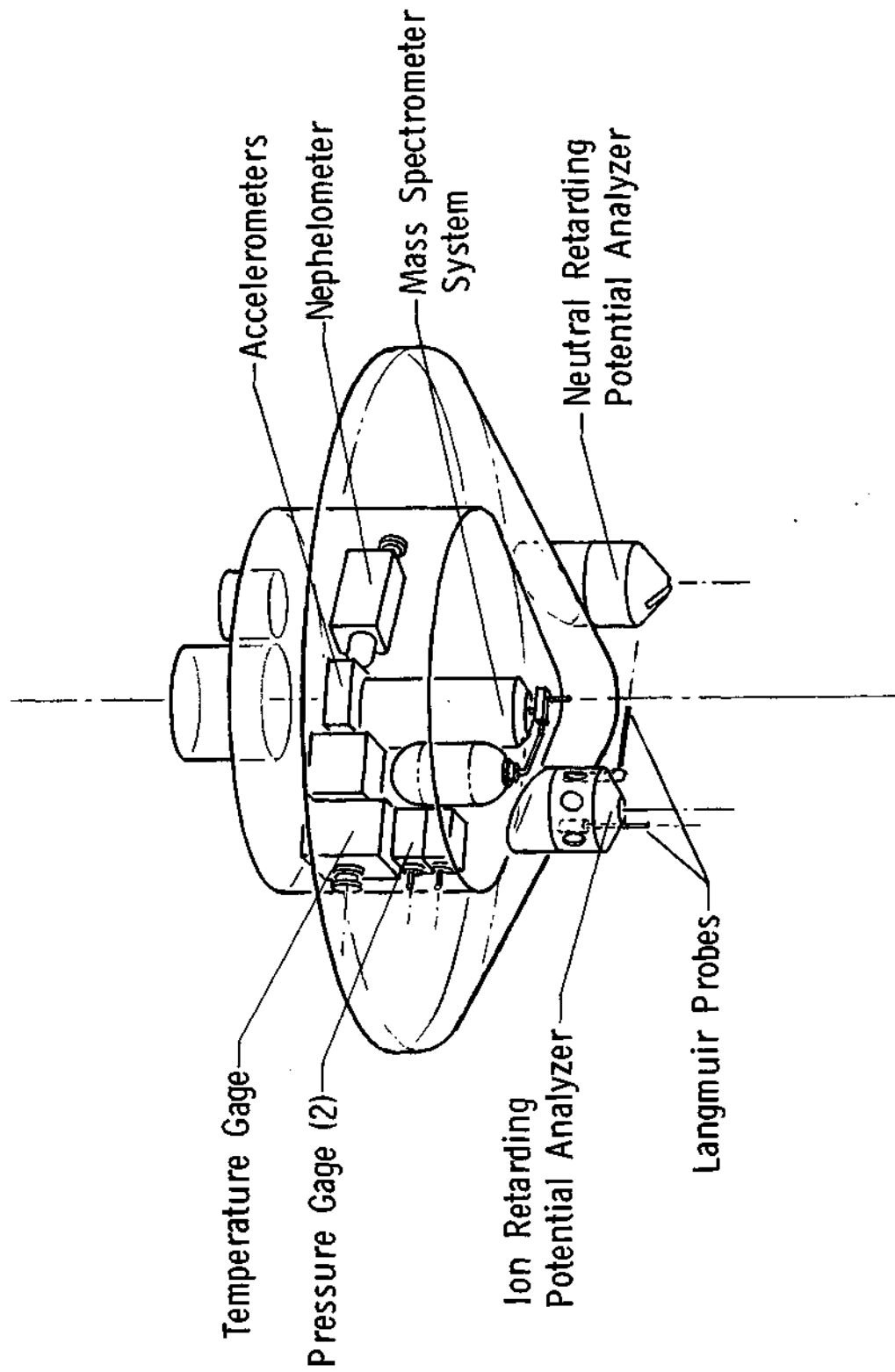


Fig. II-1 Science Instrument Locations - Expanded Science Payload

Table II-4 Descent Measurement Performance

Instrument and Sampling Time	Measurement	Criteria	Saturn/Uranus Range of Performance*
Neutral Mass Spectrometer (50 sec)	Minor Constituents Cloud Composition H/He Ratio Isotopic Ratios Molecular Weight	2 per scale height 2 inside each cloud 4 measurements	4.6/7.7 to 38 2 to 18 in CH ₄ 5 to 12 in NH ₃ 10 to 16 in H ₂ O 52 measurements
Temperature Gage (4 sec)	Temperature Profile Cloud Structure	1 per °K 2 inside each cloud	1.2/3.1 to 10.9 26 or greater in all clouds
Pressure Gage (4 sec)	Pressure Profile Cloud Structure	2 per kilometer 2 inside each cloud	1.5/4.8 to 14.4 26 or greater in all clouds
Accelerometers (8 sec)	Turbulence	1 per kilometer	0.7/2.4 to 7.2
Nephelometer (3 sec)	Cloud Location Cloud Structure	1 per kilometer 2 inside each cloud	1.3/3.2 to 19 34 or greater in all clouds

*Warm atmospheres give worst-case performance.

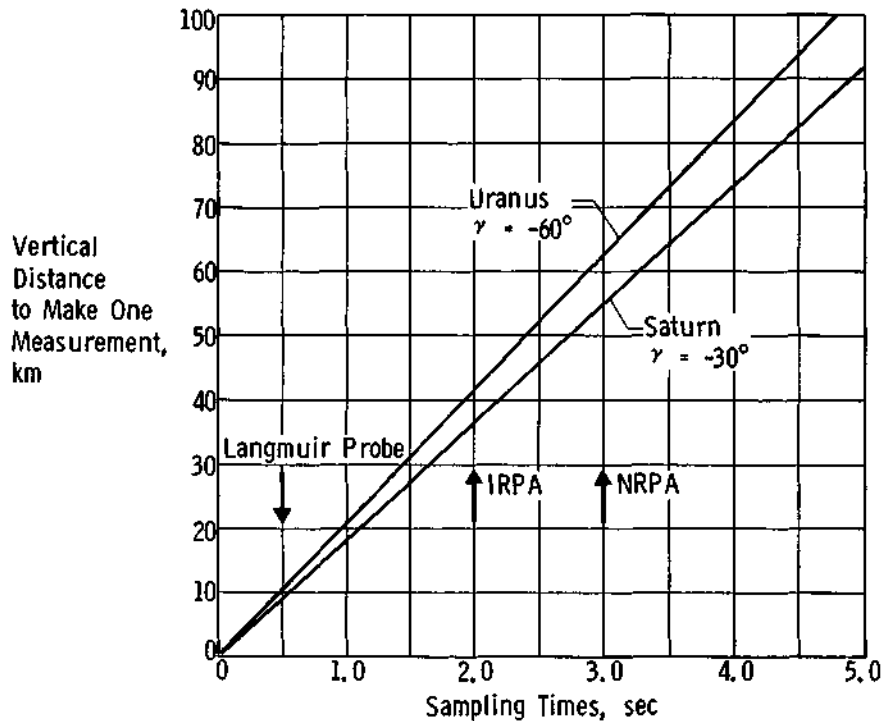


Fig. II-2 Preentry Measurement Performance

The pre-entry science instrument sampling times versus vertical distance to make one measurement for Saturn and Uranus are shown in Figure II-2.

The science constraints on the mission analysis is shown in Figure II-3 in terms of entry site selection, approach conditions, and entry attitude.

3. Mission Analysis and Design

The mission analysis and design considerations from launch through the end of mission are shown in Figure II-4. The interplanetary trajectory is selected primarily on the basis of launch payload analysis when considering such constraints as daily launch window, range safety, and parking orbit coast time. The primary goals for encounter are to send the probe to the desired entry site at the proper attitude and to establish an effective communication geometry.

The Saturn/SU 80 mission is described in Figure II-5 in terms of relative probe and spacecraft trajectories, mission summary definition and deflection summary. Just before entry, the spacecraft leads the probe and subsequently the probe catches up. Entry is at -30° and well away from the terminator on the light side.

Figure II-6 summarizes the Uranus/SU 80 mission. At entry, the probe leads the spacecraft and subsequently the spacecraft catches up. The probe is deflected below the spacecraft trace and is carried vertically by the planet rotation across the spacecraft trace. Entry is at -60° and well away from the terminator on the light side.

The mission summary for the three design missions: Saturn direct 79, Saturn/SU 80, and Uranus/SU 80 is shown in Table II-5. The first mission is a Saturn terminal mission, the next a Saturn fly-by, and the last a Uranus terminal mission. The Saturn/SU 80 mission, with a high periapsis radius of $3.8 R_s$, causes a large communication range of 1.97×10^5 km at entry, which is the worst case of the three design missions. The missions were slightly altered to provide a single spacecraft antenna pointing for both planets. The table shows the cone angle at entry to be similar for all three missions. In addition, the probe aspect angle for Uranus at the end of mission is shown to be reaching an extreme of 43° , which is an important factor of common missions. The entry time dispersion of 4.4 minutes for Saturn and 28.9 minutes for Uranus has a significant impact on power requirements and acquisition time.

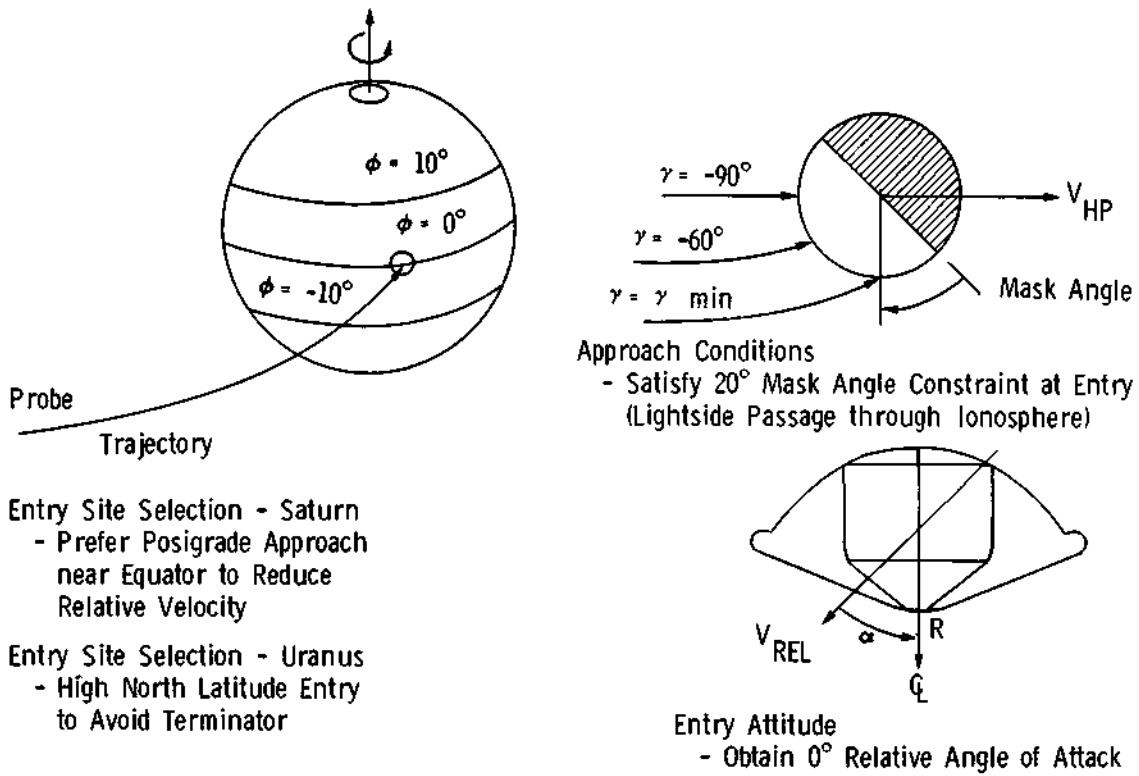


Fig. II-3 Science Constraints on Mission Analysis

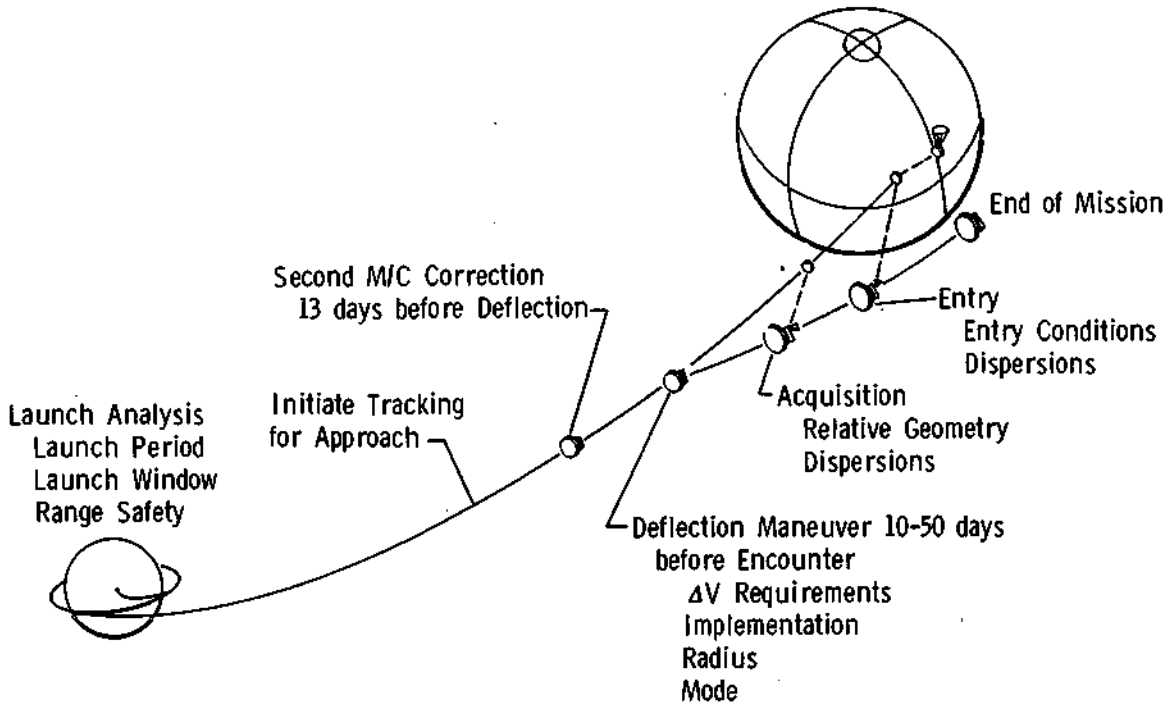


Fig. II-4 Mission Design Considerations

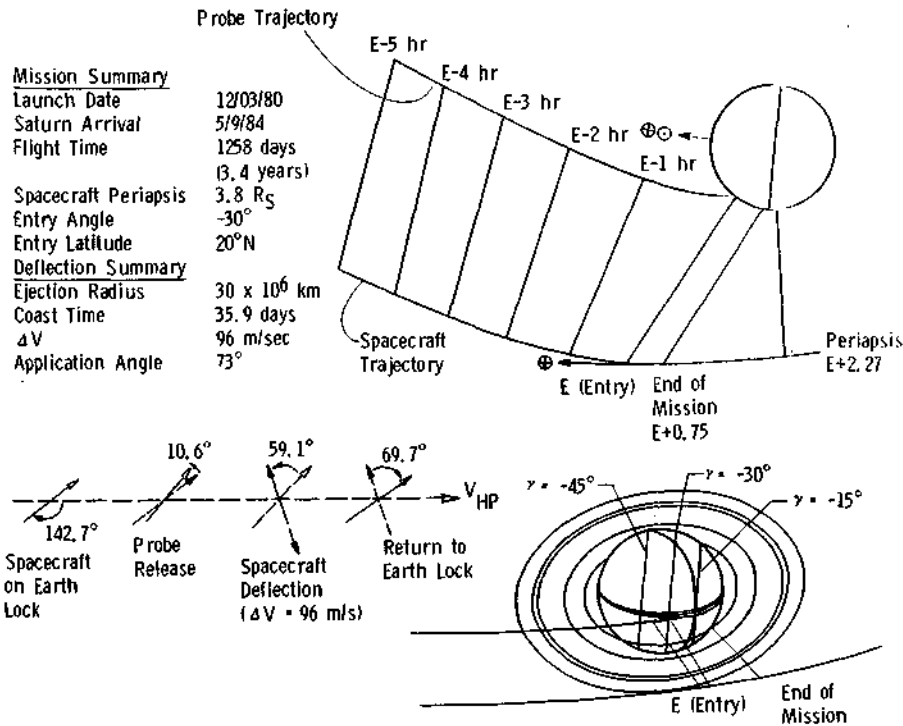


Fig. II-5 Saturn (SU'80) Mission

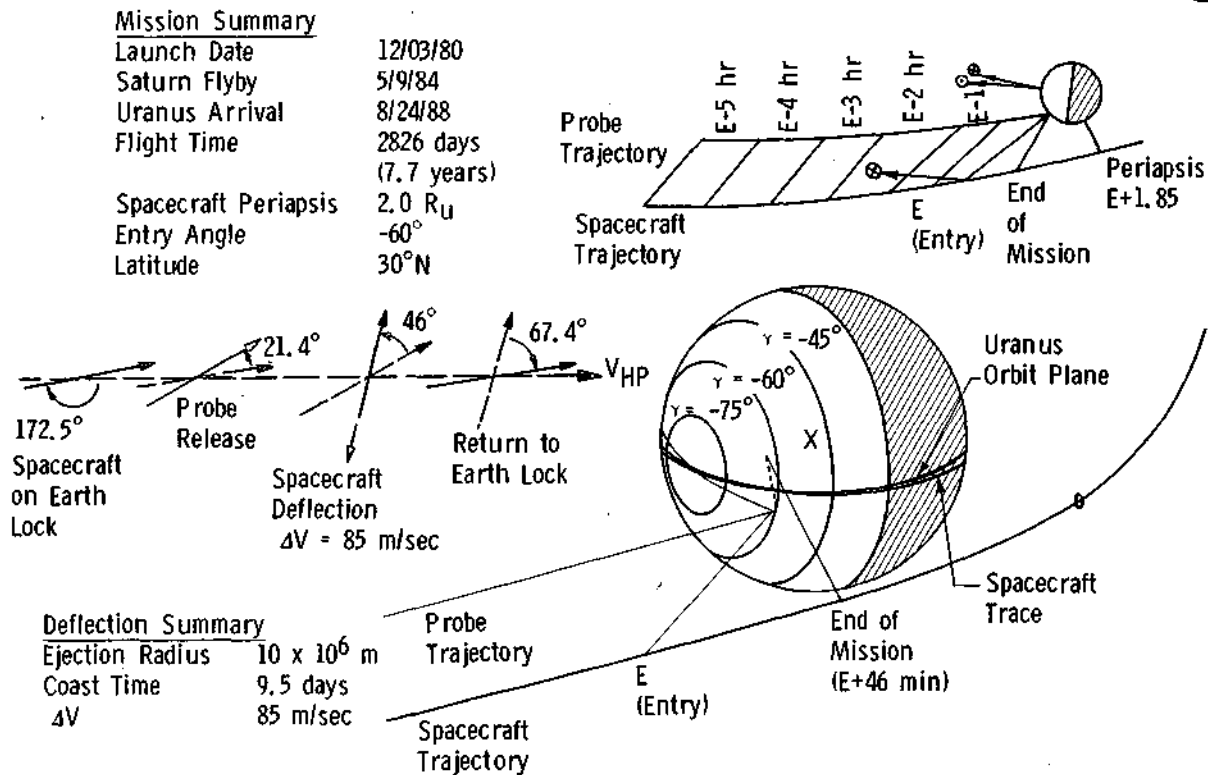


Fig. II-6 Uranus (SU'80) Mission Design

Mission	Design Missions		
	Saturn '79	Saturn (SU'80)	Uranus (SU'80)
VHP, km/sec	8.2	9.11	11.87
Entry Angle, deg	-30	-30	-60
Periapsis, R_S or R_U	2.3	3.8	2.0
Deflection Radius, 10^6 km	30	30	10
Coast Time, days	39.4	35.9	9.5
Probe Release Angle, deg	14.7	10.6	21.4
Spacecraft ΔV Angle, deg	57.3	59.1	46
ΔV Magnitude, m/sec	52	96	85
Lead Angle, deg	5.3	3.7	1.4
Lead Time, hr	1.48	2.1	1.85
Range at Entry, 10^5 km	1.08	1.97	0.87
PAA* at Entry	8.2 (42.4)	4.9 (46.7)	1.9 (31.0)
PAA at End of Mission	13.8	20.0	43
CA+ at Entry	122	118	131
CA at End of Mission	102	112	105
Entry Time Dispersion, min	4.4	4.4	28.9
Entry Angle Dispersion, deg	1.23	1.23	6.24
Angle of Attack, Dispersion, deg	2.1	2.1	3.0

*PAA = Probe Aspect Angle
+CA = Cone Angle

Table II-5 Mission Design Summary

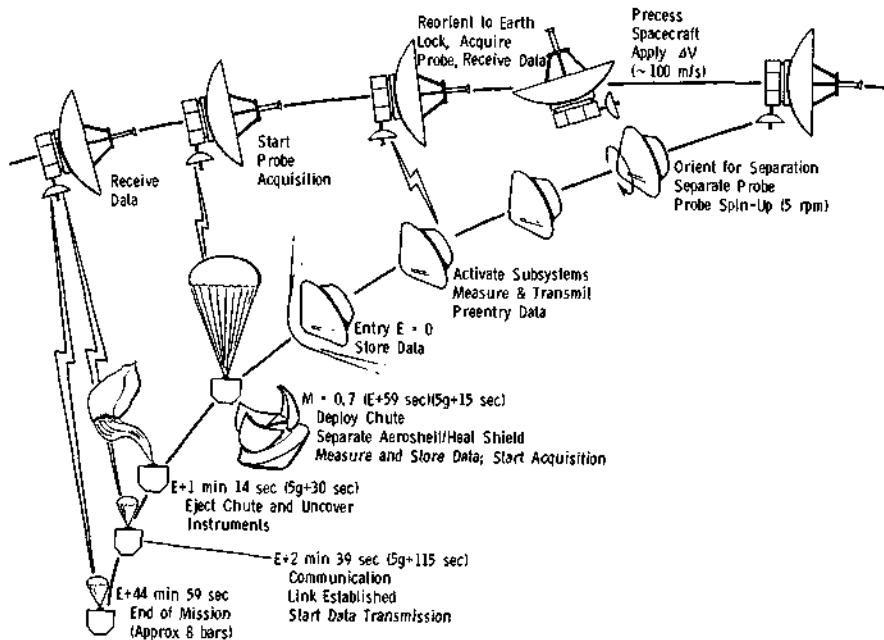


Fig. II-7 Pictorial Sequence of Events (Task I)

4. System Design and Integration

A pictorial sequence of events for the spacecraft and probe for Task I is shown in Figure II-7 from probe-to-spacecraft separation to the end of the mission. At separation, the spacecraft, targeted for an impacting trajectory, rotates and releases the probe.

The probe spins up to 5 rpm and is returned to a quiescent state until pre-entry. The spacecraft is then rotated, the delta-velocity motor is fired for the appropriate flyby geometry and is further rotated to Earth lock. At pre-entry, the Accutron timer in the probe activates the pre-entry and descent battery and the other subsystems. Engineering data is collected and transmitted after probe acquisition by the spacecraft. At entry, the transmitter is turned off and accelerometer data is stored until reacquisition. At 5 g (descending) plus 15 seconds, the main parachute is deployed to separate the heat shield and aeroshell from the descent probe. Fifteen seconds later, the large chute is ejected and the descent chute is deployed. At 100 seconds after main parachute deployment, reacquisition is complete and real-time and stored data are transmitted to the spacecraft until the end of the mission.

The data profile for Task II, Figure II-8, shows data in thousands of bits versus time for pre-entry, entry, and descent phases. At 3 minutes before entry, the Langmuir probes and IRPA begin scientific measurements at approximately 4300 km above one atmosphere and provide signals for both real-time transmission and data storage at 235 bits/sec. At entry, the accelerometer data is collected at 100 bits/sec and stored until descent. After parachute deployment, the descent data is also collected and stored until acquisition, making a total storage of 60.2×10^3 bits. After acquisition, real-time and stored data are transmitted to the spacecraft at 50.5 bits/sec.

The power profile for Task II, depicted in Figure II-9, shows the power required for the probe versus time for separation, coast, pre-entry, entry, and descent phases. The separation phase is only a few minutes duration and requires 0.67 W-hr of power. During coast, the only power required is for the Accutron timer which uses microwatts. The figure shows pre-entry requirements for late, nominal, and early arrival, using the arrival uncertainty for Uranus of 29 minutes. Late arrival is defined as the condition in which the probe arrives at entry so late that the timer times out and activates the subsystems before they are really needed. This late arrival requires the maximum energy. The arrival uncertainty for Saturn is only 4.4 minutes, therefore it is not controlling for power requirements.

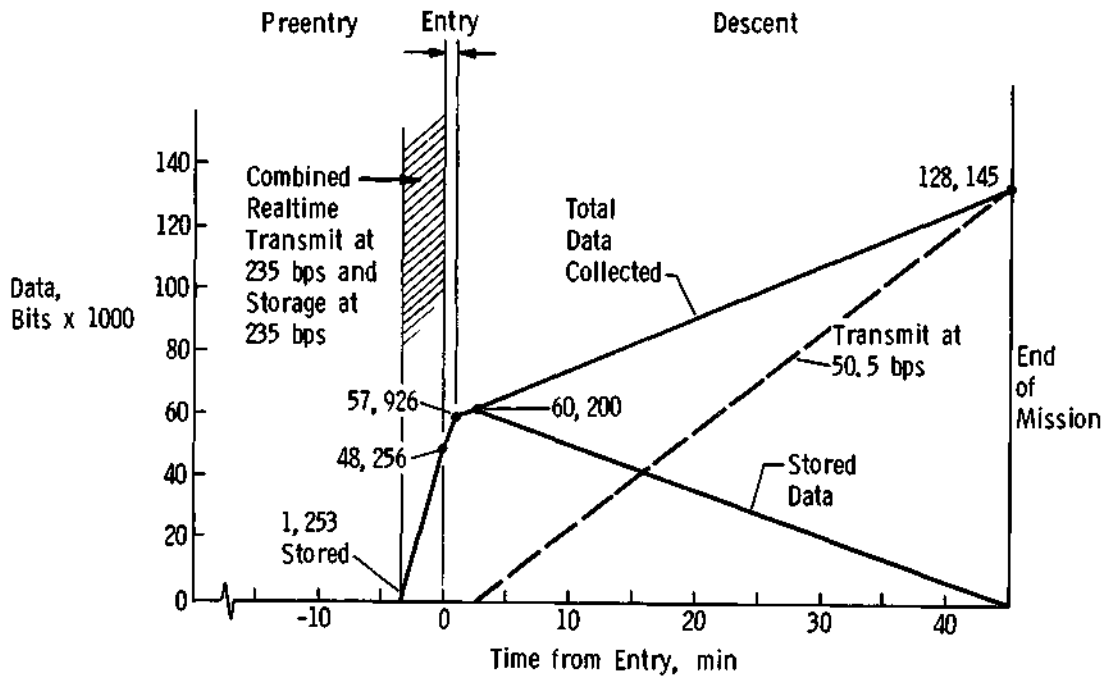


Fig. II-8 Data Profile (Task II)

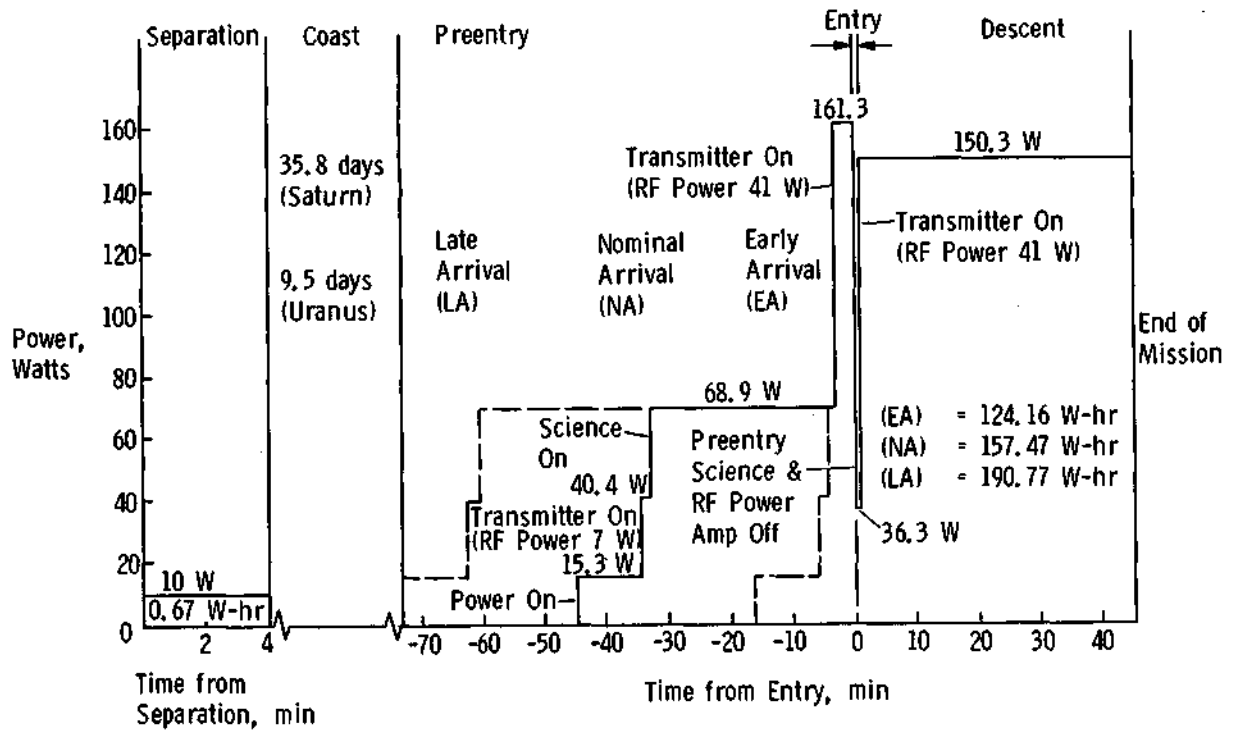


Fig. II-9 Power Profile (Task II)

5. Electrical and Electronic Subsystems

The telecommunications subsystem definitions for both study tasks are summarized in Table II-6 in terms of frequency, modulation, spacecraft and probe antennas, probe RF power, probe data rate, and probe data storage. The frequency of 0.86 GHz was selected during the basic study and used for the follow-on effort. The optimum frequency could be less than 0.86 GHz, but accommodation of the larger antennas becomes a controlling factor. Also, it was found that hardware is being developed for the frequency selected. The descent modulation was selected to be FSK because of the expected turbulence. Using the Task II pre-entry data rate of 235 bits/sec with FSK modulation required 120 watts of RF power compared with 41 watts for PSK modulation. Therefore, for Task II, PSK modulation was used for pre-entry and FSK for descent.

Two levels of RF transmitter power was required for each task: Task I descent used 25 watts and Task II pre-entry used 41 watts. These same power levels for pre-entry acquisition caused transmitter overheating due to the long RF power-on time required by the 29-minute entry arrival uncertainty for Uranus. Therefore, a pre-entry RF power of 7 watts was established as the minimum requirement. The high data rate for Task II resulted in a data storage of approximately 60×10^3 bits.

The power and pyrotechnic subsystems are essentially unchanged from the basic study. However, the definitions are summarized in Table II-7. As was seen in the power profile in Figure II-9, the separation power requirements are very small and the entry and descent batteries are determined by the RF power requirements and the entry arrival uncertainty for Uranus. The pre-entry and descent watt-hour requirements of Figure II-9 are lower than those shown on the table because the profile represents the power required at the equipment and does not reflect losses in the bus and battery margins. The separation battery was selected on the basis of availability (EP GAP 4384) rather than system optimization. The pyrotechnic subsystem uses a capacitor discharge method, dual bridgewires, and latching relays for arming and safing.

Table II-6 Telecommunication Summary

<u>Parameter</u>	<u>Value</u>	<u>Note</u>
Frequency	0.86 GHz	Minimizes Link Losses
Modulation		
Task I	PCM/FSK + Tone	Low Bit Rate
Task II, Preentry	PCM/PSK/PM	High Bit Rate
Task II, Descent	PCM/FSK + Tone	Low Bit Rate
Spacecraft Antenna	Parabolic Dish, 1.3 m Diameter 18.3 dB Gain, 20° Beamwidth	
Probe Antenna	Axial Pattern, Turnstile/Cone 6.5 dB Gain, 100° Beamwidth	
RF Transmitter		
Power, Watts		
Task I	7/25	Saturn (SU'80), End of Mission Critical
Task II	7/41	
Data Rate, bps		
Task I	1/28	Preentry/Descent
Task II	235/50.5	Preentry/Descent
Data Storage, bits		
Task I	11,600	Entry Blackout
Task II	60,200	Preentry and Entry Blackout

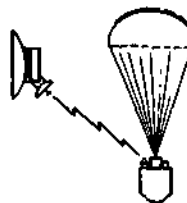


Table II-7 Power and Pyrotechnics Summary

Power Subsystem Configuration	- Remote Activated Ag-Zn Prime Power Source - Power Conditioning and Regulation at User Subsystem
Post Separation Battery Task I	- 0.25 kg, 94 cm ³
Task II	- 0.25 kg, 94 cm ³
Entry/Descent Battery Task I	- 160 Watt-hours at 28 Volts, 2.4 kg, 1196 cm ³
Task II	- 227 Watt-hours at 28 Volts, 3.3 kg, 1639 cm ³
Pyrotechnics Subsystem Configuration	- Capacitor Bank Discharge Pyrotechnic Initiation - Latching Relay Safe/Arm - Dual Bridgewire Initiation from Separate Isolated Power Conditioning
Task I	- 15 Events, 2.5 kg, 3146 cm ³
Task II	- 16 Events, 2.54 kg, 3195 cm ³

6. Mechanical and Structural Subsystems

The probe, as separated from the spacecraft, along with the three major elements, entry aeroshell and heat shield assembly, descent probe and parachutes, is shown in Figure II-10.

A general entry probe configuration, Figure II-11 depicts a cut-away showing the internal parts of the probe and the afterbody segment location. The entry probe configuration comparisons of the SAG exploratory payload (Task I) and the expanded science payload (Task II) are shown in Figure II-12. Task I configuration is 86.8 cm in diameter and weighs 89 kg compared with 92.1 cm and 103 kg for the Task II configuration. The basic difference between the two configurations is the pre-entry science and descent nephelometer which were added to the larger probe.

The descent probe configuration comparisons of the SAG exploratory payload (Task I) and the expanded science payload (Task II) are shown in Figure II-13. Task I configuration is 47.0 cm in diameter and weighs 40 kg compared with 48.9 cm and 50 kg for Task II configuration. The basic difference between the two configurations is the added nephelometer for Task II.

The structural and mechanical definitions for the two study task configurations are summarized in Table II-8. The design deceleration loads are based upon -65° entry angle in the Uranus cool atmosphere, which results in a deceleration of 865 g compared with 837 g and -60° for the design mission. Therefore, the definition considers a 5° entry angle uncertainty.

The subsystem weight buildup and dropoff for the two study task configurations is shown in Table II-9. These weights include a 15% margin for uncertainties.

7. Probe to Spacecraft Integration

The common Saturn/Uranus probe is shown mounted on a Mariner-type spacecraft in Figure II-14. The interface is briefly described in terms of mission cruise, pre-separation checkout, separation of probe and spacecraft, and post-separation.

8. Probe Comparison

An overall comparison of the two probe configurations is summarized in Table II-10.

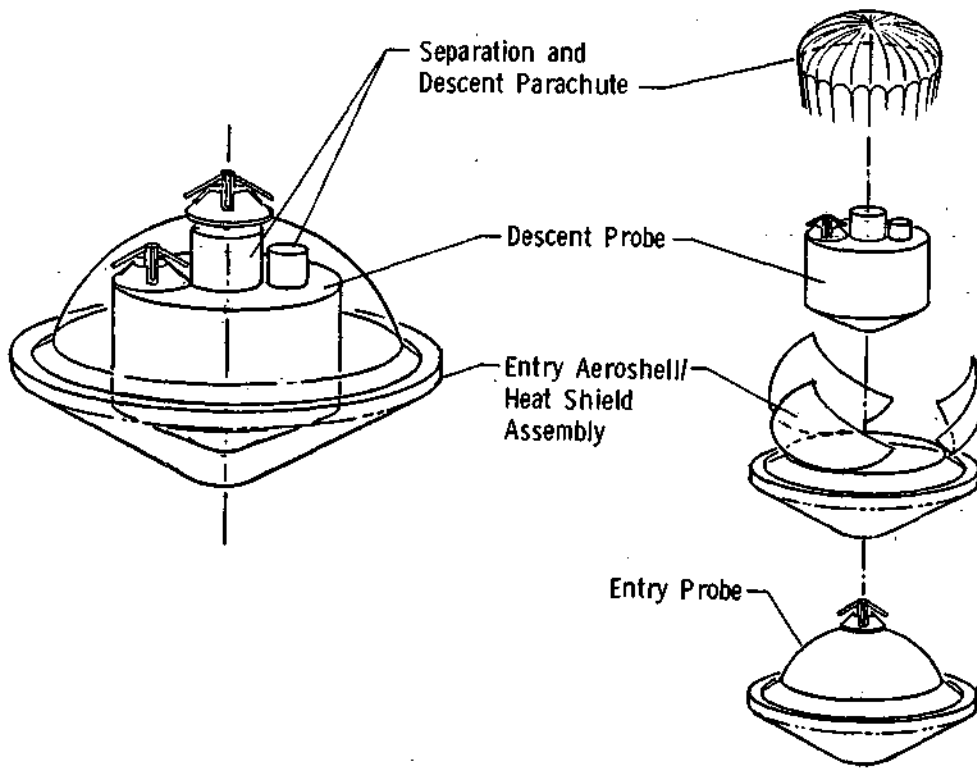


Fig. II-10 Probe Configuration Description

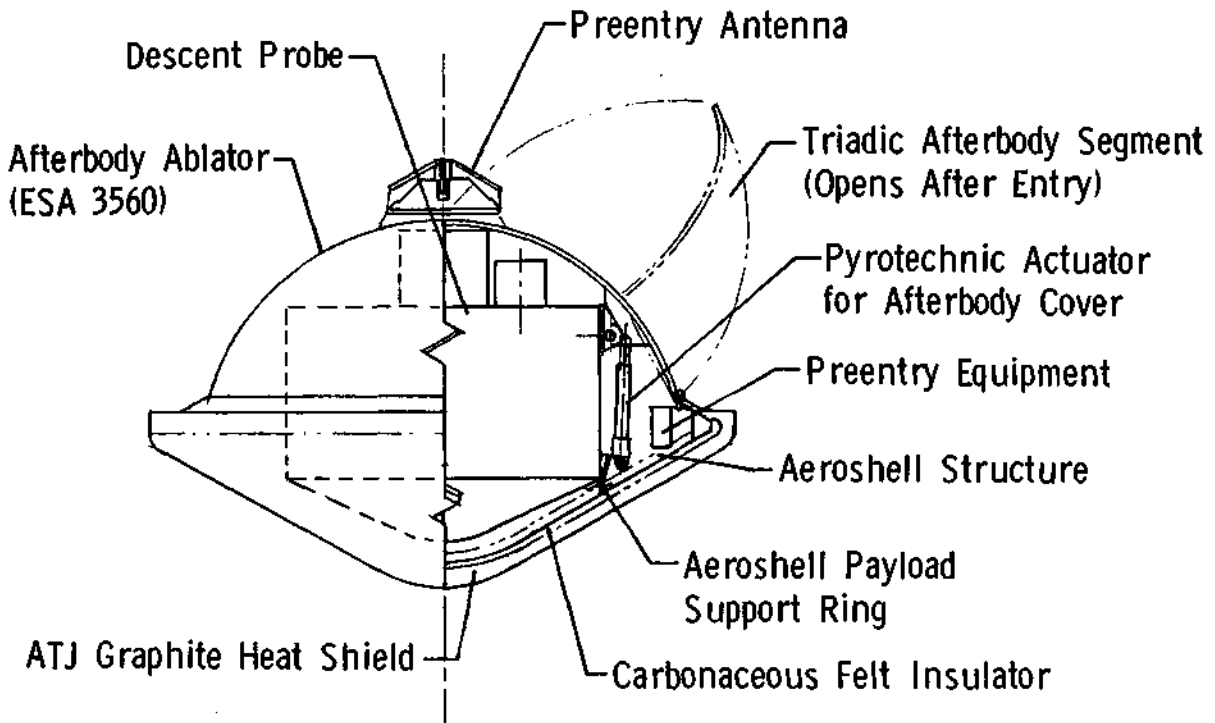


Fig. II-11 General Entry Probe Configuration

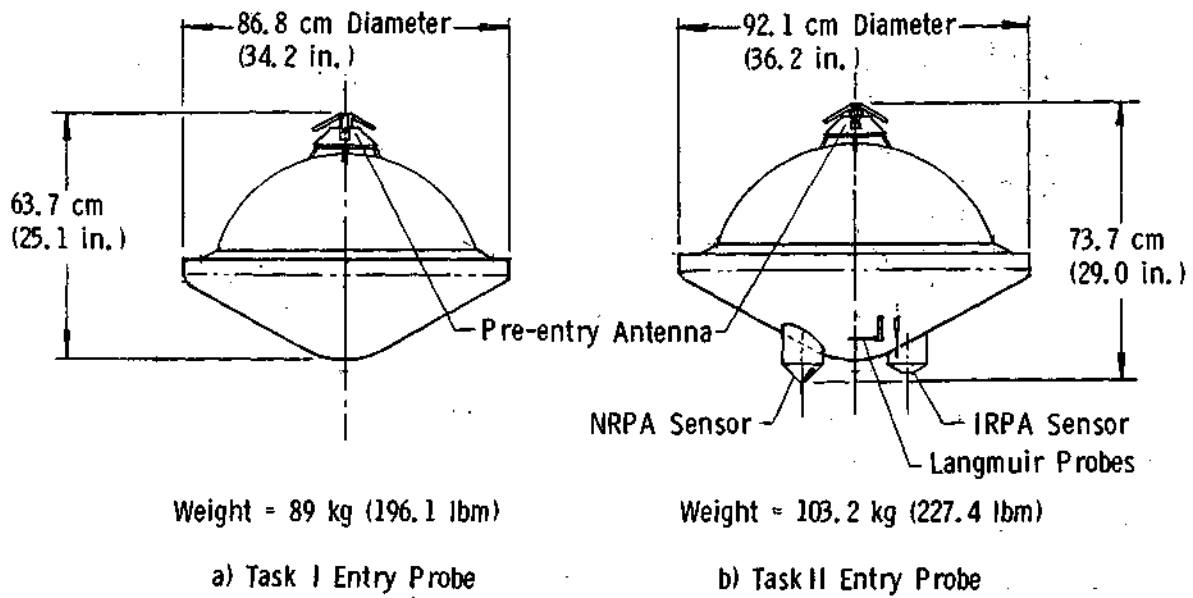


Fig. II-12 Entry Probe Configuration Comparison

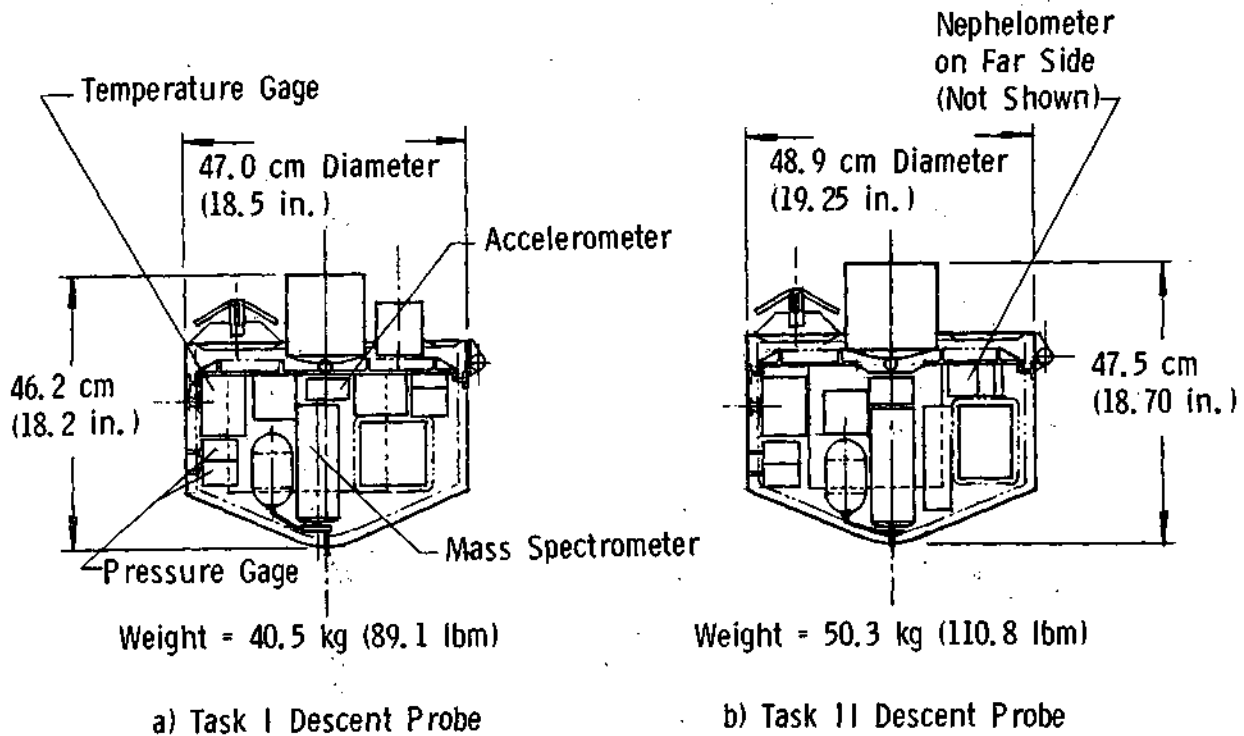
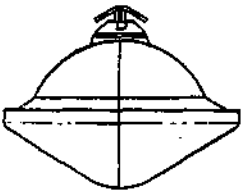
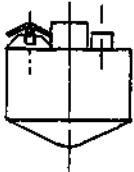


Fig. II-13 Descent Probe Configuration Comparison

	SAG Exploratory Payload (Task I)	Expanded Science Payload (Task II)
Entry Probe Weight, kg	89.0	103.2
Entry Probe Diameter, cm	86.8	92.1
Descent Probe Weight, kg	40.5	50.3
Descent Probe Diameter, cm	47.0	50.1
Separation Parachute Diameter, cm	232	250
Descent Parachute Diameter, cm	73	88
Probe Entry Deceleration Load, 65° Uranus Entry Angle	865 g	865 g
Forebody Heat Shield Mass Fraction, 35° Saturn Entry	0.21	0.21
Forebody Heat Shield Material	Graphite (ATJ)	Graphite (ATJ)
Afterbody Heat Shield Material	ESA 3560 (13.7 kg/m ²)	ESA 3560 (13.7 kg/m ²)
Spin Stabilized, rpm	5.0	5.0



Entry Probe



Descent Probe

Table II-8 Structural/Mechanical Summary

	SAG Exploratory Payload (Task I)	Expanded Science Payload (Task II)
Science	8.08 kg	14.44 kg
Power and Power Conditioning	4.70	5.79
Cabling	3.86	4.50
Data Handling	2.43	2.78
Attitude Control System	2.84	2.84
Communications	3.86	3.95
Pyrotechnic Subsystem	6.38	6.44
Structures and Heat Shield	34.00	37.12
Mechanisms	6.03	6.67
Thermal	5.22	5.22
Propulsion	0.01	0.01
Margin (15% of Above Total)	11.61	13.46
Probe Total Weight	89.02	103.22
Probe Entry Weight	89.01	103.21
Post Entry Weight	78.48	91.32
Descent Weight	40.50	50.32

Table II-9 Weight Comparisons

Spacecraft/Probe Interface

Cruise

Environmental Cover
Monitor (On Demand)
High Conduction Mechanical/Thermal Attachment

Preseparation Checkout

Power - 8 W Avg; 30 W Peak
Checkout Signals
Data Monitor - 1400 bits

Separation

Probe Pointing - 2°
Battery Activation Signal
Separation Signal
Spring Separation System ($\Delta V = 1$ m/s)
Probe Self Spin (0.52 rad/sec)

Post Separation

Track Probe
Receive Data 1 to 50.5 bps
Up to 128 Kbits

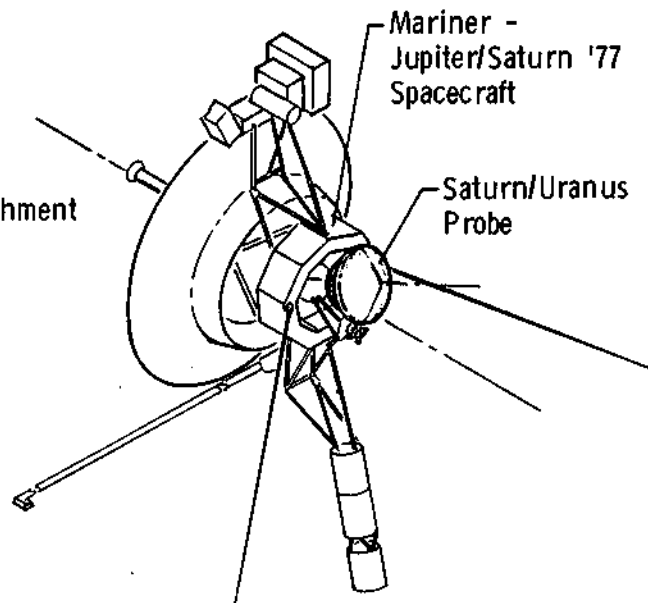


Fig. II-14 Probe Integration with Mariner Spacecraft

Table II-10 Probe Comparison Summary

<u>Parameters</u>	<u>Task I</u>	<u>Task II</u>
Mission	SU'80	SU'80
Entry Angle, deg	-30(S), -60(U)	-30(S), -60(U)
Entry Latitude, deg	20(S), 30(U)	20(S), 30(U)
Spacecraft ΔV , m/sec	96(S), 85(U)	96(S), 85(U)
Max Deceleration, g	837 (U Cool Atmosphere)	837 (U Cool Atmosphere)
Science Weight, kg	8.1	14.4
RF Power at 0.86 GHz	25(S)	41(S)
Max Realtime Data Rate, bps	28 Descent	235 Preentry, 50.5 Descent
Probe Data Storage, Kbits	11.6	60.2
Ejected Weight, kg	89.0	103.2
Heat Shield Diameter, cm	86.8	92.1

9. Influence of the Atmospheric Models

Each of the warm, nominal and cool atmosphere models for Saturn and Uranus has a different influence upon the probe design parameters. The controlling models for seven of the most significant parameters are as follows.

a. *Science Performance* - The Saturn warm atmosphere model is generally the worst case for science performance because of the large pressure and density scale heights.

b. *Pressure Height of the First Measurement* - The Saturn cool atmosphere places the first descent measurement at the highest pressure height of 122 mb due to the highest pressure at parachute deployment. The lowest pressure height for the first measurement is 51 mb in the Saturn warm atmosphere.

c. *Depth of Descent* - Using a descent ballistic coefficient of 110 kg/m² and a descent time (time from parachute deployment to the end of the mission) of 44 minutes, the deepest pressure descent of 19.2 bars is reached in the Uranus cool atmosphere compared with 3.1 bars in the Uranus warm atmosphere, as shown in Figure II-15.

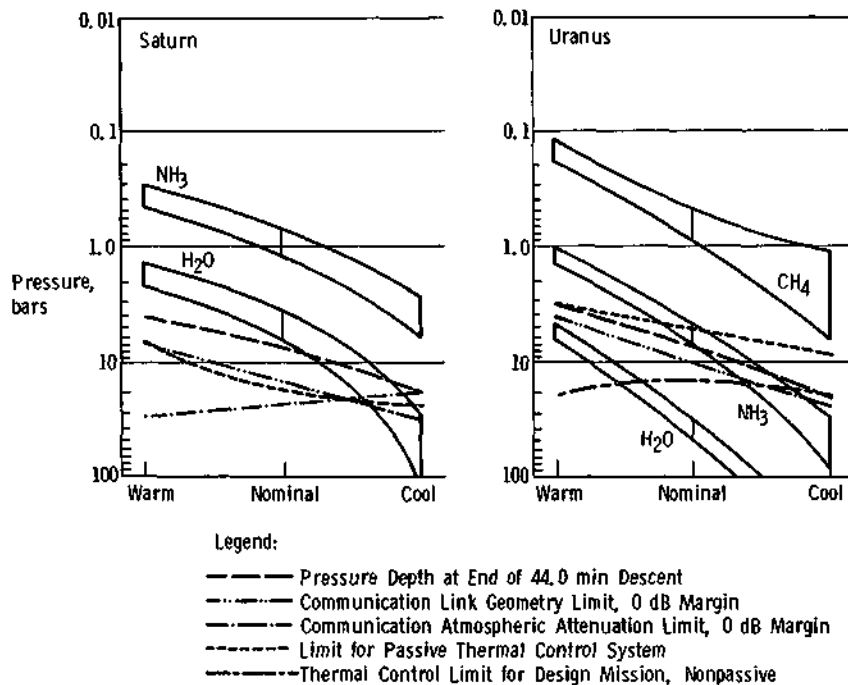


Fig. II-15 *Cloud Locations and End-of-Mission Limits for Various Model Atmospheres*

d. *Deceleration* - The Uranus cool atmospheric model, which is controlling, imposes 837 g on the probe at entry compared with 568 g for Saturn cool, and decreasing to 225 g for Uranus warm.

e. *RF Link Analysis* - The Saturn cool atmosphere model is controlling due to the higher ammonia abundance at the design depth of descent which attenuates the transmitted signal. Figure II-15 shows that for all the Uranus atmospheres and for the Saturn warm and nominal atmospheres the communication geometry is controlling.

f. *Entry Data Storage* - The Saturn warm atmosphere is the worst case. Data is stored from 0.1 g (increasing) until 5 g (decreasing) plus 15 seconds when acquisition is complete and descent transmission is started. For Saturn warm, this time is 172.5 sec compared with 166 sec for Uranus warm and decreasing to 133 sec for Uranus cool.

g. *Thermal Control* - The Uranus cool atmosphere is the worst case for the thermal control subsystem because of the severity of the cold temperature at Uranus. Figure II-15 shows that a passive subsystem is adequate for Saturn, but a nonpassive system is required for the Uranus nominal and cool atmospheres.

10. Compromises Necessary to Achieve Commonality

In designing a common probe for use at Saturn and Uranus and for all three atmospheric models at each planet, certain compromises were made. Compared with a probe optimized for a single set of constraints, such as the Saturn warm atmosphere, the compromises for this common probe are as shown in Table II-11.

11. Probe Subsystem Development Status

Some probe components are presently available while others are not. The development status of the major probe components are shown in Table II-12.

B. CONCLUSIONS AND RECOMMENDATIONS

The study showed that a common Saturn/Uranus probe is technically feasible for the 1980s using the Science Advisory Group (SAG) exploratory payload and the expanded science payload along with three atmospheric models, defined in the study monographs, for

Table II-11 Compromises for Commonality

DESIGN PARAMETER	CONTROLLING FACTORS	COMPROMISE
1. RF Power	Lead tag commonality at Saturn and Uranus	8-watt increase at Saturn
2. Temperature Control	Passive: S & UW Active: UN & UC	Active design
3. Heat Shield	Mass Fraction: S = 0.21; U = 0.13	Design for Saturn
4. Structural Design	Best Case: UW = 225 g Worst Case: UC = 837 g	Design for 837 g
5. Descent Start	Best Case: SC = 102 mb Worst Case: UC = 41 mb	Minimum Data in UC
6. NMS Performance in Cloud	Best Case: CH ₄ cloud in UC Worst Case: CH ₄ cloud in UW	Minimum Data in UW
7. Temperature Pressure Profile Performance	Best Case: UC Worst Case: SW	Minimum Data in SW
8. Entry Data	Best Case: SW = 8450 bits Worst Case: SC = 4400 bits	Minimum Data in SC
9. Battery Sizing	Shortest Pre-entry-S Longest Pre-entry-U	Design for Uranus
S = Saturn U = Uranus	C = Cool atmosphere W = Warm atmosphere N = Nominal atmosphere	

Table II-12 Probe Subsystem Development Status

SUBSYSTEM ELEMENTS	STATE OF THE ART*			DEVELOPMENT REQUIRED		
	TECH-NOLOGY	DESIGN	HARD-WARE	NONE	MINOR	MAJOR
Science						
IRPA			X		X	
NRPA	X					X
Langmuir Probe			X	X	Venus-Pioneer	
NMS			X		X	
NMS Inlet		X				X
Accelerometers			X		X	
Pressure Gages			X		X	
Temperature Gage			X	X	Viking	
Nephelometer			X	X	ISIS-B	
Electronics Subsystems						
RF Transmitter			X		X	
Antennas			X		X	
RF Switch			X	X	Titan Missile	
Modulator			X		X	
Data Handling			X		X	
Battery			X		X	
Pyrotechnics			X		X	
Structural/Mechanical Subsystems						
Heat Shield	X					X
Parachutes			X		X	
Cold Gas System			X		X	
Devices			X		X	
Thermal Control			X		X	
Radio Isotope Heaters			X	X	Pioneer Spacecraft	

*Technology--limited to concepts and ideas; no usable design.

Design--hardware definition in process; no similar hardware available.

Hardware--actual or similar hardware available.

Saturn and Uranus. The study also clearly showed that further research, design, and development activities are required in such areas as new science payloads, better atmospheric model definition, heat shield development, cloud condensation in the instrument sensing ports, NMS inlet definition, dynamic instability, communications, data handling, and parachute materials.

1. Science

Although the SAG exploratory payload definition was provided at the beginning of the basic study and the expanded science payload was provided at the start of the follow-on study, the scientists are not satisfied with either payload and continued study should ensue to obtain a better science complement.

2. Model Atmospheres

The warm, nominal, and cool atmosphere models for Saturn and Uranus were provided at the start of the basic study. The scientists believe that additional data should be generated to more precisely define these atmospheric models.

3. Heat Shield Development

NASA-ARC has done extensive development in the heat shield area in the past and has established a good reference base for further development and testing.

4. Cloud Condensation at Instrument Ports

As the probe enters the planetary atmosphere, the cloud condensation at the inlet ports for the NMS, temperature and pressure gages and on the nephelometer lense will cause erroneous readings. Further development is required to eliminate or reduce this effect.

5. NMS Inlet Definition

The inlet for the neutral mass spectrometer requires further evaluation to ensure compatibility with the masses of the primary constituents that exist in two different groups: 1 to 4 AMU and 15 to 18 AMU. The leak rates through the sintered plug might be appreciably different for each group and cause measurement distortion.

6. Dynamic Instability Due to Preentry Science "Burn-Off"

For Task II, the pre-entry science instruments are mounted external to the heat shield and are allowed to burn off during entry. Dynamic instability may result; this requires further analysis.

7. Communications

Each probe definition shows two probe antennas of the same design: one for pre-entry the other for descent. An analysis and test might show that the descent antenna with an added radome could be used for pre-entry transmission.

The thermal control analysis showed that the minimum RF transmitted power should be used during pre-entry because the entry arrival uncertainty causes the transmitter to overheat. For this reason, transmitter designs that have a variable RF power output and related dissipation control should be investigated. Reduced battery weight would also be realized.

The RF power of the binary FSK link is designed to meet $E_b/N_o = 8.9$ dB with convolutional coding and Viterbi decoding. This constraint is based on comparable improvement of PSK (BER = 5×10^{-5}). Analysis or simulation should be performed to verify the validity of this constraint.

8. Data Handling

A nonvolatile programmable memory would provide an effective approach to fault control. Memory devices and fail-safe techniques should be evaluated to provide effective failure control.

9. Parachute Materials

Data shows that the parachute material, Dacron, will withstand the Uranus cool temperatures. However, a test of the material is recommended to verify that it will withstand these temperatures under deployment conditions.

III. SATURN/URANUS PARAMETRIC ANALYSIS

This section includes the system and subsystem analyses and trade-offs that were conducted in support of the probe system definition of Sections IV (Task I) and V (Task II). The general constraints for this section follow:

Missions:

*Saturn Direct 79,

*Saturn (SU 80),

*Uranus (SU 80),

Uranus (SU 79).

Science Instruments:

Task I (Science Advisory Group's Exploratory Payload) - Neutral Mass Spectrometer (NMS), Temperature Gage, Pressure Gages and Accelerometers;

Task II - Langmuir Probes, Ion Retarding Potential Analyzer (IRPA), Neutral Particle Retarding Potential Analyzer (NRPA) and Nephelometer.

Deflection Mode: Spacecraft

Atmospheric Models: Worst Case

Entry Angles, Latitude and Descent Depth: Compatible with Mission Set and Science Objectives

*Design Missions

A. MISSION DESIGN CONSIDERATIONS

1. Launch and Interplanetary Trajectories

Opportunities for Earth-Saturn transfer occur approximately every 12.4 months when the Earth is in its appropriate orbit position for the launch of a spacecraft on a direct flight to Saturn. These launch opportunities have characteristics that vary through a cycle of 29.5 Earth-years (one revolution of Saturn about the sun). Interplanetary trajectories for the Saturn Direct 79 and SU 80 missions are shown in Figures III-1 and III-2. These missions to Saturn are characterized by trip times in excess of 3.5 years and type I transfers.

a. *Launch Energy* - Minimum energy Earth-to-Saturn transfers occur in 1970 and 1984. These missions have favorable characteristics in that they represent node-to-node trajectories approximating Hohmann transfers. The C_3 requirement for the 1984 Saturn mission is $110 \text{ km}^2/\text{sec}^2$; for the 1979 and 1980 Saturn missions, the launch energy is in excess of $130 \text{ km}^2/\text{sec}^2$. Even though the 1979 and 1980 missions are not optimal in terms of launch energy and trip time, they are still representative and feasible missions. If for any reason later launches to Saturn are considered, launch energy requirements would be improved.

Figure III-3 presents estimated Shuttle performance data; Figure III-4 Titan/Centaur performance data. The launch vehicle combinations considered for this study are (1) Titan IIIE/Centaur/BII, (2) Titan IIIE/Centaur/TE364-4, (3) Shuttle/Std. Centaur/BII, and (4) Shuttle/45,000 lb/Agena/BII. The seven-segment Titan III is no longer considered a viable launch vehicle option and accordingly it was not considered. Performance data for all vehicles assumes a 185-km parking orbit. The payload in all cases refers to probe, spacecraft, spacecraft modifications, and adapters.

A lightweight Mariner spacecraft design, not including probe, has a launch weight of about 500 kg (1100 lb) whereas an unmodified Pioneer-class spacecraft has a launch weight of about 321 kg (710 lb). Comparisons in launch vehicle performance in terms of injected payload as a function of launch period for the Saturn Direct 79 and S/U 80 mission are shown in Tables III-1 and III-2. Table III-3 summarizes the launch energy requirements for the two missions under consideration as well as the Jupiter Uranus 79 mission.

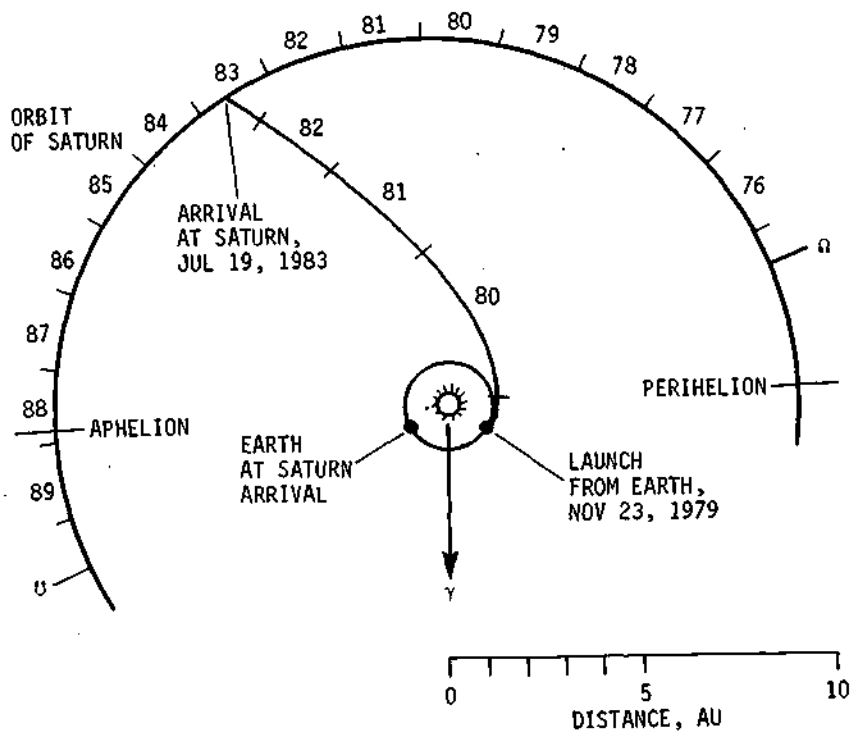


Fig. III-1 1979 Saturn Interplanetary Trajectory

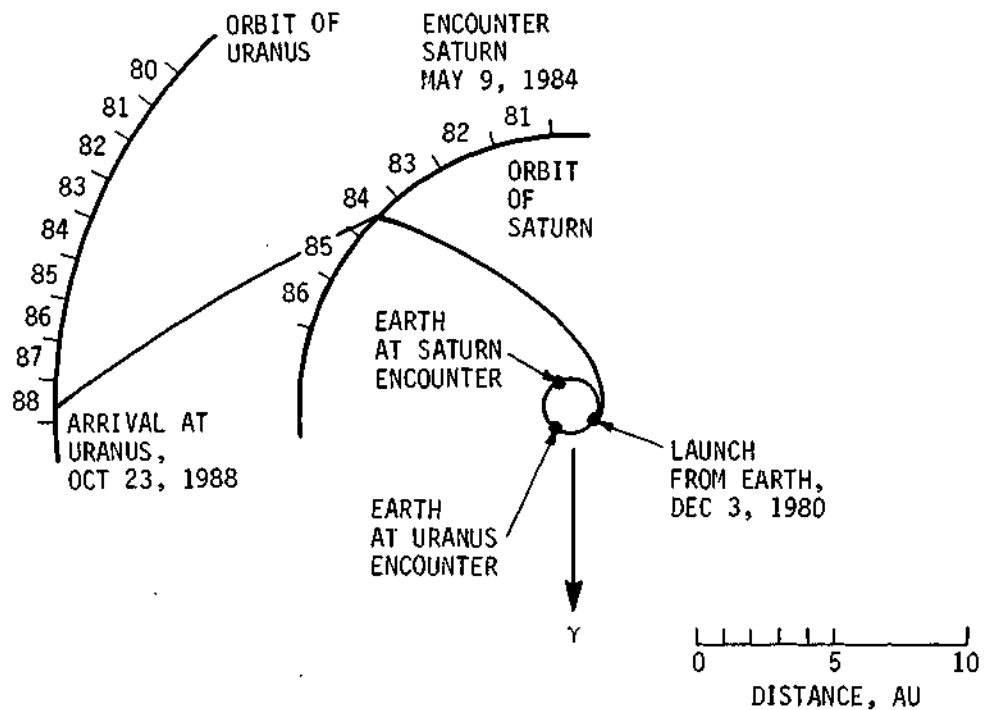


Fig. III-2 1980 Saturn/Uranus Interplanetary Trajectory

Table III-1 Saturn Direct '79 Mission Launch Capability

LAUNCH PERIOD	INJECTED WEIGHT, kg (lb)			
	TITAN IIIE/ CENTAUR/ BURNER II	TITAN IIIE/ CENTAUR/ TE 364-4	SHUTTLE/ CENTAUR/ BURNER II	SHUTTLE/ AGENA/ BURNER II
NOMINAL	480 (1060)	580 (1280)	847 (1870)	974 (2150)
5-DAY	458 (1010)	562 (1240)	806 (1780)	956 (2110)
15-DAY	417 (920)	510 (1125)	691 (1525)	861 (1900)

Table III-2 Saturn Uranus '80 Mission Launch Capability

LAUNCH PERIOD	INJECTED WEIGHT, kg (lb)			
	TITAN IIIE/ CENTAUR/ BURNER II	TITAN IIIE/ CENTAUR/ TE 364-4	SHUTTLE/ CENTAUR/ BURNER II	SHUTTLE/ AGENA/ BURNER II
NOMINAL	476 (1050)	571 (1260)	827 (1825)	956 (2110)
5-DAY	448 (990)	552 (1220)	788 (1740)	938 (2070)
15-DAY	417 (920)	510 (1125)	691 (1525)	861 (1900)

Table III-3 Mission Launch Energy Requirements

LAUNCH ENERGY, C_3 , km ² /sec ²	S 79	SU 80	JU 79
NOMINAL	132	133	102
5-DAY	133.9	134.5	105
10-DAY	135.8	136	107
15-DAY	140	140	110

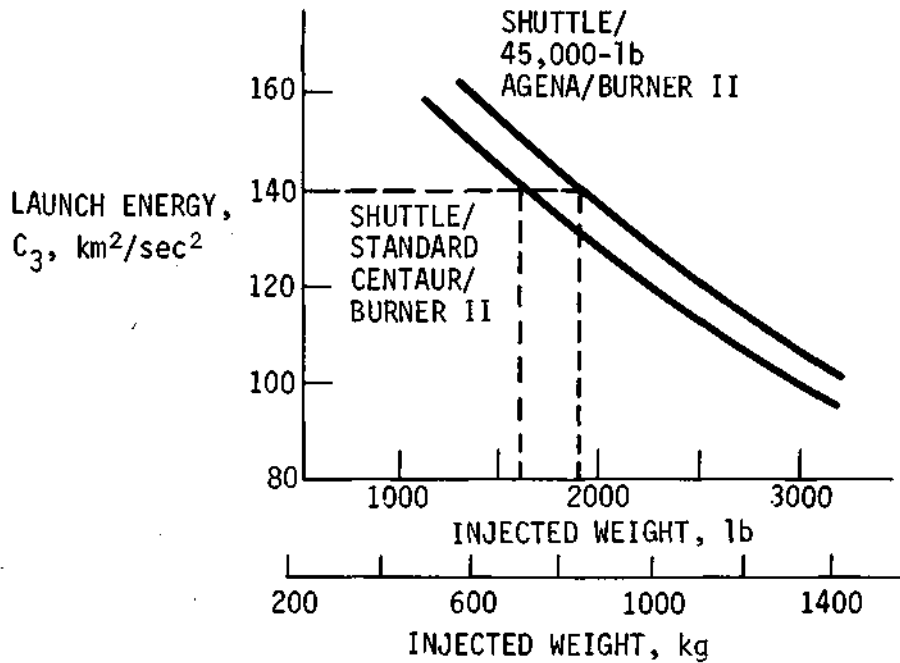


Fig. III-3 Estimated Shuttle Performance Data

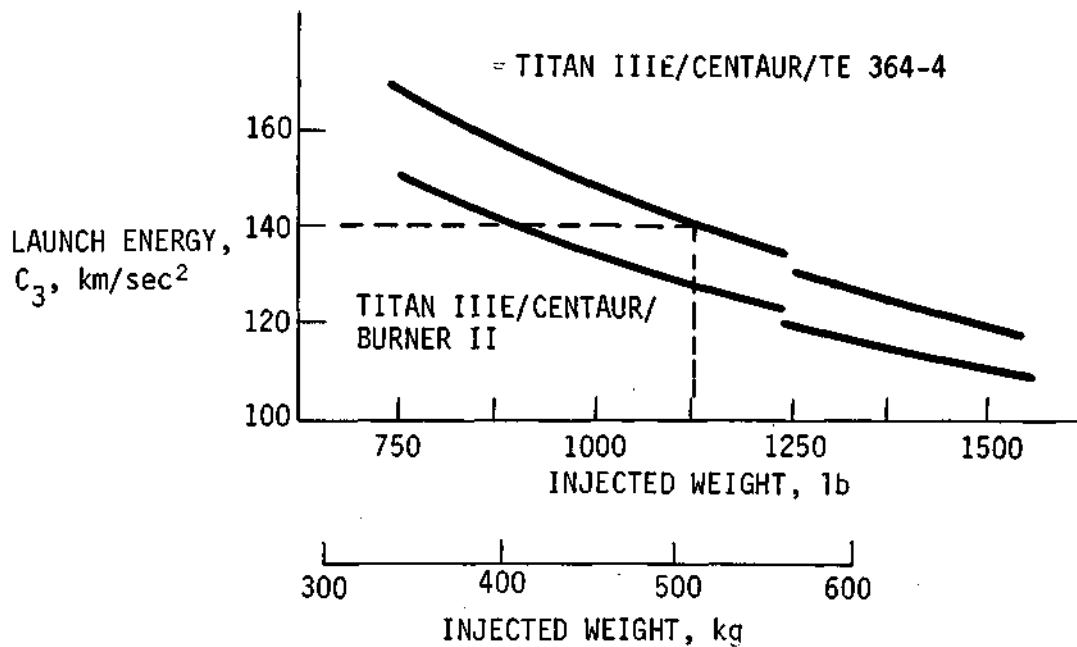


Fig. III-4 Titan III/Centaur Performance Data

Figure III-5 provides the C_3 contours for launch years 1979 and 1980. The two reference missions analyzed in this volume are indicated by the dots \odot on the C_3 contours. Since the 1979 mission has no post Saturn objectives, the end conditions in terms of periapsis radius are open and the reference mission was targeted to $R_p = 2.3 R_s$. The S/U 80 C_3 contour has the Saturn fly-by radius indicated. For the S/U mission, a trade exists between launch energy, which affects launch vehicle injected weight capability, and periapsis radius, which affects spacecraft-to-probe communication space loss; a large periapsis radius implies a large spacecraft-to-probe range at entry. The reference Saturn/Uranus mission ($R_p = 3.8 R_s$) was selected as a compromise between these two factors. By referring to Figure III-5 it is seen that launch energies for 1979 and 1980 missions to Saturn are in the range of 130 to 140 km^2/sec^2 . For comparison purposes, it is recalled that the required launch energy for the JU 79 mission was of the order of 105 km^2/sec^2 . Hence, in terms of required launch energy, trajectories that fly by Jupiter before encountering Uranus are preferred to trajectories that fly by Saturn first. The primary reason for increased launch energy for Saturn launches as opposed to Jupiter launches is simply the greater distance, 10 au versus 5 au.

b. Launch Constraints - The launch date/arrival date (LD/AD) selection must consider other requirements in addition to launch energy. Certain launch parameters constrain the choice of mission dates. The declination of the launch asymptote, DLA, is limited in magnitude to less than 36° as a result of range definition and safety considerations. This DLA constraint is most restrictive for the 1979 Saturn launch, eliminating approximately one quarter of the available period; by 1980 the DLA constraint is of no significance.

The nominal range of launch azimuths is limited between 90° and 115° , and this range determines the daily launch window. For both missions considered, the launch window was in excess of an hour.

Another constraint that is frequently imposed involves a further restriction on DLA. The accuracy of the tracking process is seriously degraded for DLAs in the vicinity of zero. Accordingly, the following constraint is considered in the launch analysis.

$$|DLA| > 2^\circ$$

This constraint is checked to ensure that it is not violated.

a. Arrival Constraints - The most critical arrival constraint is the observability of the spacecraft at encounter by Earth. If the Sun is between Earth and Saturn at encounter, neither tracking nor critical communication tasks can be performed. Therefore, the SEV angle, defined as the angle between the Sun, Earth and spacecraft, at encounter must be bounded away from zero. The constraint plotted on Figure III-5 is $|SEV| < 15^\circ$ and occurs during a noncritical spread of Saturn arrival times. A second constraint, imposed to avoid degradation of the DSN tracking process is $\delta_s = 0$, where δ_s is the geocentric declination of the spacecraft at Saturn encounter. This constraint for the missions under consideration is never violated.

Another key parameter defining the arrival geometry is the hyperbolic excess velocity V_{HP} at the planet. V_{HP} is no more than the velocity of the spacecraft relative to the planet; it varies between 7 and 11 km/sec at Saturn and 10 and 14 km/sec at Uranus. The entry velocity at either planet is not greatly affected by the magnitude of V_{HP} as is shown in Figure III-6. The magnitude of V_{HP} influences probe coast time most significantly. Of more importance than magnitude is the direction of the V_{HP} vector. Two angles, ZAP and ZAE, defined and presented in Figure III-7, are used to determine planetary lighting conditions of the approach trajectory and efficacy of approach orbit determination, respectively. Values of ZAE near 90° indicates that the velocity vector is contained in a plane perpendicular to the radius vector and hence is not conveniently determined by Doppler tracking.

2. Approach Orbit Determination and Dispersions

No new navigation analysis was performed for this phase of the study, this section includes work previously performed but not previously reported. Using knowledge and control covariances previously obtained, dispersions in entry and communication parameters were generated for trajectory parameters corresponding to a Saturn and Uranus approach from a 1980 mission. In addition, a parametric study was performed in which approach orbit determination for a range of deflection radii was investigated. The results of this study are summarized in Figure III-8; error assumptions are presented in Table III-4.

Fig. III-5 Saturn 1979 and Saturn/Uranus 1980 Launch Energy Contours

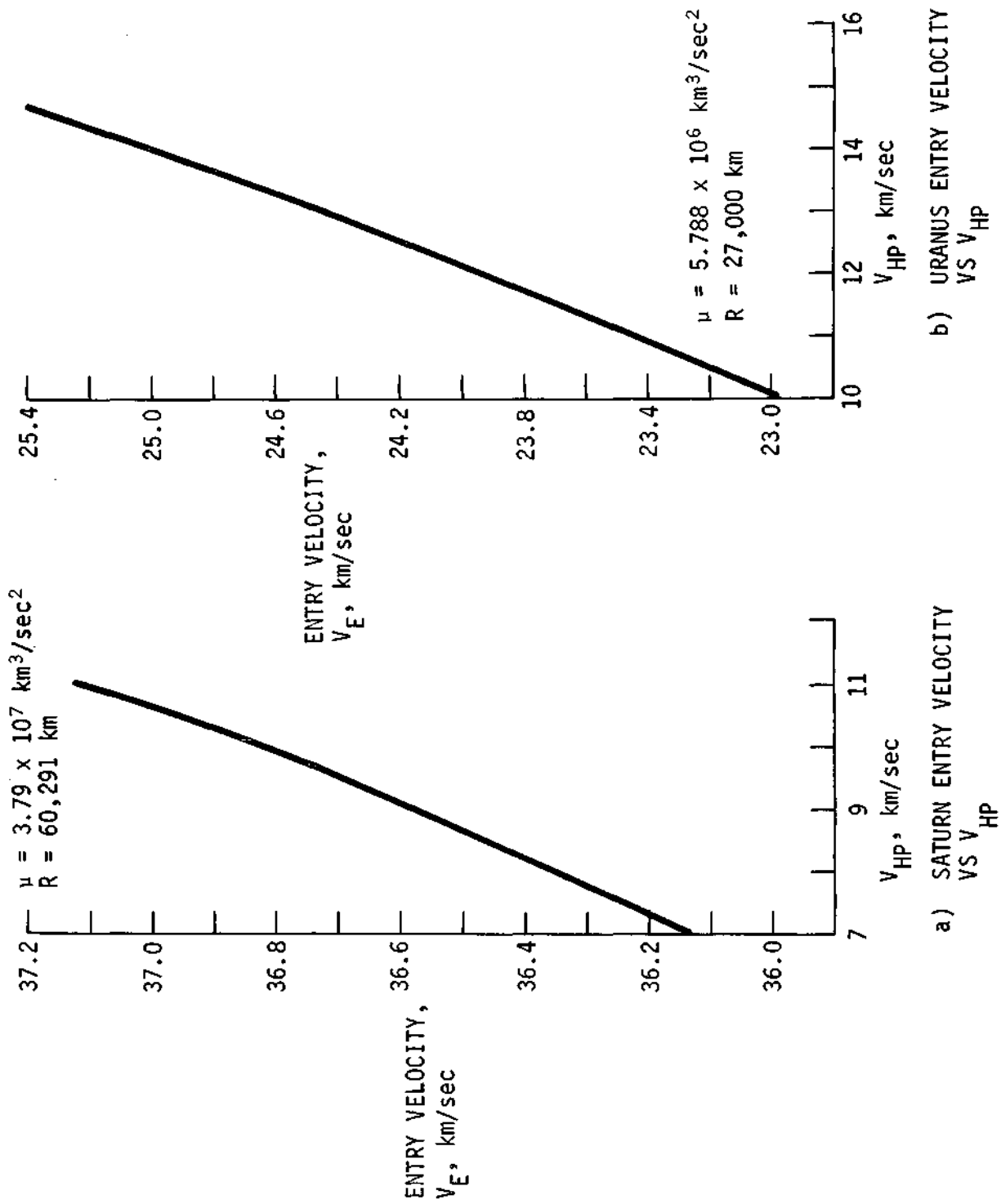


Fig. III-6 Saturn and Uranus Entry Velocity Variations with V_{HP}

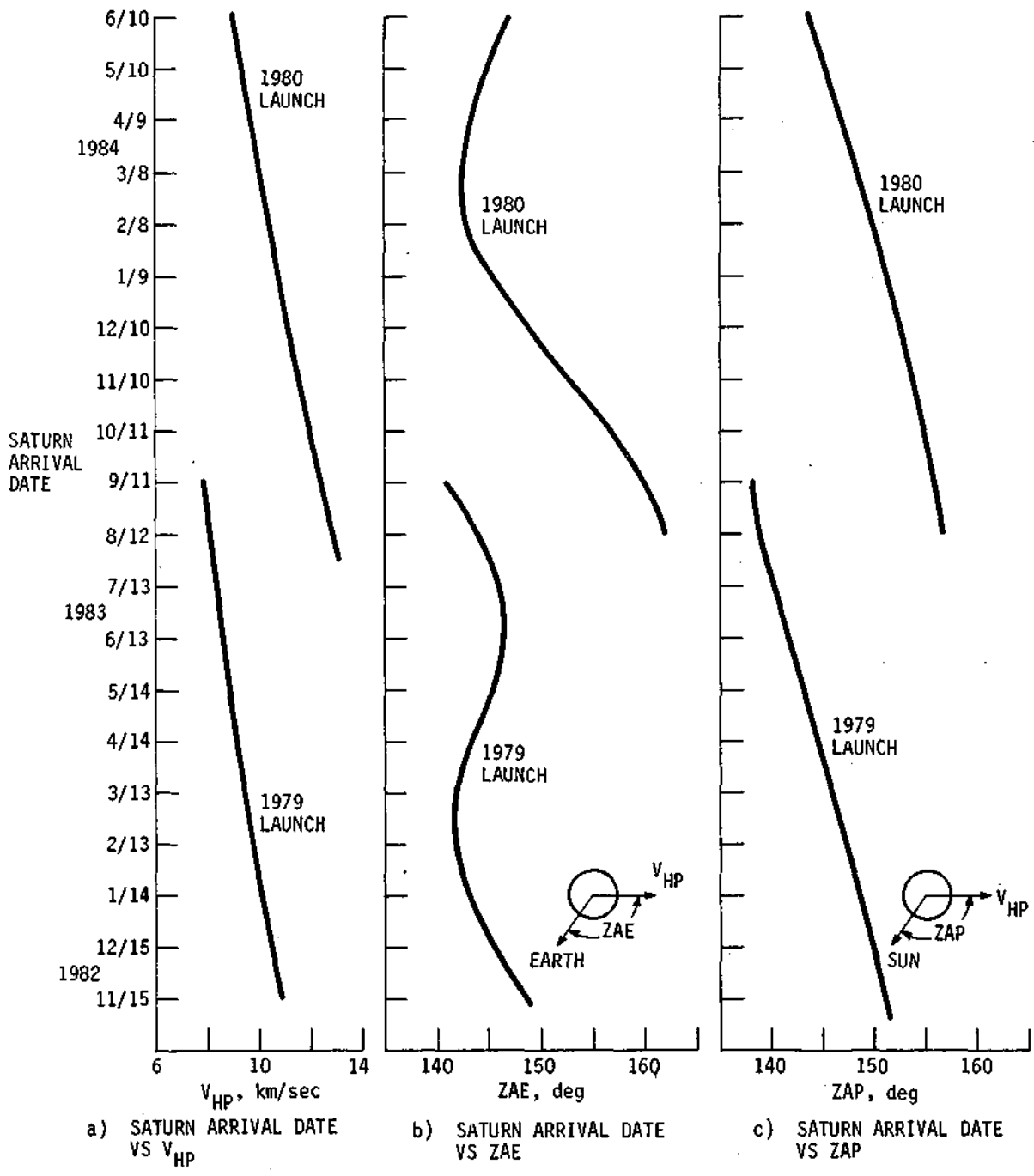


Fig. III-7 V_{HP} , ZAE, and ZAP Variations with Arrival Date

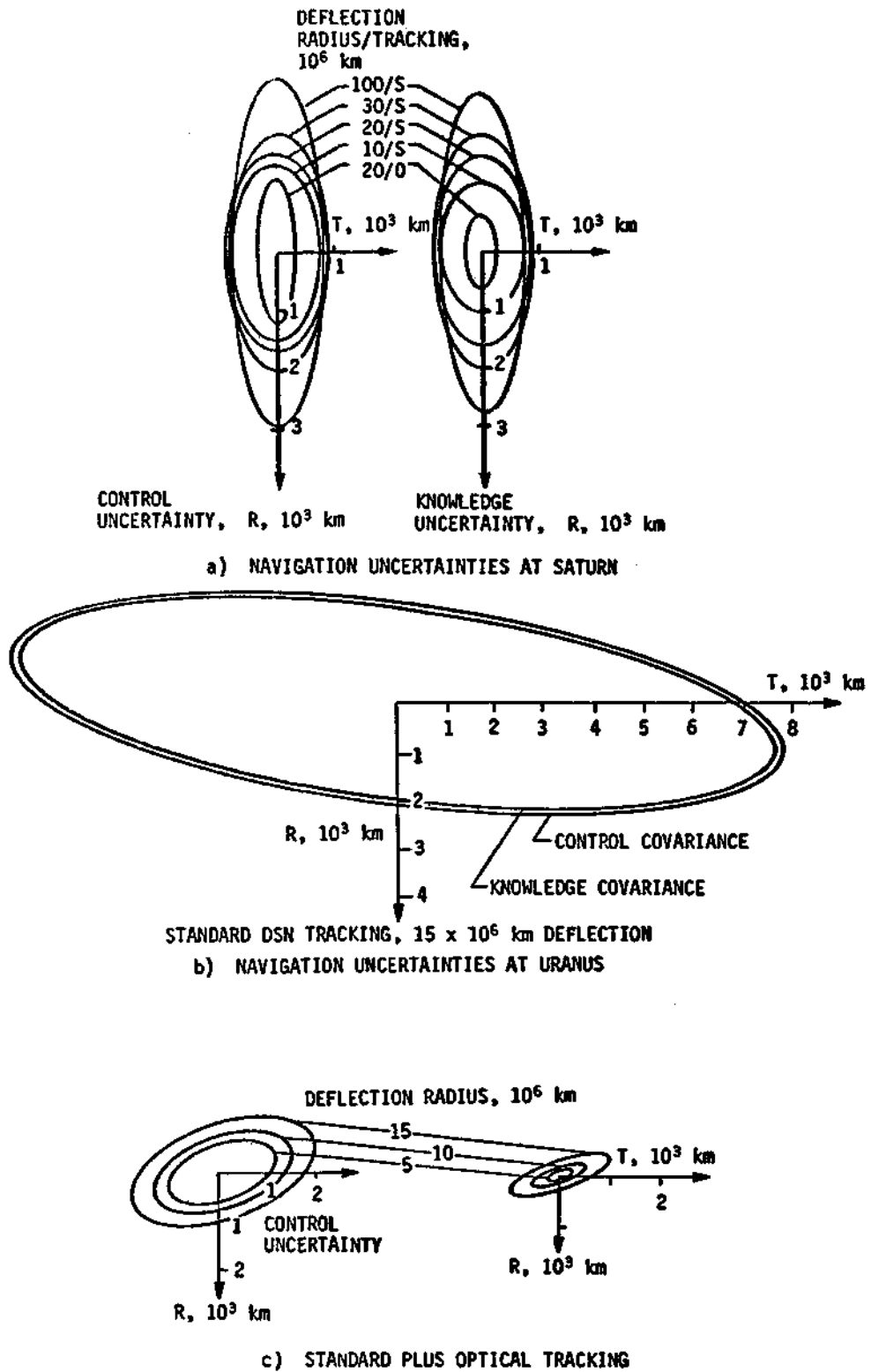


Fig. III-8 Navigation Uncertainties

Table III-4 Navigation Uncertainties at Saturn (1σ)

EPHEMERIS UNCERTAINTIES, 1σ			EQUIVALENT STATION LOCATION ERRORS, 1σ	MEASUREMENT NOISE, 1σ
	<u>SATURN</u>	<u>URANUS</u>	DISTANCE OFF SPIN AXIS, m	DOPPLER: 0.3 mm/sec (1-minute COUNT TIME)
IN-ORBIT, km	750	10,000	LONGITUDINAL DISTANCE, m	
RADIAL, km	750	10,000	Z-HEIGHT, m	
OUT-OF-PLANE, km	250	2,000	LONGITUDINAL CORRELATION	RANGE: 150 m OPTICAL: 10 arc-sec

A final midcourse maneuver was scheduled 13 days before the deflection maneuver. A 40-day tracking arc was used before initiating the midcourse maneuver. Standard tracking of 10 Doppler measurements/day plus one ranging measurement, and standard plus optical tracking that consisted of three star planet angles and one apparent planet diameter measurement per day, were evaluated for a range of different deflection radii. The S and O located between the knowledge and control ellipses in Figure III-8 refer to standard and standard plus optical tracking, respectively. Generally, standard tracking appears to be adequate at Saturn. The large ephemeris uncertainties of Uranus coupled with the large range (approximately 20 au from Earth) result in a requirement to supplement standard DSN tracking with optical measurements. The relatively minor degradation of the effectiveness of the orbit determination process at Saturn with standard tracking and Uranus with optical plus standard tracking as the deflection radius is increased, is demonstrated in Figure III-8.

The spacecraft-to-probe communications link is designed to accommodate realistic dispersion in the communication parameters. The spacecraft antenna beamwidth selection process is based on spacecraft look-direction dispersions. Figure III-9 displays the design mission look dispersions. Even though the knowledge and control covariances at Saturn and Uranus are approximately equal, the look-direction dispersions at Saturn are considerably (factor of two) larger than the dispersions at Uranus. This is explained by the respective geometries where the tail geometry yields smaller look dispersion than a side geometry. The Uranus approach approximates a side geometry, whereas the Saturn approach approximates a tail geometry.

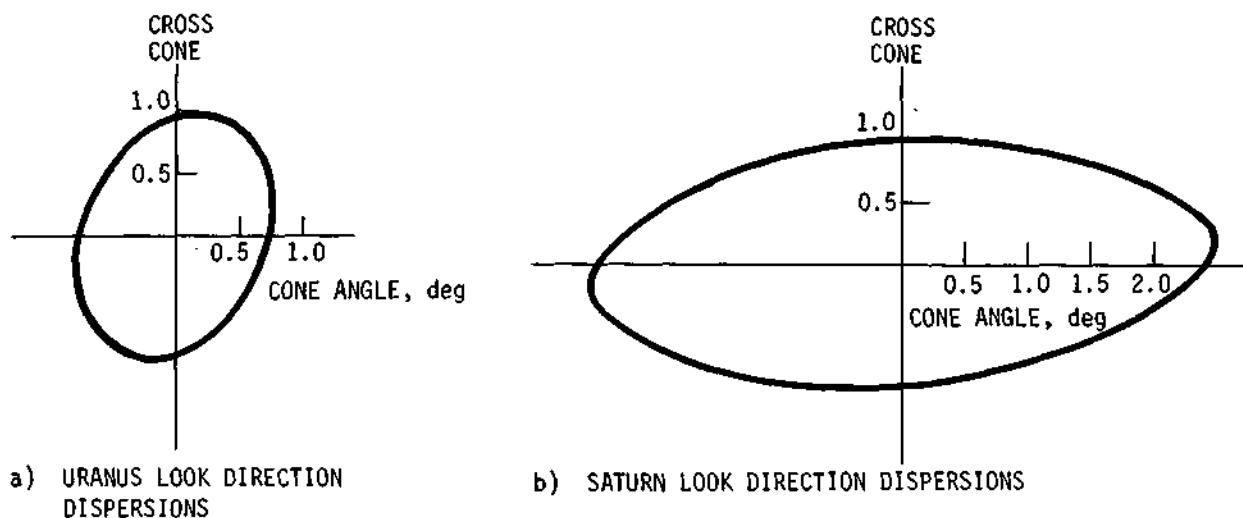


Fig. III-9 Saturn and Uranus Look Direction Dispersions

Dispersions in the probe entry parameters affect the design and operation of the probe itself. The science performance of the probe mission is affected by dispersion in entry site, entry angle, and entry angle of attack. The uncertainty in the time of entry is a critical factor in sequencing and probe power requirements. Dispersions in entry angle affect the structural requirements imposed on the probe since they impact probe thermal and aerodynamic considerations. Because the dispersions in most of these parameters are due solely to navigation uncertainties, Figures III-10, III-11 and Table III-5 present the entry dispersions used in the design of the three missions under consideration.

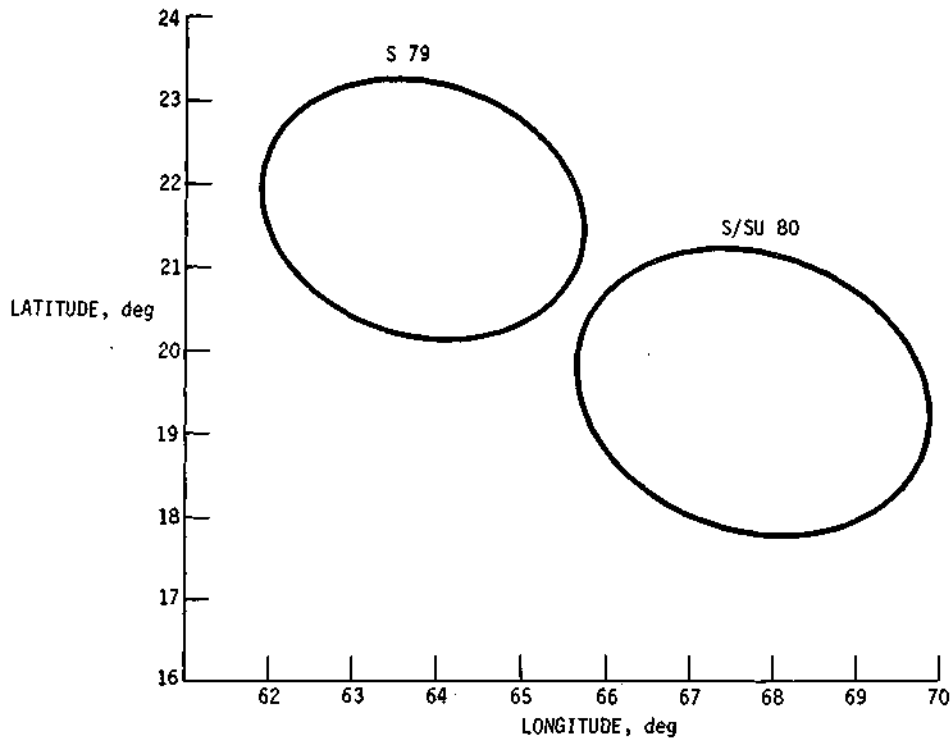


Fig. III-10 Saturn Entry Site Dispersions

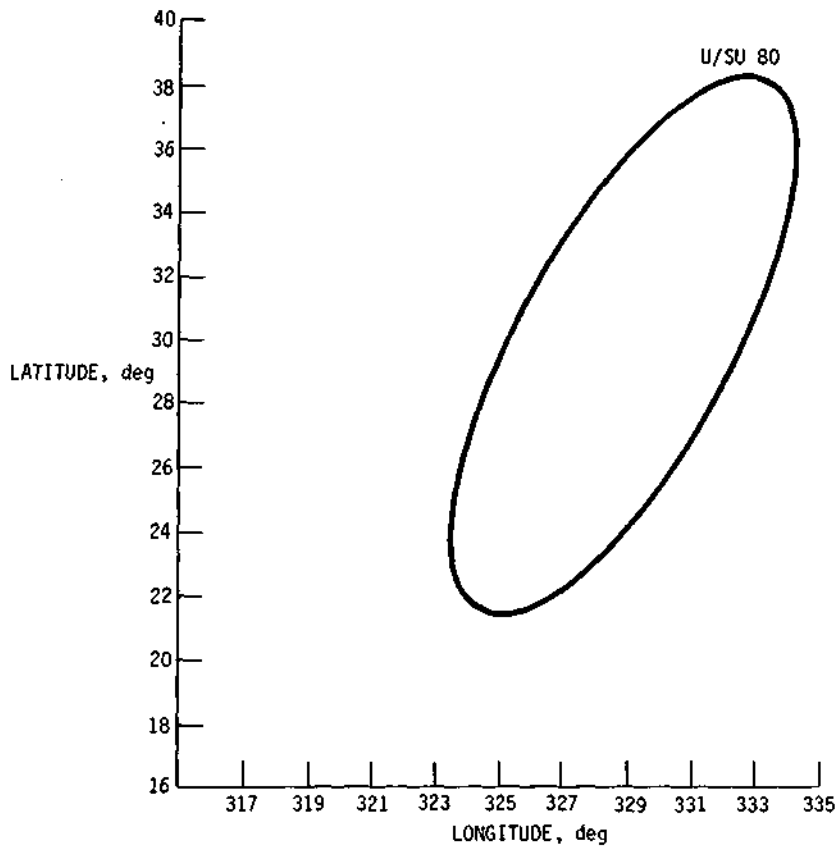


Fig. III-11 Uranus Entry Site Dispersions

Table III-5 Entry and Communication Parameter Dispersions

3 σ DISPERSIONS	S 79*	S/SU 80*	U/SU 80†
ENTRY ANGLE, deg	1.1	1.2	6.5
ANGLE OF ATTACK, deg	1.8	1.86	3.15
LEAD TIME, minutes	5.7	8.7	1.22
ENTRY TIME, minutes	4.4	4.4	28.9
PROBE ASPECT ANGLE, deg	3.3	2.59	1.17
RANGE, km	4200	5080	1240
DOPPLER VELOCITY, km/sec	1.01	0.935	0.43
DOPPLER RATE, m/sec ²	0.18	0.11	0.11
* DEFLECTION RADIUS = 30 x 10 ⁶ km.			
† DEFLECTION RADIUS = 10 x 10 ⁶ km.			

3. Planetary Encounter

The planetary encounter phase of the mission encompasses the deflection maneuver, acquisition, entry, and descent. The primary problems associated with planetary encounter include the design of the communication relay link, the selection of the approach trajectory, and the analysis of the deflection maneuver. The primary emphasis of the section will be to determine the selection of a common approach geometry for all three missions: Saturn 79, Saturn/SU 80, and Uranus/SU 80. Lesser emphasis will be placed on approach trajectory selection and the deflection maneuver. It was the intent of this study to determine a common range of spacecraft-to-probe look directions. Commonality of look directions results in a simplified spacecraft antenna design, eliminating the need for antenna gimbals on the spacecraft.

a. Design of the Relay Link - The key parameters associated with the relay link analysis are illustrated in Figure III-12. During the pre-entry phase, the probe is assumed to move on a conic trajectory in the attitude required at entry for zero relative angle of attack. During the entry phase, the probe rotates so its axis is radial relative to the center of the planet. During the descent phase, the probe is on a parachute descending along a radius vector as that vector rotates about the center of the planet at the angular rotation rate of the planet. Definitions of the relevant parameters follow.

NOTE: ϕ_E IS THE ANGLE THE PROBE ROTATES THROUGH IN GOING FROM THE PRE-ENTRY ATTITUDE TO THE DESCENT ATTITUDE.

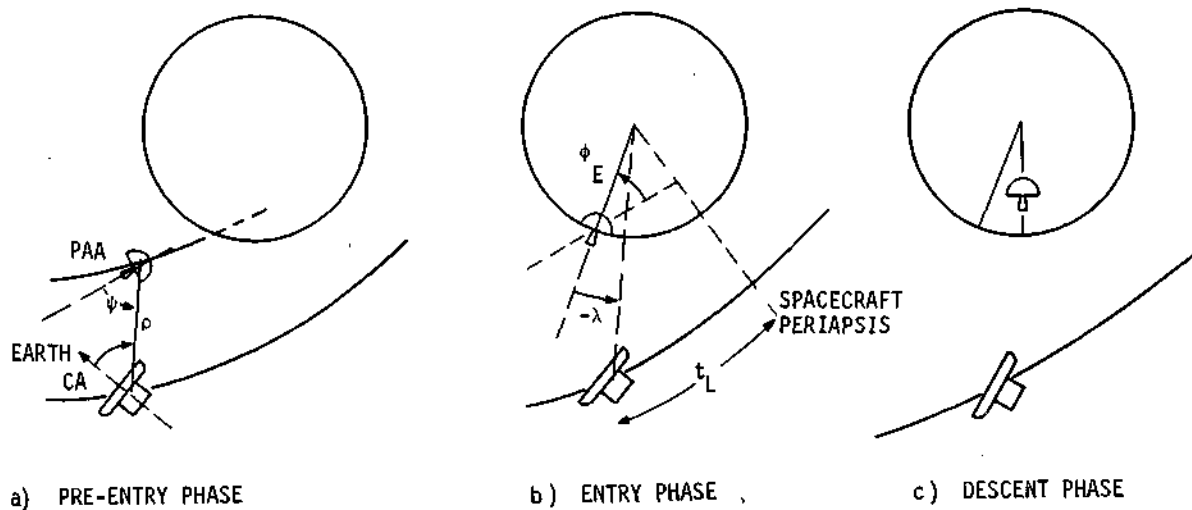


Fig. III-12 Relay Link Parameters

Probe Aspect Angle (PAA), ψ - The angle between the axis of the probe and the probe-to-spacecraft range. The PAA time history has a discontinuity at entry corresponding to the instantaneous rotation of the probe from pre-entry to descent attitude. The PAA would optimally be zero; practically, this is not possible. The larger the values of the PAA, the more power is required for the probe antenna.

Relay or Communication Range (ρ) - The distance between the probe and spacecraft. Optimally, this is held as small as possible.

Lead Angle (λ) - The angle between the spacecraft radius and the probe radius (projected into the spacecraft plane, if necessary) at entry. If negative, the probe leads the spacecraft at entry; if positive, the spacecraft leads.

Lead Time (t_L) - The time from entry to spacecraft periapsis passage. If t_L is positive (the usual case), entry occurs before the spacecraft has passed periapsis.

Cone Angle (CA) Clock Angle (CLA) - The CA and CLA are here referenced to Earth and Canopus. The CA is the angle included by the Earth-spacecraft-probe alignment; the CLA locates that direction relative to Canopus.

The selection of an effective communication geometry requires an iterative search. It was decided to first minimize the probe-to-spacecraft communication power for each of the missions under consideration. This was accomplished by targeting the spacecraft at the deflection maneuver for zero probe aspect angle at different times after descent. Four targeted trajectories corresponding to zero PAA at 5, 15, 30, and 45 minutes after entry were obtained. The nominal descent time for all three missions is approximately 44 minutes. A preliminary communication link analysis was then performed for all targeted trajectories and the minimum power case was selected as optimum. For the task one science complement, the mission determining the size of the probe transmitter was the Saturn/SU 80 mission and the resultant power was 17 watts. The increased power requirement for the Saturn/SU 80 mission relative to the Saturn/JS 77 mission was primarily a result of spacecraft-to-probe range at entry, which was 197,000 km. The range for the Saturn 1979 and Uranus/SU 80 missions was 108,000 km and 87,000 km, respectively.

The next phase in design of the relay link was to compromise each mission slightly to yield a common spacecraft-to-probe look geometry. Since the Saturn 1979 mission is a direct flight and there are no constraints on periapsis radius other than to avoid the rings, it is always possible to duplicate the Saturn/SU 80 geometry while simultaneously reducing the range. For this reason, in the subsequent discussions we shall only discuss commonality between the Saturn/SU 80 and Uranus/SU 80 missions.

The optimum Saturn/SU 80 mission had a cone and clock angle at entry of 109° and 256° , respectively, whereas the optimum Uranus/SU 80 mission resulted in $CA = 135^\circ$ and $CLA = 275^\circ$. By increasing the lead time at Saturn (and hence increasing range and PAA) and decreasing the lead time at Uranus, the differences between the respective cone angles at entry were reduced to less than 15° with $CA_{SAT} = 120^\circ$ and $CA_{URAN} = 131^\circ$. At Uranus, the approach trajectory was targeted to an inclination of 10° between the probe and spacecraft trajectory planes to minimize variations in the

PAA during the descent phase of the mission. A nonplanar deflection is desirable because the pole vector of Uranus is parallel to the ecliptic plane, resulting in probe motion during descent that is approximately perpendicular to the spacecraft trace.

To reduce the differences in clock angle at Saturn and Uranus, the deflection maneuver at Uranus was retargeted so that the inclination between the spacecraft and probe orbit planes at entry was reduced to zero. The planar deflection maneuver at Uranus had the effect of reducing the clock angle by 13° so that for the final design the difference in clock angle at Saturn and Uranus is less than 10° . This change had little effect on the cone angle.

At this point, it is interesting to point out the price that was paid to achieve Saturn and Uranus commonality. The primary criterion in determining link design effectiveness is transmitter power, and the driving mission which sizes transmitter power is Saturn/SU 80. As stated previously, the optimized Saturn/SU 80 link design resulted in a transmitter power of 17 watts. For the Saturn/SU 80 mission design to achieve commonality, this figure increased to 25 watts. Therefore, an increase of 8 watts was required to accommodate the common Saturn/Uranus link design.

Selection of Approach Trajectory - The selection of Saturn/SU 80 approach trajectory was determined primarily from launch energy considerations. Ideally, the optimum periapsis radius at Saturn to achieve effective rate matching is about $2.5 R_s$. However, the increase in launch energy to achieve the appropriate periapsis radius for rate matching was significant enough to preclude use of this trajectory and a compromise was reached. By increasing the periapsis radius to $R_p = 3.8 R_s$, the launch energy was reduced to a realistic value ($C_3 = 140 \text{ km}^2/\text{sec}^2$ for a 15-day launch period). The size of the probe transmitter design is determined by the Saturn/SU 80 mission. The approach trajectory selection for the 1979 Saturn direct and the Uranus/SU 80, while critical in the design of the communication link, is not constrained by the relationship between launch energy and periapsis radius. The Saturn 1979 approach was selected to have a periapsis radius of $R_p = 2.3 R_s$ which is the minimum value that will avoid the Saturn rings. The periapsis radius at Uranus was selected to be $R_p = 2.0 R_u$.

a. *Deflection Maneuver* - The spacecraft deflection mode was selected for each of the three missions analyzed primarily to reduce the complexity of the probe, since for this deflection scheme, the probe needs neither an attitude control system (ACS) nor a propulsion system. For a spacecraft deflection, the spacecraft trajectory is initially targeted to impact the entry site. The probe is spun up and the spacecraft is precessed so that the released probe has a zero angle of attack. The spacecraft is then deflected away from the planet to establish communication geometry and the required periapsis radius and Earth lock is reestablished.

Comparison of Deflection ΔV Requirements - Deflection ΔV requirements for a wide range of parametrics have been summarized in Volume II pages IV-31 through IV-34. The primary difference between the missions analyzed and reported in Volumes I, II, and III and those discussed in Volume IV is the deflection mode. With spacecraft deflection, greater emphasis should be placed on reducing deflection ΔV requirements. Since a ground rule of this study was to perform no new navigation work, previous navigation results were used.

The deflection radius used at Saturn and Uranus was 30×10^6 km and 10×10^6 km, respectively. These values were primarily determined as a result of availability of previous navigation results. A topic for future study would be the determination of the maximum possible deflection radius while still maintaining reasonable dispersions. It is probable that a reduction in spacecraft deflection ΔV from the present value of approximately 100 m/sec to 15 m/sec can be realized.

4. Planetary Entry

The critical phases of the probe mission are the pre-entry, entry, and descent phases. The entry phase is initiated when the probe first experiences effects of the sensible atmosphere and terminates with staging of the aeroshell. Typically, the aeroshell is staged at a subsonic velocity above a pressure level of 100 mb. Since entry is initiated at a particular pressure level and the pressure altitude profile is dependent upon atmosphere model, the altitude of entry is also dependent upon the atmosphere model. In all instances, altitudes are given above the 1-bar pressure level. For reference, the entry radius, pressure, and altitude of entry are displayed in Tables III-6 and III-7 for both Saturn and Uranus; all three (warm, nominal, and cool) atmosphere models are treated.

Table III-6 Saturn Model Atmosphere Entry
Parameter Definition

REFERENCE PARAMETER	SATURN ATMOSPHERE		
	WARM	NOMINAL	COOL
RADIUS AT 1.0 atm, km	59,735.6	59,805.9	59,863.4
ALTITUDE AT 1.0 atm, km	0.0	0.0	0.0
PRESSURE AT ENTRY, atm	1×10^{-7}	1×10^{-7}	1×10^{-7}
ENTRY ALTITUDE, km	568	366	227
ENTRY RADIUS, km	6030.6	60,171.9	60,090.4

Table III-7 Uranus Model Atmosphere Entry
Parameter Definition

REFERENCE PARAMETER	URANUS ATMOSPHERE		
	WARM	NOMINAL	COOL
RADIUS AT 1.0 atm, km	25,926.2	26,468	26,800
ALTITUDE AT 1.0 atm, km	0.0	0.0	0.0
PRESSURE AT ENTRY, atm	1×10^{-7}	1×10^{-7}	1×10^{-7}
ENTRY ALTITUDE, km	1073.8	532	200
ENTRY RADIUS, km	27,000	27,000	27,000

Typically, the entry phase of the mission lasts less than two minutes; however, it is during this phase of the mission that the probe experiences severe aerothermodynamic effects. These effects contribute in a significant manner to the sizing of the heat shield and structure. Sufficient ablative material must be available to withstand the heating encountered during entry; the structure must be sized to withstand peak decelerations.

a. Entry Ballistic Coefficient Selection - The primary considerations influencing the selection of the entry ballistic coefficient are staging conditions compatible with technology requirements and science objectives. It is desirable to commence science measurements above the 100 mb pressure level; aerodynamic considerations prefer a subsonic staging velocity. A parametric study was performed to investigate variations in staging conditions with entry angle, ballistic coefficient, and model atmosphere. The results of the study are displayed in Figures III-13 and III-14. On each figure, contours of altitude at which the prob's velocity is $M = 0.7$ for the particular ballistic coefficient indicated. Contours are displayed for the three atmospheric models and ballistic coefficients of 78.5, 157, and 235.5 kg/m². The altitude for each respective atmosphere that corresponds to the 100 mb pressure level is also indicated. Ideally, the ballistic coefficient should be as large as possible consistent with staging considerations. The worst case atmosphere with regard to entry ballistic coefficient is the cool atmosphere, and Saturn entry with entry angle of $\gamma = -30^\circ$ presents the most severe situation. To achieve desired staging conditions, the entry ballistic coefficient selected must be less than 78.5 kg/m². For consistency with previous work and also to ensure some degree of safety margin, an entry ballistic coefficient of 110 kg/m² was selected.

b. Entry Environment - The relationship between entry angle, model atmosphere, peak decelerations, maximum dynamic pressure, and their respective time profiles is shown in Figures III-15 through III-18.

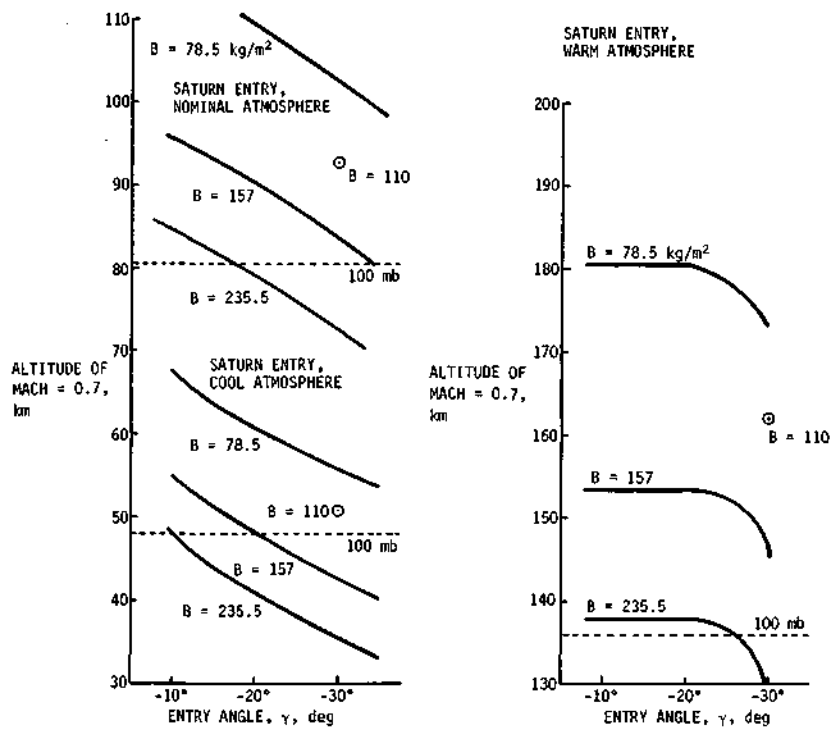


Fig. III-13 Deceleration to Subsonic Speeds at Saturn

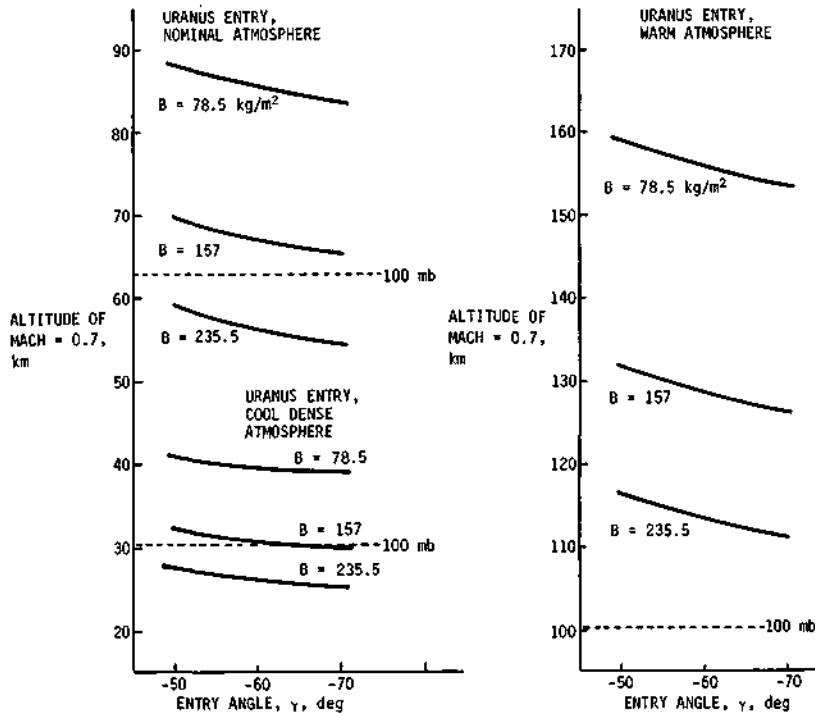


Fig. III-14 Deceleration to Subsonic Speeds at Uranus

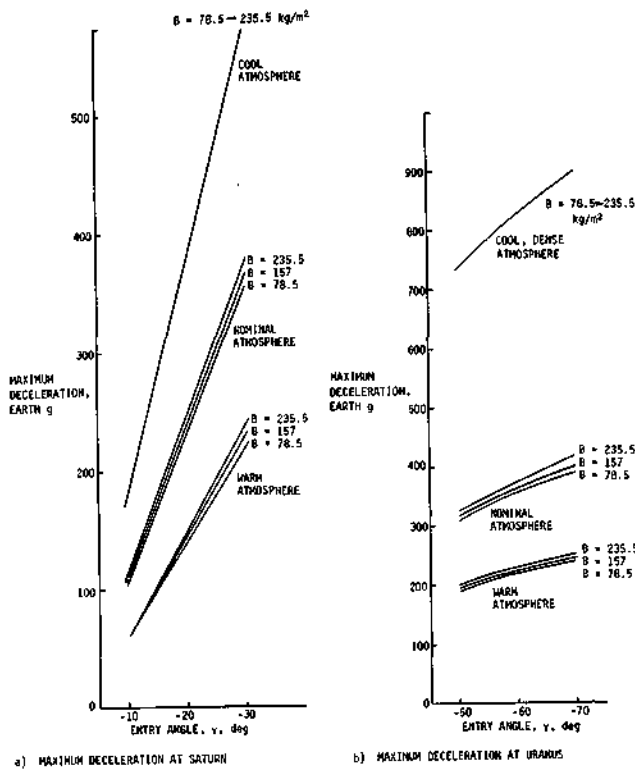


Fig. III-15 Maximum Deceleration at Saturn and Uranus vs Entry Angle

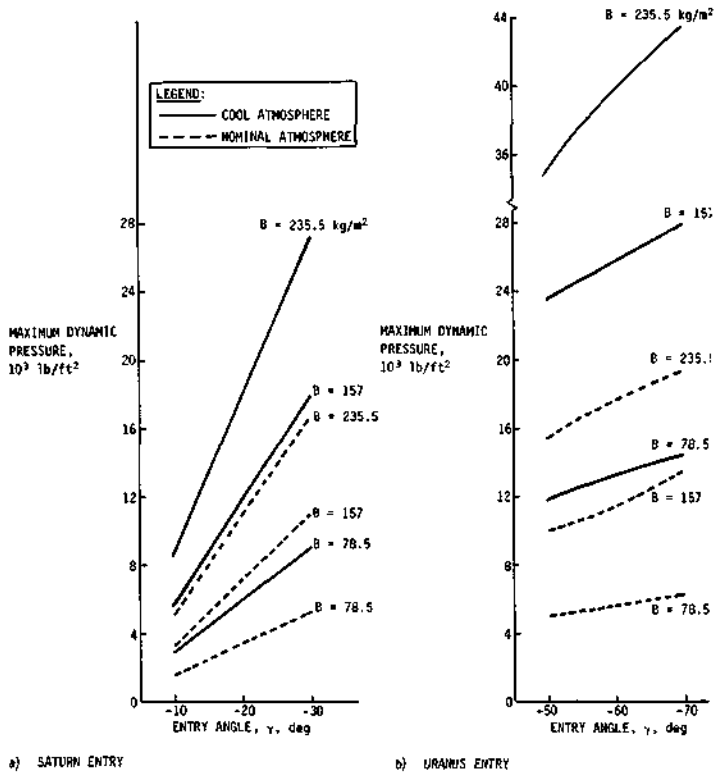


Fig. III-16 Maximum Dynamic Pressure at Saturn and Uranus vs Entry Angle

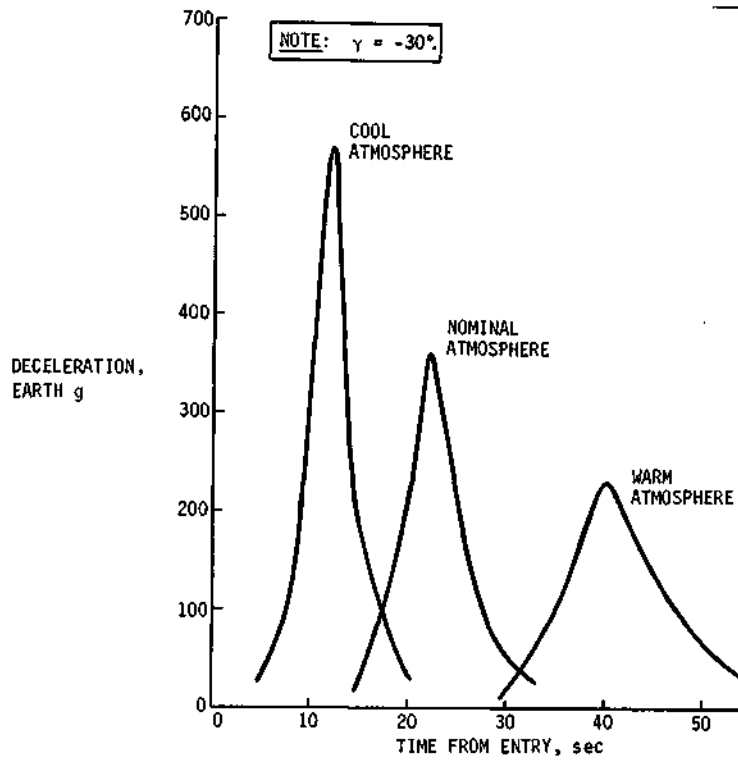


Fig. III-17 Saturn Deceleration Profile

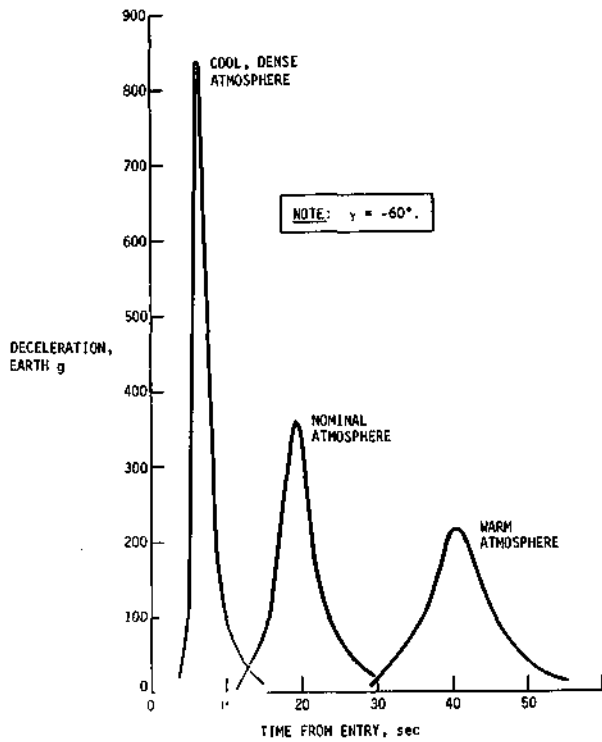


Fig. III-18 Uranus Deceleration Profile

Peak decelerations increase with increasing entry angle and are most severe for entries into the cool atmosphere. Results indicate that peak decelerations are relatively insensitive to changes in ballistic coefficient. Maximum dynamic pressure, however, is a direct function of ballistic coefficient. For a fixed ballistic coefficient, the time profiles of deceleration and dynamic pressure have a one-to-one correspondence. For this reason, time profiles of dynamic pressure were not included. Maximum decelerations are sensitive to model atmosphere. Analysis indicates (Figure III-15) that at Uranus for an entry angle of -60° , the nominal peak deceleration is 350 g; for entry into the cool atmosphere, this figure increases to 830 g. Maximum dynamic pressure follows a similar trend.

B. SCIENCE INVESTIGATIONS

1. Saturn/Uranus Atmospheric Models

In Chapter II of Volume II of this report, the model atmospheres used during the first part of the study were presented. They included the nominal models for both Saturn and Uranus as well as the models for Jupiter and Neptune. In this follow-on study, the cool and warm models for both Saturn and Uranus were used and are thus presented here along with the nominals for reference.

The models used were taken from NASA monographs given in References III-1 and III-2. Both of these models have been updated from those used in the first part of the study. Figures III-19 and III-20 present the pressure versus temperature profiles for each model atmosphere for Saturn and Uranus. At 10 bars, the temperature range is from 191°K to 424°K at Saturn and from 114°K to 300°K at Uranus.

Figures III-21 and III-22 connect pressure to altitude for each of the six models to aid in model description. The modeled clouds and their locations are shown in Figures III-19 and III-20 and tabulated in Table III-8. These are methane, ammonia, and water clouds, the last two existing in both solid and liquid phases in different models.

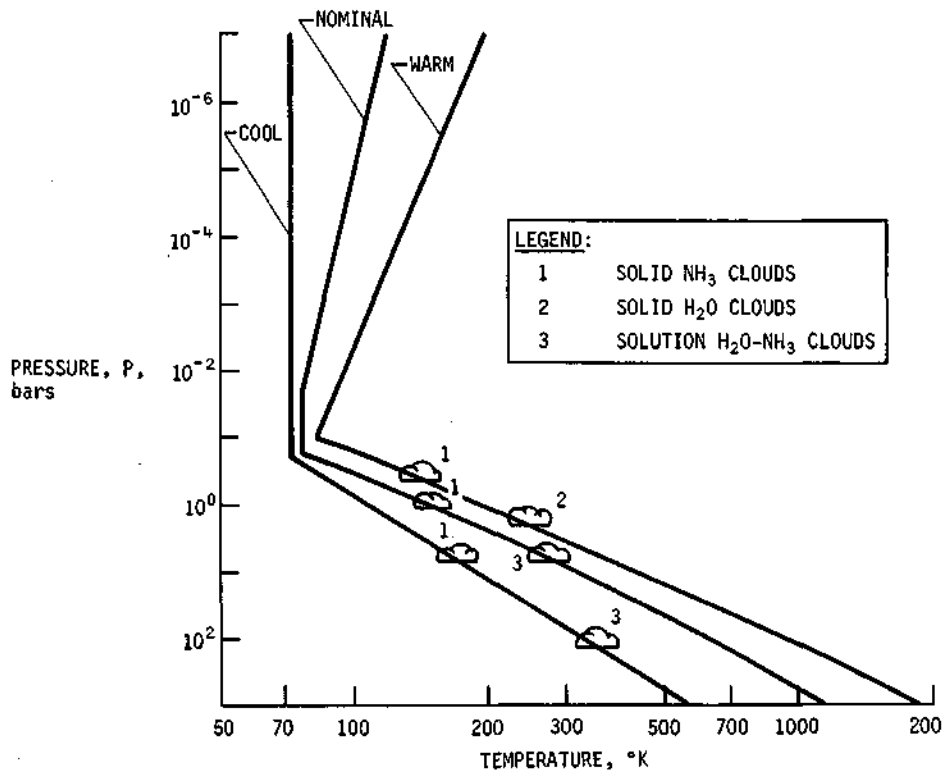


Fig. III-19 Pressure vs Temperature and Cloud Levels for Saturn Model Atmospheres

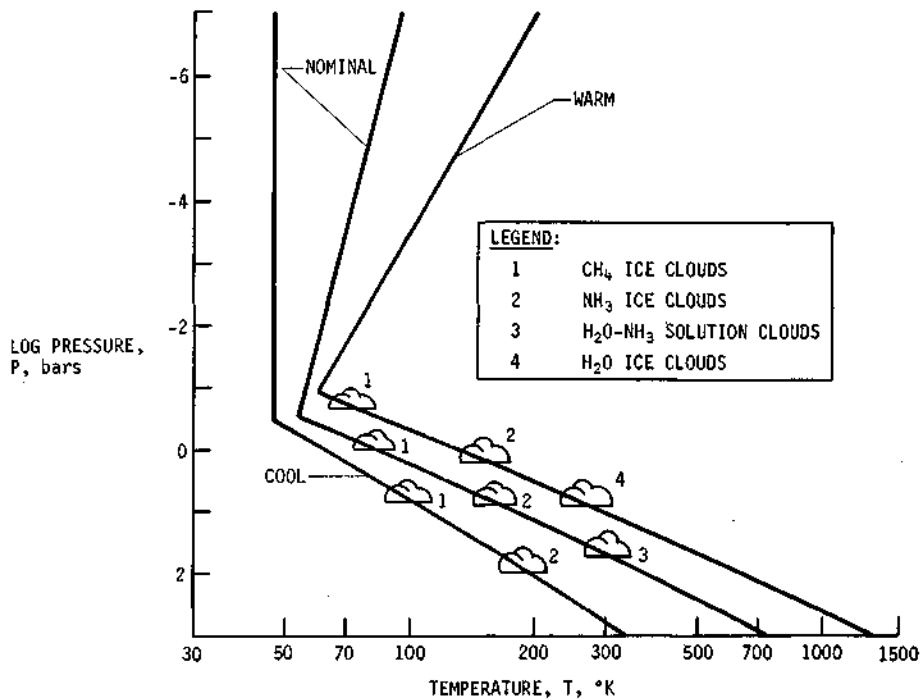


Fig. III-20 Pressure vs Temperature for Uranus Model Atmospheres

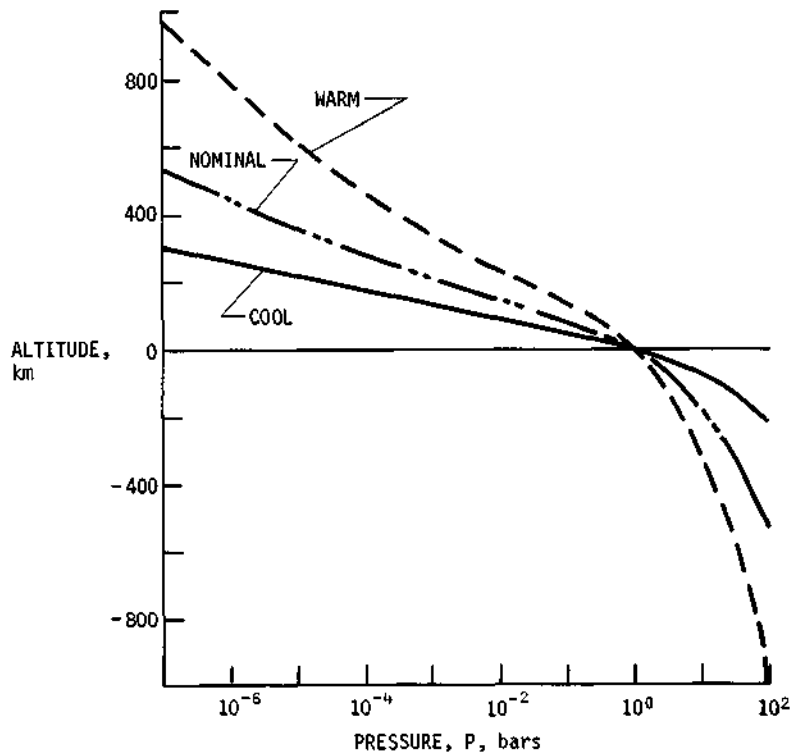


Fig. III-21 Pressure vs Altitude for Saturn Model Atmospheres

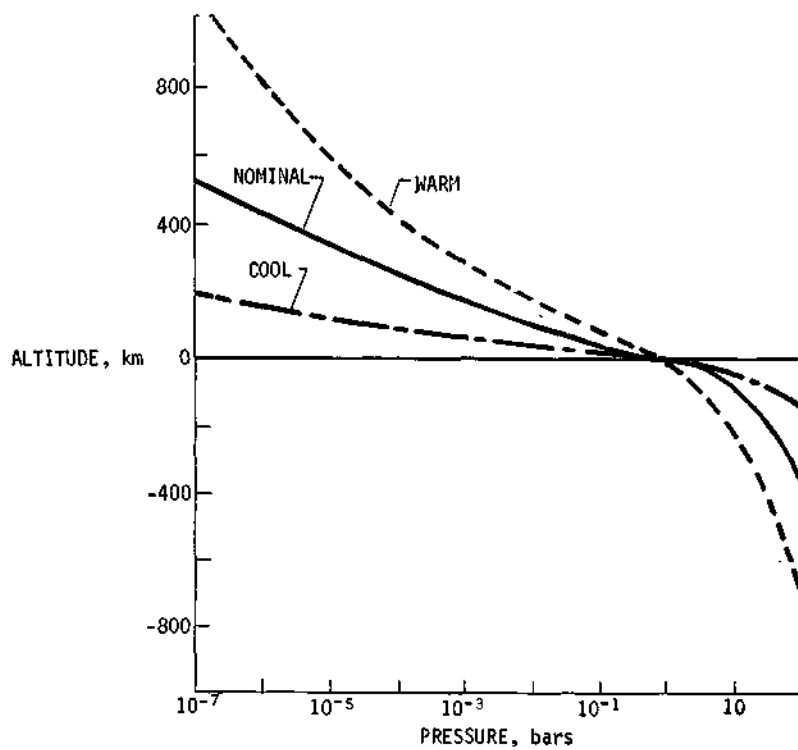


Fig. III-22 Pressure vs Altitude for Uranus Model Atmospheres

Table III-8 Saturn/Uranus Modeled Cloud Locations

ATMOSPHERE	CLOUD	PRESSURE, bar	
		CLOUD TOP	CLOUD BASE
SATURN			
COOL	NH ₃	3.00	6.34
COOL	H ₂ O	30.0	66.7
NOMINAL	NH ₃	0.727	1.12
NOMINAL	H ₂ O SOLUTION	3.94	6.92
WARM	NH ₃	0.262	0.425
WARM	H ₂ O	1.29	2.13
URANUS			
COOL	CH ₄	1.0	6.25
COOL	NH ₃	30.0	80.7
NOMINAL	CH ₄	0.49	0.93
NOMINAL	NH ₃	4.80	6.69
NOMINAL	H ₂ O SOLUTION	32.2	48.4
WARM	CH ₄	0.12	0.18
WARM	NH ₃	1.0	1.29
WARM	H ₂ O	4.71	6.80

2. Science Instrument Characteristics for Additional Instruments

The characteristics of the SAG Exploratory payload instruments were given in Section C of Chapter III of Volume II. The characteristics of those additional instruments, pre-entry and descent, that were included in the follow-on portion of the contract are included in the following paragraphs. Specifically, these are ion and neutral retarding potential analyzers, Langmuir probes, and a nephelometer.

Table III-9 relates these instruments to the measurements they are expected to perform. The descent portion, except for the nephelometer, was given in Table III-2 of Volume II, described in detail there, and is included here only for completeness. The additional nephelometer will search for condensing clouds and define their locations with respect to temperature and pressure, as a function of the density of the condensible gases.

Table III-9 Instruments Related to Measurements

MEASUREMENTS	INSTRUMENT*							
	LANGMUIR PROBES	IRPA	NRPA	TEMPERATURE GAGE	PRESSURE GAGE	ACCELEROMETERS	NEUTRAL MASS SPECTROMETER	NEPHELOMETER
PRE-ENTRY								
ION CONCENTRATION PROFILES	D	D	N					
NEUTRAL CONCENTRATION PROFILES	N	R	D					
ELECTRON DENSITY & TEMPERATURE	D	R	N					
ENTRY								
DECELERATION LOADS						D		
DESCENT								
H/He RATIO				R	R	R	D	N
ISOTOPIC RATIOS				N	N	N	D	N
MINOR CONSTITUENTS				R	R	N	D	R
ATMOSPHERIC TEMPERATURE				D	R	R	R	N
ATMOSPHERIC PRESSURE				R	D	R	R	N
CLOUD LOCATION/STRUCTURE				R	R	R	R	D
CLOUD COMPOSITION				R	R	R	D	R
ATMOSPHERIC TURBULENCE				R	R	R	N	R
*D = DIRECT MEASUREMENT; R = RELATED MEASUREMENT; N = LITTLE OR NO RELATION.								

The function of the three pre-entry instruments is to establish profiles of ion, electron, and neutral particle number densities, and electron temperatures as a function of altitude, through the ionosphere and upper atmosphere. This is accomplished before the probe's trajectory is significantly deviated from a free-space conic, and thus is prior to aerodynamic entry. This allows the pre-entry instruments to be mounted on the outside of the heat shield. They will cease to function and burn off shortly after entry.

The accelerometer triad measurements of deceleration loads during entry are indicated here to point out the distinction between the pre entry measurements and the descent turbulence measurements.

a. *Positive Ion Retarding Potential Analyzer (IRPA)* - The function of the IRPA is to establish the positive ion number density concentration profiles through the ionosphere as the probe descends in free molecular flow. The instrument has a range of 1 to 5 amu to include H_1^+ , H_2^+ , H_3^+ , He^+ , and HeH^+ . It will begin its operation at about 5000 km and take data for several minutes before passing through the turbopause where data will probably

cease due to grid wire burn-up. The sampling time for one complete measurement has been set at 2.0 seconds. Although this is not the minimum possible sampling time, it is a reasonable compromise between science data return and maximum allowable bit rate for entry velocities in the range being considered.

The characteristics of the instrument are shown in Table III-10. The total weight is 3.5 lb, the power requirement is 3 watts, and the nominal bit rate is 60 bps. The configuration of the instrument is shown in Figure III-23. It is circular with a conical entrance that has a vertex cone angle of 120° and has side vents to allow particles to flow through. The conical entrance reflects particles to the side to limit interference with incoming ions that would normally enter the aperture and be measured. The particle interference problem has been analyzed in Reference III-3 and the results used here.

The instrument is on the nose of the vehicle so that the aperture is forward of the stagnation point. This location minimizes particle reflection from the probe body and other instruments, which could interfere with incoming particles. This design resulted from References III-3 and III-4.

The aperture is circular and approximately 5 cm^2 in area; below it is a grid of 1-mil wire grounded to probe surface potential. Ions enter and are retarded by a second set of grids successively varied from -3 to 63 volts in 5.5-volt steps. The ion then passes through a third grid biased at about -20 volts and collected on a plate at about -5 volts. The purpose of the last grid is to suppress emission of secondary electrons from the collector. As voltages are varied, corresponding current values resulting from collection of various positive ions are measured and telemetered back to be coupled with the present voltage values, to establish a current-voltage (I-V) curve from which density, temperature, composition, and potential can be derived.

To obtain ion density and composition, only one current value per mass number is necessary. However, there is danger of missing a step if voltage step size equals voltage per mass number, which is about 12 v/amu; two measurements per step gives better determination of step level and length. Thus, for the 1 to 5-amu range, voltage step size has been set at the previously mentioned 5.5-volt value for the 66-volt sweep. This gives twelve current values to be sent back, and, assuming a 10-bit word at the 2.0-second sampling time, gives 60 bps.

Table III-10 IRPA Characteristics

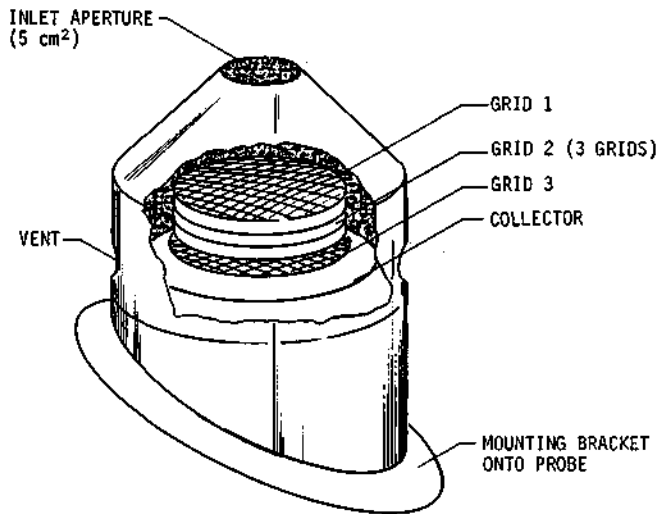
1. WEIGHT - SENSOR = 0.23 kg (0.5 lb), ELECTRONICS = 1.36 kg (3 lb),
TOTAL = 1.59 kg (3.5 lb)
2. SENSOR SIZE - 10 x 10 x 4 cm
3. SENSOR VOLUME = 400 cm³, TOTAL PACKAGE = 2200 cm³
4. MAXIMUM POWER REQUIRED - 3 w
5. WARMUP TIMES - 15 TO 30 sec
6. SAMPLING INTERVAL* - 0.5 TO 5 sec
7. DATA BITS PER SAMPLE - 120
8. DATA BIT RATE - 24 TO 240 bps
9. TEMPERATURE LIMITS - -30 TO 1000°C
10. HEAT DISSIPATED - 3 w
11. ONBOARD PROCESSING REQUIRED[†] - NOMINALLY, NO; YES FOR ION TEMPERATURES
12. OPERATIONAL ALTITUDES - 5000 km TO TURBOPAUSE (~530 km)
13. SENSITIVITY - 10 ion/cm³ → 5 ion/cm³ BY 1975
14. EXTERNAL LOCATION - ON SIDE OF PROBE FORWARD SECTION, TO BE IN LINE WITH
STAGNATION POINT, OR ON NOSE AHEAD OF STAGNATION POINT
15. ORIENTATION & POINTING - APERTURE NORMAL TO INCOMING FLUX, AND PERPEN-
DICULAR TO FLIGHT VELOCITY VECTOR
16. OTHER REQUIREMENTS - CONICAL ENTRANCE CONE AND VENTED SIDE PLATES

*TWELVE SAMPLE POINTS REQUIRED, BASED ON A 5.5-v STEP SIZE (1- TO 5-amu RANGE).

[†]FOR A MISSION THAT INCLUDES AN ONBOARD ION TEMPERATURE PROCESSOR, ADD 0.5 lb TO ELECTRONICS WEIGHT. THE DATA BIT RATE WILL NOT BE LARGER THAN THE NOMINAL VALUE GIVEN HERE.

If ion temperature is to be determined, the I-V curve must be detailed enough to accurately define the sharp drop corresponding to a given ion mass number. For ion temperatures expected, the number of data points needed to define the curve will be excessive for the telemetry system. Therefore, onboard data processing will be necessary. The electronics will be more complicated than those necessary to determine ion composition and density alone, and the corresponding weight increase has been estimated to be a half pound. However, overall bit rate could be slightly less because the output to be telemetered is now processed, and therefore condensed.

This instrument is state-of-the-art flight hardware, and except perhaps for some development for the onboard temperature processor, will cause no major development problems.



RPA ELEMENT	POTENTIAL RELATIVE TO PROBE GROUND
GRID 1	0 v
GRID 2	VARIABLE RETARDING VOLTAGE (-3 TO 63 v IN 5.5-v STEPS)
GRID 3	-20 v (TO EXCLUDE ELECTRON COLLECTION & SUPPRESS EMISSION OF SECONDARY ELECTRONS FROM COLLECTOR)
COLLECTOR	-5 v

Fig. III-23 Ion Retarding Potential Analyzer

b. *Neutral-Particle Retarding Potential Analyzer (NRPA)* - The NRPA establishes neutral-particle number density concentration profiles through the upper atmosphere as the probe flow field goes from free molecular into the transitional region. The instrument range is 1 to 20 amu, looking primarily for H, H₂, and He, but wide enough to detect compounds like CH₄, NH₃, and H₂O. The NRPA will begin operation nominally at about 5000 km altitude and take data until communications blackout or until the grid wires burn up. The sampling time for one complete measurement has been set at 3.0 seconds. Although this is not the minimum possible sampling time, it is a reasonable compromise between data return and maximum bit rate allowable.

Instrument characteristics are shown in Table III-11. Power required for the NRPA is greater than for the IRPA, primarily because an ionizing beam is required. The bit rate is larger because of the extended sweep range.

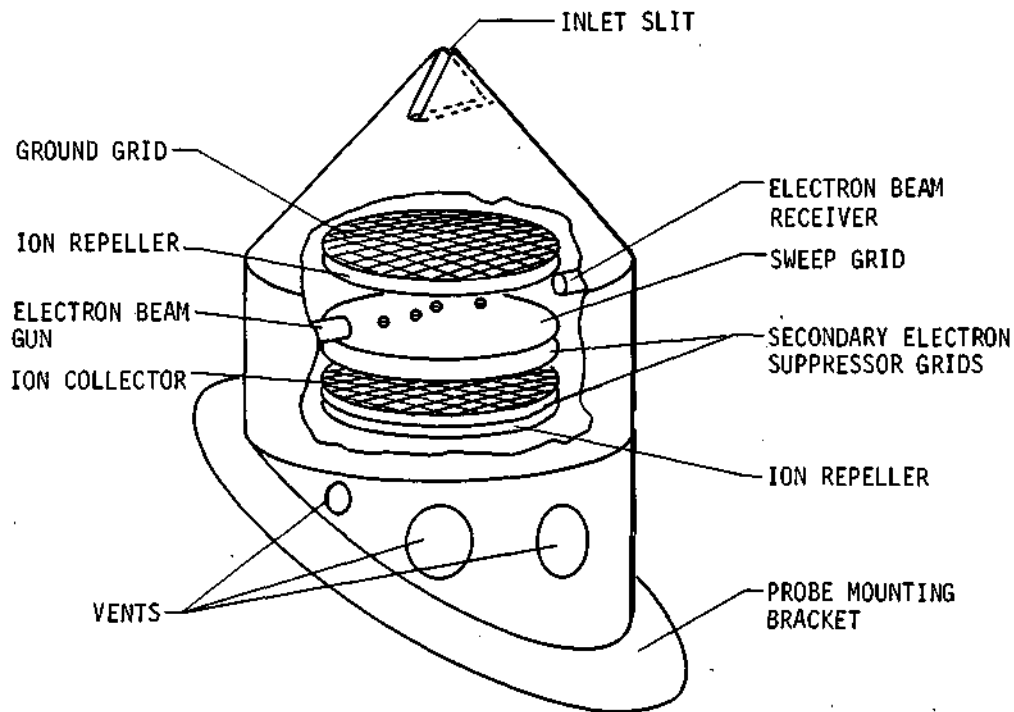
Table III-11 NRPA Characteristics

1. WEIGHT - SENSOR = 0.45 kg (1 lb), ELECTRONICS = 1.82 kg (4 lb),
TOTAL = 2.27 kg (5 lb)
2. SIZE - SENSOR = 10 x 10 x 4 cm, ELECTRONICS + SENSOR = 25 x 10 x 10 cm
3. VOLUME - SENSOR = 400 cm³, TOTAL PACKAGE = 2500 cm³
4. POWER REQUIRED - 5 w
5. WARMUP TIME - 30 sec
6. SAMPLING INTERVAL* - 1 TO 5 sec
7. DATA BITS PER SAMPLE - 280
8. DATA BIT RATE - 56 TO 280 bps
9. TEMPERATURE LIMITS - -30 TO 1000°C
10. HEAT DISSIPATED - 5 w
11. ONBOARD PROCESSING REQUIRED[†] - NOMINALLY, NO; YES FOR NEUTRAL-
PARTICLE TEMPERATURES
12. OPERATIONAL ALTITUDES - 5000 km TO TURBOPAUSE (~530 km)
13. SENSITIVITY - 10⁵ particles/cm³ → 10⁴ particles/cm³ BY 1975
14. EXTERNAL LOCATION - SAME AS IRPA
15. PROTECTION REQUIRED - FOR PROTECTION AGAINST CONTAMINANTS, ENTRANCE &
EXIT VENTS ARE COVERED AND VACUUM-SEALED UNTIL
AFTER PROBE SEPARATION
16. ORIENTATION & POINTING - APERTURE NORMAL TO INCOMING FLUX, AND PERPEN-
DICULAR TO FLIGHT VELOCITY VECTOR
17. OTHER REQUIREMENTS - CONICAL ENTRANCE CONE AND VENT IN BOTTOM

* TWENTY-EIGHT SAMPLE POINTS, BASED ON A BIAS VOLTAGE STEP SIZE OF 10 v (1- TO 20-amu RANGE).

[†] FOR A MISSION THAT INCLUDES AN ONBOARD NEUTRAL-PARTICLE TEMPERATURE PROCESSOR, ADD 0.5 lb TO ELECTRONICS WEIGHT. THE DATA BIT RATE WILL NOT BE GREATER THAN THE NOMINAL VALUE GIVEN HERE.

The configuration of the instrument is shown in Figure III-24. It is basically the same in shape and location as the IRPA. The conical entrance is designed with a vertex cone angle of only 90° to lessen interference with heavier neutral particles and because the distribution inside the instrument is not as critical. This instrument is vented at the back to allow greater flow because it operates generally in a denser portion of the atmosphere. The position of the NRPA is symmetrical to that of the IRPA on the opposite side of the probe centerline with its aperture ahead of the stagnation point.



RPA ELEMENT	POTENTIAL RELATIVE TO GROUND
ION REPELLER	300 v
BEAM RECEIVER ANODE	0 v
SWEEP GRID	0 TO 280 v
SECONDARY ELECTRON SUPPRESSOR GRID	-300 v

Fig. III-24 Neutral Retarding Potential Analyzer

The rectangular aperture is about 5 cm² with the long axis parallel to the direction of an ionizing beam inside the sensor. Below the inlet is a ground grid of 1-mil wire at zero relative potential to the probe surface. Inside are two grids charged at +300 and -300 volts to prevent all charged particles from getting inside the instrument, allowing only neutrals to enter. The electron beam gun ionizes the neutrals, which are subsequently retarded and collected as in the IRPA.

To correspond to the range of from 1 to 20 amu, the retarding sweep voltage varies from 0 to 280 volts. The steps on the resulting I-V curve will be a little greater than 13 v/amu. Only one current value per mass number is allowed because of the greater amount of data and the limitations on bit rate. However, again there is danger of missing a step (mass number) if the voltage step size equals 13 v/amu. Thus, for this study, 10 volts was chosen for the step size. One sample or sweep then consists of 28 words. With a 10-bit word and a 3.0-second sampling time, the nominal bit rate for the NRPA is 93.3 bps.

If the neutral-particle temperature is to be determined, the I-V curve must be detailed enough to accurately define the sharp drop corresponding to a given mass number. For particle temperatures expected, the number of data points needed to define the curve will be excessive for the telemetry system. Therefore, onboard data processing will be necessary to determine composition and density alone, and the corresponding weight increase has been estimated to be 0.5 lb. However, overall bit rate could be slightly less because the output is now processed, and therefore condensed.

This instrument is not state-of-the-art flight hardware, and will require considerable development, although the technology gained from the operational IRPA is applicable.

c. *Langmuir Probe (Electron Temperature/Density Probe)* - Two Langmuir probes are required to establish the electron number density concentration profiles and electron temperature profiles as the vehicle descends through the ionosphere in free molecular flow. The probe will begin operation at 5000 km and take data until near the turbopause. Sampling time for one complete measurement, including onboard processing, has been set at 0.5 second, which is not the fastest possible time, but is a reasonable compromise between data return and limiting bit rates.

Characteristics of the instrument are shown in Table III-12. Only one set of electronics is required for both probes and it weighs 1.36 kg (3 lb) and requires 3 watts to operate.

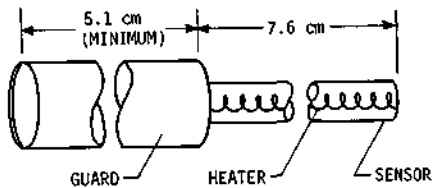
The configuration and location of the instruments are shown in Figure III-25. The guards protrude from the nose of the vehicle, roughly 90° from the RPA locations. The sensor is a 7.6-cm (3-in.) long hollow tube, 0.158 cm (1/16 in.) OD. Electrical heaters are included in the hollow tube and heated to 500°C for 10 minutes before use. The purpose of heating the probe is to remove all contaminant particles that have been collected on the sensor from launch operations, outgassing during cruise, or fuel deposits from engine firings. The probe needs a 2-minute warm-up time and no longer than 2-minutes cooling time before taking measurements; it does not have to reach ambient temperature before use. The suggested best time for performing this operation is after separation and a few hours before entry, but it could be done before separation from spacecraft power, if the separation is clean. Even a cold gas system could cause a problem; thus, any spacecraft engine firings should be performed after the probe has drifted away from the spacecraft. Power required for each heater filament is about 2.5 watts for the 10-minute period, plus a 2-minute warmup transient.

From discussions with Dr. L. H. Brace of NASA-GSFC, one Langmuir probe is perpendicular to the flight velocity vector, has a constant voltage applied, and measures the electron current as it varies with the descent altitude. These measurements are processed onboard to yield the electron number density. The other probe is fixed so that the sensor is parallel to the flight velocity vector and has variable voltage applied. When this variable voltage is high and negative, the Langmuir probe measures the ion current, which is processed onboard to give ion number density. As the voltage is swept from negative to positive, current readings are taken to obtain the slope of the I-V curve. After further onboard processing, the electron temperature is obtained.

Table III-12 Langmuir Probe Characteristics

1.	WEIGHT - SENSOR = NEGLIGIBLE, ELECTRONICS = 1.36 kg (3 lb)
2.	SIZE - SENSOR = 7.6 cm (3 in.) LONG BY 0.16 cm (0.0625 in.) IN DIAMETER ELECTRONICS = 5 x 15 x 15 cm (2 x 6 x 6 in.)
3.	VOLUME - 1200 cm ³ (SENSOR IS HOLLOW TUBE)
4.	POWER REQUIRED - 3 w (2 w BY 1975); HEATER POWER = 5 w FOR 12 minutes BEFORE ENTRY
5.	WARMUP TIME - 12 minutes (INCLUDING DECONTAMINATION)
6.	NOMINAL SAMPLING INTERVAL* - 0.5 sec
7.	DATA BITS PER SAMPLE* - 30
8.	NOMINAL DATA BIT RATE - 60 bps
9.	SENSOR TEMPERATURE LIMITS - -100 TO 700°C
10.	HEAT DISSIPATED - 3 w
11.	ONBOARD PROCESSING REQUIRED - YES*
12.	OPERATIONAL ALTITUDE - 5000 km TO TURBOPAUSE (~530 km)
13.	SENSITIVITY - 10 ¹ TO 10 ⁷ cm ⁻³ , 200 to 20,000°K (e ⁻ temp)
14.	ORIENTATION & POINTING - ONE SENSOR NORMAL TO AND ONE PARALLEL TO FLIGHT VELOCITY VECTOR

* ABOUT 30 CURRENT MEASUREMENTS ARE OBTAINED FROM ONE VOLTAGE SWEEP. AFTER ON-BOARD PROCESSING, THE NOMINAL THREE WORDS OF INFORMATION TELEMETERED BACK ARE THE ELECTRON NUMBER DENSITY, ION NUMBER DENSITY, AND ELECTRON TEMPERATURE. HOWEVER, AS AN OPTION, THE ENTIRE 30 CURRENT MEASUREMENTS COULD BE SENT BACK FROM EVERY 30th VOLTAGE SWEEP BY ADDING A FOURTH WORD OF PRESTORED CURRENT DATA TO BE TELEMETERED EVERY SAMPLE.



LANGMUIR PROBE

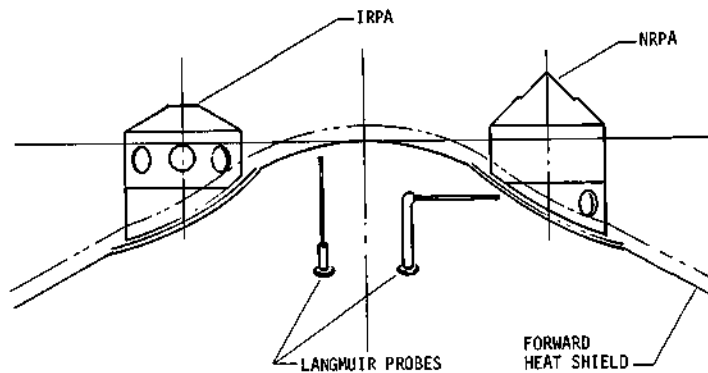


Fig. III-25 Langmuir Probe and RPA Location

The primary reasons for aligning the variable-voltage sensor parallel to the velocity vector are to (1) substantially reduce extraneous voltage induced by the planetary magnetic field as the probe moves through it; (2) keep the distribution of potential along the sensor length even; and (3) prevent translational energy of the probe from interfering with particle thermal energy measurements. This orientation is sensitive to angle of attack, the limit being about $\pm 5^\circ$.

The nominal data telemetered consists of three 10-bit words, all processed onboard--electron number density, ion number density, and electron temperature. With the half-second sampling time, the nominal bit rate is 60 bps; however, as an optional verification of the accuracy of the data, one complete set of current readings (30) along a voltage sweep could be sent back every 30th sample by adding a fourth word (current) to the data from a storage unit. This would increase the data rate to 80 bps.

The Langmuir probe and all of its electronic equipment have been flown on Earth-orbital missions, and as such, are all state of the art.

d. Nephelometer - This instrument is the sole addition to the descent payload given in Section C of Chapter III of Volume II. It is added to the payload for the purpose of better defining the location and density of the aerosol cloud formations. It will operate from the initial sequencing of descent instruments, after the parachute is deployed, until the end of the mission. The characteristics used for probe integration design are given in Table III-13 and the configuration and location of the sensor is shown in Figure III-26. It is composed of a He/Ne laser light source that emits a fine beam through a window in the descent capsule. The amount of the beam reflected is a function of the density, albedo, and size of the particles. The fraction that is reflected back through the window is diverted by optics into a photomultiplier that yields an intensity reading.

A sampling time of 3.0 seconds has been selected to ensure nephelometer readings of better than one per kilometer below 100 millibars; the instrument is capable of sampling at a faster rate but at the expense of a higher bit rate. The nominal bit rate based upon one 10-bit intensity word every 3.0 seconds is 3.33 bps. The components of this system are all currently available and are being proposed for use on Venus probes. No development will be necessary.

Table III-13 Nephelometer Characteristics

1.	WEIGHT - SENSOR = 0.45 kg (1 lb), ELECTRONICS = 0.68 kg (1.5 lb)
2.	SENSOR SIZE = 5.1 x 6.3 x ~12.7 cm
3.	VOLUME - SENSOR = 410 cm ³ (~25 in. ³), ELECTRONICS = 902 cm ³
4.	POWER REQUIRED - 3 w
5.	WARMUP TIMES - ~5 sec
6.	SAMPLING INTERVAL - 1 TO 5 sec (NOMINAL = 3 sec)
7.	DATA BITS PER SAMPLE - 10
8.	DATA BIT RATE - 2 TO 10 bps
9.	OPERATIONAL TEMPERATURE LIMITS - 240 TO 325°K
10.	HEAT DISSIPATED - 3 w
11.	ONBOARD PROCESSING REQUIRED - NO
12.	OPERATIONAL PRESSURES - 100 mb TO DESIGN LIMIT
13.	SENSITIVITY - 10 ⁴ photons/measurement
14.	LOCATION & ORIENTATION - ORIENT SENSOR SUCH THAT LOOK DIRECTION IS TO THE SIDE OF THE PROBE AND APPROXIMATELY HORIZONTAL

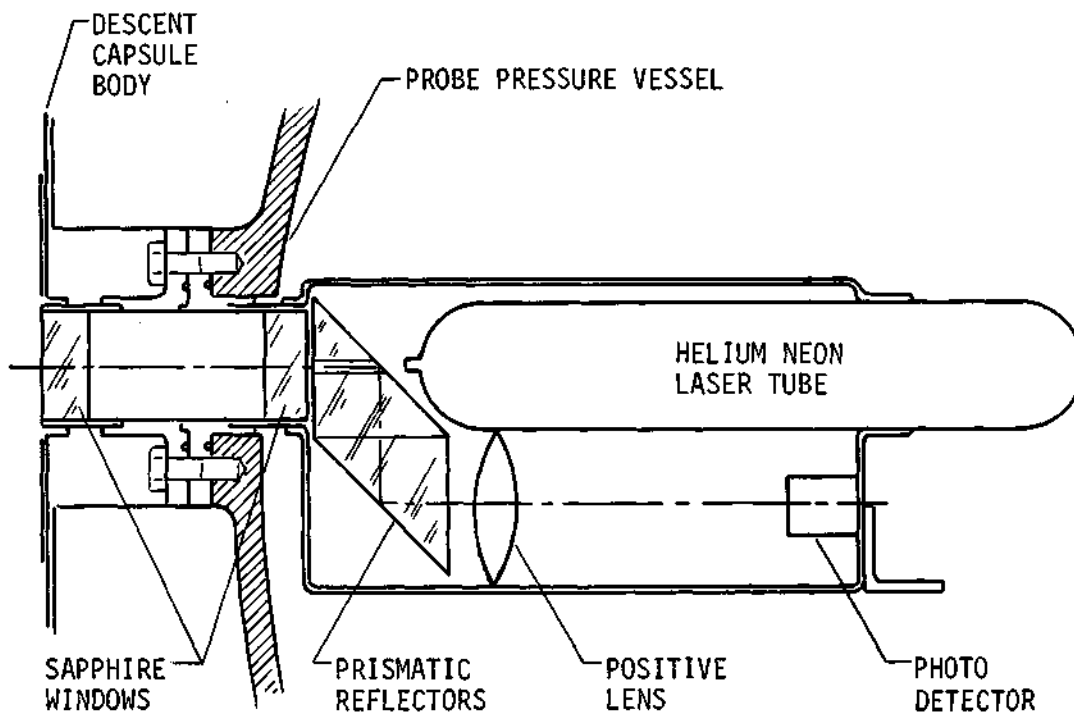


Fig. III-26 Descent Side-Looking Nephelometer

3. Science Mission Analysis and Data Collection

a. Science Event Sequence Profile (Expanded Payload) - The sequence of science events is approximately the same for all Saturn and Uranus model atmospheres, with the time of occurrence for the same events varying slightly. Heater coils inside the Langmuir probes are turned on before the other instruments to decontaminate the sensor. This occurs from 20 to 45 minutes before entry depending upon trajectory uncertainties.

The Langmuir probes begin operation no later than 5000 km altitude and the RPAs 20 seconds (~600 km) later. The probes begin transmission of real-time data to the spacecraft upon detection of nonzero (or threshold) data. If it is desired to store the data for delayed transmission during descent, both the Langmuir probes and IRPA are also monitored for the beginning of nonzero data and a signal is sent to the data handling system to begin storage, avoiding storage of the large amount of zero data due to trajectory and atmospheric uncertainties.

A g sensor will detect 0.1 g at about 5 seconds after entry, and will signal the pre-entry instruments to be turned off and the entry accelerometers to begin storing entry deceleration data. The pre-entry instruments, mounted on the heat shield, will burn off a few seconds after entry.

The remainder of entry and descent has been described in Section D.1 of Chapter III of Volume II. One important difference is that a nephelometer will begin operation simultaneously with the temperature and pressure gages, and take data on cloud densities until the end of mission. A second difference is that consideration of the cool and warm atmospheres, in addition to the nominal, has caused a wider variation in some of the times and pressure of event occurrences. Values for some of these parameters are given in the following subsection.

b. Parameter Variation With Atmosphere - In order to design a common probe for both Saturn and Uranus, the warm, nominal, and cool atmospheres of each planet were evaluated to determine the worst case environment for each design parameter. Table III-14 lists 18 parameters relating to the entry and descent in each of the six model atmospheres showing the variation and identifying the worst case for those that are important.

Table III-14 Variation of Parameters with Atmosphere

PARAMETER	SATURN ATMOSPHERE ($\gamma = -30^\circ$)			URANUS ATMOSPHERE ($\gamma = -60^\circ$)			WORST CASE*
	COOL	NOMINAL	WARM	COOL	NOMINAL	WARM	
REFERENCE RADIUS (0-km ALTITUDE), km	59,863.4	59,805.9	59,735.6	26,800	26,468	25,926.2	
ENTRY ALTITUDE, km	297	536	968.5	200	532	1073.8	UW
MAXIMUM DECELERATION, g	568	366	227	837	358	225	UC
MAXIMUM DYNAMIC PRESSURE, 10^5 N/m ²	5.6	3.6	2.2	8.3	3.5	2.2	UC
TIME TO 0.1 g, sec	2.0	5.0	12	0.5	4.0	14	
TIME TO 100 g, sec	8.5	17.5	35	4.5	15	36	
TIME TO MAXIMUM g, sec	11.5	22	40	6.5	19	40	
ALTITUDE AT MAXIMUM g, km	92.7	151.2	259	65.1	138	235	
TIME TO M = 0.7, sec	36.5	59.5	98.5	27.5	54.5	90.0	SW
CHUTE DEPLOYMENT MACH NO.	0.56	0.70	0.88	0.59	0.72	0.84	SW
CHUTE DEPLOYMENT ALTITUDE, km	48	92.5	168	35.3	78.9	145	
CHUTE DEPLOYMENT TIME (5 g + 15 sec), sec	44	59.5	84.5	33.5	53.5	80	SW
CHUTE DEPLOYMENT PRESSURE, mb	102	65	44	41	47	49	SC
ACCELEROMETER MEASUREMENT PERIOD, sec	57	69.5	87.5	48	64.5	81	SW
PRESSURE AT FIRST MEASUREMENT, mb	122	77	51	56	55	54	SC
ALTITUDE AT FIRST MEASUREMENT, km	44.3	87.8	162	32.2	74	141.3	SW
DESCENT TIME TO 7.3 bars, minute	24.4	41.1	67.5	23.8	44.0	82.0	UW
PRESSURE REACHED IN 44 minutes, bars	18.2	8.0	4.0	19.2	7.3	3.1	UC

*S = SATURN;

U = URANUS;

C = COOL ATMOSPHERE;

W = WARM ATMOSPHERE.

The first two lines in the table give the radius at zero altitude (1 atmosphere pressure), computed from equations in the NASA monographs referred to previously and the altitude of entry. The probe must traverse more vertical distance in the Uranus warm atmosphere, while the next two lines show that the Uranus cool atmosphere has the highest peak g-load and dynamic pressure. Times and altitudes to various event points are also given, the warm atmospheres requiring significantly longer times.

Parachute deployment occurs at 5 g sensing plus 15 seconds in all six atmospheres, which causes variation in the Mach number at deployment but allows for commonality of design. The worst case Mach number is 0.88 in the Saturn warm atmosphere. This atmosphere also requires the longest time for entry and thus sizes the entry accelerometer data storage capacity requirement. The first descent measurement is desired as high in the atmosphere as possible. The Saturn cool atmosphere is the worst case, the first measurement being taken at 122 mb. In all the other atmospheres, this measurement is made before the probe reaches 80 mb.

The descent depth is 7 bars with additional time to digitize and telemeter the final mass spectrometer sample, assuming that it was taken exactly at 7 bars, which is approximately the cloud base in both nominal models. This adds 50 seconds or about 0.3 bar to the depth, giving 7.3 bars. The times to descent to 7.3 bars, given in the table for each atmosphere, use a ballistic coefficient of 110 kg/m^2 , and become prohibitive for communication geometry in both warm models, exceeding one hour. However, the clouds are higher in these atmospheres and it is not necessary to descend to the same depth as for the cool and nominal atmospheres. Therefore, the worst case time is that for the Uranus nominal (44 min). Selection of a constant descent time, allows the time-dependent design values, such as bit rate and battery power requirement, to be the same for all atmospheres, as well as more closely aligning the final pressure design point with the modeled clouds. Thus, the descent is designed for 44 minutes and the final pressure reached is given in the last line of the table. The maximum pressure to be designed for is 19.2 bars in the Uranus cool.

Figure III-59 in Section F shows the cloud locations as a function of pressure depth and the relative location of the probe with respect to pressure at the end of a 44-minute descent. As can be seen, the descent time of 44 minutes was selected to allow the probe to pass through the Uranus ammonia cloud in its nominal location. If the atmosphere is actually colder than nominal, the probe would not penetrate completely through the cloud, but there is a good probability that it will obtain some measurements within the cloud. This is also true of the Saturn water cloud. If the atmospheres are like the cool models, these clouds cannot be measured without serious penalty to the overall probe design.

c. *Pre-Entry Data Collection* - The pre-entry measurements at both Saturn and Uranus are intended to define the ion and neutral particle concentrations in the ionosphere and upper atmosphere before actual aerodynamic entry. A determination of how well this can be done requires a theoretical model, with uncertainties, for the number densities of various species of particle expected to exist as a function of altitude. This has been done for Jupiter (Ref III-5 and others) but has not been attempted, to date, for Saturn or Uranus. However, the NASA monographs (previously mentioned) do give an equation for the projected electron number density, with uncertainties, that may be used as a first order approximation for proton density versus altitude. The equation is the same for both planets, but Z_1 is defined differently.

$$N_o = e \left[\frac{Z_1 - Z}{250} \right] \times 10^6 \text{ electrons/cm}^3 \text{ for } Z \geq Z_1$$

$$N_o = 0 \text{ for } Z < Z_1$$

$Z_1 = 450 \text{ km for Saturn and } 300 \text{ km for Uranus (altitudes above the 1 atm reference)}$

The uncertainties given are $10^{\pm 1}$ on the exponent and ± 200 km on Z_1 . Despite these large uncertainties, this nominal equation was used for this preliminary look at Saturn and Uranus ionospheric investigations.

From Reference III-4, the projected state of the art sensitivity for the Langmuir probe is 10 electrons/cm³, and for the IRPA it is 5 ions/cm³. Using the equation previously given, Table III-15 shows the approximate altitudes and times before entry when each instrument should begin to detect its respective particle.

Table III-15 State of Pre-Entry Measurements

INSTRUMENT & PARTICLE	SENSITIVITY, particles/cm ³	PLANET	ALTITUDE, km	TIME BEFORE ENTRY, sec
LP (e ⁻)	10	SATURN	3350	151
LP (e ⁻)	10	URANUS	3200	130
IRPA (H ₁ ⁺)	5	SATURN	3500	159
IRPA (H ₂ ⁺)	5	URANUS	3350	138
IRPA (H ₁ ⁺)	5	JUPITER	1375 (REFERENCE)	

It can be calculated from the equation that with each 576 km of altitude, the number density changes one order of magnitude. Assuming a liberal two-order-of-magnitude error in the exponent (~ 1200 km) and the 200 km error in reference altitude, the IRPA could possibly encounter protons at Saturn as high as 4900 km. Therefore, these pre-entry instruments should begin monitoring for ions at about 5000 km altitude, which is 237 seconds before entry. This time (and altitude) also does not include the trajectory errors. Twelve minutes prior to use, the Langmuir probes should be warmed up and decontaminated. The IRPA requires

only 5 to 10 seconds for warmup. However, the NRPA may require as long as 30 seconds, so that if turned on exactly at 5000 km, it may not start measurements until about 4420 km, which is still well above the required measurement altitude (probably less than 2000 km altitude for the neutral particles).

Figure III-27 shows the altitude and velocity time histories from 5000 km to nominal entry at 536 km (532 km Uranus). The probe inertial velocity, the velocity relative to an ionosphere rotating with the planet, and the vertical descent velocity component are shown for both planets. The great difference in inertial velocity between Saturn and Uranus is directly attributable to their difference in size and gravitational constant. At Saturn, the probe enters with the planet's rotation; thus the relative velocity is significantly reduced from the inertial. However, at Uranus, the inertial entry velocity vector is approximately perpendicular to the direction of motion of the planetary atmosphere; thus, the relative velocity is about 0.5 km/sec higher than the inertial. The relative velocity is that velocity at which the pre-entry instruments will intercept particles, and it differs between Saturn and Uranus by about 4 km/sec.

The difference between the radial velocities for the two planets is always less than about 2 km/sec. Since the rate of vertical descent through the upper atmosphere is used to judge measurement performance of the pre-entry instruments, the fact that these velocities are about the same allows for commonality of sampling times and bit rates. This occurs only because of the selected entry flight path angles of 30° for Saturn and 60° for Uranus. The large difference in entry angle also explains the fact that the radial velocity lines in Figure III-27 diverge. The small decrease in the flight path angle along the Saturn conic trajectory offsets the increased inertial velocity for calculation of the radial component. This does not occur for Uranus; thus the former decreases and the latter increases.

If the entry angle is varied, the performance will change with the radial velocity. Figure III-28 shows the change in the various velocities as a function of entry flight path angle for Saturn. While the inertial velocity is almost independent, the relative velocity increases significantly with increasing flight path angle, and the radial velocity increases drastically. The effect of entry angle on radial velocity dominates the effect of mission selection and VH_p . (See Figure III-6.)

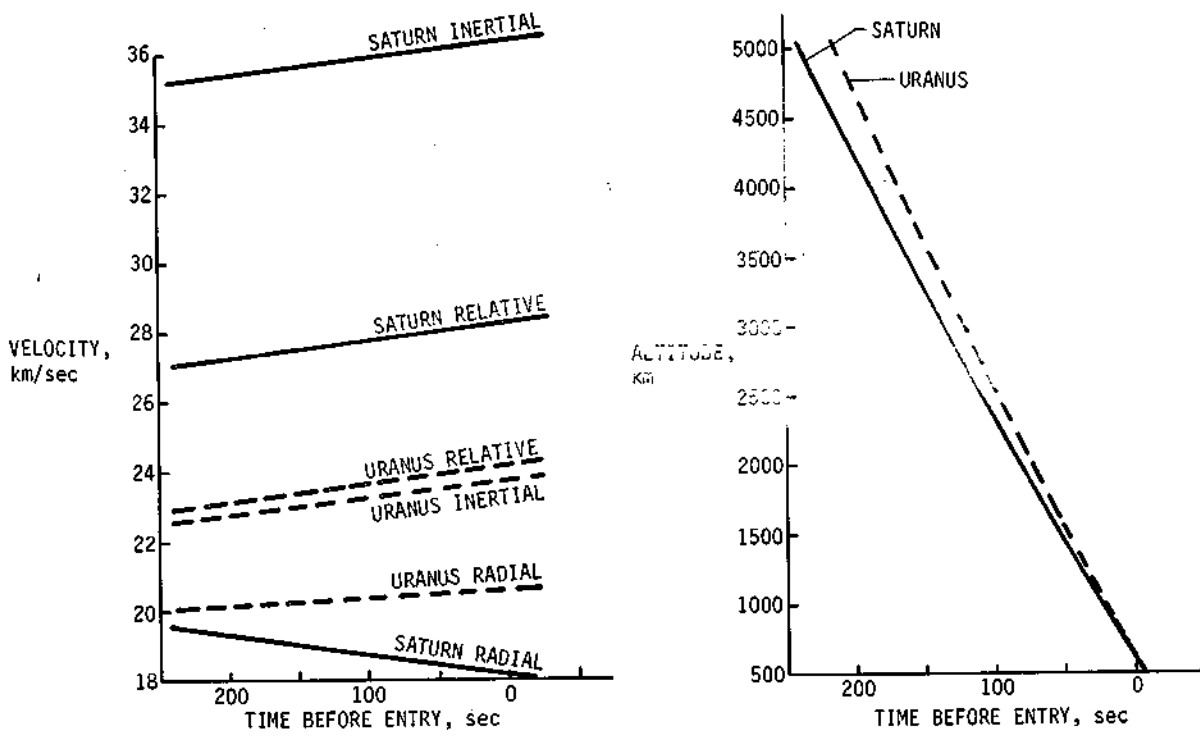


Fig. III-27 Pre-Entry Velocity/Altitude Time History

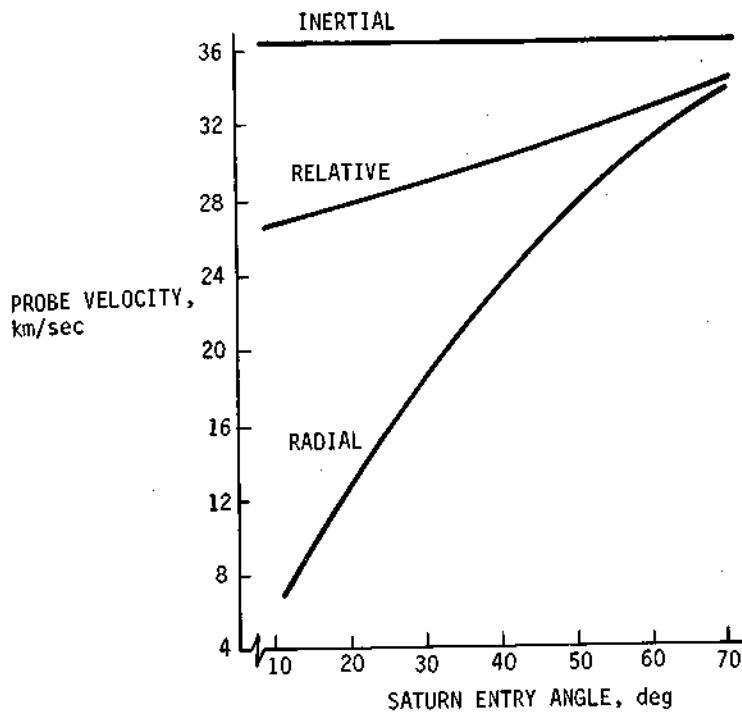


Fig. III-28 Probe Velocities at Entry vs Saturn Entry Angle

The resulting effect on pre-entry performance is given by Figure III-29 for Saturn. For a given instrument sampling time, the number of kilometers of altitude required for a single measurement increases with the entry angle, and fewer measurements are obtained for a given mission. For the specific entry angles chosen, Figure III-30 shows the variation in measurement performance with sampling time for both Uranus and Saturn. The lines are relatively close together so that the performance for a given sampling time (≤ 5 sec) is nearly the same for the two planets.

The sampling times selected for the pre-entry instruments are shown on the figure. The Langmuir probes, sampling every half second, make one measurement every 10 km, which would be on the order of 280 separate measurements of electrons and protons, based upon the previously given equation. The IRPA, sampling at 2 seconds makes one measurement in approximately 40 km, which is about 70 proton density determinations and fewer for the heavier positive ions. The NRPA sampling time has been selected at 3.0 seconds, which requires the probe to travel about 60 km (more for Uranus, less for Saturn) between measurements. Since no model for the upper atmospheric neutral particles exists, the number of measurements cannot be estimated. If the neutrals are measured at and below a conservative 1500 km altitude, a total of 16 separate measurements will be made.

Ideally, the ionosphere should be sampled along a radial line to obtain a vertical ionospheric sample. However, because of entry at angles other than 90° , the probe will traverse a small amount of latitude and longitude. Table III-16 shows these amounts for the three missions investigated. Both variations are small and are satisfactory for ionospheric measurements.

*Table III-16 Latitude and Longitude Variations**

PLANET	SATURN	SATURN	URANUS
MISSION	S 79	SU 80	SU 80
Δ LATITUDE	0.5 deg	1.3 deg	4.7 deg
Δ LONGITUDE	6.6 deg	6.6 deg	4.8 deg
*ALTITUDES FROM 5000 km TO 530 km.			

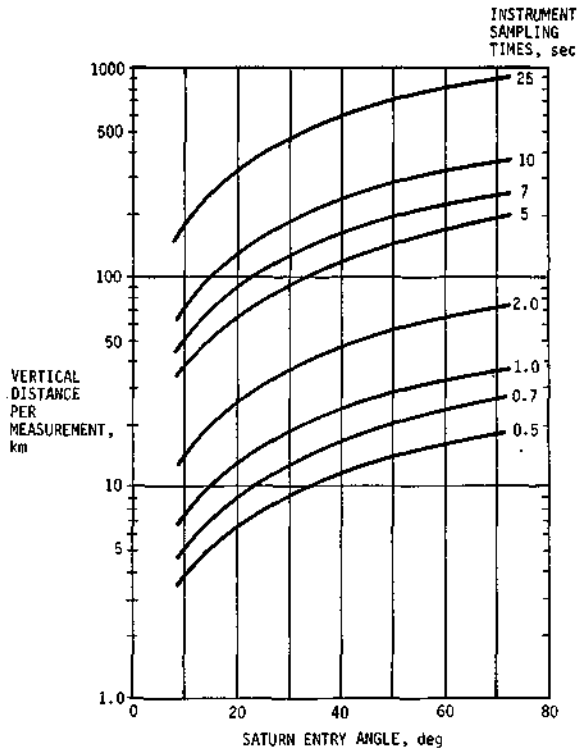


Fig. III-29 Pre-Entry Performance vs Saturn Entry Angle

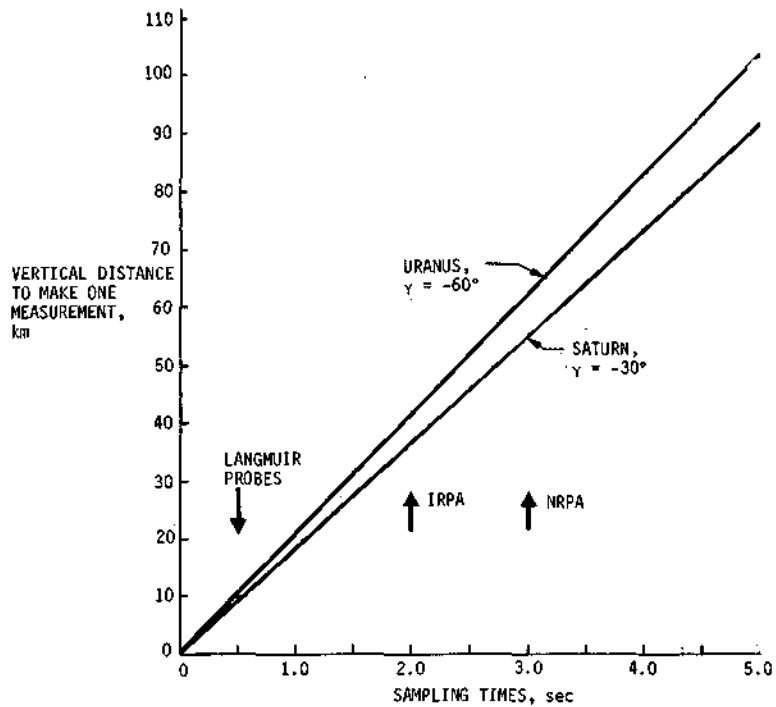


Fig. III-30 Pre-Entry Instrument Measurement Performance vs Sampling Time

d. *Entry Accelerometer Data Collection* - The entry accelerometers will begin to store data upon sensing of a steady 0.1 g at about 5 seconds after entry. As established in the previous part of the study, the axial sampling will be at a rate of 5 samples/sec and lateral sampling at a rate of 2.5 samples/sec. This gives a total collection data bit rate of 100 bps, assuming 10-bit words and two lateral sensors.

The range of accelerometer operational times given in Table III-14, show a variation from 48 seconds in the Uranus cool to 87.5 seconds in the Saturn warm atmosphere. This sizes the accelerometer data storage memory at about 8800 bits for entry into any of the six atmospheres. Additional storage is required for engineering, formatting, and some descent data.

The performance of the instrument for a given sampling time can be gaged from how detailed it defines the peak-g point on a g-time history. Figure III-32 shows these deceleration curves for all six atmospheres. Table III-17 lists the peak g values and then gives the number of separate measurements above three high-g levels, based upon the sampling times given above. Comparison of the number of points to the curve shows that the chosen sampling should be more than adequate.

Table III-17 *Accelerometer Measurement Performance*

ATMOSPHERE	PEAK ACCELERATION, g	NUMBER OF MEASUREMENTS AT		
		> 500 g	> 300 g	> 100 g
SATURN				
WARM	227	0	0	60
NOMINAL	336	0	13	50
COOL	568	8	19	39
URANUS				
WARM	225	0	0	51
NOMINAL	358	0	12	45
COOL	837	11	18	27

e. *Descent Data Collection and Transmission* - During descent, the neutral mass spectrometer, temperature and pressure gages, and the accelerometer triad (switched to the turbulence mode) will be operating. In addition, on the expanded payload, a nephelometer will search in detail for clouds. Also, during descent, the store entry accelerometer data must be played back, and with the expanded payload, the entire pre-entry collection of data may be interleaved with the real time.

The detailed data rate breakdown for each mission is given in the chapters concerning system definitions, but Table III-18 provides a summary for discussion here. The total data rate for the Exploratory payload is 27.7 bps, and with the addition of the nephelometer, it increases to 31.5 bps. This is the minimum requirement for the expanded payload descent. However, the power requirement for the pre-entry rate of 235 bps exceeds that required for descent; thus, the data could be stored and replayed for redundancy during descent for a cost of only 26 w-hr. The bit rate becomes 50.5 bps which still requires less power than pre-entry. Another option also available is to increase the descent science measurements instead of replaying pre-entry data. This is discussed further in Chapter V, Section B.

Table III-13 presented values for some of the descent parameters. Figure III-31 shows descent profiles for all atmospheres of both planets, using a descent ballistic coefficient of 110 kg/m^2 . The final pressure at the end of the design mission is indicated at the right. The descent time is a constant 44 minutes but the profiles exceed this time by an amount equal to the time from entry to parachute deployment, which is a variable. Note that for a given atmosphere, the planet has a small effect upon descent times and pressures. Descents into Saturn are deeper for all except the cool models. Further discussion on descent and the associated instrument measurement performance is given in Chapter IV, Section B and in Chapter V, Section B.

Table III-18 Descent Data Rate Composition

COMPONENT	BIT RATE, bps
EXPLORATORY PAYLOAD SCIENCE	24.7 (Table IV-4)
FORMATTING	2.5
ENGINEERING	<u>0.5</u>
EXPLORATORY PAYLOAD TOTAL	27.7
NEPHELOMETER ADDITION	3.4
FORMATTING	<u>0.4</u>
EXPANDED PAYLOAD TOTAL (LESS PRE-ENTRY)	31.5
TOTAL STORED PRE-ENTRY	16.8
STORED FORMATTING	1.7
STORED ENGINEERING	<u>0.5</u>
TOTAL DESCENT	50.5

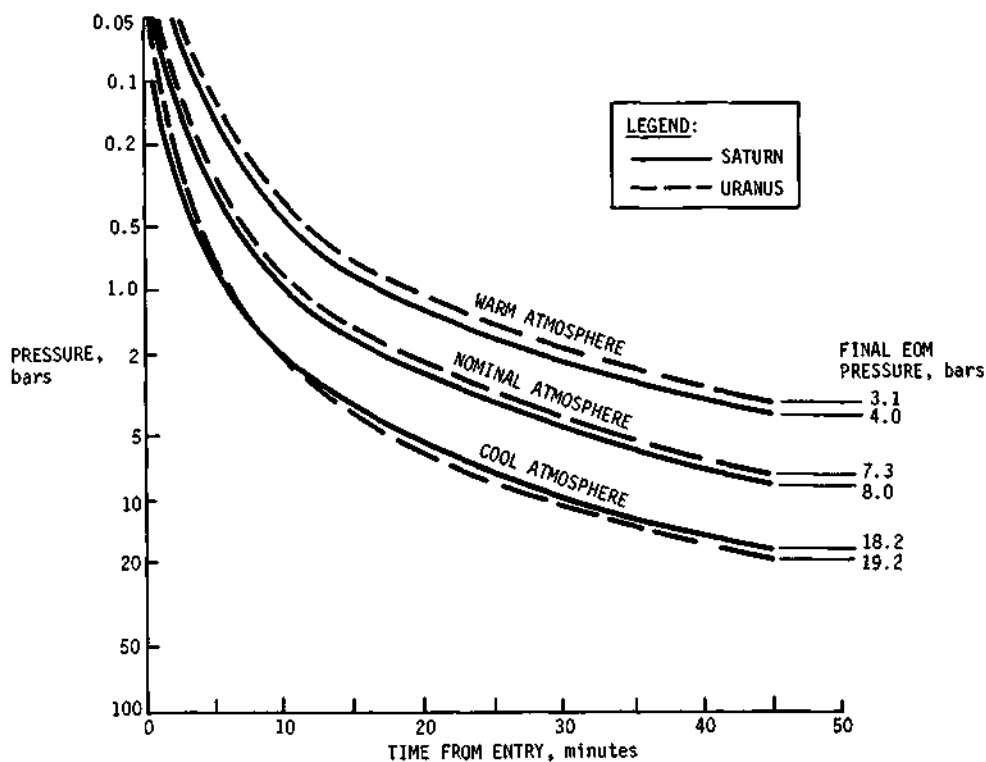


Fig. III-31 Pressure Descent Profiles

C. SYSTEM INTEGRATION

1. Parachute Deployment Analysis

The expected deceleration of the probe varies significantly for the cool, nominal, and warm atmospheric models for Saturn and Uranus as shown in Figure III-32. Accordingly, it was necessary to investigate the parachute deployment to meet the following criteria:

- 1) The parachute shall be subjected to Mach numbers no greater than 0.9.
- 2) The parachute shall be deployed at pressure altitudes higher than 100 mb (a soft constraint).

From the initial portion of the contract, the 100 mb pressure level for an entry ballistic coefficient of 102 kg/m² (0.65 slug/ft²) occurs at or near Mach 0.7. This Mach number varies from 1.38 g for the Uranus warm atmosphere to 2.4 g for the Saturn cool atmosphere. Using 2.4-g sensor to deploy the parachute would expose the chute to Mach 0.95 in the Uranus warm atmosphere and Mach 1.0 in the Saturn warm atmosphere. Using 10-g (decreasing) sensing for the Saturn nominal atmosphere plus 20 seconds, the highest velocity encountered is Mach 0.9 in the Saturn warm atmosphere. Due to errors expected in sensing devices, timers, and determining ballistic coefficients, 5 g (decreasing) plus 15 seconds was selected for parachute deployment. As a result, the following Mach numbers and pressure altitudes are expected for the various atmospheric models:

	<u>Mach No.</u>	<u>Pressure Altitude, mb</u>
Saturn Atmospheres		
Cool	0.56	102
Nominal	0.70	65
Warm	0.88	44
Uranus Atmospheres		
Cool	0.59	41
Nominal	0.72	47
Warm	0.84	49

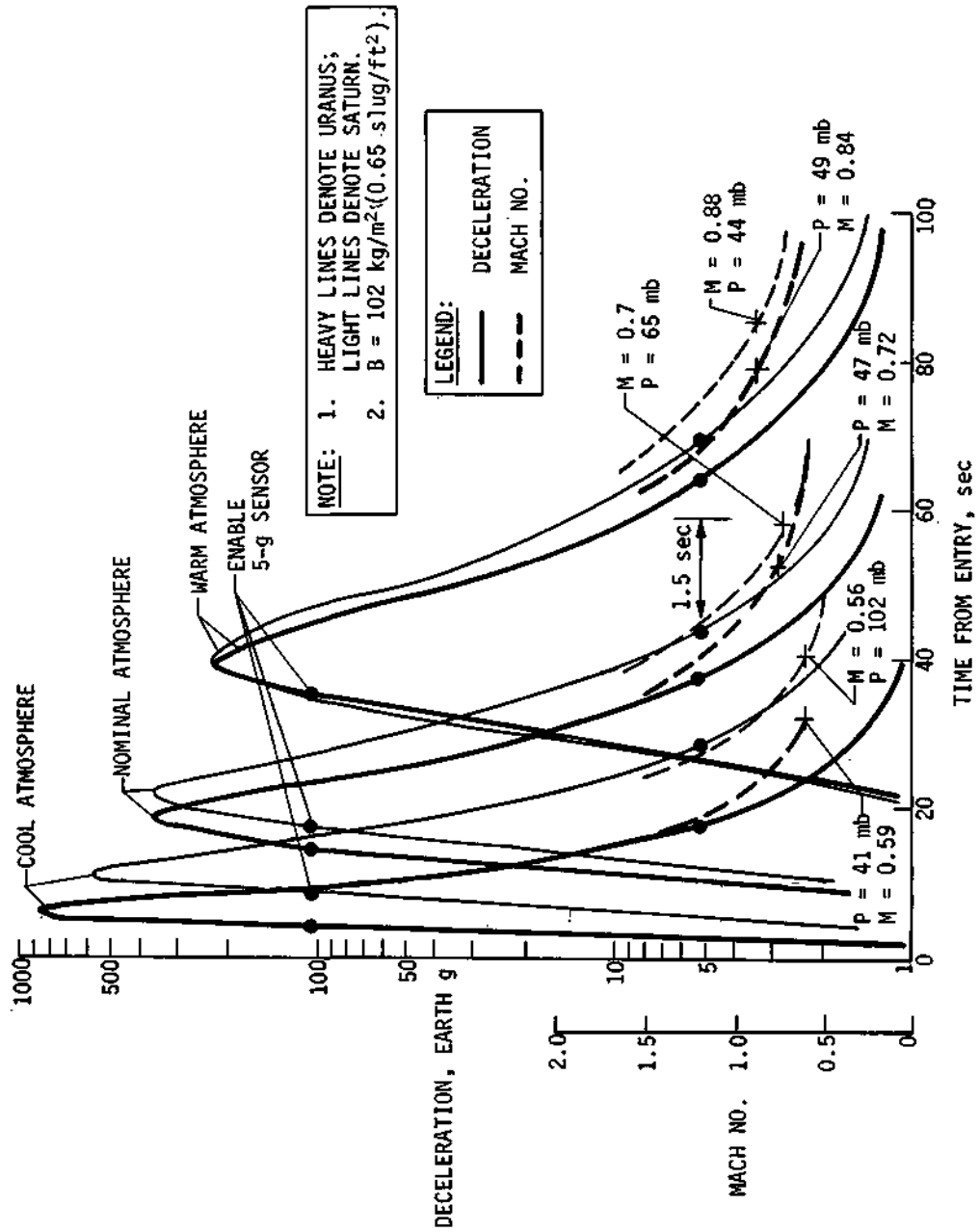


Fig. III-32 Parachute Deployment Analysis for Saturn and Uranus

The 5-g sensor would be enabled by 100 g (sensing) as shown in the figure.

2. Task II Data Mode Analysis

The data mode for Task I is very similar to that for the Probe Dedicated Jupiter Mission described in Volume II, Chapter V, Section C. Since the probe is deflected by the spacecraft, the probe separation time is very short, i.e., a few minutes, during which time data is not collected. During the pre-entry phase, engineering data is collected and transmitted in real time until entry when the transmitter is turned off due to the blackout encountered. Science and engineering data is collected and stored until probe acquisition and interleaved with real-time data during descent at approximately 28 bps.

Compared with Task I, the addition of the pre-entry science instruments and the nephelometer for Task II caused the pre-entry data rate to increase from 1 bps to 235 bps and the descent data rate to increase from 28 bps to 31.5 bps, assuming that pre-entry science data is not stored. The high pre-entry data rate precipitated a data mode tradeoff as follows:

- 1) Keeping the pre-entry transmission real time and using FSK modulation will require a high RF power; changing the modulation to PSK should reduce the RF power required.
- 2) Storing the pre-entry data (i.e., no pre-entry transmission) and interleaving it with real-time data during descent would increase data storage requirement, but decrease the RF power requirements.

The data profiles for the primary and optional data modes are shown in Figure III-33 with the optional mode corresponding to 2) above. In the primary mode, the pre-entry science starts collecting data at the time corresponding to 5000 km above 1 atmosphere, but due to the entry arrival uncertainty of 29 minutes for Uranus and 4.4 minutes for Saturn, the pre-entry science starts collecting data earlier than required. For the optional mode, the Langmuir probes and IRPAs are used to sense data at approximately 4300 km above 1 atmosphere and instruct the Data Handling Subsystem to start storing data. This adaptive science method eliminates the entry arrival uncertainty and accounts for less data collected in the optional mode.

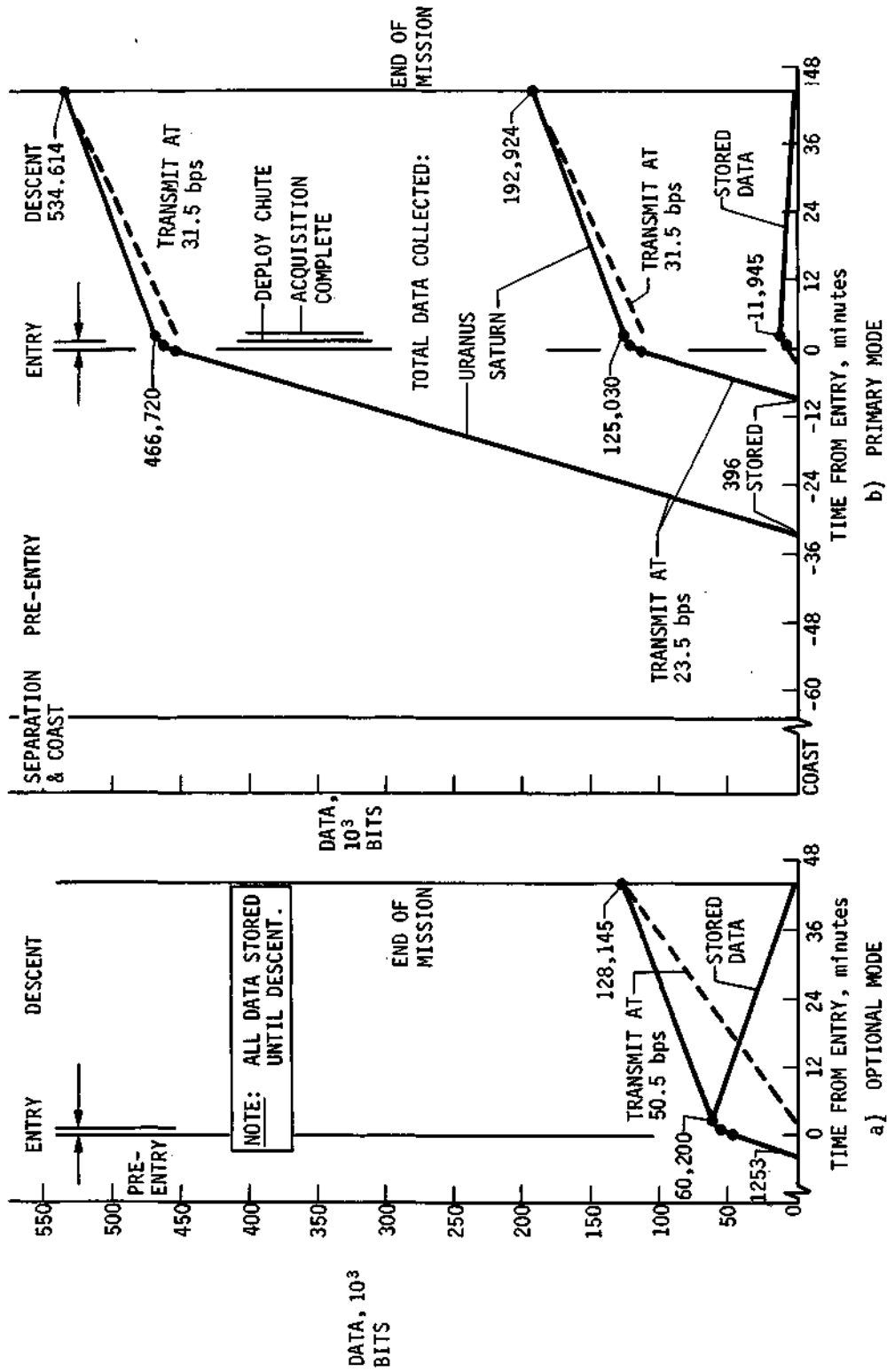


Fig. III-33 Data Profile for Task II, Data Mode Tradeoff

Results of these trades, shown in Table III-19 were presented at the Mid-Term Review held at Martin Marietta Denver Division on 13 October 1972. Since data modes 2 and 3 require the same RF power without increasing the probe weight or size, it was recommended at the Mid-Term review that the pre-entry data be transmitted real time as in mode 2 and also stored for descent transmission as in mode 3, as shown in Figure III-34. These trades are also discussed in Sections B and D.

After conducting the thermal control analysis of the combined data modes 2 and 3 shown in Figure III-34, the long real-time transmission times for Uranus caused the transmitter to exceed the upper temperature limit. As a result, a 7-watt transmitter amplifier was added for pre-entry tracking and acquisition. At 3.3 minutes before entry, the adaptive science method starts the real-time transmission at 41 watts and begins storing data. This condition is further discussed in Sections D and E.

The pre-entry RF power required for mode 2 is 41 watts and the descent RF power required is only 29 watts. As discussed in Section B, it might be more desirable to use the increased descent RF power by improving the descent science performance, i.e., increase the NMS sweeps instead of the combined data mode 2 and 3.

Table III-19 Task II Data Mode Analysis Results

DATA MODE	DATA RATE, bps	MODULATION TYPE	RF POWER, w	PROBE WEIGHT, kg	PROBE DIAMETER, cm	PROBE DATA STORAGE 10 ³ bits
PRE-ENTRY DATA, TRANSMITTED	235	FSK	120			
REAL-TIME (NO STORAGE)				116	96.5	11.9
DESCENT	31.5	FSK	29			
PRE-ENTRY DATA TRANSMITTED	235	PSK	41			
REAL-TIME (NO STORAGE)				103	91.4	11.9
DESCENT	31.5	FSK	29			
PRE-ENTRY DATA STORED & TRANSMITTED DURING DESCENT	50.5	FSK	40	103	91.4	60.2

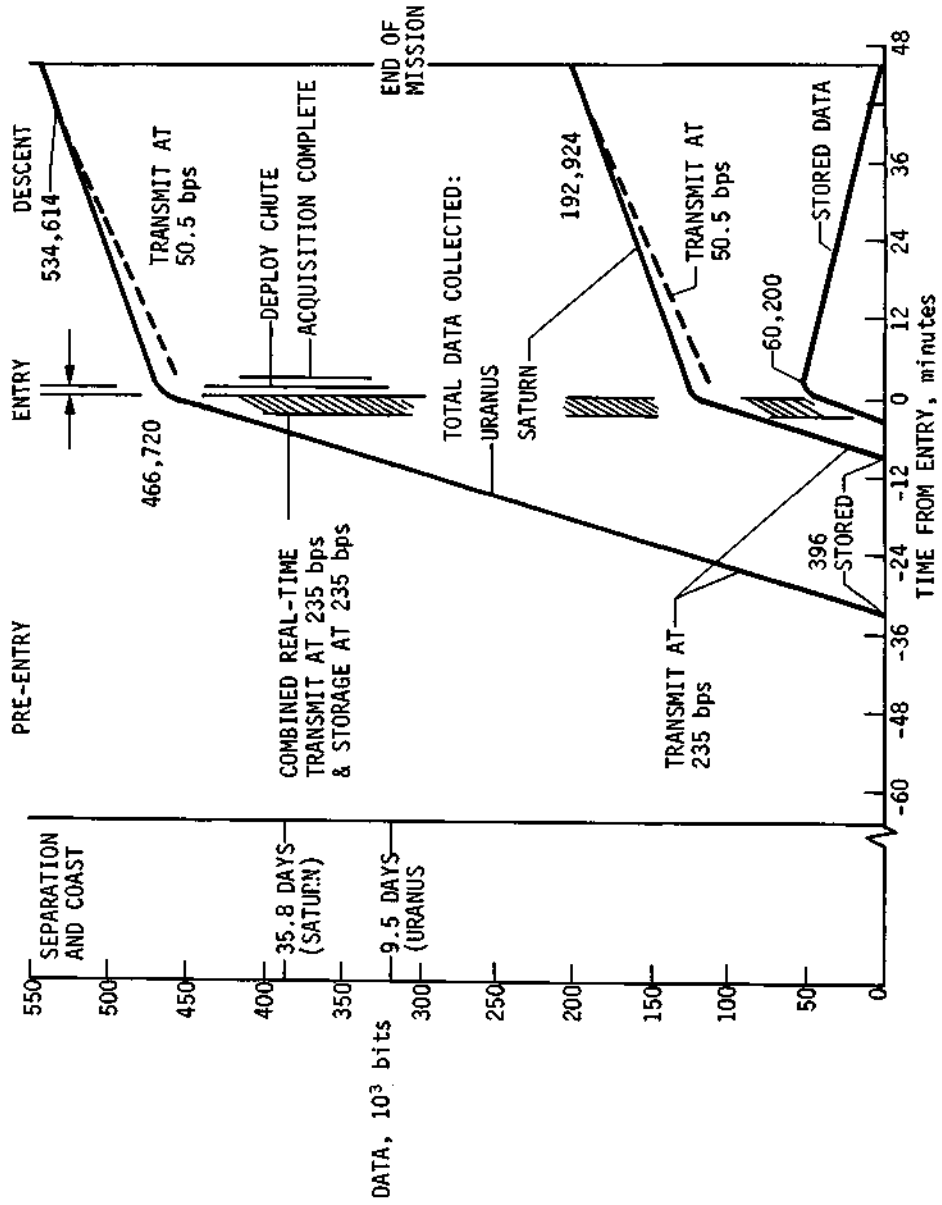


Fig. III-34 Preliminary Data Profile for Saturn/Uranus Probe (Task II)

D. ELECTRICAL AND ELECTRONIC SUBSYSTEMS

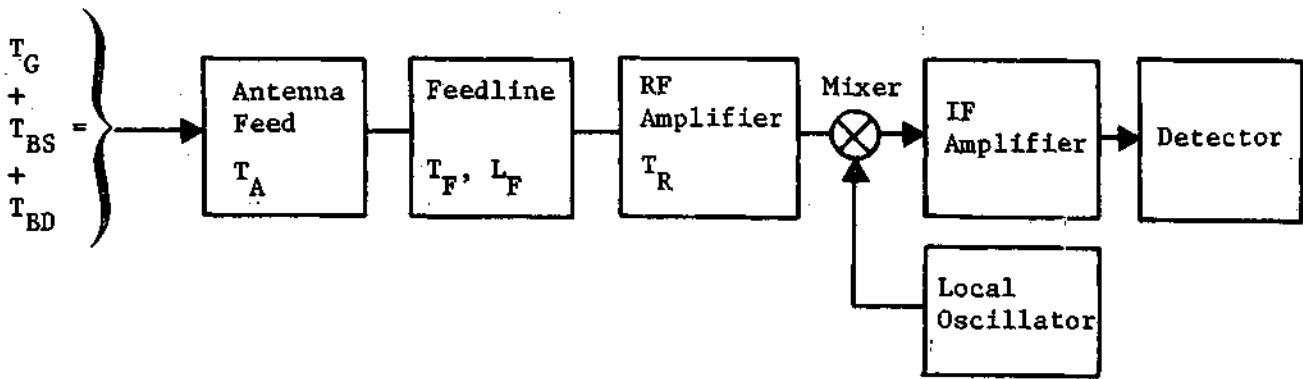
Additional analyses have been performed in several areas of the electrical and electronic subsystems to further refine hardware design criteria. Only the changes and improvements made to the original subsystem, which are described in Volumes I through III, are discussed in the following sections.

1. Telecommunication Subsystem

Parametric variations were made in arriving at an optimum geometry that results in a common Saturn/Uranus probe from the standpoint of the telecommunication subsystem. Results of parametric variations are discussed together with changes and improvements to some preliminary data used previously. New hardware information is also included.

a. *System Noise Temperature* - Previous determination of the system noise temperature did not include effects of antenna feedline noise or the location of the galactic center. Disk noise for Uranus was also preliminary data obtained before release of the Uranus design criteria monograph (Ref III-2). Improvements in system noise temperature calculations were made for Saturn and Uranus and are described in the following paragraphs.

Various noise sources reduce the useful operating range of the receiver system. There are several external sources of radio noise such as galactic, star, magnetosphere, planet, and atmospheric noise. Internally, the antenna and receiver also have a noise level which is expressed in terms of noise temperature. Noise temperature can also conveniently be expressed in terms of a noise figure as defined in Volume III, Appendix B, p B-10. The thermal noise sources affecting the probe receiver subsystem are shown in following sketch.



The system noise temperature is used in all considerations of sensitivity and in calculating the total effective noise power density per modulation bandwidth (kT_s). System noise temperature is defined as

$$T_s = T_A + T_F + L_F T_R \quad [1]$$

where T_s = receiving system noise temperature, °K

T_A = antenna noise temperature, °K

= $T_G + T_{BS} + T_{BD}$, as applicable

T_G = galactic noise temperature, °K

T_{BS} = synchrotron noise temperature, °K

T_{BD} = planet disk noise temperature, °K

T_F = antenna feedline noise temperature, °K

T_R = receiver noise temperature, °K

L_F = feedline power loss ratio.

Feedline loss affects the noise temperature of the receiver and the feedline temperature in °K is expressed by

$$T_F = 290^\circ (L_F - 1). \quad [2]$$

The loss in 3 ft of coaxial cable (from antenna feed to receiver) is 0.2 dB/ft at 0.86 GHz or 0.6 dB. The two connectors add 0.4 dB for a total loss of 1 dB (power ratio = 1.26). From Equation [2], we have

$$T_F = 290 (1.26 - 1) = 75.5^\circ\text{K}. \quad [3]$$

It is important to have the receiving antenna close to the receiver with a minimum feedline cable length. Low loss cable and connectors should be used on the spacecraft to keep reflected noise temperature to a minimum.

The receiver is an amplifier and mixer chain (see sketch) to the detector, which determines the receiver noise temperature. The receiver noise temperature, T_R , of a typical superheterodyne receiver, with RF amplifier and a mixer down converter to IF frequencies, is given by the relationship

$$T_R = T_1 + \frac{T_2}{G_1} . \quad [4]$$

where

T_R = receiver noise temperature, °K

T_1 = RF amplifier noise temperature, °K

T_2 = mixer noise temperature, °K

G_1 = power gain ratio of RF amplifier.

For an amplifier and mixer package where $T_1 = 289^\circ\text{K}$, $T_2 = 3000^\circ\text{K}$, and $G_1 = 30$ dB (ratio = 1000), the receiver noise temperature from Equation [4] is

$$T_R = 289^\circ + \frac{3000^\circ}{1000} = 292^\circ\text{K} \quad [5]$$

As can be seen, the noise temperature if this receiver is controlled by the first amplifier stage and the other, high gain stages in the receiver only add a small amount of noise.

Noise contributions from the magnetosphere and planet disk vary during the probe mission. Background cosmic noise from the galaxy can be significant, as seen in Figure III-35 (Ref III-6), depending on whether or not the center of the galaxy is within the beamwidth of the probe receiving antenna on the spacecraft. The position of the galactic center relative to the antenna look direction is dependent upon the arrival date, the planet of interest, and the spacecraft-to-probe geometry. As seen in Figure III-36a, the galaxy is occulted by Saturn during probe acquisition and during the active portion of the probe mission. The planet disk subtends an angle at the spacecraft of 28° and galactic background noise is overshadowed by the disk noise. Cosmic noise present between the outer limit of the magnetosphere and the spacecraft is negligible ($< 10^\circ\text{K}$). The direction to the center of the galaxy is also shown in the figure; it is 19° off the spacecraft antenna boresight at acquisition.

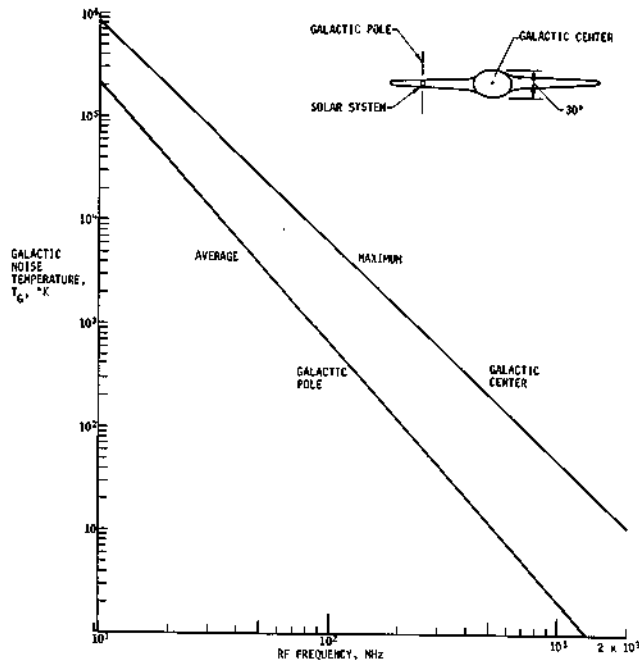


Fig. III-35 Thermal Noise Temperature of the Milky Way Galaxy

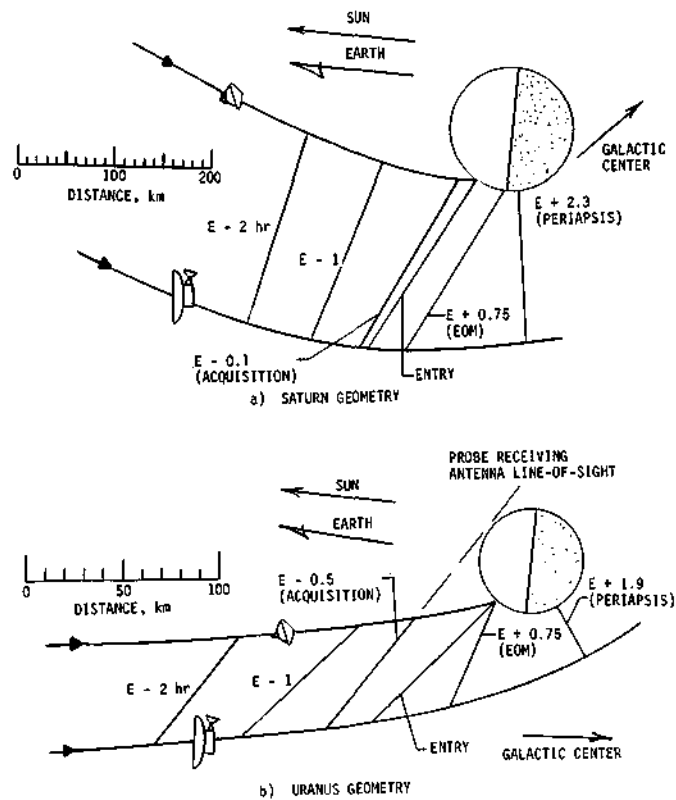


Fig. III-36 Trajectory Geometry for the Saturn/Uranus 1980 Mission

Therefore, only the variable synchrotron and planet disk noise is present at Saturn encounter as a function of the relative geometry of the probe, planet, and spacecraft. Within the operating frequency range of the probe receiving antenna on the spacecraft, noise power produced by black body radiation from the planet disk and magnetosphere is received through the antenna radiation envelope and is coupled to the receiver through the radiation resistance of the antenna. The fraction of noise power received by the spacecraft antenna is a function of the directivity of the antenna with most of the power received via the main beam. The noise temperature of the antenna from each direction is a function of the power (flux) emitted into the antenna from that particular direction.

The revised receiving system noise temperature for Saturn is shown in Figure III-37. The original curve is shown in Figure VI-7 of Volume II. The revised curve represents an increase of 149°K at 0.86 GHz, resulting from feedline noise and its impact on receiver front-end noise temperature. A feedline loss of 1 dB is used for 0.88 m (3 ft) of coaxial cable. The antenna temperature remains unchanged, based on the latest values for synchrotron and disk brightness temperatures for Saturn (Ref III-1).

The trajectory geometry for Uranus is shown in Figure III-36b and indicates that the line-of-sight (LOS) of the receiving antenna grazes the planet disk at acquisition. For a 20° antenna beamwidth, half of the beam encounters space noise and half disk thermal noise with the planet disk emanating the higher noise level. Also depicted in the figure is the direction to the galactic center. The LOS vector is 53° away from the galactic center at acquisition. Therefore, the antenna noise temperature is attributed only to the influence of the planet disk. The planet disk subtends an included angle of 24° at the spacecraft position during acquisition.

The revised receiving system noise temperature for Uranus is shown in Figure III-38. The original curve is shown in Figure VII-2 of Volume II. The revised figure depicts a new upper-limit curve for the planet disk brightness temperature based on measured data reported in the planet monograph (Ref III-2). The basic study assumed a constant disk brightness temperature of 300°K. The monograph also discusses the possibility of trapped radiation belts existing at Uranus. The conclusion is that radio emission measurements do not establish the planet as a synchrotron source since the existing measurements are in rough agreement with what would be expected of thermal emission from the atmosphere (Ref III-2, p 28). Therefore, the antenna noise temperature is equal to the planet disk brightness temperature, as shown in the figure, and is constant during the active portion of the probe mission.

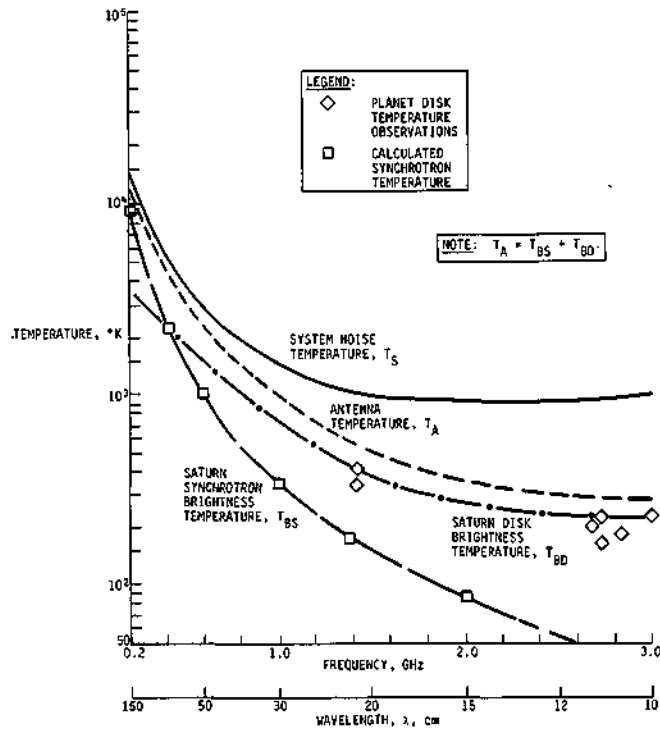


Fig. III-37 Receiving System Noise Temperature for Saturn

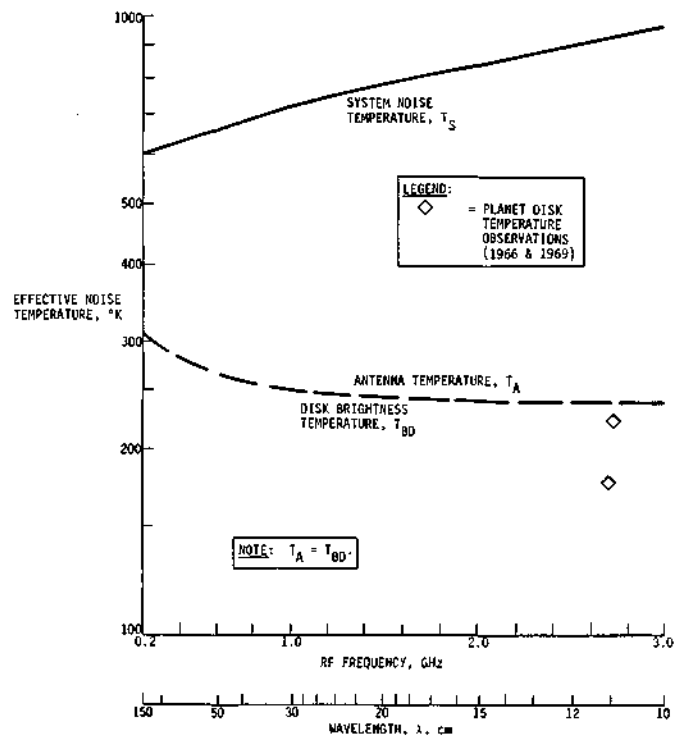


Fig. III-38 Receiving System Noise Temperature for Uranus

The average receiver noise temperature curve of Figure V-11, p V-21, Volume II, is used and a feedline loss of 1 dB is used for 0.88 m (3 ft) of coaxial cable. The revised system noise temperature curve represents an increase of 102°K at 0.86 GHz resulting from feedline noise and its impact on receiver front-end noise temperature and a revised antenna noise curve. The revised system noise temperature curves are used to determine the receiver noise spectral density in the RF link analysis.

b. Atmosphere Microwave Losses - The basic method of computing absorption and defocusing losses in the planetary atmosphere is described in Volume III, Appendix A. Results were given only for the nominal atmosphere models of Saturn and Uranus. For the common probe design, the worst-case atmosphere was used to define the communication subsystem.

For an atmosphere such as that found on Saturn and Uranus, the principal source of microwave absorption is gaseous ammonia. Water vapor and liquid water/ammonia solution clouds also contribute to absorption losses. Absorption in solidified ammonia or water clouds is negligible. During descent, the solid ammonia clouds are encountered before the water/ammonia solution clouds, as seen in Figure III-39. In general, the atmosphere model having the highest ammonia concentration will result in the greatest microwave absorption if the probe penetrates the ammonia saturation level; descent into the cool Uranus atmosphere is an exception because the probe does not reach the saturation level (80.7 bars) as seen in the figure. The saturation level is approximately 6.7 bars for the nominal Uranus atmosphere and the probe descends to approximately 7.3 bars at mission completion. Ammonia abundances are shown in Table III-20 for Saturn (Ref III-1, p 43) and Uranus (Ref III-2, p 33). As seen in the table, the warm models for both planets are very low in ammonia and were therefore not investigated because the resulting microwave absorption will be smaller than for the nominal or cool models. Methane clouds were not considered in the analysis since their microwave absorption is negligible.

There have been two changes made in the computation method described in Volume III, Appendix A. The improvements, which are based on more recent analysis, did not have a large effect on the numerical results. The nominal planet atmosphere models for Saturn and Uranus were also recalculated to update the data on microwave absorption.

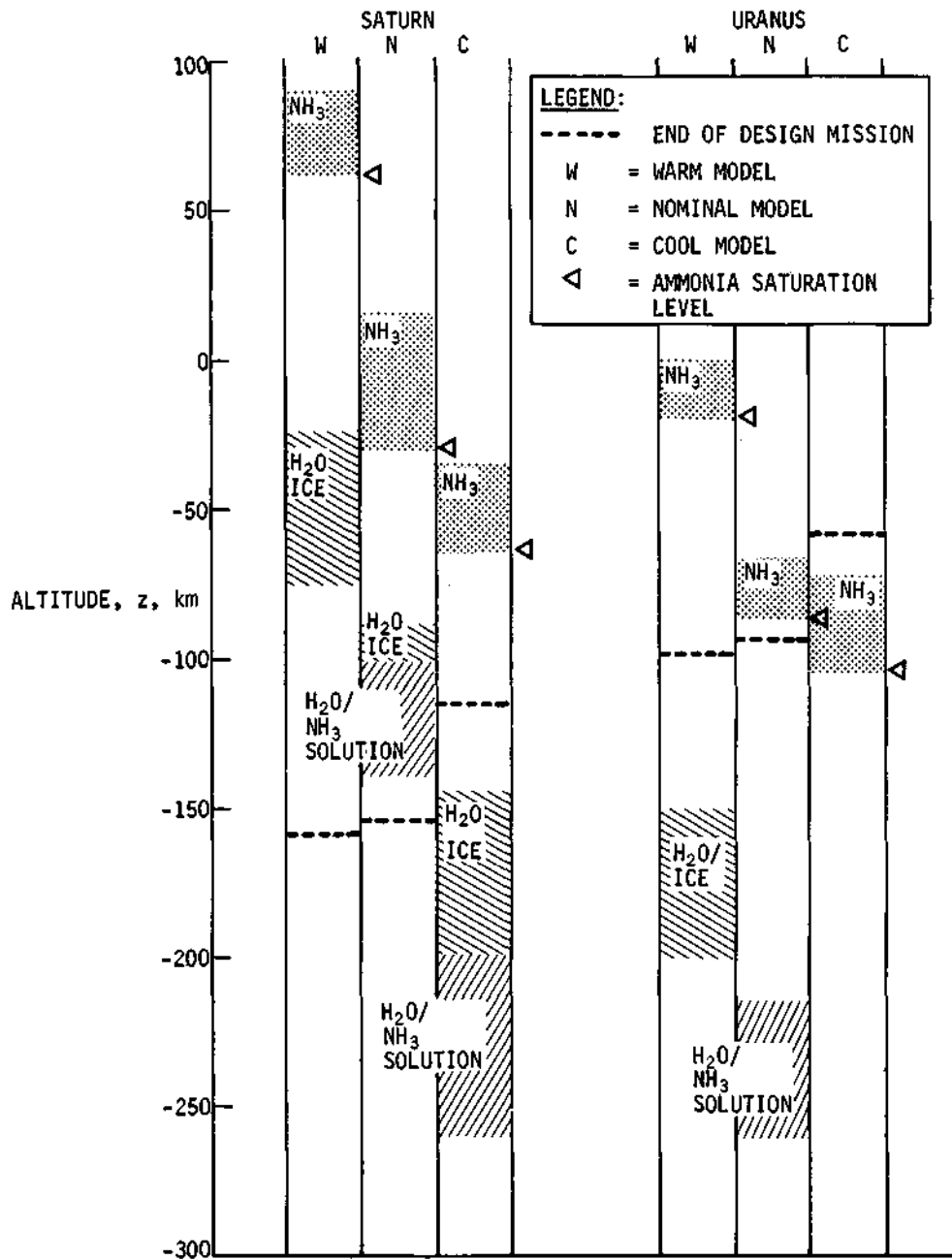


Fig. III-39 Location of Clouds that Affect Microwave Absorption

Table III-20 Ammonia Abundance in the Atmosphere Models

	SATURN ATMOSPHERE			URANUS ATMOSPHERE		
	WARM	NOMINAL	COOL	WARM	NOMINAL	COOL
Ammonia Mass Fraction, %	0.037	0.113	0.34	0.038	0.095	0.168

The first change consisted of an alteration of the method used to compute ammonia (NH₃) absorption coefficients. The method outlined in Volume III, Appendix A was based on work done by A. A. Maryott at National Bureau of Standards, Gaithersburg, Maryland and used in the original analysis (Ref III-7). The new method is based on work recently completed by D. A. DeWolf of RCA, Princeton, New Jersey (Ref III-8).

Figure III-40 shows a comparison of the two methods of computing absorption coefficients, $\alpha(z)$, using the Jupiter cool atmosphere at 1 GHz. Jupiter is shown because an atmosphere profile that extended to very high pressures was needed to show the turnover that occurs at -100 km (approximately 65 bars). Above this altitude, the two coefficients are very close. Below this point, the high pressure asymptotic forms prevail: T^{-1} for Maryott's coefficients and $T^{-1.4}$ for the DeWolf coefficients. Therefore, the curves will continue diverging as depth and temperature are increased. Similar differences in the two methods of computing the coefficient exist for Saturn and Uranus, which result in differences in absorption as seen in Figure III-41. The zenith microwave absorptions for the nominal and cool Saturn atmosphere models and the Uranus nominal atmosphere model are shown in Figure III-41, through III-46. Each model has two figures associated with it to depict absorption as a function of altitude and pressure at two selected frequencies, or as a function of frequency at several selected altitudes as represented by pressure. Use of the coefficients developed by Maryott and DeWolf is shown for the nominal atmospheres for purposes of comparison. The curves were calculated only to a pressure of 30 bars and extrapolated to higher pressures. The zenith absorption is equal to the total microwave attenuation since the defocusing losses are zero at zenith. The zenith absorption is the integral of the coefficients given in a plot such as shown in Figure III-39. The difference between the two methods of computation is only about 23% over the altitude range of interest for this program. However, the change to the DeWolf method was made because it is based on more recent and extensive experimental work. Defocusing losses for the two planets are similar to Figures A-8 and A-9 in Volume III, Appendix A, and are less than 0.1 dB for the altitudes and aspect angles encountered during the missions.

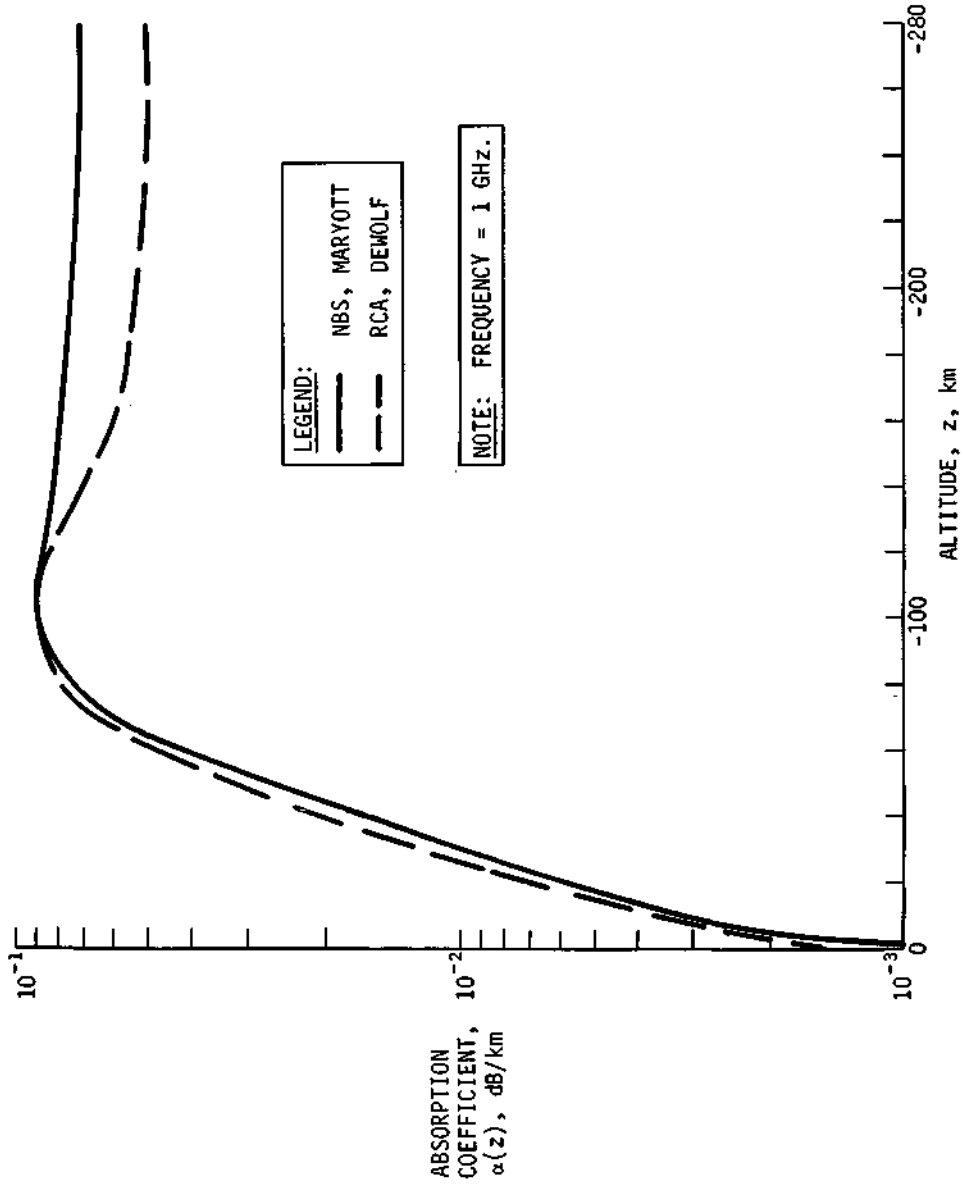


Fig. III-40 Absorption Coefficients for the Cool Jupiter Atmosphere

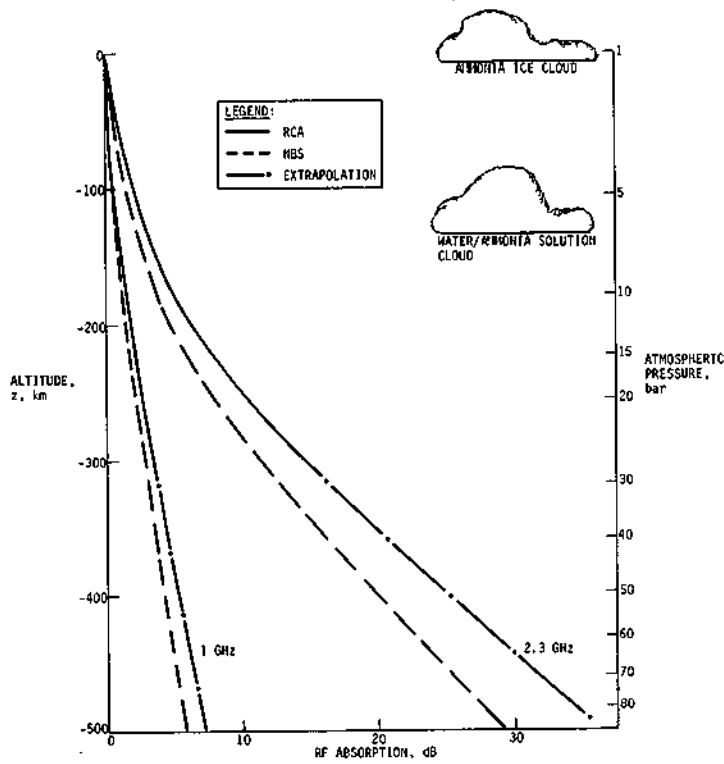


Fig. III-41 Zenith Absorption for the Saturn Nominal Atmosphere

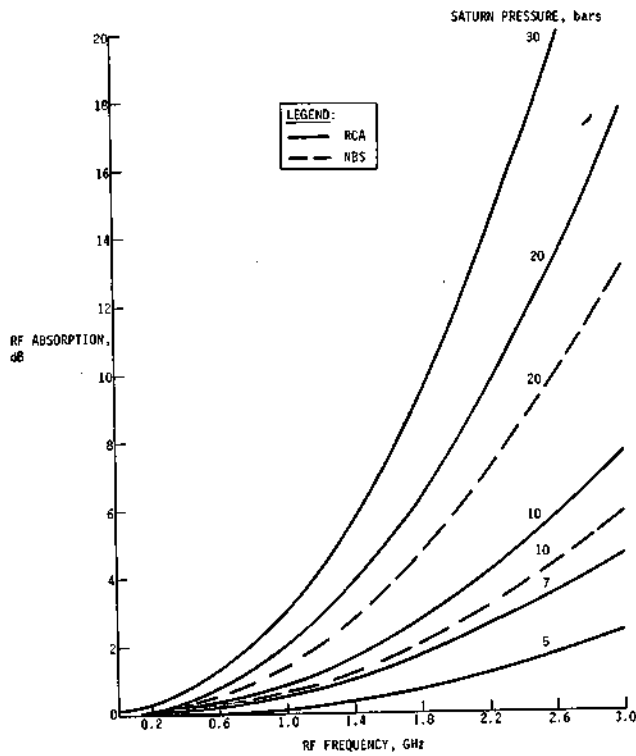


Fig. III-42 Zenith Absorption at Selected Pressures for the Saturn Nominal Atmosphere

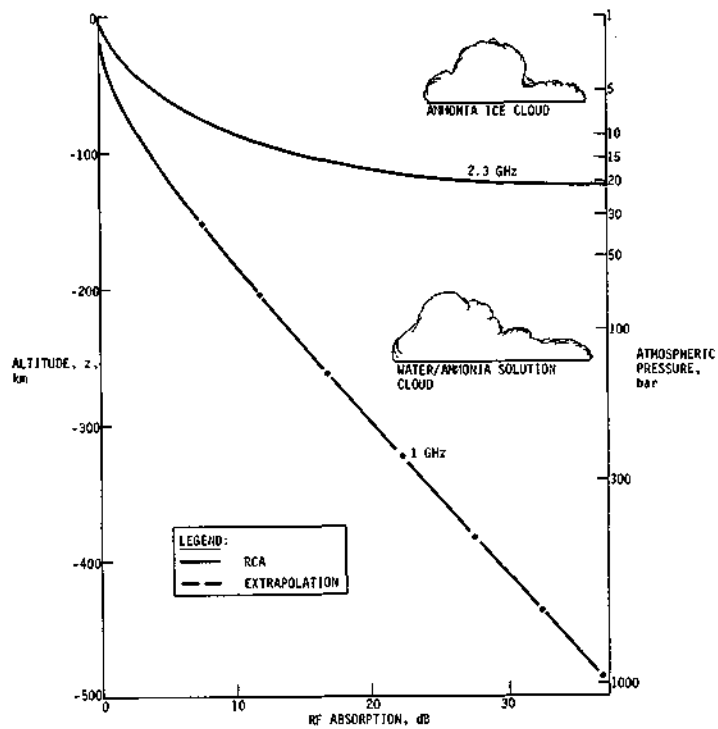


Fig. III-43 Zenith Absorption for the Saturn Cool Atmosphere

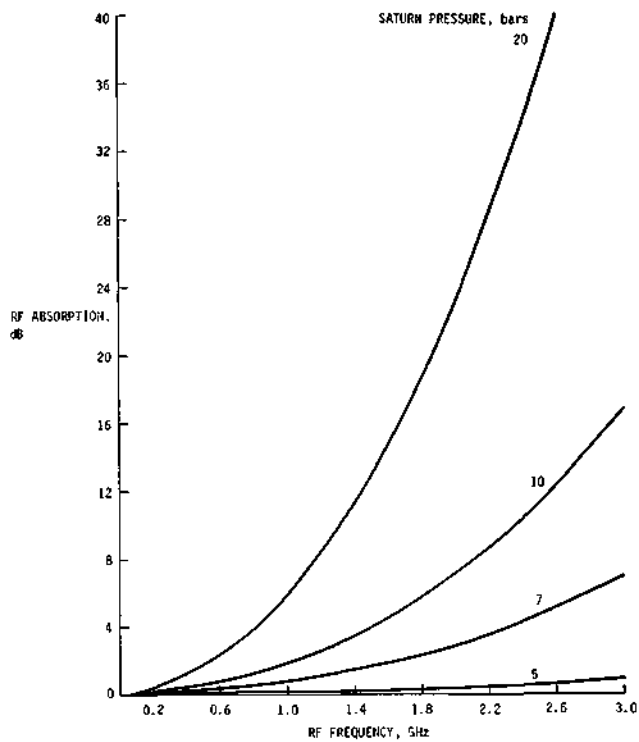


Fig. III-44 Zenith Absorption at Selected Pressures for the Saturn Cool Atmosphere

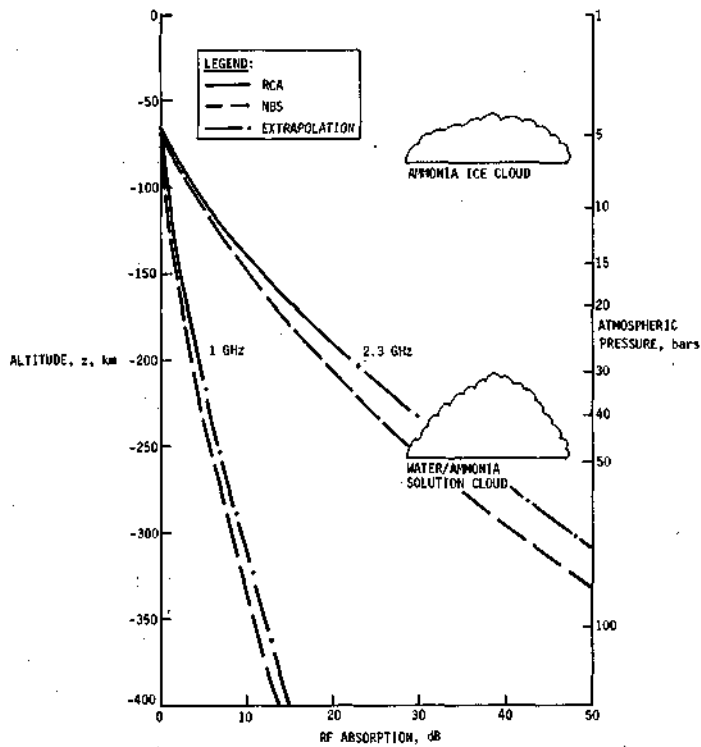


Fig. III-45 Zenith Absorption for the Uranus Nominal Atmosphere

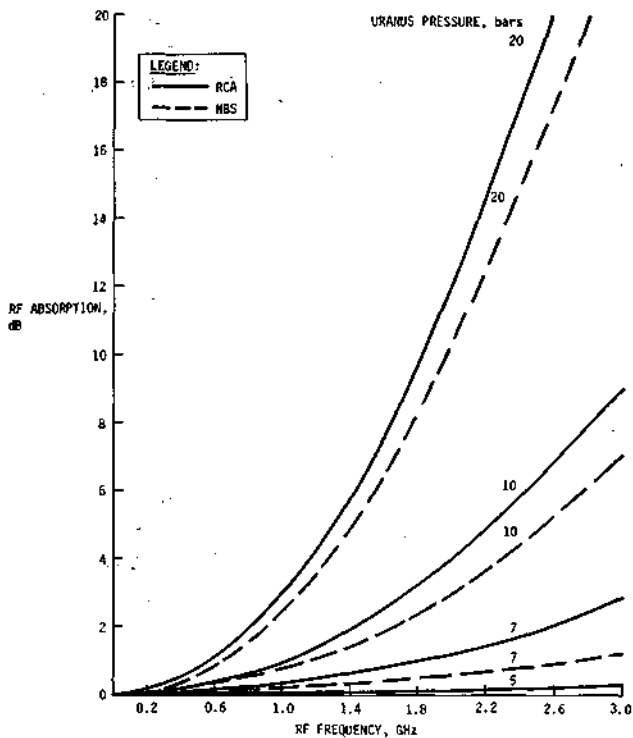


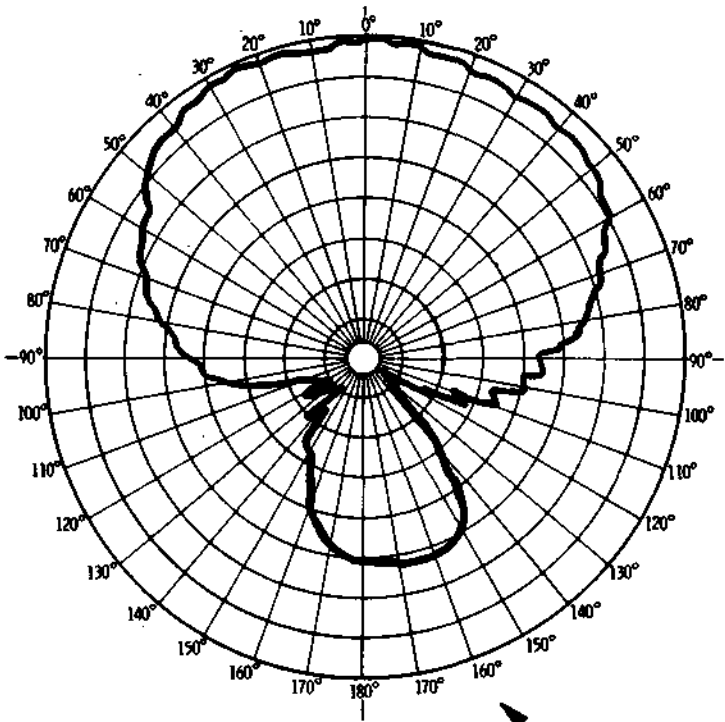
Fig. III-46 Zenith Absorption at Selected Pressures for the Uranus Nominal Atmosphere

The second change in the computation consists of implementing a calculation of the variable ammonia and water abundances in the saturated region in and above the clouds, rather than setting the abundances equal to zero above the saturation elevation. Absorption in this region is very low compared to that below the saturation elevation. Therefore, it can be neglected for probe missions that penetrate any distance below the ammonia saturation elevations, shown in Figure III-39 by the triangles. The necessity of adding this computation arose from examination of the cool Uranus model. The ammonia saturation level occurs at a pressure of 80.7 bars, so a 20-bar mission would be flown completely in the saturated region of the atmosphere. The equation used to compute ammonia abundance is shown as Equation [IVK-25], page IV-99 of Reference III-7, and was taken from Reference III-9. A similar expression was also used for the water abundance.

Computation of the absorption loss in the cool Uranus atmosphere model indicates that it is completely negligible due to the very low ammonia abundance in the saturation region and the fact that the mission is over before the ammonia cloud level is reached. Zenith absorption at 1 GHz and a depth of 28 bars was only 0.007 dB. At 3 GHz and 28 bars, absorption is only 0.06 dB. Absorption curves for the cool Uranus atmosphere similar to Figures III-45 and III-46 were therefore not plotted because the absorption is essentially zero to 28 bars. The nominal Uranus atmosphere and cool Saturn atmosphere are the two worst case atmospheres, with the cool Saturn model providing the greatest microwave absorption as seen in Figures III-43 and III-44.

c. Probe Antenna - One result of the parametric study to achieve a common probe design for the Saturn and Uranus missions was a decrease in probe aspect angles before entry. An axial pattern with 100° beamwidth will satisfy the requirements for pre-entry and descent antennas. A pair of identical antennas will satisfy the design requirements; the turnstile/cone antenna provides the most compact design among several considered.

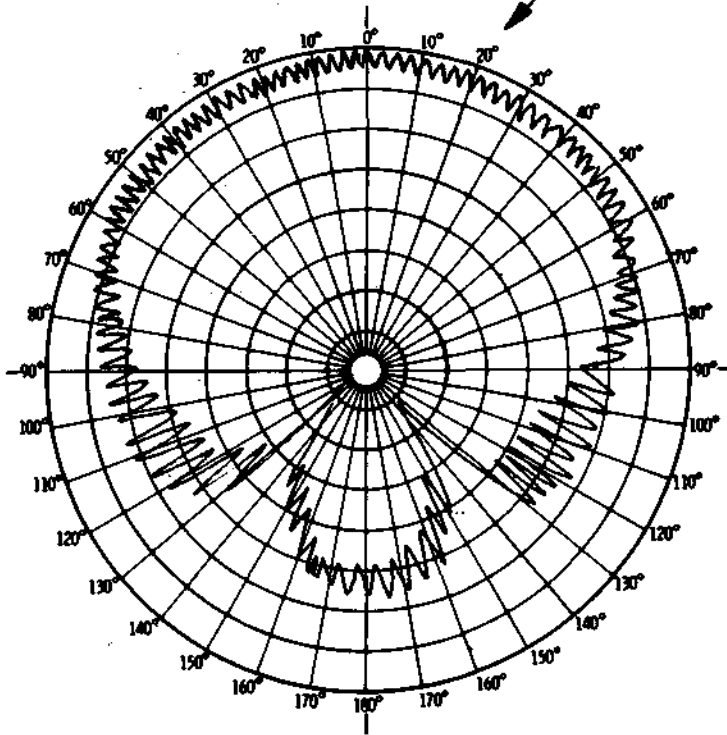
An internally funded study (Ref III-10) has developed prototype turnstile/cone antenna design with circular polarization. The measured radiation and polarization patterns are shown in Figure III-47. The main beam radiation pattern is uniform and approximately symmetrical in both the E- and H-planes. The on-axis ratio is 1.8 dB and only 2.8 dB at the 3-dB points. High circularity is a result of improved feed and ground-plane design.



CONDITIONS
E-PLANE VOLTAGE
100° BEAMWIDTH
0.86 GHz
LINEAR SOURCE

a) RADIATION PATTERN

AXIAL SCALE = 5 dB/RING



b) CIRCULAR POLARIZATION PATTERN

Fig. III-47 Circularly Polarized Turnstile/Cone Probe Antenna Patterns

A revised probe antenna design is shown in Figure III-48 for the turnstile/cone antenna. Comparison with the original design (Vol III, Figure D-7, p D-12) indicates an envelope diameter reduction from 20.3 to 15.2 cm (8 to 6 in.) and slightly increased (0.6 cm, 0.25 in.) height. The dipoles are equal in length, and wings have been added to the truncated cone apex to control pattern circularity. The weight is unchanged. As seen in the perspective view of the figure, the dipoles and wings must be supported by dielectric material (Teflon, etc) in order to withstand the high g-forces during planet entry. The antenna patterns were measured using a prototype antenna design mounted on an aluminum hemisphere 61 cm (24 in.) in diameter. The test model is shown in Figure III-49. Patterns were measured on domes of several sizes and the ground plane area affects the backlobe distribution. Therefore, full-scale radiation and circularity patterns should be recorded during hardware development to verify the predicted pattern coverage.

Thermal analysis of the descent probe indicates that the antenna will be exposed to a temperature of approximately 50°K (-370°F). The turnstile/cone antenna was qualified for operation at 172°K (-150°F) for the Viking mission. Cryogenic operation at the low temperature could result in problems with the printed circuit balun feed and the dipole elements. Preliminary analysis indicates that a radome may be required over the probe descent antenna with a heating element or thermal insulation such as spun fiberglass. Fiberglass or Teflon would be a suitable radome material and would provide thermal insulation.

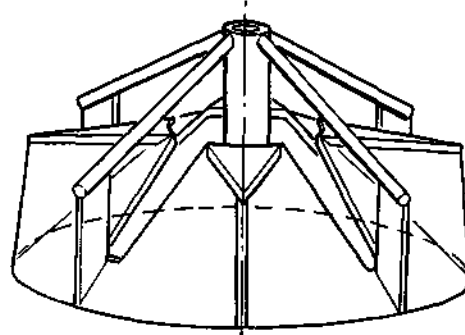
d. Polarization Loss - In the previous study an arbitrary value of 0.2 dB was used throughout all the RF link analyses as an adverse tolerance resulting from polarization loss between the probe and spacecraft antennas. During the follow-on study, an equation was added to the computer program (LINK) to calculate the cross-polarization loss as a function of the axial ratios of the two antennas and the ellipse axis aspect angle. The equation that relates this loss is expressed by:

$$P_L = 10 \log_{10} \left\{ \frac{1}{2} + \frac{2 R_1 R_2}{(1 + R_1^2)(1 + R_2^2)} + \frac{(1 - R_1^2)(1 - R_2^2)}{2(1 + R_1^2)(1 + R_2^2)} \cos (2\beta) \right\} \quad [6]$$

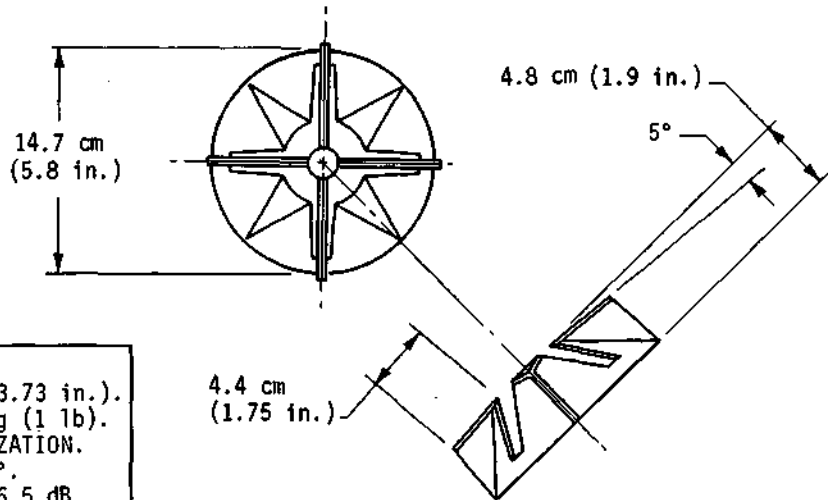
where

P_L = polarization loss, dB

R_1 = probe antenna axial ratio (voltage)



PERSPECTIVE VIEW



- NOTE:**
1. $f = 0.86 \text{ GHz.}$
 2. $\lambda = 34.88 \text{ cm (13.73 in.)}$
 3. **WEIGHT = 0.45 kg (1 lb).**
 4. **CIRCULAR POLARIZATION.**
 5. **BEAMWIDTH = 100°.**
 6. **MAXIMUM GAIN = 6.5 dB**

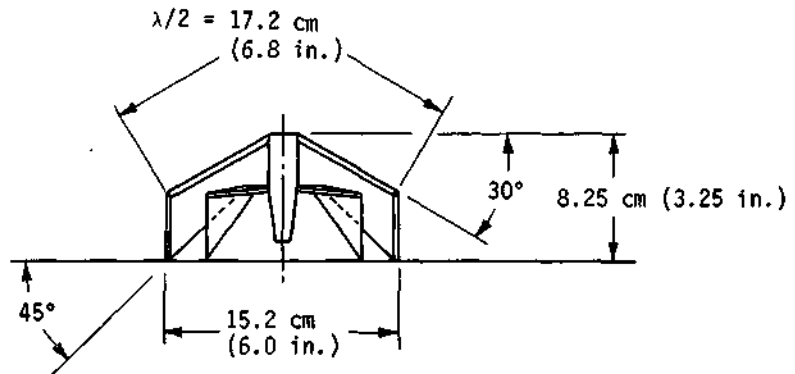


Fig. III-48 Probe Turnstile/Cone Antenna

Reproduced from
best available copy. 

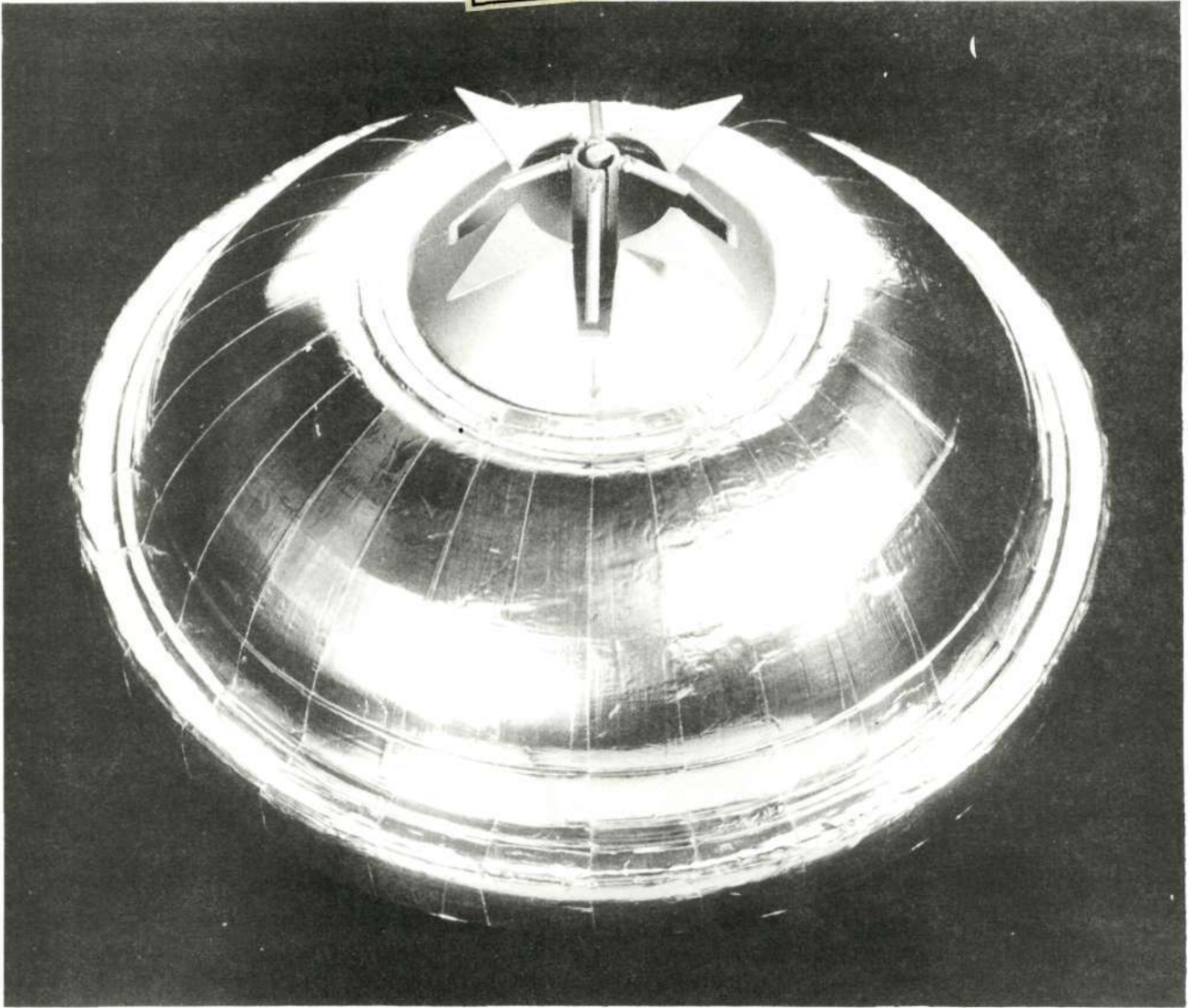


Fig. III-49 Prototype Turnstile/Cone Antenna Mounted on Probe Model

R_2 = spacecraft antenna axial ratio (voltage)

β = ellipse axis aspect angle as defined in Figure III-50, deg
($0 \leq \beta \leq 90^\circ$).

The equation is plotted in Figure III-50 along with a definition of the ellipse axis aspect angle (Ref III-11). As seen from the insert in the figure, the best case is when the ellipses are coincident ($\beta = 0^\circ$); the worst case is when the two patterns are orthogonal ($\beta = 90^\circ$).

A circularly polarized antenna pattern may be considered as an elliptical pattern with a certain circularity expressed in terms of the axial ratio. As the probe rotates about its spin axis, the probe antenna pattern will rotate in space with respect to the spacecraft antenna pattern. As seen in Figure III-47, the axial ratio for the probe antenna is 2.9 dB at the half-power points. An axial ratio of 2 dB was used for the parabolic dish antenna on the spacecraft and $\beta = 90^\circ$ for worst-case relative position. As seen from Figure III-50, the polarization loss is 0.35 dB and this value was used in all RF link calculations.

e. Probe Transmitter - Another attempt was made to survey the industry and determine availability of transmitters in the 0.8 to 1.2 GHz frequency range. Technical information was requested of 19 suppliers and 13 did not respond with data. The six suppliers who did respond provided various technical brochures on hardware that could be modified for the frequency and/or type of modulation required. Philco-Ford Western Development Labs Division, supplied the most technical information. Transmitter efficiency and package density remain the same as determined previously (Vol III, p V-23) since additional technical data indicated the same general values.

f. Spacecraft Receiver - Seventeen suppliers were requested to furnish technical information on hardware that could be modified to the probe mission requirements. Eleven vendors did not have receiver hardware that could be modified to the probe mission, and six suppliers sent general technical brochures that were not particularly applicable to the specific requirements of the receiver with the unique modulation and tone. Therefore, noise figures, weights, and package densities remain unchanged from the values used on the original portion of the study (Vol III p V-23).

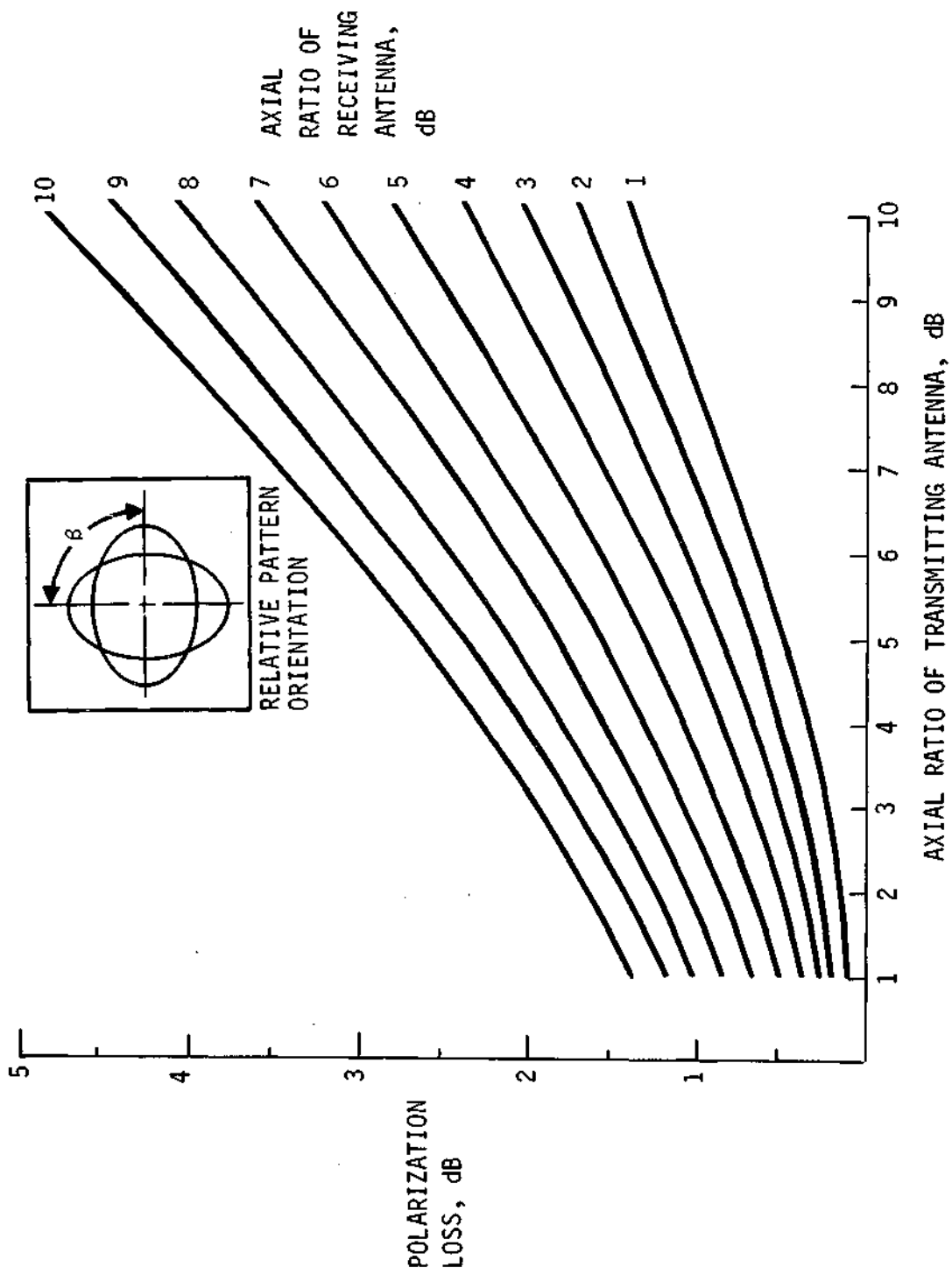


Fig. III-50 Antenna Pattern Polarization Loss

g. Parametric Designs - RF link analyses were performed first to optimize several critical parameters for the individual missions to Saturn and Uranus using the Task I science payload. This initially sized the beamwidths of the pre-entry and descent antennas and the spacecraft antenna for the optimum trajectory to each planet. Key mission communication parameters are shown in Table III-21 under Configuration 1. Parameters that were not varied are listed at the bottom of the table. The second configuration considered using the optimum probe descent antenna beamwidth for Saturn for the Uranus mission, and vice versa. As seen in the table, the RF power requirement for Saturn increased 1.2 w.

Early in the analysis, it was evident that the Saturn encounter from the common Saturn/Uranus-1980 trajectory would create the worst-case conditions. (See Table III-21.) The direct Saturn mission (Saturn 1979) did not create worst-case conditions since the trajectory could be tailored to accommodate the communications geometry required for the Saturn/SU 80 mission. The communication range is also smaller because the direct mission has a periapsis radius of $2.3 R_S$ as compared to $3.7 R_S$ for the Saturn/SU 80 mission. Saturn also has the higher atmosphere microwave absorption of the two planets, as discussed in subparagraph b. Because of these reasons, the direct Saturn mission was not investigated fully until a common probe trajectory had been finalized.

Configuration 3 considered two identical axial-beam antennas on the probe that would satisfy the probe aspect angle requirements for both planets. This was achieved by varying trajectory lead times for the two trajectories until a similar probe aspect angle profile versus mission time was established. At the same time, attempts were made to achieve a common spacecraft look direction for probe tracking at both planets. This was achieved by trajectory variations that resulted in a common spacecraft cone angle to cover both planet missions. The clock angles were also close at this time but not as close as the cone angles.

The position of the spacecraft antenna pointing for the common missions was further refined for Configuration 4, as seen in Table III-21. Minor modifications were made at this time to reduce the cone angle and optimize the spacecraft antenna gain, which further reduces the RF power required. The modifications had more impact on the RF power for Saturn than for Uranus. Configuration 4 results in missions that are common from the communications hardware standpoint, except for the disparity in spacecraft clock angle.

Table III-21 Telecommunication Subsystem Parameters for Common Probe Development

PARAMETER	CONFIGURATION									
	1-S**	1-U	2-S	2-U	3-S	3-U	4-S	4-U	5-U	5-SD
FIXED LOSSES, dB	5.9	5.9	5.4	7.1	6.3	7.4	6.2	7.3	9.0	6.2
PROBE ANTENNA PATTERN TYPE*	T/A	A/A	T/A	A/A	A/A	A/A				
PROBE ANTENNA BEAMWIDTH, deg†	30/90	90/110	30/110	90/90	100/100	100/100				
PROBE ANTENNA BEAM DIRECTION, deg	60/0	0/0	60/0	0/0						
SPACECRAFT ENTRY CONE ANGLE, deg	105	125	105	125	119	119	116	116	116	116
SPACECRAFT ENTRY CLOCK ANGLE, deg	256	275	256	275	257	275	256	275	263	254
MAXIMUM RF TRANSMITTER OUTPUT POWER, w	17.4	2.2	18.6	2.6	28	5.5	25	5.3	9.2	18.4

INVARIENT PARAMETERS
 SPACECRAFT ANTENNA BEAMWIDTH = 20°
 FREQUENCY = 0.86 GHz
 BIT RATE = 28 bps (TASK 1 DESCENT)
 $E_b/N_0 = 8.9$ dB
 BER = 5×10^{-5}
 BINARY FSK MODULATION, K = 8
 CONVOLUTIONAL ENCODER, M = 2, V = 2, Q = 8
 SIGNAL-TO-NOISE RATIO = 10 dB

DATA CHANNEL LOSSES = 2 dB
 POLARIZATION LOSS = 0.35 dB
 SATURN COOL AND URANUS NOMINAL ATMOSPHERE MODELS USED
 FIXED LOSSES INCLUDE CIRCUIT LOSSES, ADVERSE TOLERANCES, AND 3σ VALUES OF SPACE LOSS, PROBE POINTING AND SPACECRAFT POINTING LOSSES
 SYSTEM NOISE TEMPERATURE
 1750°K FOR SATURN
 690°K FOR URANUS

* PROBE ANTENNA PATTERN AND TYPE
 T = TORUS (BUTTERFLY), ANNULAR SLOT
 A = AXIAL, TURNSTILE/CONE

† DUAL VALUES ARE FOR PRE-ENTRY/DESCENT TRAJECTORY CONFIGURATION
 **MISSIONS
 S = SATURN/SU 80 MISSION
 U = URANUS/SU 80 MISSION
 SD = SATURN 79 DIRECT MISSION

Adjustments were made in probe deflection for Uranus to reduce the clock angle and provide for a common spacecraft receiving antenna LOS direction. Configuration 5 in the table shows the results after adjustment was made for Uranus. The spacecraft clock angle was reduced 12° with only a slight change in cone angle. The 116° nominal cone angle position covers the mission satisfactorily. The probe aspect angle increased from 35° to 43° at mission completion. The increased fixed losses result in the RF power increase to 9.2 w required at probe entry, which is the worst-case point for the Uranus mission.

With the communication parameters determined for the common Saturn/Uranus 1980 mission, the direct Saturn 1979 mission was investigated to determine the RF power required. The results are shown in Table III-21 as Configuration 5-SD. To satisfy the common mission requirements, 18.4 w of RF power is required.

Parametric variations in certain key communication parameters (probe aspect angle, clock angle, cone angle, etc) have resulted in a common probe design with a communication subsystem that will operate for either the S/U 80 or S 79 missions. The Saturn/SU 80 mission (Configuration 4-S) contains worst-case conditions from the standpoint of communication subsystem design. The direct Saturn 1979 mission (Configuration 5-SD) was second and Uranus/SU 80 mission (Configuration 5-U) was third in order of RF transmitter output power required for the Task I science payload, as seen in Table III-21. Design details of the Saturn/SU 80 mission are described in Chapter IV, and used in Chapter V, Section D since it is the worst-case mission.

Table III-22 depicts a comparative summary of the three missions for the follow-on study and the two missions for Saturn (JST 77) and Uranus (JU 79) of the basic study described in Volume II, Section B of Chapters VI and VII. Communication parameters that were sensitive to the communication geometry are shown in the table for the five missions. The new Saturn mission (S/SU 80) has increased range, bit rate, fixed losses, and atmosphere attenuation. The new Uranus mission (U/SU 80) uses a spacecraft antenna with higher gain to offset a smaller probe antenna gain, higher bit rate, and increased fixed losses in the link. The net result is 2.7 w more RF power required for the Uranus encounter from the S/U 80 trajectory.

Table III-22 Telecommunications Subsystem Characteristics Comparison Summary

PARAMETER	SATURN			URANUS	
	JST 77	S/SU 80	S 79	JU 79	U/SU 80
ENTRY ANGLE, γ_E , deg	-25	-30	-30	-60	-60
PERIAPSIS RADIUS, R_p	2.3 R_S	3.8 R_S	2.3 R_S	2.4 R_U	2.0 R_U
EJECTION RADIUS, 10^6 km	10	30	30	10	10
DEFLECTION MODE	PROBE	SPACECRAFT	SPACECRAFT	PROBE	SPACECRAFT
ENTRY COMMUNICATION RANGE, km	9.6×10^4	2×10^5	10^5	1.5×10^5	8.8×10^4
PROBE ASPECT ANGLE, ψ , deg					
ACQUISITION	55	46	45	19	34
ENTRY	48	44	42	18	31
END OF MISSION	8	24	14	10	43
SPACECRAFT CONE ANGLE, ϕ , deg					
ENTRY	91	120	122	159	132
END OF MISSION	59	113	103	150	106
SPACECRAFT CLOCK ANGLE, θ , deg					
ENTRY	177	257	254	260	263
END OF MISSION	173	254	250	257	251
PROBE PRE-ENTRY ANTENNA					
ANTENNA TYPE	SLOT	TURNSTILE	TURNSTILE	TURNSTILE	TURNSTILE
PATTERN TYPE	TORUS	AXIAL	AXIAL	AXIAL	AXIAL
BEAMWIDTH, deg	30	100	100	90	100
MAXIMUM GAIN, dB	5.2	6.5	6.5	7	6.5
PROBE DESCENT ANTENNA					
ANTENNA TYPE	TURNSTILE	TURNSTILE	TURNSTILE	TURNSTILE	TURNSTILE
PATTERN TYPE	AXIAL	AXIAL	AXIAL	AXIAL	AXIAL
BEAMWIDTH, deg	90	100	100	90	100
MAXIMUM GAIN, dB	7	6.5	6.5	7	6.5
SPACECRAFT RECEIVING ANTENNA					
ANTENNA TYPE	HELIX	DISH	DISH	HELIX	DISH
BEAMWIDTH, deg	35	20	20	35	20
MAXIMUM GAIN, dB	13.5	18.3	18.3	13.5	18.3
FREQUENCY ACQUISITION TIME, sec	40	31	29	25	18
RF POWER OUTPUT AT 0.86 GHz, w	6.5	25	18.4	6.5	9.2
BIT RATE, bps	26	28	28	26	28
WORST-CASE POINT	END OF MISSION	END OF MISSION	END OF MISSION	ENTRY	ENTRY
WORST-CASE ATMOSPHERE	NOMINAL	COOL	COOL	NOMINAL	NOMINAL

The three major communications geometry parameters that determine a common telecommunications subsystem design are variations in probe aspect angle, spacecraft cone angle, and spacecraft clock angle. Differences in communications range relate directly to the RF power required to overcome greater space loss. These three angles were varied to achieve commonality that results in a common probe pre-entry and descent antenna beamwidth and a probe receiving antenna on the spacecraft that is fixed in look direction as defined by the cone and clock angles.

Probe aspect angles for the three missions are shown in Figure III-51. End-of-mission conditions for the Saturn/SU 80 mission was used to size the descent antenna beamwidth because maximum gain and minimum beamwidth is required for that mission. The angle is 24° and 3° for 3σ variations and 20° to account for parachute swing is added to the nominal value. The antenna should have a half-power (3 dB) point at approximately 50° ($24^\circ + 20^\circ + 3^\circ$) or a beamwidth of 100° . As seen in the figure, the end-of-mission angle for Uranus is 43° and 3σ variations are 6° . An optimum beamwidth for Uranus is 140° . The 100° beamwidth for Uranus is down by 6 dB from a maximum of 6.5 dB. The 140° beamwidth requirement for Uranus is less severe on a 100° beamwidth than the performance requirements at Saturn. Adverse tolerances have been added to the Uranus RF link design to compensate for the low probe antenna gain. Therefore, two identical probe antennas are used for the common probe design. A circularly polarized axial beam antenna with a maximum gain of 6.5 dB and 100° beamwidth will cover probe aspect angle variations for the three missions and is optimized for the Saturn/SU 80 encounter, which requires maximum antenna gain.

Spacecraft cone and clock angles for the three missions are shown in Figure III-52. Relative probe movement in the elevation plane is accurately depicted by the cross-cone angle as defined in Volume II, Chapter IV.E.1, pp IV-37 through IV-39. The cross-cone angle has a zero reference at a particular clock angle (Vol II, Figure IV-16, p IV-39), and plots of several missions on the same cross-cone angle versus cone angle would not be realistic because each zero-reference cross-cone point has a different clock angle value. For the three missions of interest, the cone angle is near 115° and the clock and cross-cone plots are nearly identical. Therefore, plots were made of the relative probe movement including 3σ dispersions on a cone angle versus clock angle plot as shown in the figure. A common plot was required in order to optimize the position of the probe receiving antenna on the spacecraft, and modify the trajectories so that clock and cone angles were within 10° of each other. The design goal was to eliminate spacecraft antenna pointing complexity by having the relative probe positions for the three missions occurring in the same general point in space. Thus, a fixed antenna could be employed on the spacecraft.

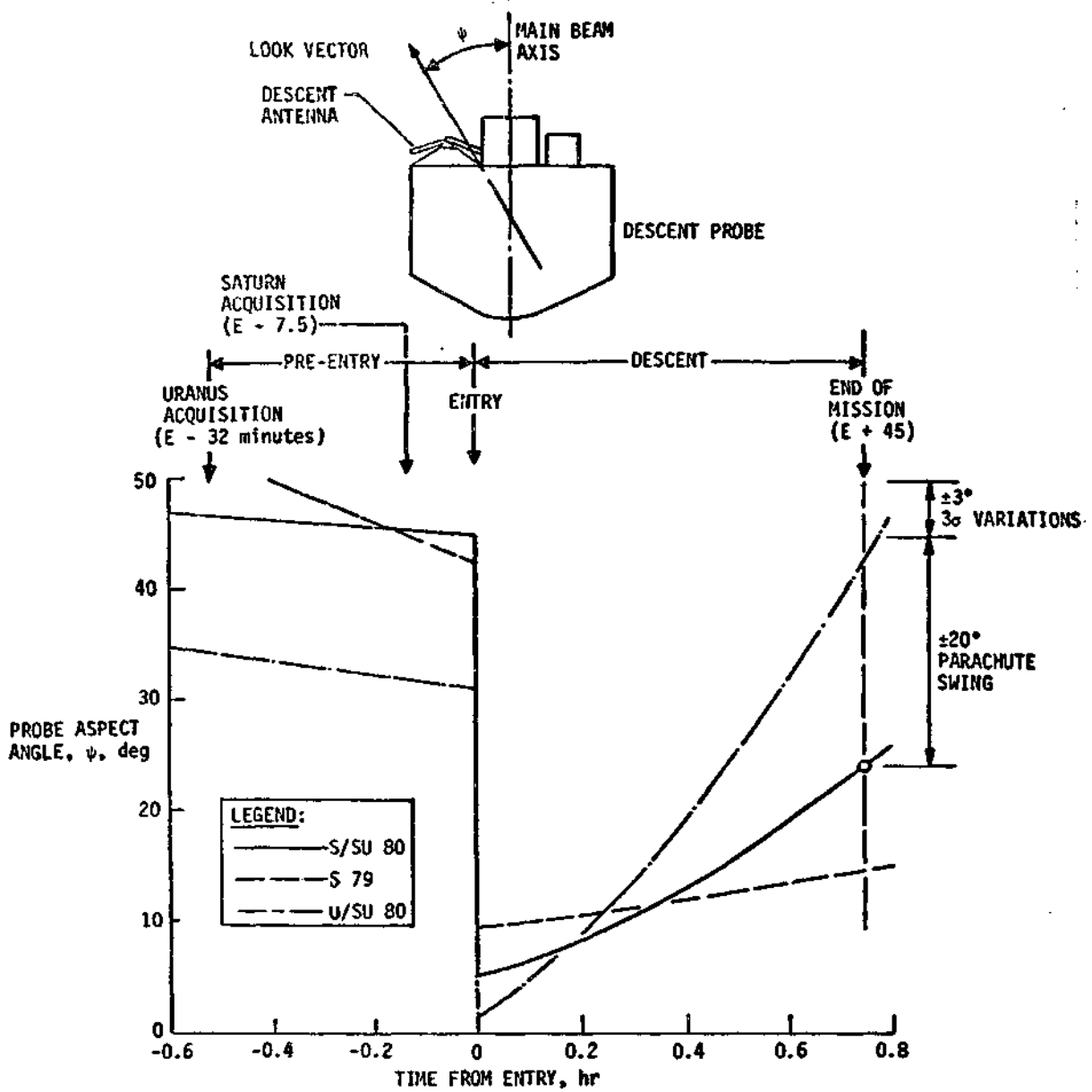


Fig. III-51 Probe Aspect Angle for the Three Missions

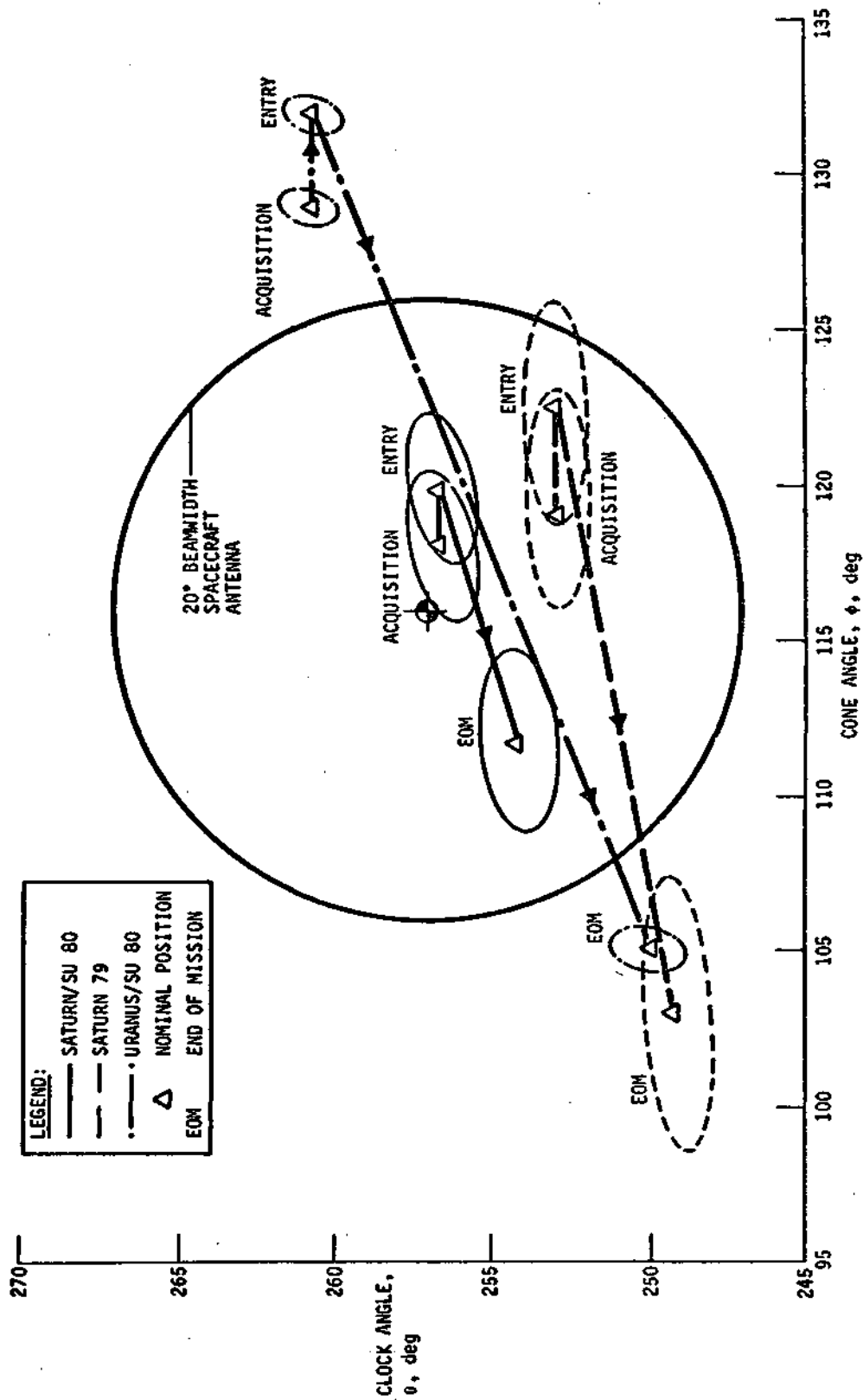


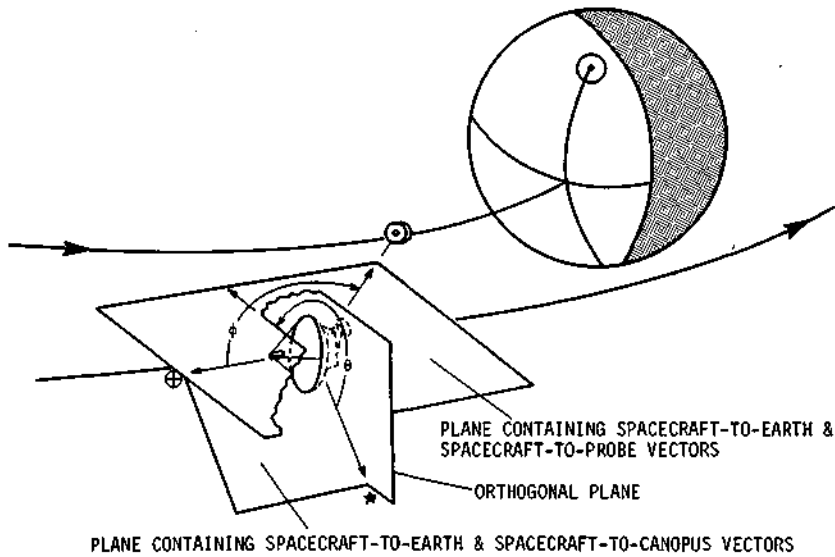
Fig. III-52 Spacecraft Antenna Requirements for the Three Missions

The cone and clock angles are defined in Figure III-53. These two angles determine a vector direction that represents relative probe movement from a fixed reference system on the spacecraft. The probe vector direction also defines the probe receiving antenna boresight position. The planes shown in the figure contain the Canopus meridian and cone meridian. The cone angle is the angle included by the Earth-to-spacecraft-to-probe alignment; the clock angle is the angle between the Canopus meridian and the cone meridian measured as shown in the figure.

The parametric studies indicated the Saturn encounter from the SU 80 trajectory as having maximum communications range; therefore, the spacecraft antenna gain was maximized in order to minimize the RF power required in a manner similar to the probe aspect angle adjustment. As seen in Figure III-52, the antenna boresight (look direction) was chosen for optimum coverage with minimum beamwidth for the Saturn/US 80 mission. A beamwidth of 20° with a peak gain of 18.3 dB and circular polarization was chosen, which can be met with a parabolic dish antenna. The chosen beamwidth will also cover the other two missions, but less efficiently. The end of mission is outside the 3-dB beamwidth for the direct Saturn mission and conditions are worst for the Uranus mission. Entry is 17° off boresight with a gain of 8.6 dB at that point. The gain improves during descent and then is again 14° off boresight at mission completion and moving away rapidly. The gain at the end of mission is 12.1 dB. The Uranus mission certainly is not optimized from the standpoint of antenna gains, but less gain is required since the communications range and atmosphere losses are less.

2. Data Handling and Sequencing (DHS) Subsystem

The basic concepts of the DHS are unchanged from those of the previous volumes of this report. The functions provided are data acquisition from digital and analog science and engineering interfaces, storage, sequencing, formatting, and coding. There are no provisions for data compression or adaptive control with the minor exception of the use of discrete signals from the science instruments and g-switches to provide effective control of data storage and descent format. A functional block diagram of the DHS is shown in Figure III-54.



NOTE: 1. ϕ = CONE ANGLE MEASURED FROM EARTH VECTOR TO PROBE VECTOR, $0 \leq \phi \leq 180^\circ$
 2. θ = CLOCK ANGLE MEASURED FROM CANOPUS VECTOR TO PROBE VECTOR, COUNTERCLOCKWISE LOOKING AT ANTI-EARTH, $0 \leq \theta \leq 360^\circ$

Fig. III-53 Definition of Spacecraft-to-Probe Look Direction

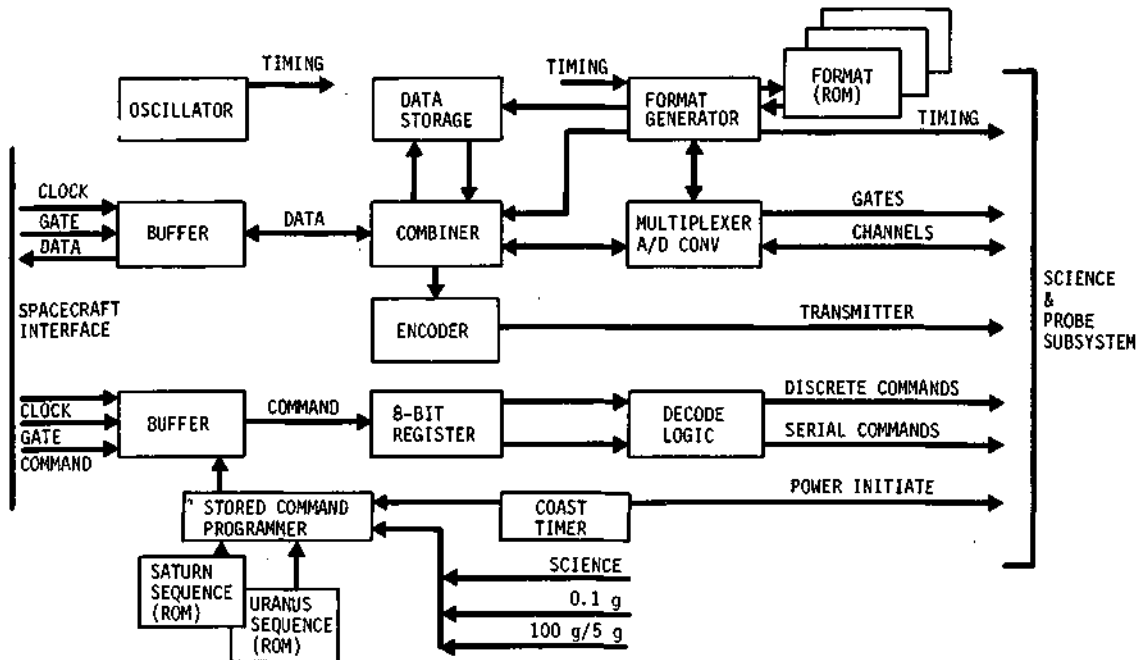


Fig. III-54 Data Handling Subsystem

a. *Probe/Spacecraft Interface Functions* - All probe checkout functions are implemented by commands from the spacecraft through the in-flight disconnect to the probe DHS. Although launch and cruise operations have not been defined, it is expected that the DHS and accelerometers will be operating during launch and some minor maintenance functions such as removal of outgassing products from the science instruments, will probably be required during cruise. The capability to operate the probe subsystems individually and in reduced modes is necessary in order to maintain the peak power demand from the spacecraft during cruise and pre-separation checkout within acceptable limits. This capability is provided by the power distribution unit (power and pyrotechnic subsystem) which is controlled by the DHS. Pre-separation checkout must be initiated early enough to allow at least one update by the ground station. Capability is provided to switch out failed subsystems that are not essential to the operation of the probe in a reduced data mode mission, and it is recommended that pre-separation checkout be initiated early enough to allow several revisions of the probe programming. The present concept of the coast sequencing is implemented by an Accutron timer. Since this component is factory set and not continuously programmable, operation must be initiated at a precise interval prior to probe entry. In order to meet requirements for the two-planet mission, an extra set of output contacts must be provided and will be selected by latching relay before separation. The coast timer is the only active component in the probe subsystem during the coast period, and it contains its own power source. Although basically a sequencing function, the timer is shown as part of the power and pyrotechnic subsystem since its only purpose is to initiate the first pre-entry pyrotechnic event. The only other active component during separation is the spin-up electronics. Spinup is implemented by a simple timer and two pyrotechnic valves. These pyrotechnics will be operated directly off the post-separation battery through relay contacts. An RC timer will provide adequate accuracy and is naturally resistant to EMI produced by the pyro events. Operation will be initiated by the separation event that removes a ground from the timer. The first pyro event occurs 0.5 seconds after separation; the second at 1.26 seconds after separation (0.76 seconds spin-up time).

b. *Data Handling Subsystem Design* - As stated, the basic concept of the DHS is unchanged from the design described in previous volumes of this report, but some modifications have been made to optimize the design for the two-planet mission. Program sequencing is provided by a timer and two ROMs; the correct ROM is selected during the pre-separation period by a latching relay.

An additional discrete is included in this design to improve descent sequencing. Sensing of the deceleration decreasing to 5.0 g subsequent to 100-g deceleration provides more accurate data for descent sequence control than the 100-g discrete alone.

The memory electronics have been modified from previous bipolar IC design to COS/MOS electronics. Considering the present state of the art, this approach provides a more realistic design. It is anticipated that in the expected time frame of hardware development, all the DHS electronics will be COS/MOS. It is also estimated that a completely redundant DHS would have weight volume, and power characteristics similar to that of the present nonredundant bipolar data processing electronics alone (2.13 kg, 6.9 w, 2330 cm²). The basis used for sizing the memory consisted of the following assumptions:

- 1) use of 1024-bit chip (Intel-1103 or TI-TMS4062JC)
- 2) 30 chips plus 10% of memory for peripheral circuits
- 3) 5 μ w/bit, standby; 25 μ w/bit, operating
- 4) 50% power conditioning efficiency
- 5) 9.7 cm²/chip, 0.76 cm board thickness, 1.5 cm board spacing
- 6) 0.91 gm/cm³ (board only)

On this basis the following memory parametrics were generated:

- 1) volume = 443 + 16.0 M (10⁻³) cm³
- 2) weight = 0.2 + 0.715 M (10⁻⁵) kg
- 3) power (standby) = 0.2 + 11.0 M (10⁻⁶) w
- 4) power (operate) = 1.0 + 55.0 M (10⁻⁶) w
- 5) memory = M (number of bits stored)

The DHS begins initial descent sequence shortly after the descent battery is energized. The initiation of the sequence and the initial state of the DHS will be established by a timing circuit working off battery voltage. This will ensure that the turn-on battery transient has subsided, and will eliminate the need of an additional event from the coast times. The required sequence

of events is illustrated in Table IV-1 (Saturn Sequence of Events, Task I). The pre-entry sequence occurs from item 19 to item 22 inclusive. The actual time with respect to entry of these events will vary (± 4.4 min, Saturn; ± 29 min, Uranus) due to trajectory uncertainties. The control state established at item 22 will remain fixed regardless of the actual time before entry until 0.1-g sensing (item 24). The functions required of the DHS formats with respect to the Task I Saturn sequence are as follows.

FROM ITEM	TO ITEM	FORMAT
19	22	STORE ENGINEERING DATA
22	24	INTERLEAVE STORED AND REAL-TIME ENGINEERING DATA
24	30	STORE ENTRY ACCELEROMETER SCIENCE AND ENGINEERING DATA
30	31	STORE DESCENT SCIENCE AND ENGINEERING DATA
31	33	INTERLEAVE STORED AND REAL-TIME SCIENCE AND ENGINEERING DATA

During periods 22 to 24 and 31 to 33, the interleaved data is sequenced to the encoder and RF transmitter. The sequence and formatting for Task II follows a similar pattern (Table V-1).

FROM ITEM	TO ITEM	FORMAT
19	25	STORE ENGINEERING DATA
25	27	INTERLEAVE REAL-TIME PRE-ENTRY SCIENCE AND ENGINEERING DATA WITH STORED ENGINEERING DATA
25	27	STORE PRE-ENTRY SCIENCE AND ENGINEERING DATA
27	33	STORE ENTRY ACCELEROMETER AND ENGINEERING DATA
33	34	STORE DESCENT SCIENCE AND ENGINEERING DATA
34	35	INTERLEAVE REAL-TIME DESCENT SCIENCE AND ENGINEERING DATA WITH STORED SCIENCE AND ENGINEERING DATA IN THIS ORDER: (a) ITEM 27 TO 34; (b) ITEM 25 TO 27

The interleaved data (item 22 to 27 and item 34 and 35) is sequenced through the encoder to the RF transmitter. The retransmission of the pre-entry data (items 34, 35) is an option that provides some data redundancy, however, other options such as increased descent science may eventually prove more favorable.

c. Coding - On these missions, the purpose of coding is to provide a significant reduction in RF power. The selection of convolutional encoding is recommended because of the simplicity of the circuitry. The constraint length selection will ultimately be influenced by the capabilities of the spacecraft relay link and ground station decoding cost. Long constraint lengths will decrease required probe power but increase the complexity of the decoding equipment. Although the Viterbi decoding algorithm is recommended for this design, longer constraint lengths would favor sequential decoding. The trades between decoding methods would depend on a critical evaluation of the required equipment for each approach with variations in constraint length and code rate. The result would be weighted by the available onboard computational capability of the spacecraft if decoding on the spacecraft is a consideration. Since adequate models for such an evaluation are not defined, this trade is considered beyond the scope of this study. The classic comparisons between convolutional and block codes are also applicable. The use of block codes would suggest decoding at the ground station due to the cost of possible loss of block synchronization. The increased number of symbols of coded data place an increased burden on the spacecraft relay link and/or data storage. If sufficient spacecraft storage is available or it is considered feasible to relay the coded data in real time, it is recommended that decoding be performed at the ground station. With the code presently recommended, the total number of symbols of the coded data is increased by a factor of eight over the basic data due to the rate 1/2 code and the required quantization. The Viterbi algorithm is recommended for the decoder (constraint length = 8) if decoding is required on the spacecraft. If additional storage capability is required on the spacecraft for probe data, the state of the art of tape recorders must be traded off against COS/MOS approaches. A tape recorder in general represents an overdesign of spacecraft memory with respect to total probe data link storage requirements. It is anticipated that state of the art design could reduce the estimated COS/MOS weight, size, and power by a factor of four. Reliability of either approach represents the greatest uncertainty at this time. Present development of COS/MOS for space applications is advancing rapidly. It is anticipated that a COS/MOS memory could be tested in flight and failed blocks programmed out by spacecraft control. Catastrophic failure of data storage would then be an extremely remote possibility. This is the recommended approach.

3. Power and Pyrotechnic Subsystem

The configuration of the power and pyrotechnic subsystem is illustrated in Figure III-55 and is unchanged from the basic concepts of previous volumes of this report.

Power is supplied, as required, to the probe from the spacecraft power system during all periods before separation. Remote activated Ag-Zn batteries provide probe power during post-separation activity (~4 min) and the entry and descent period (<2 hr). Two Hg-Zn batteries provide power for the coast timer (1.3 v) and the first pre-entry pyrotechnic event (36 v). The power distribution unit responds to commands from the DHS to provide all required power sequencing of the probe subsystems; latching relays provide the switching function. The pyrotechnic subsystem uses capacitor bank discharge to fire entry and descent ordnance devices. SCR switches discharge the banks and latching relays perform arming and safing. The pyrotechnic electronics provide requires power conditioning, ordnance circuitry isolation, and logic required to decode the commands from the DHS. The two pyrotechnic events that occur during spinup derive initiation energy directly from the battery. This avoids the necessity of activating the descent pyrotechnic subsystems and the DHS. A simple RC timer that is highly resistant to pyrotechnic EMI is sufficiently accurate to provide the required discrete signals.

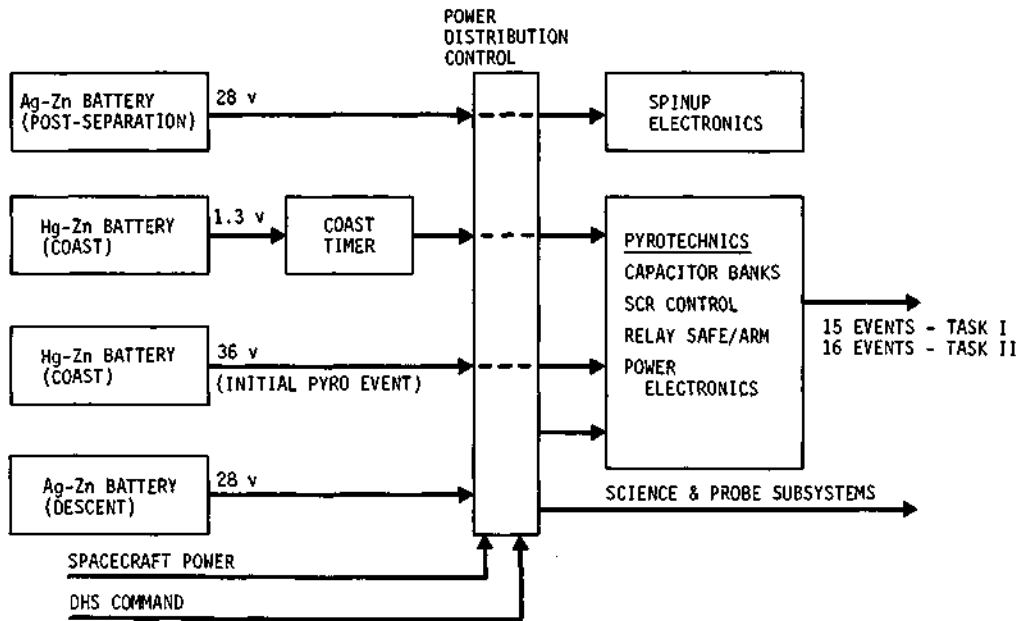


Fig. III-55 Power and Pyrotechnic Subsystem

a. *Power Sources* - The post-separation battery energy requirement is composed of power required for the spin-up electronics and two pyrotechnic events. The battery selection was based on available rather than optimum design. Energy requirements for the simple circuitry indicated would not exceed 0.1 w-hr as compared to the indicated capability of approximately 12.0 w-hr of the selected battery. The excess capacity provides capability for limited pyrotechnic firing. Some test verification or cell redesign may be required. The battery characteristic and the number of cells (20) indicate a voltage of 1.4 volts per cell at 1.0 amperes. Assuming a typical linear characteristic and a minimum battery voltage of about 10.0 volts, a maximum current of approximately 10.0 amperes could be developed. The basis of these estimates is as follows:

$$I_{\min} = 5.0 \text{ amp (minimum bridgewire current)}$$

$$R = 2.0 \text{ ohms (assumed total bridgewire and circuit resistance)}$$

$$V_{\min} = 10.0 \text{ volts} = 5.0 \text{ amp} \times 2.0 \text{ ohms}$$

$$I_b = 10 \text{ amp (minimum battery current for two bridgewires)}$$

$$V_c(1.0) = 1.4 \text{ volts (28 volts per 20 cells at 1.0 amp)}$$

$$V_c(0.0) = 1.5 \text{ volts } \Delta V_c(1.0) = 0.1 \text{ volts}$$

$$\Delta V_c(10.0) = 1.0 \text{ volt } V_c(10.0) = 0.5 \text{ volt}$$

These calculations are based on the preliminary test data for this battery. The cell voltage as a function current density is higher than that indicated from standard sources (NASA SP-172 Batteries for Space Power Systems) but is conservative with respect to more recent data provided by the MMA-D battery area for new Ag-Zn primary cells. Since this battery has very short required life and the circuitry may be designed around the voltage fluctuations, a significant decrease in post-separation system complexity may be achieved by using direct battery operated pyrotechnics.

The weight and volume of Ag-Zn remote activated battery for the entry and descent phase are estimated on the same basis as in previous volumes of this report (Vol III, Appendix G). The required commonality necessitates the use of the higher power at Saturn and the longer trajectory (due to uncertainties) as Uranus.

Hg-Zn batteries are selected for the 1.3-volt coast timer and the 36-volt pyrotechnic battery. The coast timer battery is required to deliver less than ten micro-amperes for a maximum period of 35 days (Saturn). The pyrotechnic battery provides power to charge at least two banks of capacitors and supply associated leakage current for one hour. At that time a contact on the timer closes operating a relay to fire the ordnance device which activates the entry/descent battery. Each battery is required to meet storage life requirements for the maximum cruise period (approximately 8 yr). The two principal contending types are a Hg-Cd battery and a Hg-Zn battery. Information from Electrochem (Hg-Cd) and Mallory (Hg-Zn) indicates that both batteries have sufficient shelf life for this application. Preliminary studies show that the Hg-Zn battery has approximately a 30% advantage in size and weight. However, since the total volume and weight involved is small, the ultimate decision should be based on confidence in expected storage life. The major reliability problems in storage are the achievement of a lead-proof seal and the effect of chemical changes within the battery. The Hg-Cd cell is more resistance to extreme temperature environments but is not at present manufactured in appropriate sizes for this low-power application; leakage of small cells is indicated as a design problem which needs further study. Hg-Zn cells have an extensive history of application and long-life reliability problems are under study for pacemaker applications. The major reliability consideration for long storage life for either type of cell appears to be internal chemical changes, although test data indicate this is a solvable problem. The obvious major difficulty with either cell design is predicting long-term failure rates on primary cells; accelerated testing (at high temperature) of cells from the same manufactured lot is the most promising solution at this time. Detailed X-ray examination and hard vacuum test to detect leakage induced outgassing are techniques that could be applied during flight acceptance testing. For the purposes of this study, the selection of the Hg-Zn cell is academic, pending further study of long shelf-life problems. The weight and volume specified for this application will accommodate either type cell.

b. Pyrotechnic Subsystem - The two contending approaches for initiating entry/descent ordnance devices are capacitor bank discharge and deriving current directly from a battery. The use of battery-initiated descent pyrotechnics would require isolation (approximately 40-amp pulse) from the main power bus and ground. The initial pyrotechnic event would require the use of Ni-Cd batteries (5 w-hr/lb) or hybrid system that incorporated capacitor banks from this event alone. The application of the capacitor bank approach has greater inherent redundancy, decreased EMI problems, and, for the low total number of events (15 events), is a weight effective design.

The subsystem defined for the Saturn/Uranus entry probe uses SCR switches to initiate firing. The requirements and constraints for for this design are:

- 1) maximum current less than 34.5 amp
- 2) minimum current greater than 8.0 amp 0.5 msec after current initiation;
- 3) all fire energy 100 m joules in less than 5.0 msec;
- 4) bridge wire resistance 0.95 to 1.15 ohms;
- 5) SCR voltage drop defined by $E = V + IR$, $V = 1.25$ volts, $R = 0.043$ ohms;
- 6) maximum rate of SCR current 150 amp/ μ sec;
- 7) capacitor, tantalum porous plug, $C = n82 \mu f \pm 5\%$;
- 8) equivalent series resistance (ESR) less than 4.2 ohms/capacitor over temperature range.

For total capacitance less than 1000 μf , 5.0 msec is long compared to the circuit time constant and the energy dissipated is:

$$H = \frac{E_o^2}{2R} R_I C$$

R_I = bridgewire resistance = $1.05 \pm 10\%$ ohms

C = total capacitance = $n82 \pm 5\%$ μf

n = number of 82 μf capacitors

R = series resistance at bridgewire, SCR, relay contacts, ESR ($4.2/n$) and circuit wiring

E_o = charge voltage minus SCR drop = $36 \pm 10\% - 1.25$ volts

$$H = \frac{0.034 n}{1.35 + \frac{4.2}{n}} \text{ Joules}$$

$H = 0.146$ Joules $n = 8$

Nominal capacitance/band = $8(82) = 656 \mu f$.

The current rate of rise constraint is met with the use of a 2.0 μ h choke in series with the SCR. This does not have a significant influence on the delivered energy at 5.0 msec. For actual hardware design, the total resistance and inductance of the initiator circuit must be carefully scrutinized; however, this analysis closely approximates values determined in Viking tests.

4. Attitude Control

The attitude control dynamics are minimal for the design configuration considered for the Saturn/Uranus probe. The errors involved are:

- 1) initial error due to spacecraft pointing;
- 2) drift error accumulation during period between separation and spinup due to tipoff rate;
- 3) error due to tipoff rate combined with spinup;
- 4) error due to spinup jet misalignment.

Only momentum vector errors are of significance in this analysis since nutation errors are damped out and the spin axis (principal moment of inertia) will align with the momentum vector. The momentum vector errors involved are discussed in the following:

- 1) Initial error is a function of the spacecraft and will not be discussed.
- 2) Drift error - Assuming an initial tipoff rate of 0.5 deg/sec about a nominal X-axis, the spin axis is displaced in the minus y direction.

$$\theta_T = W_T t_D$$

$$\theta_T = \text{drift error}$$

$$W_T = \text{tipoff rate}$$

$$t_D = \text{drift period}$$

- 3) Tipoff rate combined with spinup - This error was analyzed in Vol III, Appendix F of this report. The analysis results in a series solution. The initial (significant) terms are summarized:

$$\theta_x(p) = P_x(o)/P [1 + q^2/24 - q^4/2688 + q^6/506880 \dots]$$

$$\theta_y(p) = P_x(o)/P [-q/2 + q^3/240 - q^5/54569 \dots]$$

the position of the spin axis is given by

$$\theta_x(\hat{K}) = P_x(o)/P [q^2/6 - q^4/366 + q^6/42260 \dots]$$

$$\theta_y(K) = P_x(o)/P [-q + q^3/40 - q^5/5456 \dots]$$

P = angular momentum

$$q = P^2/mI_t$$

m = torque

I_t = transverse moment of inertia

R = spin-axis unit vector

- 4) Spin jet misalignment - Lower moments of inertia and higher torques enable a simpler analysis of the effect of this misalignment. Since the probe rotates less than 15° for Task I and Task II, the error due to the spin jets may be based on impulse analysis. From Appendix F, Vol III, the 3σ tolerances involved are as follows. The resulting RSS error applies to Task I and Task II.

Nozzle/flange, cm	0.0254
Flange, cm	0.0762
Cg location, cm	0.038
Mounting surface, deg	0.1
Thrust moment arm, cm	38
Thrust vector, deg	0.1
Number of thrusters	2
RSS torque vector error, deg	0.136

The time constant of the damper for the previous study was calculated to be twenty hours at 5 rpm. The spin moment of inertia for that calculation was 12.1 kg-m². Since the time constant is proportional to this parameter, the time constant for Task I and II is

$$\tau = \frac{20}{12.1} I_s = 2.22 I_s \text{ hr}$$

τ = time constant

I_s = spin moment of inertia

It appears that some reduction in size and weight of the nutation damper could be made, but since

$$\tau \propto \frac{1}{R^3} \text{ (effect of radius and mass)}$$

$$m \propto \frac{1}{R} \text{ (annular ring),}$$

the decrease in size and weight would be small and was not evaluated. The design constraints for damper with spacecraft deflection mode have not been established. The prime concerns are the effect of nutation on the entry conditions and pre-entry instrumentation. In the absence of more definitive constraints, it has been assumed that the damping time constant should be less than one-tenth of the probe coast time. Analysis of the final battery configuration may show that the stored electrolyte for the remote activated entry/descent battery provides sufficient damping and eliminates all need for a nutation damper.

E. THERMAL CONTROL SUBSYSTEM

Thermal control is provided as an integral part of the mechanical subsystem design to ensure that all probe systems and individual subsystem components will be maintained within acceptable temperature limits during all phases of the mission. During recent studies (GSFC NAS5-1145 and JPL 953311), various conceptual thermal control approaches for outer planet probe missions were investigated. The results of these studies identified important tradeoffs as well as logical thermal design; these results have been used to arrive at the baseline probe thermal control design presented here. A detailed discussion of the important parameters and thermal design approach and analysis have been previously presented in Volume II, Chapter V, Section A.10, (pp V-79 through V-103).

The most critical thermal control problem from a standpoint of thermal design is the high rate of thermal energy heat loss to the the cryogenic atmospheric environment during descent. To compensate for the cold atmospheres encountered, elevation of the probe internal temperature to maximum before entry allows optimum leeway for internal temperature decrease during descent. Since the probe must be thermally self-sufficient during coast, the probe internal temperature desired for planetary encounter becomes an important consideration.

To satisfy the mission constraints imposed by the anticipated environments, the thermal control concept shown in Figure III-56 was parametrically evaluated for common Saturn/Uranus probe design. The concept uses:

- 1) radioisotope heaters located in the service area within the aeroshell to provide heating during spacecraft cruise and coast;
- 2) multilayer insulation to encapsulate and isolate the probe from the space environment;
- 3) an environmental spacecraft cover for meteoroid protection during spacecraft cruise;
- 4) thermal coatings to conserve the internal heating required during probe coast;
- 5) graphite ablator and fibrous aeroshell insulation for probe entry and to isolate the descent probe capsule from the entry heat pulse;

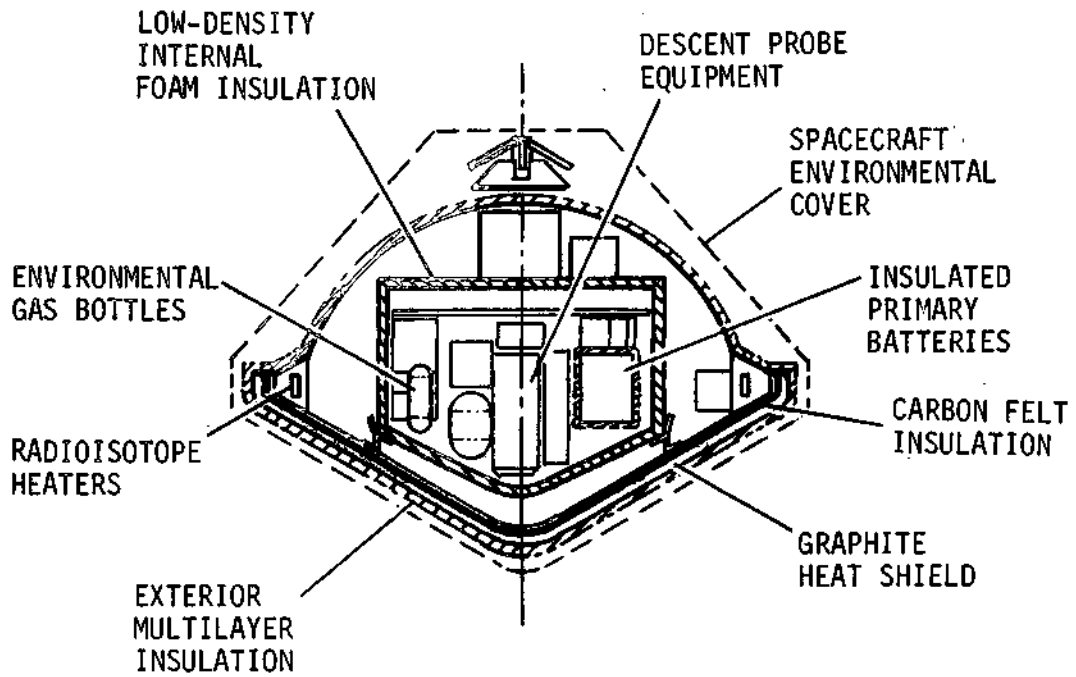


Fig. III-56 Probe Thermal Control Concept

- 6) internal probe low-density foam insulation, located adjacent to the structural probe shell, for thermal isolation of the internal components from the descent atmospheric environment.

To evaluate the thermal control subsystem, worst-case atmospheric encounters and navigation uncertainties were analyzed for the SAG exploratory payload. Figure III-57 presents the Saturn/Uranus worst-case model atmosphere temperature profiles for descent, using the baseline descent ballistic coefficient of 110 kg/m^2 (0.70 slug/ft^2). To increase the passive ability of previous probe designs, the probe arrival temperature was optimized to maximum and the more critical primary descent batteries were insulated with 1-cm foam insulation.

Table III-23 presents typical probe equipment temperature limits. As previously discussed, the probe batteries bound the allowable payload storage limit during spacecraft cruise (300°K upper limit to maintain the dry stored battery charge characteristics). Figure III-58 presents the cruise/coast probe thermal control radioisotope heating requirement. Since cool-biased probe cruise temperatures are desired for long-term equipment storage and warm-biased probe temperatures are desired for descent, the probe/spacecraft structural attachments were carefully considered for heat rejection. Results indicated that approximately 8 watts could be dissipated to establish the desired cruise equilibrium temperatures. The hard-mount attachments disconnect at separation and thus provide for probe temperature increase during coast. On the basis of preliminary probe analysis, an internal probe coast temperature of 302°K with a $\pm 10^\circ\text{K}$ uncertainty would provide optimum leeway for probe temperature decrease and an acceptable margin for possible over-temperature problems at the beginning of descent. Although not included in the probe design for this study, the use of a probe louver system warrants consideration to establish the probe coast temperature and reduce the thermal uncertainty at planetary encounter.

Using the optimum probe entry temperature of 302°K , the SAG exploratory probe was evaluated for a 100% passive thermal control protection system. Late arrival uncertainties were assumed for warm atmospheric encounters where over-temperature conditions would terminate the mission, and early arrival uncertainties were assumed for cool atmospheric encounters where under-temperature conditions would terminate the mission.

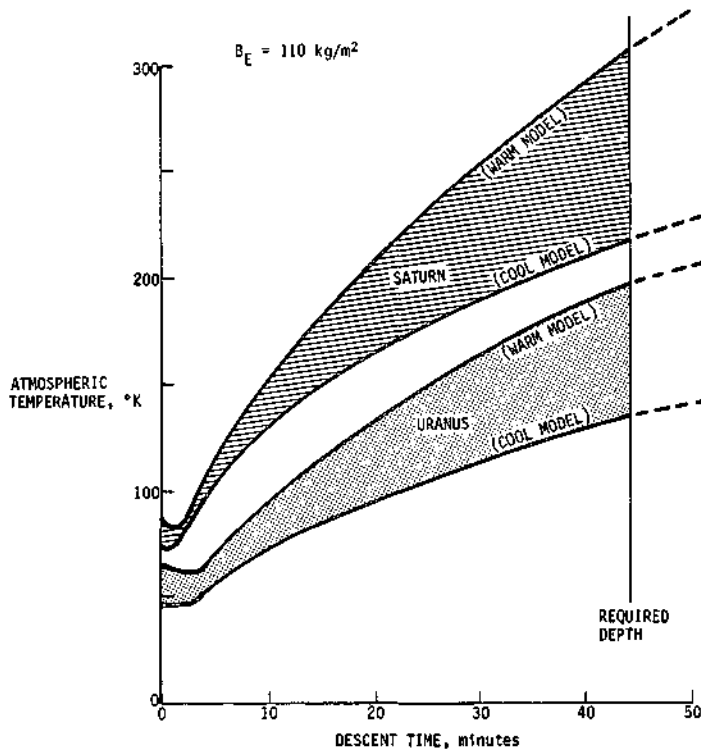


Fig. III-57 Worst-Case Saturn/Uranus Atmospheric Temperature Profiles

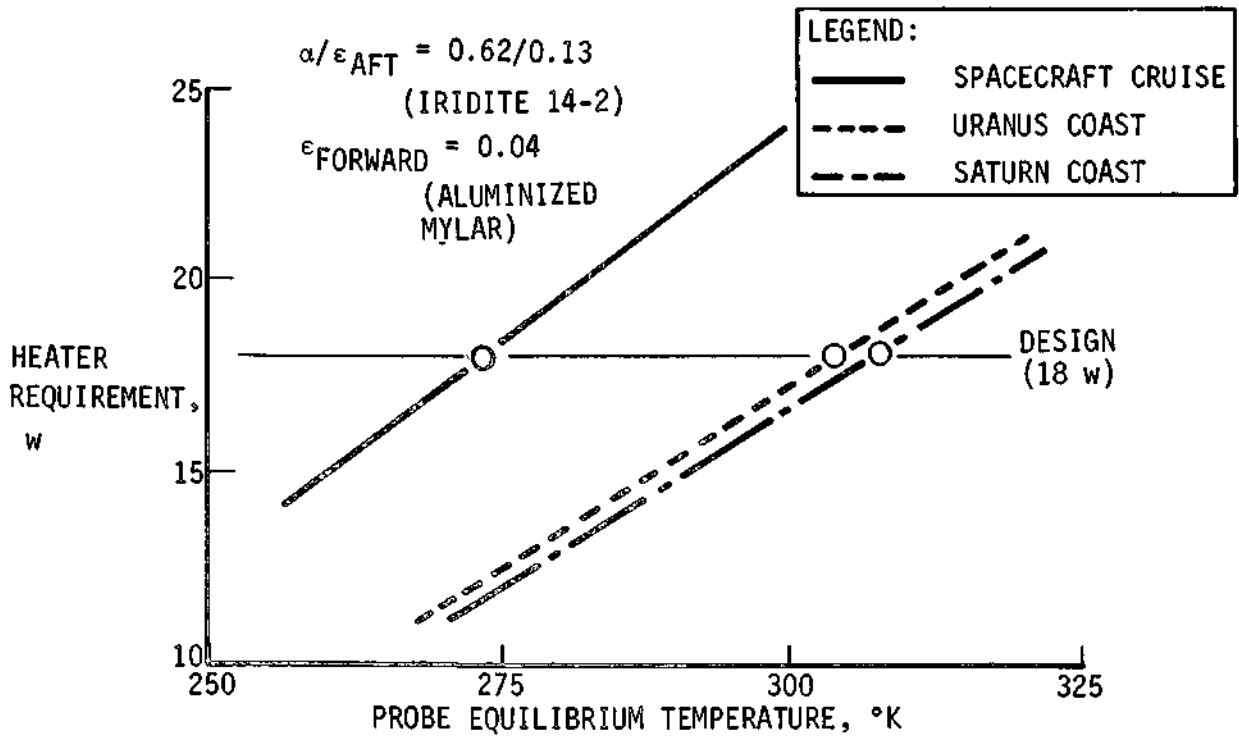


Fig. III-58 Cruise/Coast Probe Equilibrium Temperatures Based on Thermal Coating Selection

Table III-23 Typical Probe Equipment Temperature Limits

PROBE SUBSYSTEM & SCIENCE COMPONENTS	TYPICAL TEMPERATURE LIMITS, °K	
	STORAGE (MIN/MAX)	OPERATING (MIN/MAX)
SCIENCE INSTRUMENTS & ELECTRONICS		
NEUTRAL MASS SPECTROMETER	235/325	250/320
TEMPERATURE PROBE	175/700	175/500
TEMPERATURE PROBE ELECTRONICS	210/350	230/325
PRESSURE GAGES	220/325	240/325
ACCELEROMETERS	225/375	230/370
ION RETARDING POTENTIAL ANALYZER	240/500	240/500
NEUTRAL-PARTICLE RETARDING POTENTIAL ANALYZER	240/500	240/500
LANGMUIR PROBE	175/700	175/500
LANGMUIR PROBE ELECTRONICS	230/350	235/350
NEPHELOMETER	240/325	240/325
COMMUNICATIONS		
RF TRANSMITTER	225/350	250/345
POSTENTRY ANTENNA	125/365	125/365
DATA HANDLING SYSTEM		
ELECTRONICS	220/400	250/350
MEMORY UNIT	220/400	250/350
POWER & PYROTECHNICS		
POWER CONDITIONER	225/350	250/340
POWER DISTRIBUTION BOX	225/340	250/340
PYROTECHNICS (Hg-Zn BATTERY)	225/325	255/325
PRIMARY ENTRY BATTERY	225/300	275/325
PYROTECHNIC ELECTRONICS	225/350	250/350
COAST TIMER	240/350	280/350

For passive thermal control protection, the results are as follows:

DEPTH OF DESCENT (100% PASSIVE)	SATURN			URANUS		
	WARM	NOMINAL	COOL	WARM	NOMINAL	COOL
TIME (min)	64	74	55	45	35*	27*
PRESSURE (bar)	6.8	17.4	25.9	3.1	5.2	8.9
TEMPERATURE LIMIT EXCEEDED	UPPER	UPPER	LOWER	LOWER	LOWER	LOWER
*DOES NOT MEET MINIMUM MISSION REQUIREMENT (44 min)						

For Saturn encounters, the passive thermal control is sufficient to satisfy the mission requirement. For Uranus, electrically heating the payload was first evaluated for the penalizing atmospheres. Results show that 38 w-hr of electrically supplied energy would satisfy the nominal atmosphere encounter (0.55 kg of batteries), but 135 w-hr would be required for the cool atmosphere encounter (2.00 kg of batteries). Additional analyses show that an extended mission to obtain measurements in the cool atmosphere NH₃ cloud (35-bar descent) would require approximately 300 w-hr of heating, or 4.36 kg of batteries.

Since electrical heating of the probe payload requires complex concepts as well as severe volume and weight penalties, an alternative scheme of thermal protection was considered. Although the required cool Uranus atmosphere calls for a descent to 19.2 bars, results indicate that an onboard supply of neon gas to purge the probe for the first 2.5 bars of descent would be sufficient to eliminate the requirement of electrical heating. Neon gas was chosen over nitrogen gas because of cooler probe shell temperatures anticipated in the Uranus cool atmosphere and the increased probability of condensation and freezing of nitrogen gas at the insulation/probe shell boundary. A 100% redundant gas supply system has, therefore, been integrated into the baseline probe design of this study. The 0.25 kg of gas required occupies approximately 0.40 liters of volume in two bottles with a total delta weight of 0.54 kg. This penalty compares with 2.0 kg of batteries and associated heating circuits and switches. For extended descent to 35 bars in the Uranus cool atmosphere, the neon gas approach would not be adequate. The use of a gas pressurization system rapidly reaches a point of diminishing return, and a descent to 35 bars would require neon environment control for the entire descent.

The parametric studies, therefore, indicate that a minimum weight passive thermal control approach with neon gas initially inside the probe for the first 2.5 bars of the planetary descent will satisfy the mission and system design criteria. Chapters IV and V present complete probe thermal histories from launch to descent for the SAG exploratory payload and the expanded science complement probe designs. The temperature limits of any exposed external equipment or components during the atmospheric descent phase (i.e., temperature probe, antenna, parachute) also are important for these missions. Since these components will be directly exposed to cryogenic temperatures (50°K or less) during descent, they must be able to withstand not only the severity of such extreme temperatures, but also the sudden thermal shock that will occur when these components are deployed.

F. PARAMETRIC ANALYSIS SUMMARY

This section summarizes results of analyses conducted during the study and presented in detail in previous sections of this chapter.

1. Mission Analysis and Design

A comparison of the three design missions is shown in Table III-24. Saturn direct (S-79) is a terminal mission and is more flexible to compromises than the Saturn/SU 80 mission which flies by Saturn for a subsequent Uranus encounter. The Uranus/SU 80 mission is also a terminal mission with some flexibility to constraints. The periapsis radius of $3.8 R_g$ for the Saturn/SU 80 mission causes a large range of 197×10^3 km at entry, which is significant for the RF link analysis and is the worst case of the three design missions.

An analysis was conducted to obtain the same spacecraft antenna look direction and the same probe pre-entry antenna for both planets. Some modifications to the missions were made so that the cone angles at entry are nearly the same. Further, the Table III-24 shows that the probe aspect angle at Uranus at the end of the mission is reaching extreme limits and is an important factor in making the missions similar for both planets.

Entry deceleration varies from 225 g in the Uranus warm atmosphere to 837 g in the Uranus cool atmosphere.

2. Science Analysis

The science analysis is summarized in Table III-25. The table denotes that the addition of the pre-entry science and nephelometer instruments, used in Task II, increase the weight, power, and volume compared to that for Task I; however, these increases are small compared to the same factors for the overall probe. The science objectives are achieved with a single descent time of 44 minutes with the Saturn warm atmospheric model controlling the instrument performance.

Table III-24 Comparison of Mission Designs

MISSION	DESIGN MISSIONS		
	S 79	S/SU 80	U/SU 80
V_{HP} , km/sec	8.2	9.11	11.87
ENTRY ANGLE, deg	-30	-30	-60
PERIAPSIS, R_S OR R_U	2.3	3.8	2.0
DEFLECTION RADIUS, 10^6 km	30	30	10
COAST TIME, days	39.4	35.8	9.5
PROBE RELEASE ANGLE, deg	14.7	10.6	21.4
SPACECRAFT ΔV ANGLE, deg	57.3	59.1	46
ΔV MAGNITUDE, m/sec	52	96	85
LEAD ANGLE, deg	5.3	3.7	1.4
LEAD TIME, hr	1.48	2.1	1.85
RANGE AT ENTRY, 10^5 km	1.08	1.97	0.87
PROBE ASPECT ANGLE AT ENTRY, deg	8.2 (42.4)	4.9 (46.7)	1.9 (31.0)
PROBE ASPECT ANGLE AT EOM, deg	13.8	20.0	43
CONE ANGLE AT ENTRY, deg	122	118	131
CONE ANGLE AT EOM, deg	102	112	105
ENTRY TIME DISPERSION, minutes	4.4	4.4	28.9
ENTRY ANGLE DISPERSION, deg	1.23	1.23	6.24
ANGLE-OF-ATTACK DISPERSION, deg	2.1	2.1	3.0

Table III-25 Science Analysis Summary

• PLANETARY ATMOSPHERIC VARIATIONS ALLOW FOR INSTRUMENT COMMONALITY		
• EXPANDED PAYLOAD ALLOWS DETERMINATION OF UPPER ATMOSPHERE AND IONOSPHERE AND BETTER DEFINES DESCENT CLOUD LOCATIONS FOR THE FOLLOWING INSTRUMENT INCREASES:		
	79% GREATER WEIGHT	
	104% GREATER VOLUME (93% INSIDE PROBE)	
	72% MORE POWER REQUIRED	
• A CONSTANT DESCENT TIME OF 44 minutes SATISFIES THE OBJECTIVES		
FINAL DESCENT PRESSURE:	3.1 TO 19.2 bars	
VERTICAL DISTANCE COVERED ON CHUTE:	92 TO 320 km	
DESCENT BALLISTIC COEFFICIENT:	110 kg/m ²	
• MEASUREMENT PERFORMANCE IS SATISFACTORY FOR WORST-CASE SATURN WARM ATMOSPHERE AND IMPROVES WITH COOLER MODELS AND WITH URANUS		
• THREE MODES OF DATA TRANSMISSION ARE POSSIBLE:		
	<u>PRE-ENTRY</u>	<u>DESCENT</u>
1. EXPLORATORY PAYLOAD ONLY	0 bps	27.7 bps
2. REAL-TIME PRE-ENTRY TRANSMISSION (EXPANDED PAYLOAD)	235 bps	31.5 bps
3. PRE-ENTRY DATA STORAGE AND RETRANSMISSION	235 bps	50.5 bps

3. System Design Analysis

a. *Parachute Deployment Analysis* - Since the warm, nominal, and cool atmospheric models for Saturn and Uranus cause the entry deceleration to vary from 225 g to 837 g, an analysis was conducted to determine parachute deployment such that the chute is subjected to Mach numbers no greater than 0.9. A secondary constraint was deployment of the chute at pressure altitudes at 100 mb and higher. As a result, the parachute is deployed at 5 g (decreasing) plus 15 seconds. Table III-26 shows the related Mach number and pressure altitude for each atmosphere.

Table III-26 *Parachute Deployment Results*

	MACH NO.	PRESSURE (mb)
SATURN ATMOSPHERES		
COOL	0.56	102
NOMINAL	0.70	65
WARM	0.88	44
URANUS ATMOSPHERES		
COOL	0.59	41
NOMINAL	0.72	47
WARM	0.84	49

b. *Data Mode Analysis for Task II* - Results of the Task II data mode analysis are shown in Table III-27. The pre-entry science required a data rate of 235 bps. If the FSK modulation used during Task I were retained, the RF power requirement was 116 watts as shown in data mode 1. The resulting probe weight was 116 kg with a size of 96.5 cm. Data mode 2 changes the modulation from FSK to PSK, reducing the RF power requirement to 41 watts, and resulting in reduced size and weight. Data mode 3 stores all pre-entry data and transmits it during descent, using 40 watts of RF power, and increasing the storage. Task II definition uses data modes 2 and 3.

Table III-27 Task II Data Mode Analysis Results

DATA MODE	DATA RATE, bps	MODULATION TYPE	RF POWER, w	PROBE WEIGHT, kg	PROBE DIAMETER, cm	PROBE DATA STORAGE, 10 ³ bits
1. PRE-ENTRY DATA TRANSMITTED REAL-TIME (NO STORAGE)	235	FSK	116	116	96.5	11.9
DESCENT	31.5	FSK	29			
2. PRE-ENTRY TRANSMITTED REAL-TIME (NO STORAGE)	235	PSK	41	103	91.4	11.9
DESCENT	31.5	FSK	29			
3. PRE-ENTRY DATA STORED & TRANSMITTED DURING DESCENT	50.5	FSK	40	103	91.4	60.2

c; *Descent Depth Sensitivity* - Figure III-59 shows the probe system definition depth at the end of the mission for all three atmospheric models at Saturn and Uranus. For Saturn, the communication subsystem is sized for the cool atmosphere primarily because of the attenuation; the nominal and warm atmospheres, however, are more critical to the link geometry. For Uranus, the communication geometry is critical because the axis of rotation for Uranus is approximately in the ecliptic plane.

Thermal control, sized by the Uranus cool atmosphere, shows that for the design mission a depth capability of 20 bars in the Uranus warm atmosphere is feasible using a nonpassive system. The atmospheres at Saturn are much less severe so that a passive system could be used for that planet.

4. Telecommunication Analysis

Table III-28 presents the communications analysis summary to achieve common spacecraft antenna pointing and a common probe pre-entry antenna for use at both planets, as mentioned in paragraph III.F.1 for the mission impact. The table shows that when tailored for each planet, the RF power required was 17 watts for

Table III-28 Communications Parameters

PARAMETER	S/SU 80	U/SU 80	S/SU 80	U/SU 80	S 79
PROBE ANTENNA PATTERN TYPE	TORUS/AXIAL	AXIAL/AXIAL	AXIAL/AXIAL	AXIAL/AXIAL	AXIAL/AXIAL
PROBE ANTENNA BEAMWIDTH, deg	30/90	90/110	100/100	100/100	100/100
SPACECRAFT ANTENNA BEAMWIDTH, deg	20	20	20	20	20
SPACECRAFT-TO-PROBE NOMINAL CONE ANGLE, deg	105	125	116	116	116
SPACECRAFT-TO-PROBE ENTRY CLOCK ANGLE, deg	256	275	256	263	256
MAXIMUM TRANSMITTER POWER, w	17.4	2.2	25	9.2	18.4

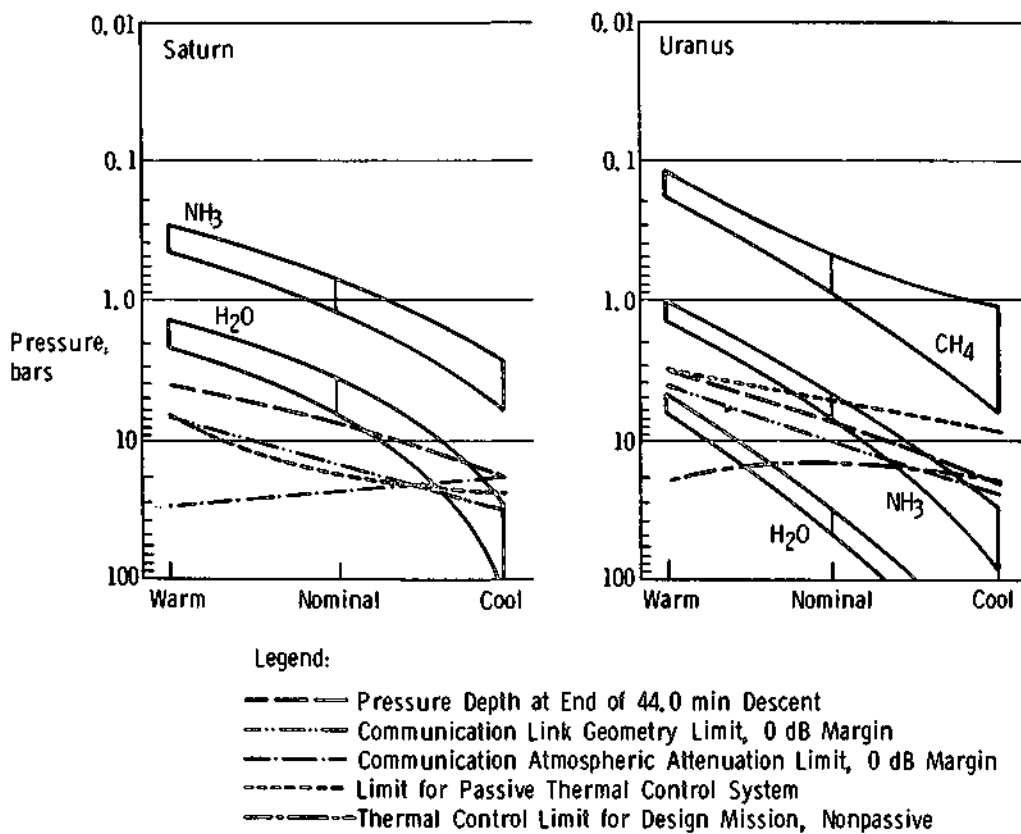


Fig. III-59 Cloud Locations and End-of-Mission Limits for Various Model Atmospheres

Saturn and 2 watts for Uranus. When the mission definition was revised for the desired commonality, the RF power requirement was increased to 25 watts at Saturn. This definition is reflected in Chapter IV (Task I) data.

G. REFERENCES

- III-1 *The Planet Saturn (1970), NASA Space Vehicle Design Criteria (Environment)*. NASA SP-8091, June 1972.
- III-2 *The Planets Uranus, Neptune and Pluto (1970), NASA Space Vehicle Design Criteria (Environment)*. NASA SP-8103, Nov. 1972.
- III-3 S. G. Chapin, Program Manager: *Jupiter Turbopause Probe Gas Physics Environment and Instrument Response Study, Final Report*. Martin Marietta Corporation Report No. MCR-71-142, August 1971.
- III-4 R. S. Wiltshire, Program Manager: *Systems Level Study of a Non-survivable Jupiter Turbopause Probe, Final Report*. Martin Marietta Report No. MCR-72-91, June, 1972.
- III-5 D. M. Hunten: "The Upper Atmosphere of Jupiter", *Journal of Atmospheric Sciences*, Vol 26, No. 5, Part 2, September 1969.
- III-6 J. D. Krams: *Radio Astronomy*. McGraw-Hill, New York, New York, 1966, p 237.
- III-7 S. J. Ducsay: *Jupiter Atmospheric Entry Mission Study, Final Report*. Martin Marietta Corporation, Denver, Colorado, MCR-71-1 (Vol III) Contract JPL 952811, April 1971, pp IV-82 through IV-158.
- III-8 D. A. DeWolf and G. S. Kaplan: *Investigation of Line-of-Sight Propagation in Dense Atmosphere: Phase III, Part I, Final Report*. RCS Labs, Princeton, New Jersey, NASA CR-114416, NASA/ARC Contract NAS2-5310, November 1971, pp 5 through 11.
- III-9 J. S. Hogan, S. I. Rasool, and T. Encrenaz: "The Thermal Structure of the Jovian Atmosphere." *Journal of the Atmosphere Sciences*, Vol 26, No. 5, Pt 1, September 1969, pp 898 through 905.
- III-10 J. D. Osborn: *An Investigation of Low Gain Antennas for Spacecraft and Planetary Probes*. Martin Marietta Corporation, Denver, Colorado, Research Report, D72-48728-001, December 1972.
- III-11 D. G. Fordham, Jr. and R. S. Brazil: "Polarization Loss for Elliptically Polarized Antennas." *Microwave Journal*, Vol 8, No. 12, December 1969, pp 50 through 52.

IV. SATURN/URANUS PROBE SYSTEM DEFINITION WITH SCIENCE ADVISORY GROUP'S EXPLORATORY PAYLOAD

This section summarizes the common Saturn/Uranus probe system definition (Task 1) which uses the Science Advisory Group's (SAGs) exploratory payload and was defined in Volume II, Chapter III. The definition uses concepts that were generated during the basic study and extended to be compatible with the three new missions, the "worst case" atmospheric models, and spacecraft deflection mode. Results of the system and subsystem tradeoffs and analysis from Chapter III are included in the definition.

A. MISSION DEFINITION

1. 1979 Saturn Mission Definition

The Saturn Direct 1979 mission is shown in Figure IV-1 and detailed in Table IV-1. Important mission design results are summarized in this Chapter.

a. Interplanetary Trajectory Selection - The type I Interplanetary trajectory from Earth to Saturn is shown in Figure IV-1a with 1-year intervals noted. The launch date of November 23, 1979 and a Saturn arrival date of July 19, 1983 results in a total trip time of 3.7 years.

b. Launch Analysis - The launch analysis is provided in Figure IV-1b. Available payload is plotted against the launch period for four sets of launch vehicle performance data. The nominal launch window and parking orbit coast times were checked and found satisfactory.

c. Approach Trajectories - The probe trajectory was constrained to enter and remain in the sunlit side of the planet until the end of the mission (E + 44 min). This requirement set the entry angle at $\gamma = -30^\circ$. The resulting approach trajectory is pictured in Figure IV-1d and summarized in Table IV-1b. Since Saturn is the terminal planet for this mission, a spacecraft periapsis radius was selected to be $2.3 R_s$ to miss encountering the rings.

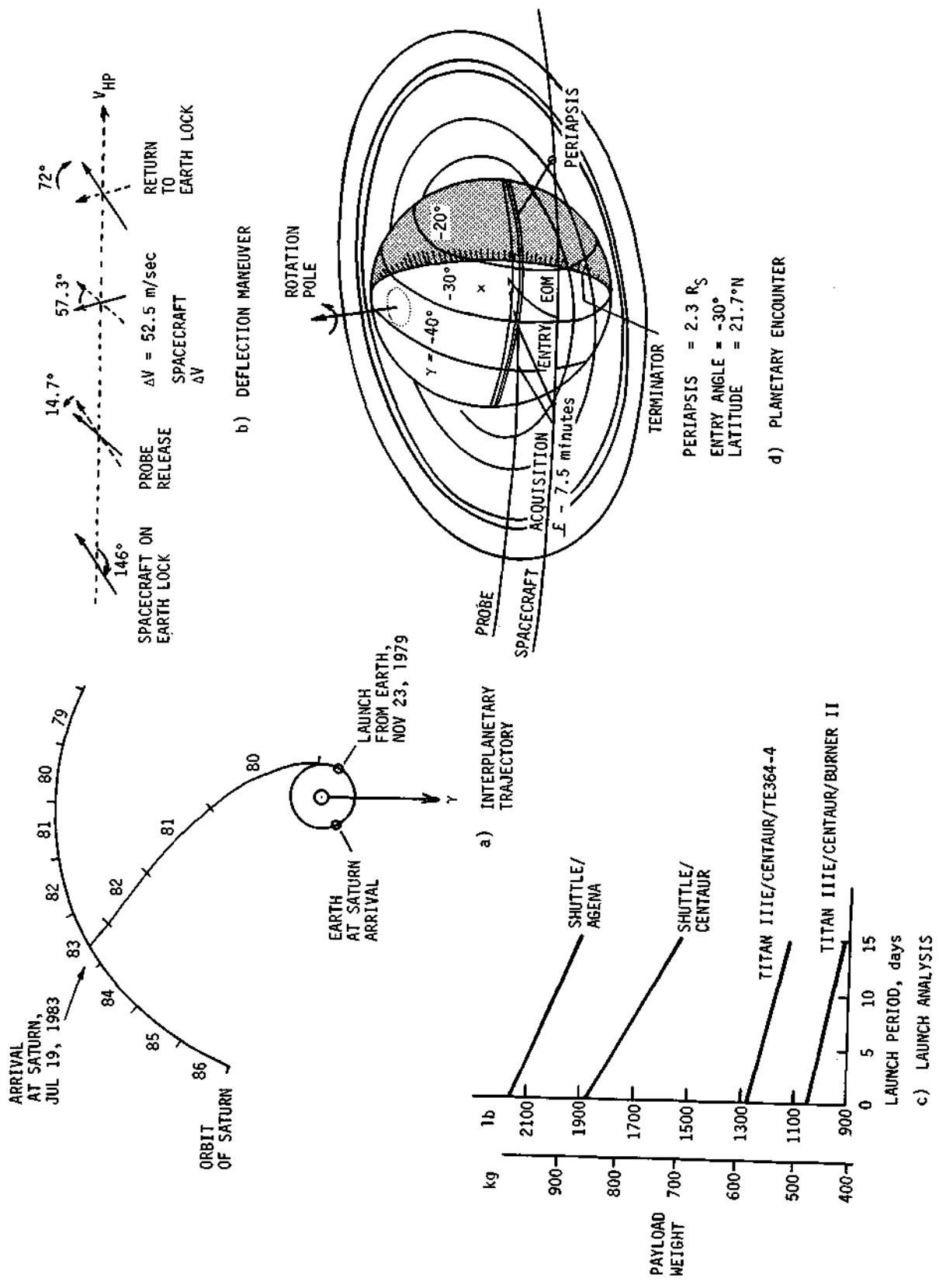


Fig. IV-1 1979 Saturn Mission Definition

Table IV-1 Saturn 1979 Mission Summary Data

a) CONIC TRAJECTORY DATA

INTERPLANETARY TRAJECTORY	LAUNCH TRAJECTORY	ARRIVAL TRAJECTORY
LAUNCH DATE: 11/23/79	NOMINAL C_3 : 132 km ² /sec ²	V_{HP} : 8.2 km/sec
ARRIVAL DATE: 7/19/83	NOMINAL DLA: 34.5°	RA: 173.88°
FLIGHT TIME: 3.7 yr	C_3 (5-day): 133.9 km ² /sec ²	DEC: -0.163°
	C_3 (10-day): 135.8 km ² /sec ²	ZAE: 146.0°
	C_3 (15-day): 140 km ² /sec ²	ZAP: 140.1°
		INC: 3.97°
		R_p : 2.3 R_S

b) DEFLECTION MANEUVER AND PROBE CONIC

DEFLECTION MANEUVER		PROBE CONIC DEFINITION	
DEFLECTION MODE:	SPACECRAFT	ENTRY ANGLE:	-30°
DEFLECTION RADIUS:	30 x 10 ⁶ km	ENTRY LATITUDE*:	-4.4°
COAST TIME:	39.4 days	ENTRY LONGITUDE*:	59.9°
ΔV :	52.5 m/sec	LEAD TIME:	1.48 hr
APPLICATION ANGLE:	74.4°	LEAD ANGLE:	5.3°
OUT-OF-PLANE ANGLE:	10.9°	PROBE/SPACECRAFT RANGE (ENTRY):	1.08 x 10 ⁵ km
PROBE RELEASE ANGLE:	14.7°	PROBE ASPECT ANGLE (ENTRY -):	42.4°
SPACECRAFT DEFLECTION ANGLE:	57.3°	PROBE ASPECT ANGLE (ENTRY +):	8.2°
SPACECRAFT REORIENTATION ANGLE:	72°	PROBE ASPECT ANGLE (EOM):	13.8°

*SUBSOLAR ORBITAL PLANE.

c) DISPERSION ANALYSIS SUMMARY

NAVIGATION UNCERTAINTIES	EXECUTION ERRORS (3 σ)	DISPERSIONS (3 σ)
TRACKING: DOPPLER & RANGE (40-DAY ARC)	ΔV PROPORTIONALITY: 1%	ENTRY ANGLE: 1.1°
SMAA: 2009 km	ΔV POINTING: 2°	ANGLE OF ATTACK: 1.8°
SMIA: 833 km	PROBE ORIENTATION POINTING: 2°	DOWNRANGE: 2.02°
β : 93°		CROSSRANGE: 1.47°
TOF: 87.7 sec		LEAD ANGLE: 2.4°
		LEAD TIME: 5.7 minutes
		ENTRY TIME: 4.9 minutes

d) ENTRY AND DESCENT SUMMARY

ENTRY PARAMETERS	ATMOSPHERE MODEL					
	WARM		NOMINAL		COOL	
ENTRY VELOCITY, km/sec	36.3	36.4	36.4	36.5	36.5	36.5
ENTRY ALTITUDE, km	968.5	536	536	297	297	297
ENTRY B , kg/m ²	102	102	102	102	102	102
MAXIMUM DECELERATION, g	227	366	366	568	568	568
MAXIMUM DYNAMIC PRESSURE, N/m ²	2.2 x 10 ⁵	3.6 x 10 ⁵	3.6 x 10 ⁵	5.6 x 10 ⁵	5.6 x 10 ⁵	5.6 x 10 ⁵
EOM PRESSURE, bar	4.0	8.0	8.0	18.2	18.2	18.2
DESCENT B , kg/m ²	110	110	110	110	110	110

CRITICAL ENTRY EVENTS	ATMOSPHERE MODEL					
	WARM		NOMINAL		COOL	
	TIME, sec	ALTITUDE, km	TIME, sec	ALTITUDE, km	TIME, sec	ALTITUDE, km
$g = 0.1$	12.2	734	5.0	445	1.5	268
$g = 100$	35.0	329	17.5	218	8.5	139.5
MAXIMUM DECELERATION	40	259	22	151.2	11.5	92.7
MACH = 0.8	89.5	166	54.5	94.5	33.5	51.5
MACH = 0.7	98.5	162	59.5	92.5	36.5	50.5

The probe aspect angle at start of descent is 8.2° and increases to 14° at the end of the mission. The spacecraft periapsis radius is such that approximate angular rate matching is achieved, which accounts for the small change in probe aspect angle for the duration of descent.

d. Deflection Maneuver - A spacecraft deflection maneuver is used in this mission at a deflection radius of 30 million km, or 39.4 days from entry. A deflection ΔV of 52.5 m/sec is applied to the spacecraft to establish the desired communication geometry. The implementation sequence is shown in Figure IV-1c.

e. Navigation and Dispersions - The navigation and dispersion results are given in Table IV-1c. A forty-day standard Doppler range tracking arc was used. The entry time dispersion was 4.4 min (3 σ). The communication parameter dispersions are discussed in Chapter III, Section A.

f. Entry and Descent Trajectories - Table IV-1d summarizes the entry and descent phases of the mission. For the nominal atmosphere, the entry phase starts 536 km above the 1 atmosphere pressure level and ends 59 seconds later. The descent phase starts after the aeroshell is staged and lasts until the end of the mission, 44 minutes later. Parametric data showing critical events times and altitudes for the warm, nominal, and cool atmospheres is also shown in Table IV-1d. Maximum deceleration of 568 g is experienced in the cool atmosphere.

2. Saturn/SU 80 Mission Definition

The Saturn/SU 80 mission is shown in Figure IV-2 and detailed in Table IV-2. The important mission design results are summarized in this section.

a. Interplanetary Trajectory Selection - The type I interplanetary trajectory from Earth to Saturn is pictured in Figure IV-2a. The launch date is May 9, 1984. The total trip time is 3.4 years.

b. Launch Analysis - Available payload weight is plotted against launch period for four sets of launch vehicle performance data in Figure IV-2b. The nominal launch window and parking orbit coast times were checked and found satisfactory.

c. Approach Trajectories - The probe trajectory was constrained to enter and remain in the sunlit side of the planet until the end of the mission (E + 44 min). An entry angle of $\gamma = -30^\circ$ was found satisfactory. The resulting approach trajectory is pictured

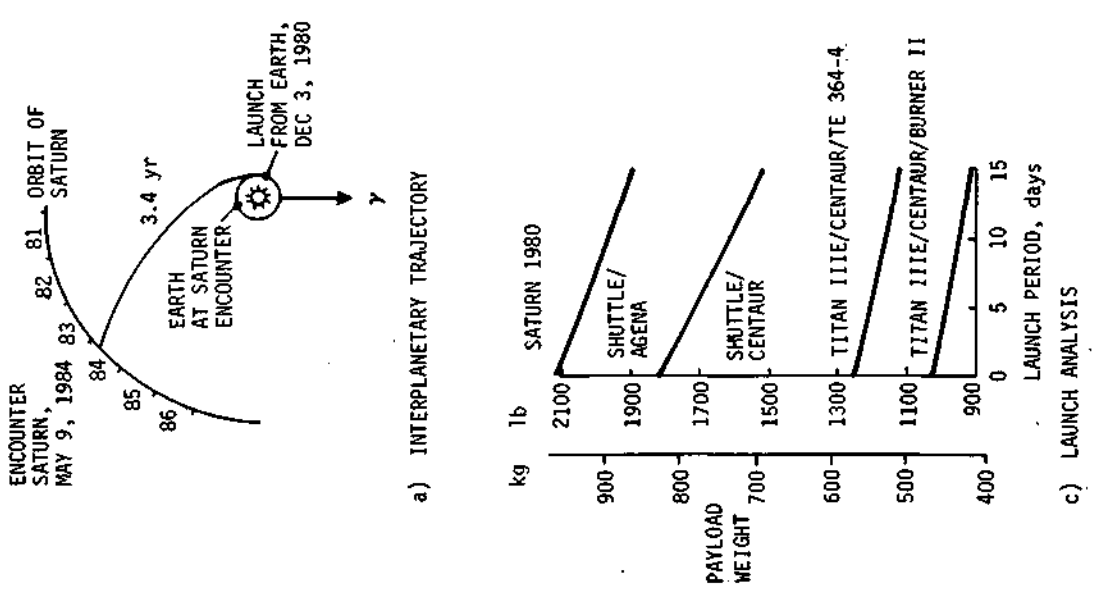
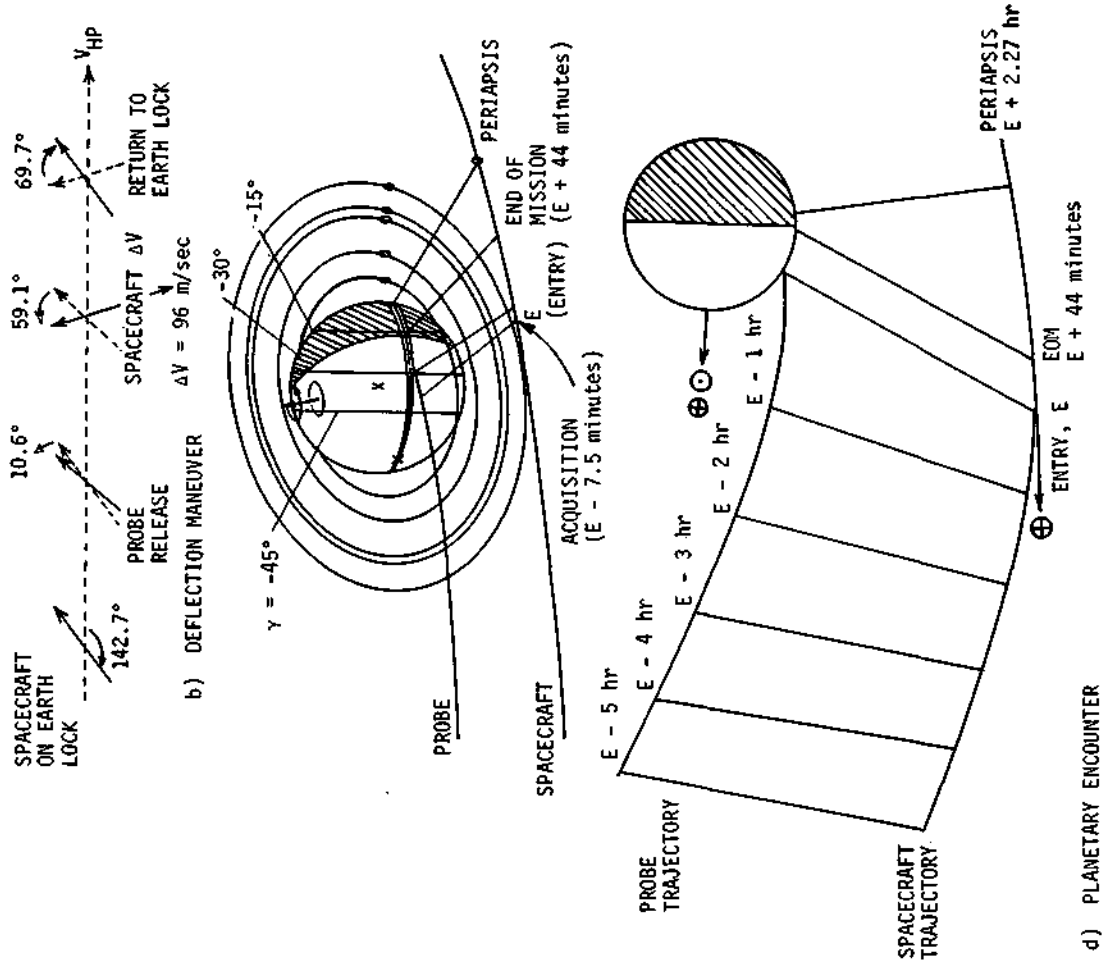


Fig. IV-2 Saturn/SU 80 Mission Definition

Table IV-2 Saturn/SU 1980 Mission Summary Data

a) CONIC TRAJECTORY DATA

INTERPLANETARY TRAJECTORY	LAUNCH TRAJECTORY	ARRIVAL TRAJECTORY
LAUNCH DATE: 12/3/80	NOMINAL C_3 : 132.7 km ² /sec ²	V_{HP} : 9.11 km/sec
ARRIVAL DATE: 5/9/84	NOMINAL DLA: 27.5°	RA: 188.27°
FLIGHT TIME: 3.4 yr	C_3 (5-day): 134.5 km ² /sec ²	DEC: 0.192°
	C_3 (10-day): 135 km ² /sec ²	ZAE: 142.7°
	C_3 (15-day): 140 km ² /sec ²	ZAP: 145.9°
		INC: 2.8°

b) DEFLECTION MANEUVER AND PROBE CONIC

DEFLECTION MANEUVER	PROBE CONIC DEFINITION
DEFLECTION MODE: SPACECRAFT	ENTRY ANGLE: -30°
DEFLECTION RADIUS: 30 x 10 ⁶ km	ENTRY LATITUDE*: -4.969°
COAST TIME: 35.8 days	ENTRY LONGITUDE*: 63.3°
ΔV : 95.9 m/sec	LEAD TIME: 2.1 hr
APPLICATION ANGLE: 73.0°	LEAD ANGLE: 3.8°
OUT-OF-PLANE ANGLE: 13.9°	PROBE/SPACECRAFT RANGE (ENTRY): 1.97 x 10 ⁶ km
PROBE RELEASE ANGLE: 10.6°	PROBE ASPECT ANGLE (ENTRY -): 46.8°
SPACECRAFT DEFLECTION ANGLE: 59.1°	PROBE ASPECT ANGLE (ENTRY +): 4.9°
SPACECRAFT REORIENTATION ANGLE: 69.7°	PROBE ASPECT ANGLE (EOM): 20.7°

*SUBSOLAR ORBITAL PLANE.

c) DISPERSION ANALYSIS SUMMARY

NAVIGATION UNCERTAINTIES	EXECUTION ERRORS (3 σ)	DISPERSIONS (3 σ)
TRACKING: DOPPLER & RANGE (40-DAY ARC)	ΔV PROPORTIONALITY: 1%	ENTRY ANGLE: 1.2°
SWAA: 1950 km	ΔV POINTING: 2°	ANGLE OF ATTACK: 1.86°
SMIA: 833 km	PROBE ORIENTATION POINTING: 2°	DOWNRANGE: 2.2°
β : 93°		CROSSRANGE: 1.58°
TOF: 85.5 sec		LEAD ANGLE: 1.9°
		LEAD TIME: 8.7 minutes
		ENTRY TIME: 4.6 minutes

d) ENTRY AND DESCENT SUMMARY

ENTRY PARAMETERS	ATMOSPHERE MODEL					
	WARM		NOMINAL		COOL	
ENTRY VELOCITY, km/sec	36.8	36.8	36.8	36.8	36.8	36.8
ENTRY ALTITUDE, km	968.5	536	297	297	297	297
ENTRY β , kg/m ²	102	102	102	102	102	102
MAXIMUM DECELERATION, g	227	366	568	568	568	568
MAXIMUM DYNAMIC PRESSURE, N/m ²	2.2 x 10 ⁵	3.6 x 10 ⁵	5.6 x 10 ⁵			
EOM PRESSURE, bar	4.0	8.0	18.2	18.2	18.2	18.2
DESCENT β , kg/m ²	110	110	110	110	110	110

CRITICAL ENTRY EVENTS	ATMOSPHERE MODEL					
	WARM		NOMINAL		COOL	
	TIME, sec	ALTITUDE, km	TIME, sec	ALTITUDE, km	TIME, sec	ALTITUDE, km
g = 0.1	12.2	734	5.0	445	1.5	268
g = 100	35.0	329	17.5	218	8.5	139
MAXIMUM DECELERATION	40.0	259	22.0	151.2	11.5	92.7
MACH = 0.8	89.5	166	645	94.5	33.5	51.5
MACH = 0.7	98.5	162	59.5	92.5	36.5	50.5

in Figure IV-2d and summarized in Table IV-2b. The spacecraft periapsis radius of $R_p = 3.8 R_s$ was selected as a compromise between launch energy and communication link power requirements, as discussed in Chapter III, Section A.3. The probe aspect angle at the beginning of descent is 5° and increases to 21° at the end of the mission. Approach geometry for all three missions was selected to achieve a commonality in spacecraft-to-probe directions. As a result, the probe aspect angle is not minimized, but rather is simply kept within acceptable bounds. The probe leads the spacecraft for the duration of descent.

d. Deflection Maneuver - A spacecraft deflection maneuver requiring 96 m/sec is used in this mission at a deflection radius of 30 million km. The corresponding coast time is 36 days. The implementation sequence is shown in Figure IV-2.

e. Navigation and Dispersions - The navigation and dispersion results are given in Table IV-2c. A standard Doppler tracking arc of forty days with supplementary ranging measurements was used. The three-sigma entry time dispersion was 4.4 minutes. The communication parameter dispersions are discussed in Chapter III, Section B.

f. Entry and Descent Trajectories - Table IV-2d summarizes the entry and descent phases of the mission. For the nominal atmosphere, the entry phase starts 536 km above the 1 atmosphere pressure level and ends 59 seconds later. The descent phase starts after the aeroshell is staged and lasts to the end of the mission 44 minutes later. Parametric data showing the critical event times and altitudes for the warm, nominal, and cool atmospheres is also shown in Table IV-2d. Maximum deceleration of 568 g is experienced in the cool atmosphere. The entry and descent trajectory for the 1979 Saturn and the Saturn/SU 80 missions are identical.

Uranus/SU 80 Mission Definition

The 1980 Saturn/Uranus mission is shown in Figure IV-3 and detailed in Table IV-3. The important mission design results are summarized in this section.

a. Interplanetary Trajectory Selection - The interplanetary trajectory from Earth to Uranus with an intermediate Saturn swing-by is pictured in Figure IV-3a. The launch date is December 3, 1980 and the Uranus arrival date is October 23, 1988. The total trip time is 7.7 years.

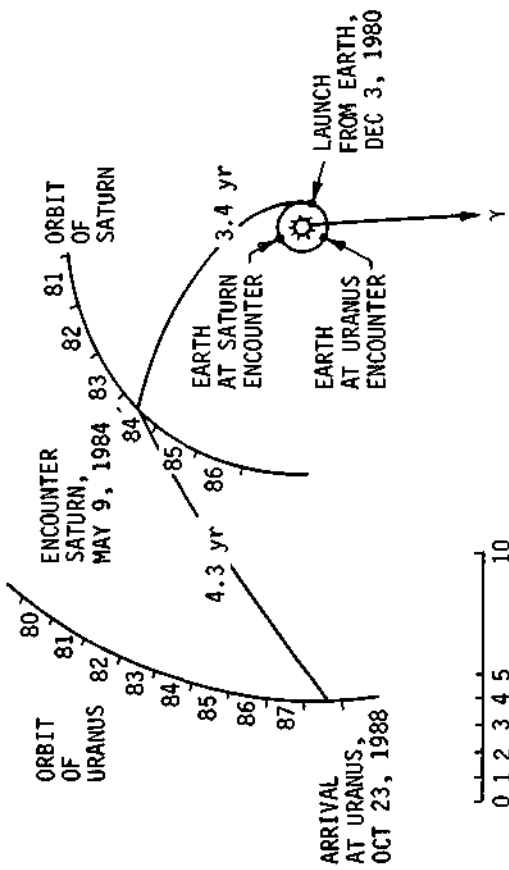
b. *Launch Analysis* - Available payload weight is plotted against launch period for four sets of launch vehicle performance data in Figure IV-3b.

c. *Approach Trajectories* - The probe trajectory entry angle, γ , of -60° was selected. The resulting approach trajectory is pictured in Figure IV-3d and summarized in Table IV-3b. The spacecraft periapsis radius of $2.0 R_U$ results in an acceptable spacecraft-to-probe communication range at entry. The probe aspect angle at beginning of descent is 2° and increases to 43° at the end of the mission. The relatively large EOM probe aspect angle is the result of targeting for common spacecraft to probe look direction for the three missions being considered.

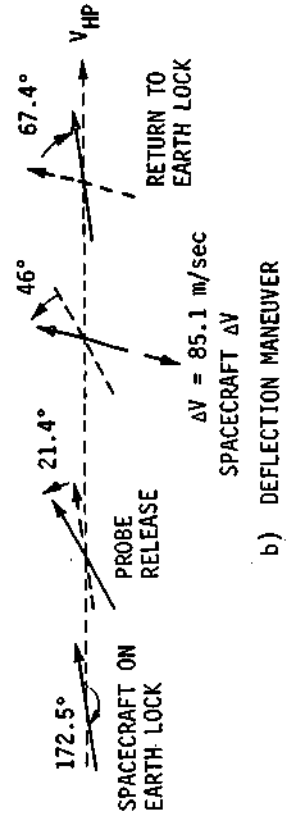
d. *Deflection Maneuver* - A spacecraft deflection maneuver was used to establish the above defined link geometry and acquire the entry site. A deflection radius of 10×10^6 km was used with a resulting spacecraft ΔV requirement of 85 m/sec. The implementation sequence is pictured in Figure IV-3c.

e. *Navigation and Dispersions* - This design mission requires optical tracking to supplement the standard Earth-based tracking, because Uranus' ephemeris uncertainties are about ten times greater than those of Saturn. The navigation results provided in Table IV-3c are approximately equivalent to those obtained at Saturn with standard Earth-based tracking.

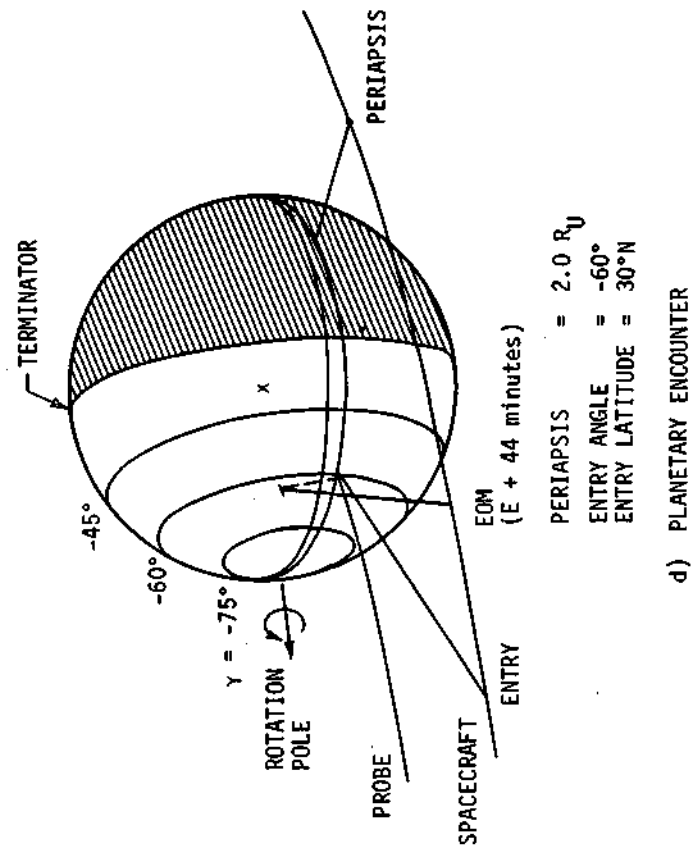
f. *Entry and Descent Trajectories* - Table IV-3d summarizes the entry and descent phases of the mission. Both entry and descent were simulated using all three atmosphere models. The variation in entry duration is from 27 seconds for the cool atmosphere to 90 seconds for the warm. During this phase of the mission, a peak deceleration of 837 g is attained 6.5 seconds after entry into the cool atmosphere.



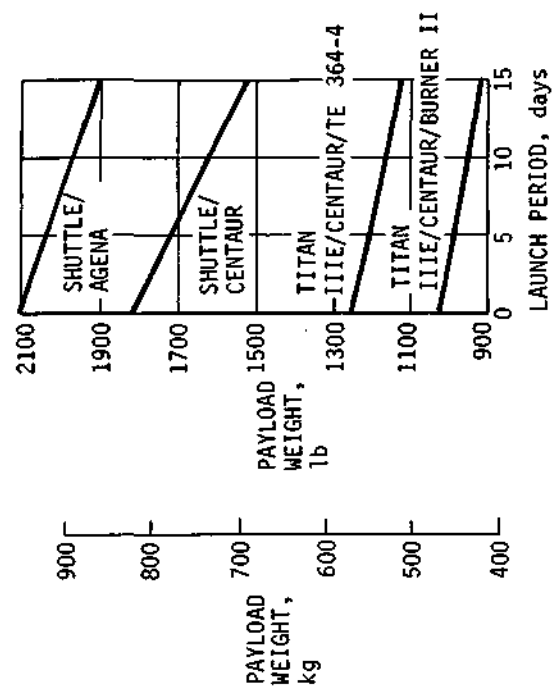
a) INTERPLANETARY TRAJECTORY



b) DEFLECTION MANEUVER



d) PLANETARY ENCOUNTER



c) LAUNCH ANALYSIS

Fig. IV-3 Uranus/SU 80 Mission Definition

Table IV-3 Uranus/SU 1980 Mission Summary Data

a) CONIC TRAJECTORY DATA

INTERPLANETARY TRAJECTORY	LAUNCH TRAJECTORY	ARRIVAL TRAJECTORY
LAUNCH DATE: 12/3/80	NOMINAL C_3 : 132.7 km ² /sec ²	V_{HP} : 11.87 km/sec
ARRIVAL DATE: 10/23/88	NOMINAL DLA: 27.6°	-RA: 276.5°
FLIGHT TIME: 7.7 yr	C_3 (5-day): 134.5 km ² /sec ²	DEC: -2.17°
	C_3 (10-day): 135 km ² /sec ²	ZAE: 169.7°
	C_3 (15-day): 140 km ² /sec ²	ZAP: 172.47°
		INC: 5.9°

b) DEFLECTION MANEUVER AND PROBE CONIC

DEFLECTION MANEUVER		PROBE CONIC DEFINITION	
DEFLECTION MODE:	SPACECRAFT	ENTRY ANGLE:	-60°
DEFLECTION RADIUS:	10 x 10 ⁶ km	ENTRY LATITUDE*:	-2.5°
COAST TIME:	9.5 days	ENTRY LONGITUDE*:	47.3°
ΔV :	85.1 m/sec	LEAD TIME:	1.8 hr
APPLICATION ANGLE:	127°	LEAD ANGLE:	1.5°
OUT-OF-PLANE ANGLE:	180°	PROBE/SPACECRAFT RANGE (ENTRY):	8.7 x 10 ⁴ km
PROBE RELEASE ANGLE:	21.3°	PROBE ASPECT ANGLE (ENTRY -):	31°
SPACECRAFT DEFLECTION ANGLE:	22.4°	PROBE ASPECT ANGLE (ENTRY +):	2°
SPACECRAFT REORIENTATION ANGLE:	43.7°	PROBE ASPECT ANGLE (EOM):	43°

*SUBSOLAR ORBITAL PLANE.

c) DISPERSION ANALYSIS SUMMARY

NAVIGATION UNCERTAINTIES	EXECUTION ERRORS (3 σ)	DISPERSIONS (3 σ)
TRACKING: OPTICAL & DOPPLER	ΔV PROPORTIONALITY: 1%	ENTRY ANGLE: 6.5°
SMAA: 1682 km	ΔV POINTING: 2°	ANGLE OF ATTACK: 3.15°
SMIA: 702 km	PROBE ORIENTATION POINTING: 2°	DOWNRANGE: 9.3°
β : 20°		CROSSRANGE: 3.4°
TOF: 635.8 sec		LEAD ANGLE: 13.7°
		LEAD TIME: 1.22 minutes
		ENTRY TIME: 31 minutes

d) ENTRY AND DESCENT SUMMARY

ENTRY PARAMETERS	ATMOSPHERE MODEL					
	WARM		NOMINAL		COOL	
ENTRY VELOCITY, km/sec	22.1	22.2	22.3			
ENTRY ALTITUDE, km	1073.8	532	200			
ENTRY β , kg/m ²	102	102	102			
MAXIMUM DECELERATION, g	225	358	837			
MAXIMUM DYNAMIC PRESSURE, N/m ²	2.2 x 10 ⁵	3.5 x 10 ⁵	8.3 x 10 ⁵			
EOM PRESSURE, bar	3.1	7.3	19.2			
DESCENT β , kg/m ²	110	110	110			

CRITICAL ENTRY EVENTS	ATMOSPHERE MODEL					
	WARM		NOMINAL		COOL	
	TIME, sec	ALTITUDE, km	TIME, sec	ALTITUDE, km	TIME, sec	ALTITUDE, km
g = 0.1	14.0	770	4.0	444	0.5	188
g = 100	36	300	15	208	4.5	102
MAXIMUM DECELERATION	40	235	19	138	6.5	65
MACH = 0.8	82.5	143	49.5	80.3	24.5	37.3
MACH = 0.7	90	140	54.5	78.5	27.5	36.5

B. SCIENCE INSTRUMENTATION AND PERFORMANCE

The instruments for the basic common Saturn/Uranus probe are the SAG Exploratory payload instruments. Their characteristics were given in Table V-29 of Volume II and are also given in the first part of Table V-1 of this volume. They are discussed in detail in Chapter III, Section C.1 of Volume II. These instruments are unchanged from the first part of the study.

The descent profiles shown in Figure III-31 are different from those in the previous part of the study only because three atmospheres are considered. The ballistic coefficient is 110 kg/m^2 for all descents. Values for descent parameters are given in Table III-14. It shows the parachute deployment pressure varying from 41 to 102 millibars while the pressure at the first descent measurement varies from 51 to 122 millibars. The final pressure for a descent designed at 44 minutes varies from 3.1 bars in the Uranus warm to 19.2 bars in the Uranus cool temperature. However, the probe falls 238 km in the Uranus warm, while descending only 92 km in the Uranus cool atmosphere. The distance in the Saturn warm atmosphere corresponding to the same 44 minutes is 320 km.

The entry and descent times, instrument sampling times, and resulting bit rates are shown in Table IV-4. The transmission bit rates for descent are slightly higher than the collection bit rates because the descent data collected during probe acquisition by the spacecraft must be stored and later interleaved with real-time data for transmission. The difference between this table and Table VI-2 of Volume II is that the mass spectrometer sampling time has been reduced to 50 seconds. Both the entry and descent times are slightly longer because of consideration of other model atmospheres; thus the bit rate to telemeter the stored accelerometer data is coincidentally 3.4 bps in both tables despite the fact that more data is collected here (8750 bits plus formatting, etc).

The descent mission measurement performance is given in Table IV-5 for Saturn and in Table IV-6 for Uranus. The first column gives the instrument, its sampling interval, and the measurement to be made. The second column gives the criteria set forth in Volume II. The remaining columns give the performance numbers in the units specified by the criteria. The minimum values are those at the highest point in the atmosphere that the measurement is to be evaluated, and are specified individually for each atmosphere to allow determination of worst case atmospheres. The maximum value given in the last column is the maximum performance of all the atmospheres at the end of the design mission (44 min from parachute deployment).

First, note that the mass spectrometer makes two full 1 to 40 amu sweeps inside the methane cloud in the Uranus warm atmosphere at the 50-second sampling time. At 60 seconds, it was only completing one sweep and a partial sweep inside this extremely low-pressure cloud. Since definition of the atmospheric clouds is an important objective, it was necessary to reduce the sampling time to the lower value in order to adequately sample this cloud.

Secondly, note that in most cases, the performance is lowest in the warm atmospheres. In fact, the pressure and turbulence accelerometer measurements are below the criteria at the highest evaluated point in both warm atmospheres. However, since the number of measurements per kilometer increases with descent and an adequate number of measurements is obtained within the highest modeled cloud (26 to 38), this does not necessitate a modification of the instrument sampling time.

Table IV-4 Instrument Sampling Times and Data Rates for Common Saturn/Uranus Probe with Exploratory Payload

PHASE	INSTRUMENT	SAMPLING TIMES, sec	COLLECTION BIT RATE, bps	TRANSMISSION BIT RATE, bps
ENTRY (84.5 sec MAXIMUM)	ACCELEROMETERS			
	AXIAL	0.2	50	0
	LATERAL	0.4	25	0
DESCENT (2640 sec CONSTANT)	LATERAL	0.4	25	0
	TEMPERATURE GAGE	4	2.5	2.6
	PRESSURE GAGE	4	2.5	2.6
	NEUTRAL MASS SPECTROMETER	50	8.0	8.3
	ACCELEROMETERS			
	TURBULENCE	8	7.5	7.8
	STORED	0	0	3.4

SCIENCE TOTAL	24.7
ENGINEERING	0.5
FORMATTING	<u>2.5</u>
TOTAL	27.7 bps

Table IV-5 Saturn Descent Measurement Performance - Exploratory Payload

INSTRUMENT	SAMPLING TIME	MEASUREMENT	CRITERIA	MINIMUM PERFORMANCE			MAXIMUM PERFORMANCE
				COOL	NOMINAL	WARM	
MASS SPECTROMETER	50 sec	MINOR CONSTITUENTS CLOUD COMPOSITION H/He RATIO ISOTOPIC RATIO MOLECULAR WEIGHT	2 PER SCALE HEIGHT*	5.8	7.7	6.5	37
			2 INSIDE EACH CLOUD	10.4 in NH ₃ 16 in H ₂ O	4.0 in NH ₃ 10.5 in H ₂ O	3.0 in NH ₃ 10.5 in H ₂ O	
TEMPERATURE GAGE	4 sec	TEMPERATURE PROFILE CLOUD STRUCTURE	1 PER °K 2 INSIDE EACH CLOUD	1.5 137 in NH ₃	1.2 46 in NH ₃ 196 in H ₂ O	1.3 38 in NH ₃ 47 in H ₂ O	8.1
PRESSURE GAGE	4 sec	PRESSURE PROFILE TURBULENCE CLOUD STRUCTURE	2 PER km } 1 PER km } * 2 INSIDE EACH CLOUD	2.7 137 in NH ₃	2.0 46 in NH ₃ 196 in H ₂ O	1.5 38 in NH ₃ 47 in H ₂ O	7.8
ACCELEROMETERS	8 sec	TURBULENCE	1 PER km*	1.3	1.0	0.7	3.9

* BELOW CLOUD TOPS.

Table IV-6 Uranus Descent Measurement Performance - Exploratory Payload

INSTRUMENT	SAMPLING TIME	MEASUREMENT	CRITERIA	MINIMUM PERFORMANCE			MAXIMUM PERFORMANCE
				COOL	NOMINAL	WARM	
MASS SPECTROMETER	50 sec	MINOR CONSTITUENTS CLOUD COMPOSITION H/He RATIO ISOTOPIC RATIO MOLECULAR WEIGHT	2 PER SCALE HEIGHT*	5.6	6.1	4.6	38
			2 INSIDE EACH CLOUD	18.3 in CH ₄	4.4 in CH ₄ 12 in NH ₃	2.0 in CH ₄ 5 in NH ₃	
TEMPERATURE GAGE	4 sec	TEMPERATURE PROFILE CLOUD STRUCTURE	1 PER °K 2 INSIDE EACH CLOUD	3.0 230 in CH ₄	3.0 48 in CH ₄ 113 in NH ₃	3.1 26 in CH ₄ 63 in NH ₃	10.9
PRESSURE GAGE	4 sec	PRESSURE PROFILE TURBULENCE CLOUD STRUCTURE	2 per km } 1 PER km } * 2 INSIDE EACH CLOUD	4.8 230 in CH ₄	2.5 48 in CH ₄ 113 in NH ₃	1.6 26 in CH ₄ 63 in NH ₃	14.4
ACCELEROMETERS	8 sec	TURBULENCE	1 PER km*	2.4	1.4	0.9	7.2

* BELOW CLOUD TOPS.

C. SYSTEM DESIGN AND INTEGRATION

1. Functional Sequence

Figure IV-4 shows a pictorial sequence of events with emphasis on the probe activity. It depicts the major probe and spacecraft events and shows the relationship between the probe and spacecraft after probe separation. Pre-entry times are omitted because they are different for each planet due to entry arrival uncertainty. Tables IV-7 and IV-8 show the detailed sequence of events for Saturn and Uranus, respectively, and are similar to the sequence for the probe-dedicated Jupiter mission shown in Table V-33 of Volume II. These sequences are based upon the nominal atmospheric models but show the variation of the various parameters (time, Mach No., pressure level, and altitude) for the cool and warm atmospheric models. As an example, the main parachute is deployed at Saturn at 5 g (decreasing) plus 15 seconds. This event occurs at entry (E) plus 59.5 seconds in the nominal atmosphere, E plus 44 seconds in the cool atmosphere, and E plus 84.5 seconds in the warm atmosphere. This event concludes the entry phase and starts the descent phase. Since accelerometer data is stored during the entry phase at a high data rate, the warm atmosphere duration, being the longest, is used for sizing the data storage.

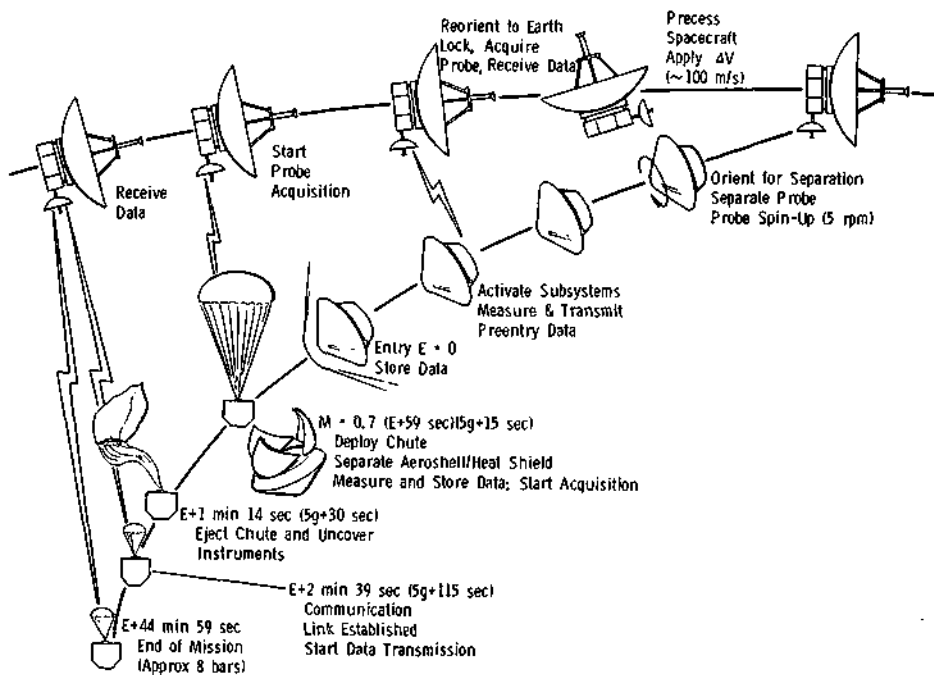


Figure IV-4 Sequence of Events (Task 1)

Table IV-7 Saturn Sequence of Events (Task I)*

ITEM	TIME	EVENT	COMMENTS†
1.	L * 0	LAUNCH (DEC 3, 1980)	
2.		SEPARATE SPACECRAFT FROM LAUNCH VEHICLE	
3.	L + 2h to L + 1221.8d	CRUISE	
4.	S - 7h, 30m, 0s	SPACECRAFT POWER TO PROBE; EJECT ENVIRONMENTAL COVER	
5.	S - 7h, 17m, 0s	START PROBE CHECKOUT	
6.	S - 0h, 17m, 0s	PROBE CHECKOUT COMPLETE; START SPACECRAFT ORIENTATION (10.6°)	
7.	S - 0h, 2m, 0s	SPACECRAFT ORIENTATION COMPLETE; ACTIVATE SEPARATION SUBSYSTEM	
8.	S = 0 (L + 1222.1d)	SEPARATE PROBE FROM SPACECRAFT	
9.	S + 0m, 0.5s	START PROBE SPINUP TO 5 rpm	
10.	S + 0m, 30s	START SPACECRAFT ORIENTATION FOR ΔV (59.1°)	
11.	S + 4m, 0s	PROBE SPINUP COMPLETE; DEACTIVATE PROBE SYSTEM	
12.	S + 15m, 30s	COMPLETE SPACECRAFT ORIENTATION FOR ΔV	
13.	S + 17m, 36s	APPLY SPACECRAFT ΔV (96 m/sec)	
14.	S + 18m, 0s	START SPACECRAFT ORIENTATION TO EARTH LOCK (69.7°)	
15.	S + 33m, 0s	SPACECRAFT ORIENTATION COMPLETE	
16.	L + 1222.12d to L + 125.79d	COAST	
17.	E - 43m, 57.5s	START BATTERY ACTIVATION PYRO CAPACITOR CHARGE	
18.	E - 23m, 57.5s	ACTIVATE BATTERY	
19.	E - 23m, 27.5s	POWER ON (DATA HANDLING SYSTEM & PYRO)	
20.	E - 8m, 9.5s	TURN ON SCIENCE & TRANSMITTER (WARM-UP)	
21.	E - 7m, 39.5s	START PROBE ACQUISITION	
22.	E - 5m, 59.5s	COMPLETE PROBE ACQUISITION; START DATA TRANSMISSION	ENGINEERING DATA AT ~1 bps
23.	E = 0	ENTRY (536 km ABOVE 1 atm; 1×10^{-7} atm)	297 km (C); 968.5 km (W)
24.	E + 0m, 5s	RF POWER AMPLIFIER OFF (0.1-g SENSING); START DATA STORAGE	1.7s (C); 12s (W)
25.	E + 0m, 17.5s	ENABLE PROBE DESCENT PROGRAM (100-g SENSING)	8.5s (C); 35s (W)
26.	E + 0m, 44.5s [5g (Ref)]	START DESCENT PROGRAM (5-g SENSING); OPERATE BASE COVER BAND CUTTERS	29s (C); 69.5s (W)
27.	E + 0m, 56.5s (5g + 12s)	DEPLOY BASE COVER QUADRANTS	41s (C); 81.5s (W)
28.	E + 0m, 59.5s (5g + 15s)	DEPLOY MAIN PARACHUTE (M = 0.7; ~65 mb); RF POWER AMPLIFIER ON; START ACQUISITION	{ 44s (C); 84.5s (W) M = 0.56 (C); M = 0.88 (W) { 102 mb (C); 44 mb (W)
29.	E + 1m, 9.5s (5g + 25s)	EJECT AEROSHELL	
30.	E + 1m, 14.5s (5g + 30s)	RELEASE MAIN CHUTE; DEPLOY TEMPERATURE GAGE; UNCOVER NEUTRAL MASS SPECTROMETER	
31.	E + 2m, 39.5s (5g + 115s)	PROBE ACQUISITION COMPLETE; START DATA TRANSMISSION	28 bps
32.	E + 44m, 59.5s (5g + 2655s)	END OF DESIGN MISSION (~8 bars)	45m, 24.5s (W) 18 bars (C); 4 bars (W)
33.	E + 2h, 12m (L + 1258d)	SPACECRAFT PERIAPSIS (3.8 R _G); MAY 9, 1984	

*ASSUMES AN ENTRY ARRIVAL UNCERTAINTY OF 4.4 minutes, A DESCENT BALLISTIC COEFFICIENT OF 110 kg/m² (0.7 slug/ft²), AND A NOMINAL ATMOSPHERE.
†(C) = COOL ATMOSPHERE; (W) = WARM ATMOSPHERE.

Table IV-8 Uranus Sequence of Events (Task I)*

ITEM	TIME	EVENT	COMMENTS [†]
1.	L = 0	LAUNCH (DEC 3, 1980)	
2.	L + 2h	SEPARATE SPACECRAFT FROM LAUNCH VEHICLE	
3.	L + 2h to L + 2816.7d	CRUISE	
4.	S - 13h, 30m, 0s	SPACECRAFT POWER TO PROBE; EJECT ENVIRONMENTAL COVER	
5.	S - 13h, 17m, 0s	START PROBE CHECKOUT	
6.	S - 0h, 17m, 0s	PROBE CHECKOUT COMPLETE; START SPACECRAFT ORIENTATION (21.4°)	
7.	S - 0h, 2m, 0s	SPACECRAFT ORIENTATION COMPLETE; ACTIVATE SEPARATION SUBSYSTEMS	
8.	S = 0 (L + 2817.3d)	SEPARATE PROBE FROM SPACECRAFT	
9.	S + 0m, 0.5s	START PROBE SPINUP TO 5 rpm	
10.	S + 0m, 30s	START SPACECRAFT ORIENTATION FOR ΔV (46°)	
11.	S + 4m, 0s	PROBE SPINUP COMPLETE; DEACTIVATE PROBE SYSTEM	
12.	S + 15m, 30s	COMPLETE SPACECRAFT ORIENTATION FOR ΔV	
13.	S + 17m, 36s	APPLY SPACECRAFT ΔV (86 m/sec)	
14.	S + 18m, 0s	START SPACECRAFT ORIENTATION TO EARTH LOCK (67.4°)	
15.	S + 33m, 0s	SPACECRAFT ORIENTATION COMPLETE	
16.	L + 2817.32d to L + 2824.6d	COAST	
17.	E - 1h, 8m, 39.5s	START BATTERY ACTIVATION PYRO CAPACITOR CHARGE	
18.	E - 48m, 39.5s	ACTIVATE BATTERY	
19.	E - 48m, 9.5s	POWER ON (DATA HANDLING SYSTEM & PYRO)	
20.	E - 32m, 51.5s	TURN ON SCIENCE & TRANSMITTER (WARM-UP)	
21.	E - 32m, 21.5s	START PROBE ACQUISITION	
22.	E - 30m, 41.5s	COMPLETE PROBE ACQUISITION; START DATA TRANSMISSION	ENGINEERING DATA AT ~1 bps
23.	E = 0	ENTRY (532 km ABOVE 1 atm; 1×10^{-7} atm)	200 km (C); 1074 km (W)
24.	E + 0m, 4s	RF POWER AMPLIFIER OFF (0.1-g SENSING); START DATA STORAGE	0.5s (C); 14s (W)
25.	E + 0m, 15s	ENABLE PROBE DESCENT PROGRAM (100-g SENSING)	4.5s (C); 36s (W)
26.	E + 0m, 38.5s [5g (Ref)]	START DESCENT PROGRAM (5-g SENSING); OPERATE BASE COVER BAND CUTTERS	18.5s (C); 65s (W)
27.	E + 0m, 50.5s (5g + 12s)	DEPLOY BASE COVER QUADRANTS	30.5s (C); 77s (W)
28.	E + 0m, 53.5s (5g + 15s)	DEPLOY MAIN PARACHUTE (M = 0.72; ~47 mb); RF POWER AMPLIFIER ON; START ACQUISITION	{ 33.5s (C); 80s (W) M = 0.59 (C); = 0.84 (W) 41 mb (C); 49 mb (W)
29.	E + 1m, 3.5s (5g + 25s)	EJECT AEROSHELL	
30.	E + 1m, 8.5s (5g + 30s)	RELEASE MAIN CHUTE; DEPLOY TEMPERATURE GAGE; UNCOVER NEUTRAL MASS SPECTROMETER	
31.	E + 2m, 33.5s (5g + 115s)	PROBE ACQUISITION COMPLETE; START DATA TRANSMISSION	28 bps
32.	E + 44m, 53.5s (5g + 2655s)	END OF DESIGN MISSION (~7.3 bars)	19 bars (C); 3.1 bars (W)
33.	E + 1h, 51m (L + 2826.9d)	SPACECRAFT PERIAPSIS (2R _J); AUGUST 24, 1988	

*ASSUMES AN ENTRY ARRIVAL UNCERTAINTY OF 29 minutes, A DESCENT BALLISTIC COEFFICIENT OF 110 kg/m² (0.7 slug/ft²) AND A NOMINAL ATMOSPHERE.
[†](C) = COOL ATMOSPHERE; (W) = WARM ATMOSPHERE.

2. Functional Block Diagram

The functional block diagram is the same as Figure V-76 of Volume II with the four subsystem areas deleted or reduced as follows for spacecraft deflection mode: propulsion and ACS electronics are deleted, ACS propulsion is reduced by 75%, and separation power is reduced by 50%.

3. System Data Profile

The data profile for the Saturn/Uranus probe shown in Figure IV-5 is very similar to Figure V-101 of Volume II for the probe-dedicated Jupiter mission. As in the earlier data profile, the separation phase is very short (approximately 4 min) because the probe is deployed by the spacecraft, and because of the short duration, data is not collected during this interval. Due to the entry arrival uncertainty of 4.4 minutes for Saturn and 29 minutes for Uranus, the pre-entry activity is different for each planet and therefore requires a different sequence to be stored onboard the probe and selected by Earth commands to the spacecraft. The entry and descent data profile is the same for both planets, i.e., total data collected is 70,300 bits, maximum storage on the probe is 11,637 bits, and the probe-to-spacecraft data transmission rate is approximately 28 bits/sec.

4. System Power Profile

Figure IV-6, showing the power profile for the Saturn/Uranus probe, is similar to that for the probe-dedicated Jupiter (Volume II, Chapter V, Section C3) except that the "worst case" entry arrival uncertainty of 29 minutes for Uranus is shown. The figure shows the effect of this arrival uncertainty on the power requirements. The late arrival condition requires 133 w-hr of power at the equipment. Late arrival is the condition where the probe has not yet arrived at the planet when the timer (preset before separation) runs out and starts the sequence before it is really needed.

5. System Weight Summary

Table IV-9 shows the weight breakdown for the Saturn/Uranus probe. Ejected weight is 89.02 kg (196.08 lb), entry weight is 89.01 kg (196.05 lb), and the final descent weight is 40.46 kg (89.11 lb). Compared with the Saturn probe weight shown in Table VI-6 of Volume II, this probe ejection weight is lighter because of the absence of a ΔV motor, but the entry weight is heavier due to higher decelerations, longer entry and descent time, which increases the battery weight, and to the small amount of propulsion weight that is carried to entry instead of being ejected with the service module as was the previous case.

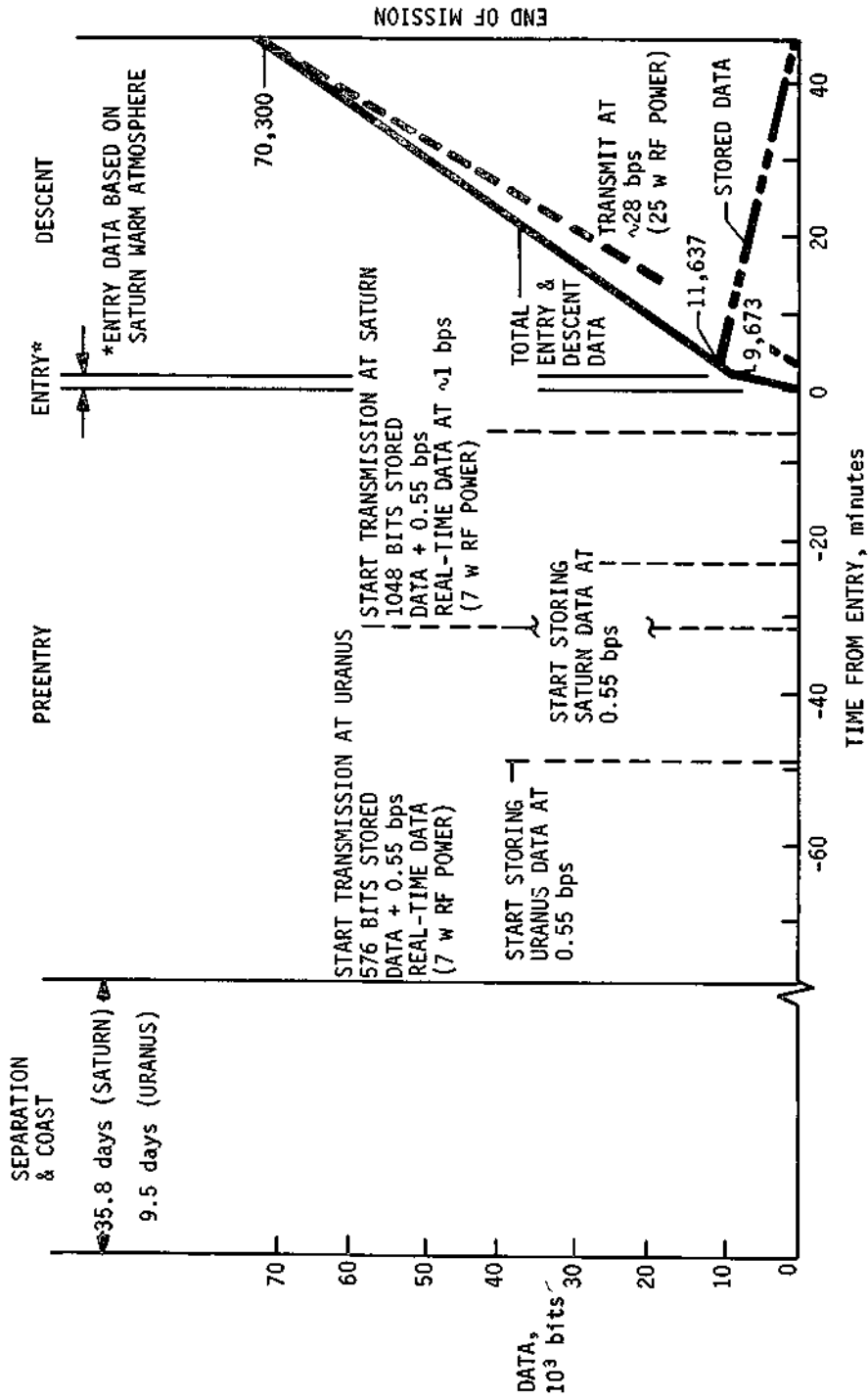


Fig. IV-5 Data Profile for Saturn/Uranus Probe (Task I)

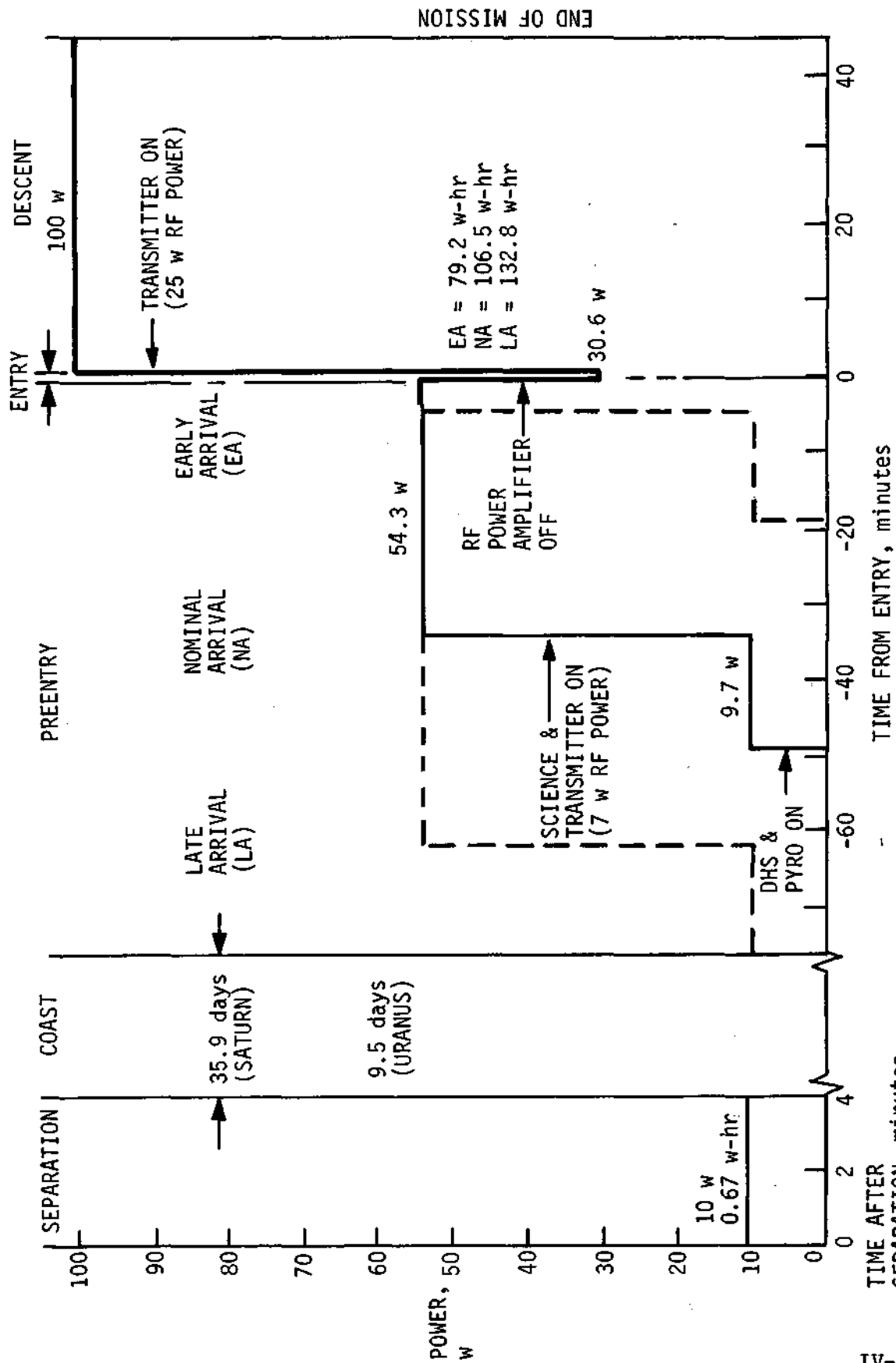


Fig. IV-6 Power Profile for Saturn/Uranus Probe (Task I)

Table IV-9 Weight Summary for Saturn/Uranus Probe with
SAG Exploratory Payload

	WEIGHT	
	kg	lb
SCIENCE	8.08	17.80
POWER & POWER CONDITIONING	4.70	10.35
CABLING	3.86	8.50
DATA HANDLING	2.43	5.35
ATTITUDE CONTROL SUBSYSTEM (DRY)	2.84	6.25
COMMUNICATIONS	3.86	8.50
PYROTECHNICS	6.38	14.05
STRUCTURES & HEAT SHIELD	34.00	74.89
MECHANISMS	6.03	13.28
THERMAL	5.22	11.50
PROPELLANT (ACS)	0.01	0.03
ENGINEERING INSTRUMENTATION	0.00	0.00
15% MARGIN	<u>11.61</u>	<u>25.58</u>
EJECTED WEIGHT	89.02	196.08
ENTRY WEIGHT	89.01	196.05
DESCENT WEIGHT (FINAL)	40.46	89.11

D. TELECOMMUNICATIONS SUBSYSTEM

Results of the parametric study performed to arrive at a common Saturn/Uranus probe design were used to define the telecommunications subsystem. The Saturn/SU 80 mission trajectory generates the worst-case communications geometry due mainly to the large communications range of 2×10^5 km at entry. The cool Saturn atmosphere model has the greatest microwave absorption at 0.86 GHz (see Figures III-43 and III-44). Therefore, the Saturn/SU 80 trajectory, as developed in Chapter III, Section D.1 as configuration 4-S, is used to define the telecommunications subsystem for the Task I science payload.

The system noise temperatures were reevaluated for the follow-on effort. Revised curves are shown in Figures III-37 and III-38 for Saturn and Uranus, respectively. The revised curves indicate a slightly higher system noise (due to cable attenuation) and its impact on receiver front-end noise temperature. The antenna noise temperature is unchanged for Saturn. A revised antenna noise temperature curve for Uranus was used based on data from a monograph published by NASA (see Ref III-2). Feedline noise was also considered for the revised Uranus system noise temperature calculation. Values for receiver noise temperature were also investigated and found to be in agreement with the predicted receiver state of the art by several suppliers. Therefore, the original values in Vol II, Figure V-11, p V-21 were used in the updated analysis.

As discussed in detail in Chapter III, Section D.1, trajectory adjustments were made in order to optimize the communications geometry for Saturn encounter from the SU 80 trajectory and at the same time develop common trajectories for Saturn and Uranus. Probe-to-spacecraft communications range is shown in Figure IV-7 for the Saturn/SU 80 mission. Increasing range before entry is caused by the relative motion of the probe and spacecraft with the spacecraft moving ahead of the probe as the probe begins descent into the atmosphere. Maximum range occurs at entry and decreases by approximately $0.2 R_s$ (12,000 km) at mission completion. The spacecraft reaches periapsis after the mission is over (E+2.3 hr).

The probe aspect angle as a function of mission time is shown in Figure IV-8. The angle steadily increases during descent from 7.5° at entry to 24° at mission completion. Three-sigma variations in the angle are 3° , based upon a 100-sample Monte Carlo

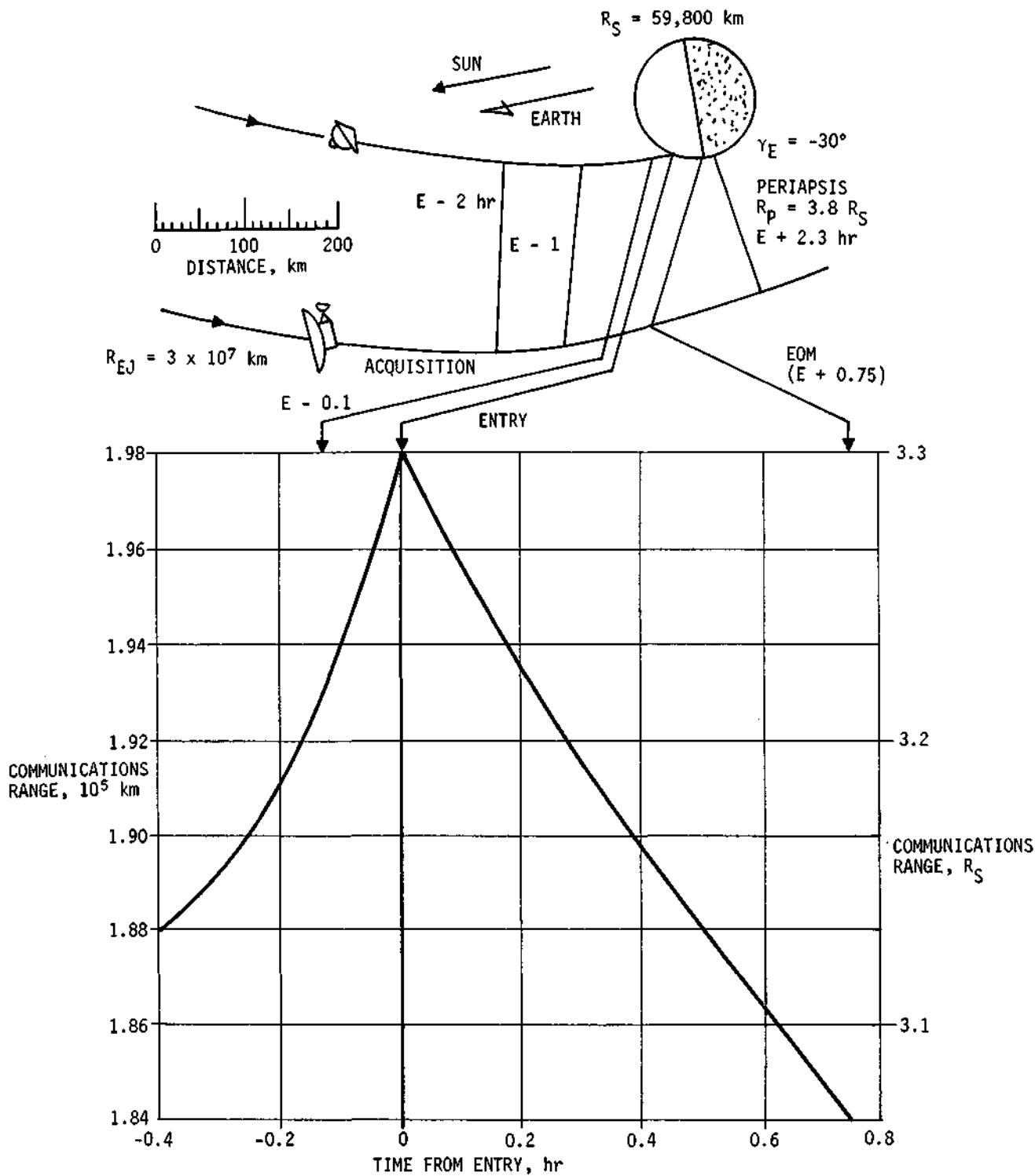


Fig. IV-7 Probe-to-Spacecraft Communications Range for the Saturn/SU-1980 Mission

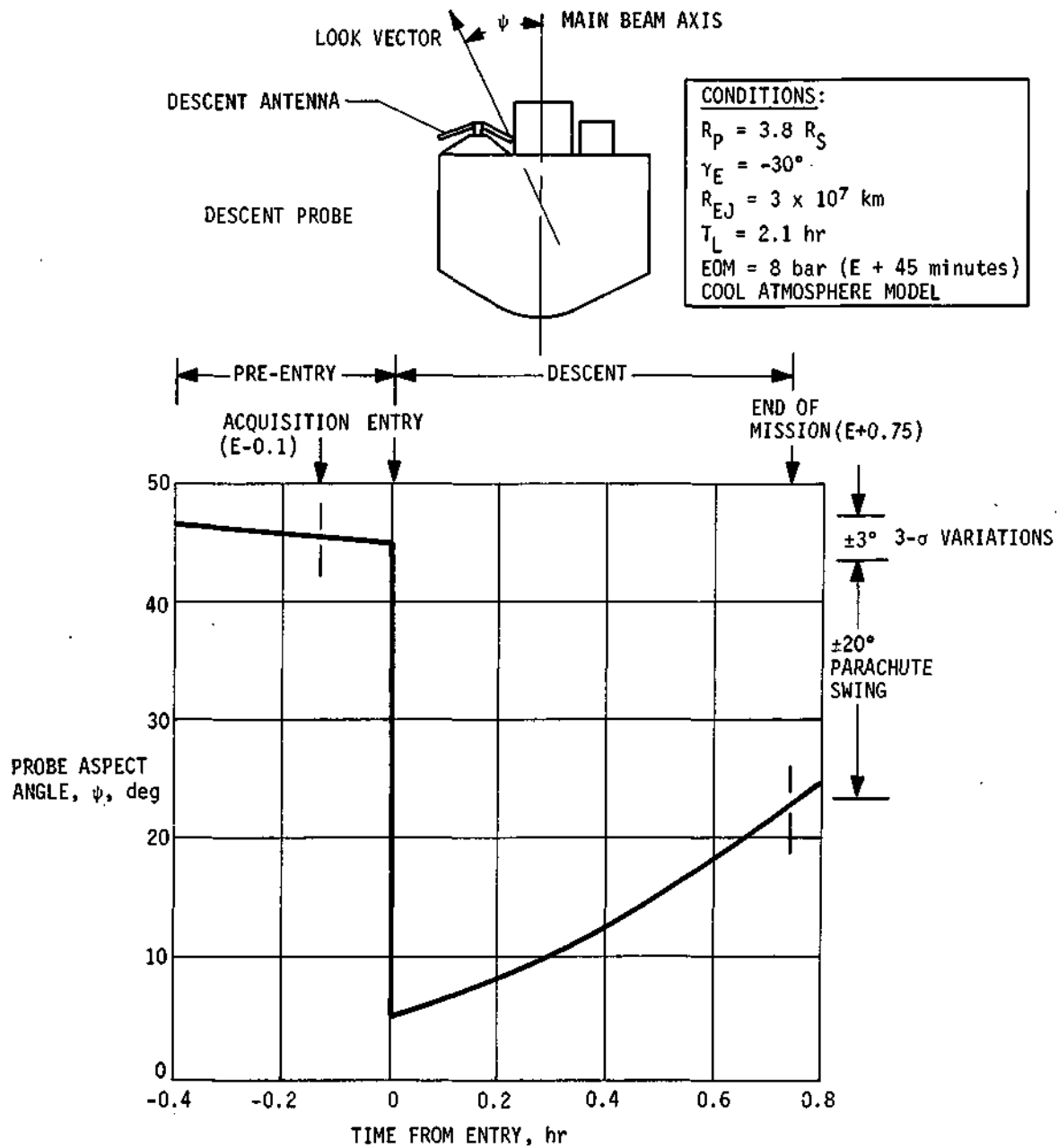


Fig. IV-8 Saturn/SU 1980 Mission Proba Aspect Angle

analysis. Also included is 20° to account for parachute swing resulting from atmosphere turbulence and lateral winds. The resulting probe descent antenna beamwidth is 100° with circular polarization.

Relative probe positions during the mission are shown in Figure III-52. The ellipses account for navigation uncertainties and execution errors used with a 100-sample Monte Carlo error analysis. Nominal positions are shown by the triangles. Whether the ellipse major axis is aligned with the cone or clock axes is determined by the direction of rotation of the planet relative to the spacecraft trajectory. For Saturn, elevation angle (cross-cone angle) dispersions are small with the major differences occurring in cone angle. Decreasing cone angle during descent results from the spacecraft pulling ahead of the descending probe. A 20° beamwidth probe receiving antenna on the spacecraft covers the relative probe positions including uncertainties for Saturn encounter from the SU 80 trajectory.

Probe transmitter output power requirements as a function of mission time are shown for the three missions in Figure IV-9 for Task I data rates. The curves are the result of considering all the RF link parameters using binary FSK modulation. RF power requirements for Saturn are increasing rapidly at mission completion due to increasing atmosphere attenuation (Figure III-44) and decreasing spacecraft antenna gain (Figure III-52). Two frequencies are shown for the worst-case mission. As seen in the figure, a small increase in the RF operating frequency results in large increases in RF power required. Also indicated on the curves are descent pressures for the two worst-case atmosphere models. The curves indicate that the worst-case mission is a Saturn encounter from the SU 80 trajectory.

Parameters of the RF link are depicted in Table IV-10 for the Saturn/SU 80 mission at mission completion which is the worst-case point. An RF power of 25 w is required at this point with the Task I science payload. This is the power level that defines the probe transmitter output power requirement and is the worst-case trajectory, atmosphere, and descent point.

Table IV-11 depicts design details of the RF components that comprise the telecommunications subsystem for the common Saturn/Uranus probe with Task I science payload. The probe transmitter has two RF power levels available for the mission, 7 and 25 w. Thermal control at Uranus prior to entry requires 7 w. The transmitter operates at 0.86 GHz and uses binary FSK modulation with a tracking tone. At the present state of the art, a mechanical RF switch may be used, but the possibility exists that a lighter, solid-state switch may be available by 1976. Identical pre-entry and descent turnstile/cone antennas are used on the probe, and the probe receiving antenna on the spacecraft is positioned at a single point in space to cover the three missions (Figure III-52). Polarization of probe and spacecraft antennas are right-hand circular.

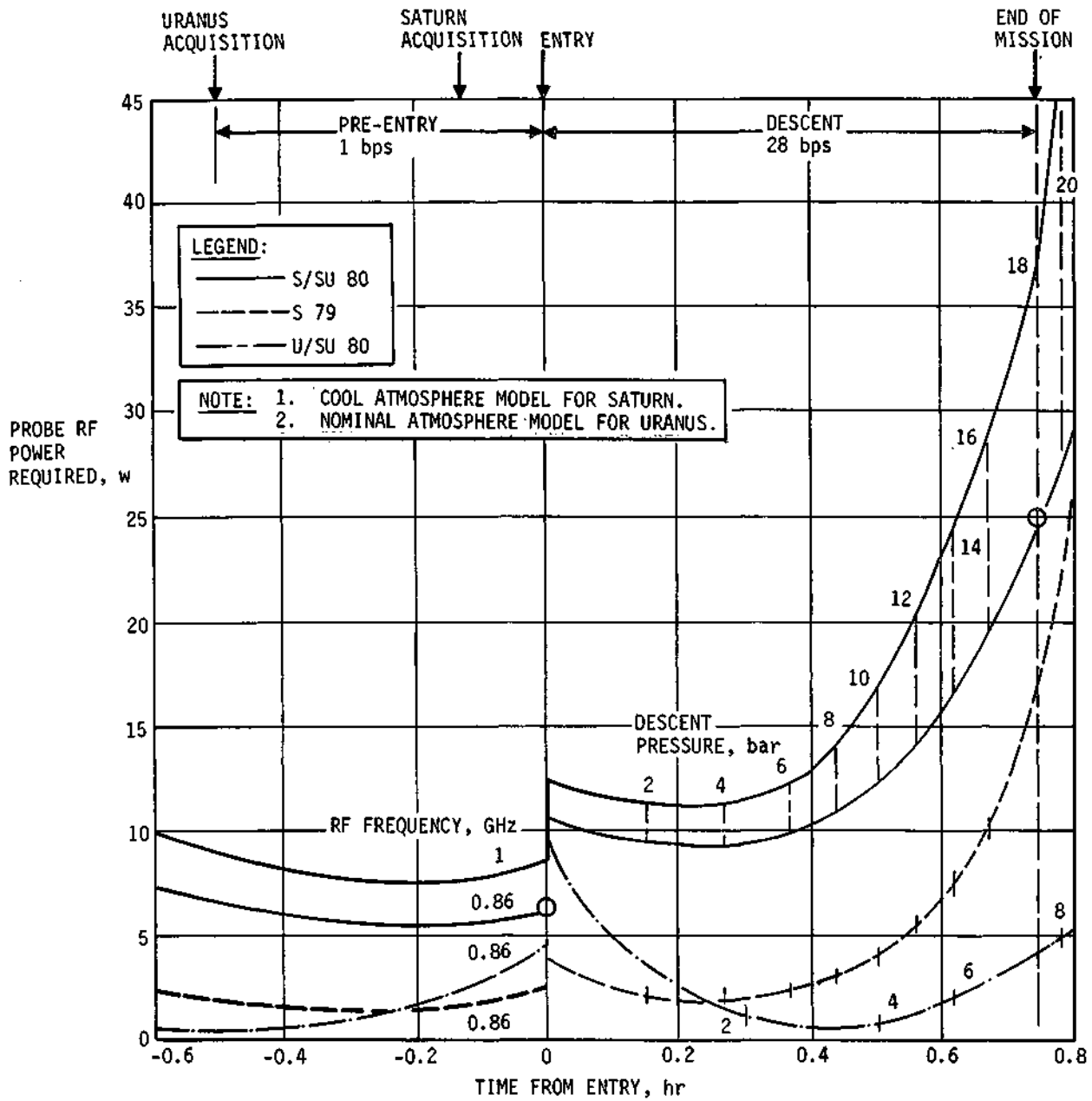


Fig. IV-9 Task I Probe RF Power Requirements

Table IV-10 Probe Telemetry Link Design Table for the Saturn/SU 1980 Mission with Task I Science*

PARAMETER	NOMINAL VALUE	ADVERSE TOLERANCE	REMARKS
1. TOTAL TRANSMITTER POWER, dBw	14.0	0	25.1 w at 0.86 GHz
2. TRANSMITTING CIRCUIT LOSS, dB	-1.1	0.1	CABLE & SWITCH
3. TRANSMITTING ANTENNA GAIN, dB	6.0	1.8	100° BEAMWIDTH
4. COMMUNICATIONS RANGE LOSS, dB	-196.5	0.3	1.8×10^5 km
5. PLANET ATMOSPHERE & DEFOCUSING LOSS, dB	-4.1	0.2	COOL, 18 bar
6. POLARIZATION LOSS, dB	-0.3	0	
7. ANTENNA PATTERN RIPPLE LOSS, dB	0	0.2	
8. RECEIVING ANTENNA GAIN, dB	17.9	1.0	20° BEAMWIDTH
9. RECEIVING CIRCUIT LOSS, dB	-1.0	0.1	CABLE
10. NET CIRCUIT LOSS, Σ (2 + 9), dB	-179.1	3.7	
11. TOTAL RECEIVED POWER (1 + 10), dBw	-165.1	3.7	
12. RECEIVER NOISE SPECTRAL DENSITY, dBw/Hz	-196.2	0.4	$T_s = 1750^\circ\text{K}$ $NF_s = 8.5$ dB
<u>TRACKING TONE</u>			
13. TONE POWER/TOTAL POWER, dB	-4.6	0	$P_t = 8.7$ w
14. RECEIVED TONE POWER (11 + 13), dBw	-169.7	3.7	
15. TRACKING THRESHOLD BANDWIDTH, dB	12.4	0	17.5-Hz BANDWIDTH
16. THRESHOLD SIGNAL/NOISE RATIO, dB	10.0	0	
17. THRESHOLD TRACKING POWER (12 + 15 + 16), dBw	-173.8	0.4	
18. TRACKING PERFORMANCE MARGIN (14 - 17), dB	4.1	4.1	
<u>DATA CHANNEL</u>			
19. DATA POWER/TOTAL POWER, dB	-1.6	0	$P_d = 17.4$ w
20. RADIO SYSTEM PROCESSING LOSS, dB	-1.0	0	
21. FADING LOSS, dB	-1.0	0	
22. RECEIVED DATA POWER (11 + 19 + 20 + 21), dBw	-168.7	3.7	
23. DATA BIT RATE, dB	14.5	0	28 bps
24. THRESHOLD E_b/N_o , dB	8.9	0	
25. THRESHOLD DATA POWER (12 + 23 + 24), dBw	-172.8	0.4	
26. PERFORMANCE MARGIN (22 - 25), dB	4.1	4.1	
27. NOMINAL LESS ADVERSE VALUE (26 - 26 adv), dB	0		
<p><u>*CONDITIONS:</u> 1. S/SU 80 COMMON PROBE MISSION (WORST-CASE TRAJECTORY). 2. WORST-CASE (END OF MISSION) CONDITIONS AT 0.86 GHz. 3. CONVOLUTIONAL ENCODER, M = 2, V = 2, Q = 8. 4. BER = 5×10^{-5} FOR BINARY FSK WITH K = 8 code.</p>			

Table IV-11 Telecommunications RF Subsystem for the Task I Mission*

COMPONENT	CHARACTERISTIC	VALUE
TRANSMITTER	RF POWER OUT	7 AND 25 w
	OVERALL EFFICIENCY	45%
	MAXIMUM dc POWER IN AT 28 vdc	55.5 w
	TOTAL WEIGHT	2.73 kg (6 lb)
RF SWITCH	VOLUME	3440 cm ³ (210 in. ³)
	TYPE	MECHANICAL SPDT
	INSERTION LOSS	0.3 dB
	WEIGHT	0.23 kg (0.5 lb)
PROBE PRE-ENTRY & DESCENT ANTENNAS	VOLUME	443 cm ³ (27 in. ³)
	TYPE	TURNSTILE/CONE
	MAIN BEAM ANGLE	0 deg
	BEAMWIDTH	100 deg
	MAXIMUM GAIN	6.5 dB
SPACECRAFT ANTENNA	SIZE (DIAMETER x HEIGHT)	15.1 x 8.25 cm (6 x 3.25 in.)
	WEIGHT	0.45 kg (1.0 lb)
	TYPE	PARABOLIC DISH
	BEAMWIDTH	20 deg
SPACECRAFT RECEIVER	MAXIMUM GAIN	18.3 dB
	SIZE (DIAMETER)	128 cm (50.4 in.) (4.2 ft)
	WEIGHT	4.54 kg (10 lb)
	DESPIN	NO
	POSITION SEARCH	ONE
	FREQUENCY ACQUISITION	31 sec
	CLOCK ANGLE, θ	257 deg
	CONE ANGLE, ϕ	116 deg
NOISE TEMPERATURE	300°K	
NOISE FIGURE	3.1 dB	
dc POWER IN AT 28 vdc	3.0 w	
WEIGHT	0.9 kg (2.0 lb)	
<p>*CONDITIONS: 1. PLANETS: SATURN & URANUS. 2. MARINER SPACECRAFT. 3. FREQUENCY = 0.86 GHz. 4. BIT RATE = 28 bps.</p>		

E. DATA HANDLING SUBSYSTEM

The data processing electronics are essentially unchanged from the previous study, as indicated in Chapter III, Section D2 of this report. The modifications necessary to provide the inflight target planet selection consist of approximately ten ROMs for the additional formats and a latching relay to implement the selection. The increase in weight associated with these additional elements is offset by a decrease in power conditioning and thermal dissipation equipment requirements. As discussed in Chapter III, Section D2 of this volume, COS/MOS data storage design has been employed for this mission. The physical and electrical characteristics are approximated by the following equations:

$$V = \text{volume} = 443 + 16.0 M (10^{-3}) \text{ cm}^3$$

$$W = \text{Weight} = 0.2 + 0.715 M (10^{-5}) \text{ kg}$$

$$\text{Power (stand-by)} = P_s = 0.2 + 11.0 M (10^{-6}) \text{ w}$$

$$\text{Power (operate)} = P_o = 1.0 + 5.50 M (10^{-6}) \text{ w}$$

M = memory = number of bits stored

The assumption is made that twelve 1024-bit chips ($M = 12,288$ bits) will be required to store the blackout data. This results in the following values for the memory electronics, physical and electrical interface characteristics.

$$V = 640 \text{ cm}^3 \quad W = 0.29 \text{ kg} \quad P_s = 0.34 \text{ w} \quad P_o = 1.7 \text{ w}$$

Comparable characteristics for data processing electronics are assumed to be identical to the previous study (Vol I thru III).

$$V = 2330 \text{ cm}^3 \quad W = 2.13 \text{ kg} \quad P = 6.9 \text{ w}$$

The DHS begins the initial descent sequence shortly after the descent battery is energized. The initiation of the sequence and the initial state of the DHS will be established by a timing circuit working off battery voltage. This will ensure that the turn-on battery transient has subsided and will eliminate the need of an additional event from the coast timer. The required sequence of events is illustrated in Table IV-7 (Saturn Sequence of Events Task I). The pre-entry sequence occurs from item 19 to item 22 inclusive. The actual time with respect to entry of these events will vary (± 4.4 min, Saturn; ± 29 min, Uranus) due to trajectory

uncertainties. The control state established at item 22 will remain fixed regardless of the actual time before entry until 0.1 g sensing (item 24). The functions required of the DHS formats with respect to the Task I Saturn sequence are tabulated.

From Item	To Item	Format
19	22	Store engineering data
22	24	Interleave stored and real-time engineering data
24	30	Store entry accelerometer science and engineering data
30	31	Store descent science and engineering data
31	32	Interleave stored and real-time science and engineering data

During periods 22 to 24 and 31 to 32, the interleaved data is sequenced to the encoder and RF transmitter.

F. POWER AND PYROTECHNIC SUBSYSTEM

The configuration of the power and pyrotechnic subsystem for Task I is unchanged from the previous study (Vol I thru III) as indicated in Chapter III, Section D3 of this volume. Remote activated Ag-Zn batteries provide power during the brief post-separation activity and the entry and descent phase, Hg-Zn batteries provide power for the coast timer (1.3 volts, 7 μ amp, 35 days max) and the initial entry pyro event (36 volts, 25 ma peak, 5 ma average, 1.0 hr).

The selection of the post-separation battery (EP GAP 4384; 0.25 kg, 93.5 cm³) is based on an available battery rather than an optimum battery. During the previous study, it was assumed that the DHS (6.9 w) and the pyrotechnics subsystem (0.5 w) would be operating at this time for approximately 4.0 minutes. Assuming some engineering functions, the total load was estimated to be 10.0 w. The battery is designed to deliver 1.0 amp (28 w) for 16 minutes. At lower loads, the capability of the battery may be expected to be greater. For purposes of decreased sequencing complexity, consideration of direct pyrotechnic initiation from the battery has been considered. A small RC timer may be used for the timing function, eliminating the need for operating the DHS and the pyrotechnic subsystems. Assuming this battery can provide the initiation currents for the dual squibs, the complexity of the separation activity is significantly reduced. The battery peak current capability remains to be fully validated (Chapter III, Section D.3); however, since the original option (activation of DHS and pyrotechnics) is available and there is no significant difference in the physical description of the two approaches, the original size and weight specification remains the same.

The entry and descent battery specification is based on the power required for subsystem components plus losses and margins and the sequence of events for a late arrival probe. The maximum transmitter power at Saturn and a late arrival probe at Uranus provide the worst case requirement for the battery. The nominal power demands of the various subsystems are tabulated.

<u>Subsystem</u>	<u>Power (w)</u>	<u>Subsystem</u>	<u>Power (w)</u>
Transmitter	25/69.4	NMS	14.0
DHS (pre-entry/descent)	7.2/8.6	Pressure	1.3
		Temperature	1.4
Engineering Housekeeping	2.0	Accelerometer	2.8
Distribution losses	9.7 (max)*		

*Assumes 5% of total power.

The margins that are applied consist of ± 29 minutes trajectory uncertainty at Uranus, $\pm 5\%$ descent time uncertainty, and 10% overall uncertainty in power levels. These calculations result in a total required energy storage of 160 w-hr and a peak demand of 105 w at 28 volts. Using an energy density of 13.6 w-hr/kg and 0.138 w-hr/cm³, the entry/descent battery physical specification is 2.41 kg and 1200 cm³.

The physical specification of the power and pyrotechnic subsystem is based on a summation of the estimated required equipment as listed.

SCR - two per (dual bridgewire) event

Relays - one per event

Capacitor banks - six discharges allowed per bank; sufficient banks must be allowed to provide separate banks for simultaneous (less than 15 sec apart) discharges.

Electronics - engineering estimate.

The number of capacitor banks (8) is controlled by the number of simultaneous events (4) for these missions. The total of 15 events requires 30 SCRs and 15 relays. The physical characteristics of the pyrotechnics is listed .

<u>Component</u>	<u>Size/Weight</u>	<u>Number Required</u>	<u>Total Size/Weight</u>
Capacitor bank	164 cm ³ /81.9 g	8	1310 cm ³ /0.66 kg
Relays	14 cm ³ /34.1 g	15	210 cm ³ /0.51 kg
SCR	13.6 cm ³ /14.1 g	30	410 cm ³ /0.42 kg
Electronics	1230 cm ³ /0.91 kg	1	1230 cm ³ /0.91 kg

The size and weight of each element includes 10% to 15% for packaging

G. ATTITUDE CONTROL

The attitude control dynamics are minimal for the design configuration considered for the Saturn/Uranus probe. The errors involved are:

- 1) initial error due to spacecraft pointing;
- 2) drift error accumulation during period between separation and spinup due to tipoff rate;
- 3) error due to tipoff rate combined with spinup;
- 4) error due to spin-up jet misalignment.

Only momentum vector errors are of significance in this analysis since nutation errors are damped out and the spin axis (principal moment of inertia) will align with the momentum vector. The momentum vector errors involved are discussed in the following paragraphs.

- 1) Drift error - Assuming an initial tip off rate of one-half deg/sec about a nominal X-axis, the spin axis is displaced in the minus y direction.

$$\theta_T = W_T t_D \quad \theta_T = \text{drift error}$$

$$W_T = \text{tip off rate} = 0.5^\circ/\text{sec} \quad t_D = \text{drift period} = 0.5 \text{ sec}$$

$$\theta_T = 0.25^\circ$$

- 3) As indicated in Chapter III, Section D4 of this volume, the error may be calculated from knowledge of the spin momentum, transverse moment of inertia and spin torque.

$$W = 0.52 \text{ rad/sec} \quad I_s = 4.9 \text{ kg-m}^2$$

$$m = 3.4 \text{ N-m} \quad I_t = 4.2 \text{ kg-m}^2$$

$$q = p^2/mI_t = 0.465 \quad P_x(o)/P = 0.795 \text{ (deg)}$$

$$\theta_x(P) \leq 0.802 \quad \theta_y(P) \leq -0.19^\circ$$

Since the combination of the drift and spinup/tipoff error is not random, the error due to (2) and (3) combined is:

$$\theta_x(P) \leq 0.802^\circ$$

$$\theta_y(P) \leq -0.44^\circ = -0.25^\circ - 0.19^\circ$$

- 4) The analysis of Chapter III Section D4 of this volume indicated the spin torque vector offset $\theta_s = 0.136^\circ$. The total rss momentum vector error is then

$$\theta_E = 0.92^\circ.$$

H. STRUCTURAL AND MECHANICAL SUBSYSTEMS

The approach to design of the structural and mechanical subsystems for the Saturn/Uranus baseline common probe is essentially the same as that presented in Volumes I and II of the report for the earlier outer planet atmospheric probes. This probe design, however, uses a spacecraft-deflect mode for the trajectory deflection maneuver rather than a probe-deflect. Therefore, this configuration deletes the solid propellant deflection motor and the spin-despin-precess service module of prior configurations. The probe utilizes an aeroshell/heat shield structure to withstand the high heating of planetary entry at either Saturn or Uranus, and to provide an entry ballistic coefficient satisfying science mission requirements for initiation of atmospheric descent. The aeroshell structure and heat shield remaining after entry are jettisoned after completion of entry and before planetary atmospheric descent. This approach rids the descent probe of the heat shield and its absorbed heat load, and eliminates contamination of the descent probe mass spectrometer by carbon and other elements originating from the heat shield. The descent probe is separated from the aeroshell after entry by means of a separation parachute, and then descends on a second parachute through the planetary atmosphere to accomplish the scientific mission.

The entire probe is designed to withstand the entry loads encountered during planetary entry at Saturn and Uranus. For the selected missions, the entry heating is most severe for Saturn entry, while structural loadings are more severe for Uranus entry. The structural and mechanical design for the common probe are described in the following paragraphs.

1. Configuration and General Arrangement

The common Saturn/Uranus probe is a two-stage configuration using one configuration for the cruise/coast/entry phases of flight and a second configuration for planetary atmospheric descent. These configurations are depicted in Figure IV-10. The cruise/coast/entry configuration is depicted on the right hand side of the figure, and the descent configuration on the left. The total weight breakdown for the entire probe before entry, and the sequential configuration weights are presented in Table IV-12. The descent probe contains all the scientific instrumentation plus the supporting electrical and electronic components necessary to successfully complete the descent science mission. That probe equipment required prior to entry, but not for descent, is located within the aeroshell/heat shield structural assembly.

The descent probe has a diameter of 47.0 cm (18.5 in.) and weighs 40.5 kg (89.1 lbm) as it descends on the parachute. The equipment within the descent probe is protected from the hostile cold environment after planetary atmospheric entry by a layer of low density foam insulation within the descent probe shell structure. In addition, the equipment support deck is thermally isolated from the cold outer structure by a thermal standoff isolator ring at the periphery of the deck located between the deck and the outer structure.

The mass spectrometer inlet is located at the center of the lower cone of the entry probe such that it is exposed to the incoming uncontaminated atmosphere of the planet. The temperature gage is located on the cylindrical side of the probe, with the temperature probe extended from the shell after separation of the descent probe from the entry aeroshell. The pressure ports for the pressure instruments are also on the side of the probe, and these ports are continuously open. The descent antenna and a dual parachute system, for descent probe separation from the aeroshell and for atmospheric descent, are located on the aft end of the descent probe.

The entry probe consists of the descent probe contained and encapsulated within the aeroshell/heat shield entry structure. The nose of the entry probe has been baselined as a 60° half angle conical shape. The nose cone is capped with a spherical segment having a ratio of nose radius to cone base radius (R_N/R_B) of 0.2. The aft closure of the probe is a spherical segment. The entry probe has a diameter of 86.8 cm (34.2 in.) and a weight of 89.0 kg (196.1 lbm). The ballistic coefficient of the entry probe is 102 kg/m² (0.65 slugs/ft²), meeting science entry requirements. The total weight breakdown for the entire probe is presented in Section H4.

A graphite forebody heat shield protects the aeroshell and the descent probe during planetary entry heating. An ESA 3560 ablator protects the afterbody structure from entry heating. The entire aeroshell/heat-shield structure and its contained equipment is jettisoned after planetary atmospheric entry. This is accomplished by opening the three-segment afterbody cover, releasing the clamp band retaining the descent probe, and deploying a separation parachute to drag the descent probe from the aeroshell. The aeroshell then follows a separate trajectory from that of the descent probe, eliminating interference during descent.

Page intentionally left blank

Table IV-12 Baseline Common Saturn/Uranus Probe Weight Breakdown

	WEIGHT	
	kg	lb
SCIENCE		
TEMPERATURE GAGE	0.45	1.00
PRESSURE TRANSDUCER	0.68	1.50
ACCELEROMETER SENSOR	0.59	1.30
ELECTRONICS (CONVERTER)	0.91	2.00
NEUTRAL MASS SPECTROMETER ANALYZER	1.82	4.00
ELECTRONICS	2.73	6.00
PUMP	0.45	1.00
BALLAST TANK	0.45	1.00
	<u>8.08</u>	<u>17.80</u>
POWER & POWER CONDITIONING		
POWER CONDITIONER	0.22	0.50
POWER DISTRIBUTION BOX	0.50	1.10
POWER FILTERS	0.91	2.00
ENTRY BATTERIES	2.41	5.30
POST-SEPARATION BATTERIES	0.25	0.55
COAST BATTERY	<u>0.41</u>	<u>0.90</u>
	4.70	10.35
CABLING		
INNER PROBE	2.36	5.20
EXTERNAL STRUCTURE	<u>1.50</u>	<u>3.30</u>
	3.86	8.50
ATTITUDE CONTROL SYSTEM (LESS PROPELLANT)		
ACS SYSTEM & TANKS	1.63	3.60
MUTATION DAMPER	1.09	2.40
COAST TIMER	<u>0.12</u>	<u>0.25</u>
	2.84	6.25
COMMUNICATIONS		
PRE-ENTRY ANTENNA	0.45	1.00
POST-ENTRY ANTENNA	0.45	1.00
RF TRANSMITTER	2.73	6.00
RF ANTENNA SWITCH	<u>0.23</u>	<u>0.50</u>
	3.86	8.50
PYROTECHNIC SUBSYSTEM		
PYRO ELECTRONICS	0.91	2.00
PYRO CAPACITORS (PROBE)	0.33	0.72
PYRO CAPACITORS (EXTERNAL)	0.33	0.72
PYRO RELAYS (PROBE)	0.17	0.37
PYRO RELAYS (EXTERNAL)	0.34	0.75
SCR (PROBE)	0.14	0.31
SCR (EXTERNAL)	0.28	0.63
PYRO SQUIBS	0.27	0.60
PYRO THRUSTER	<u>3.61</u>	<u>7.95</u>
	6.38	14.05
DATA HANDLING		
DATA HANDLING SUBSYSTEM	2.13	4.70
MEMORY BANKS	<u>0.30</u>	<u>0.65</u>
	2.43	5.35
STRUCTURES AND HEAT SHIELDS		
DESCENT PROBE STRUCTURE	3.92	8.65
EQUIPMENT SUPPORT DECK	3.54	7.80
BASE COVER	4.04	8.90
AEROSHELL (2 lb FOR PAYLOAD RING)	4.99	11.00
FORWARD HEAT SHIELD (16.6 lb ABLATED DURING ENTRY)	16.43	36.16
AFT HEAT SHIELD (BASE COVER)	<u>1.08</u>	<u>2.38</u>
	34.00	74.89
MECHANISMS		
PIN PULLER	0.66	1.44
LATCHES & BANDS	0.91	2.00
MAIN PARACHUTE	3.45	7.60
SECONDARY PARACHUTE (DESCENT)	0.54	1.20
CLAMP SEPARATORS	<u>0.47</u>	<u>1.04</u>
	6.03	13.28

	WEIGHT	
	kg	lb
THERMAL		
EXTERNAL INSULATION BLANKET (FORWARD HEAT SHIELD)	1.27	2.80
EXTERNAL INSULATION BLANKET (BASE COVER)		
PROBE HULL INSULATION (INTERNAL)	1.59	3.50
ISOTOPE HEATERS	1.82	4.00
ENVIRONMENTAL TANK & N ₂	<u>0.54</u>	<u>1.20</u>
	5.22	11.50
PROPULSION		
ACS PROPELLANT	<u>0.01</u>	<u>0.03</u>
TOTAL	77.41	170.50
15% CONTINGENCY	<u>11.61</u>	<u>25.58</u>
	89.02	196.08
1. PRE-ENTRY WEIGHT		
ACS PROPELLANT	0.01	0.03
15% CONTINGENCY	--	--
	<u>(196.08 - 0.03 = 196.05 lb)</u>	
	<u>89.02 - 0.01 = 89.01 kg</u>	
2. POST-ENTRY WEIGHT		
FORWARD HEAT SHIELD (ABLATED)	7.44	16.37
AFT HEAT SHIELD (ABLATED) = 0		
FORWARD INSULATION BLANKET	1.27	2.80
AFT INSULATION BLANKET	0.54	1.00
PRE-ENTRY ANTENNA	<u>9.25</u>	<u>20.17</u>
15% CONTINGENCY	<u>1.38</u>	<u>3.03</u>
	10.63	23.20
<u>(196.05 - 23.20 = 172.85 lb)</u>		
<u>89.01 - 10.63 = 78.38 kg</u>		
3. INITIAL WEIGHT ON PARACHUTE		
SEPARATION PARACHUTE	1.18	2.60
15% CONTINGENCY	<u>0.18</u>	<u>0.39</u>
	1.36	2.99
<u>(172.85 - 2.99 = 169.86 lb)</u>		
<u>78.48 - 1.36 = 77.12 kg</u>		
4. WEIGHT ON PARACHUTE		
PYRO THRUSTERS	3.61	7.95
PYRO CAPACITORS	0.33	0.72
PYRO RELAYS	0.34	0.75
PYRO SQUIBS	0.18	0.40
AEROSHELL	4.99	11.00
FORWARD HEAT SHIELD (NOT ABLATED)	8.96	19.79
BASE COVER HEAT SHIELD & BASE COVER	5.12	11.28
SEPARATION PIN PULLERS (BASE COVER & PARACHUTE)	0.66	1.44
LATCHES & BANDS	0.91	2.00
ISOTOPE HEATERS	1.82	4.00
EXTERNAL CABLING	1.50	3.30
MUTATION DAMPER	1.09	2.40
ACS SYSTEM	1.63	3.60
SEPARATION BATTERY	0.25	0.55
CLAMP SEPARATORS	<u>0.47</u>	<u>1.04</u>
	31.88	70.22
15% CONTINGENCY	4.78	10.53
	36.66	80.75
<u>(169.86 - 80.75 = 89.11 lb)</u>		
<u>77.12 - 36.66 = 40.46 kg</u>		

The cruise/coast/entry probe is completely enclosed within a multi-layer high-performance insulation blanket to assist thermal control of the probe and its components during cruise/coast phases of flight. Only the probe attachments to the carrier spacecraft, the spin nozzles, and the entry antenna penetrate the insulation. In the proposed design, the insulation is allowed to remain on the probe through entry and should ablate away without excessive asymmetrical drag. An alternative approach would be to jettison the insulation prior to entry; however, this is not believed to be necessary.

2. Structural Design

The structural design of the Saturn/Uranus common probe is conventional in most respects. Both the entry and descent probe structures are vented, obviating the need for structural capability of withstanding external atmospheric pressures and the consequent weight penalties. The structure of the entire probe is designed for entry of the planet Uranus, the most severe environment. For the entry angle selected (60°), and the cool atmospheric model, the peak deceleration is 865 g, including a 5° dispersion in the entry angle. The corresponding dynamic pressure acting on the aeroshell is $8.6 \times 10^5 \text{ N/m}^2$ (18,000 psf) at peak load.

The descent probe is designed entirely of 7075-T6 aluminum alloy. The structural configuration is shown in Figure IV-11. The equipment support deck is an integral-rib-stiffened disc machined from a solid plate. All components, with minor exceptions are mounted on or suspended from this deck. The deck structure in turn rests directly on a circumferential deck-support ring attached to the descent probe cylindrical walls, with the inertia loads transferred by multiple compression longerons from this ring to the forward ring frame. This forward ring frame in turn mates with the aeroshell. A forward nose fairing and a flat honeycomb aft closure complete the descent probe structural configuration. These two structural components largely support their own weight during entry of the planetary atmosphere.

Even though the descent probe is vented during planetary atmospheric descent, it is temporarily pressurized to a level of approximately $200,000 \text{ N/m}^2$ (2 bars) just at entry to delay entry of planetary gases. This is accomplished as part of probe thermal control, and is discussed in Section J. The descent probe structure can accept this pressure load with a negligible penalty in weight.

Page intentionally left blank

The planetary entry aeroshell configuration is a ring frame stiffened monocoque structure with an end closure box frame, incorporating a "saddle" ring frame at approximately the mid-diameter of the conical surface to accept the descent probe. The analysis of this structure is presented in Appendix O of Volume III. The structure has been designed of titanium alloy 6Al-4V for this study. A more refined analysis of the temperature-time history may show that an aluminum aeroshell will be compatible with the anticipated temperatures. If so, a weight saving of some 1.8 kg (4 lbm) may be achieved.

The afterbody cover is a three-segment 7075-T6 aluminum structure hinged at the base of each segment. The three segments are shell structures reinforced along the free edges and locally at the points of attachment of the development thrusters. These are opened after entry for descent probe separation.

3. Mechanisms

The primary mechanisms of the Saturn/Uranus probe are the spacecraft/probe separation mechanism, the aft closure opening thruster system, the descent probe retention/release mechanism, the parachute deployment system, and the parachute release mechanism. The latter two are described in the parachute system description of Section H5; the first three are depicted in Figure IV-11.

The spacecraft/probe separation mechanism is simply a bolted joint, three-point attachment to the spacecraft. Pyrotechnically actuated nuts retain the attachment of the probe to the spacecraft and are activated for probe release. Three matched-performance springs push the probe away from the spacecraft at separation, imparting a delta velocity of 1 m/s (\approx 3 fps).

The base cover is opened in three segments, after completion of atmospheric entry, to permit separation of the descent probe from the spent aeroshell/heat shield assembly. The opening is accomplished by activation of three pyrotechnic thrusters, one attached to each of the three base-cover segments. The thrusters open the segments wide enough to permit separation of the descent probe, reach the end of their stroke, and lock the aft cover segments in the open position. Before opening the base cover segments, the segments are held in the closed position by pyrotechnic pin pullers that are activated just prior to opening the base cover segments. Not shown in Figure IV-11 is the pre-entry antenna. This unit is

attached to one of the aft cover segments, and after entry heating separates with the cover segment as it is opened.

The descent-probe retention/release mechanism is simply a clamp ring around the descent probe with tension links attaching the clamp ring to the aeroshell structure, and thereby holding the descent probe in the aeroshell. The descent probe is released by dual pyrotechnic clamp separators releasing the tension of the clamp ring. A separation parachute then pulls the descent probe from the aeroshell.

4. Mass Properties

The weight breakdown for the probe is presented in Table IV-12. This table presents the weights tabulation for the baseline configuration Saturn/Uranus probe by subsystems, which are summed to establish the total weight of the probe. The last portion of the table reduces the weight sequentially, in keeping with the normal mission sequence of events to indicate the probe weight for the various phases of the mission.

The moment of inertia data for this probe has been computed for use in attitude control propulsion propellant calculations and as an indicator of stability about the spin axis. The moment of inertia data are tabulated.

	<u>Descent Probe</u>	<u>Entry Probe</u>
I_{spin}	0.612 slug-ft ²	3.61 slug-ft ²
$I_{\text{pitch/yaw}}$	0.475 slug-ft ²	3.07 slug-ft ²

It is seen that the moment of inertia about the spin axis is approximately 17.5% larger than that of pitch and yaw as presently configured, and should be adequate. This value can be increased to approximately 20%, if desired, by rearrangement of equipment in the aeroshell.

5. Parachute Subsystem

The parachute subsystem consists of two parachutes that are deployed in sequence. A large main parachute is deployed after completion of atmospheric entry and is used to separate the descent probe from the spent heat shield/aeroshell structure. This parachute is then jettisoned and a descent parachute is deployed and used for the scientific mission descent through the atmosphere.

The size of the main parachute is large enough to assure prompt separation of the descent probe from the entry probe assembly. The aeroshell/heat shield assembly with its contained equipment weighs 36.7 kg (80.8 lbm) after entry (with the descent probe removed). It has a ballistic coefficient of approximately 59.5 kg/m^2 (0.38 slugs/ft^2) when traveling subsonic (Mach 0.7). To assure separation of the descent probe, the main parachute selected gives the descent probe a ballistic coefficient of 18.8 kg/m^2 (0.12 slug/ft^2). This value is somewhat arbitrary, but will assure prompt separation. The resulting parachute diameter for a 40.5 kg (89.1 lbm) descent probe is 2.29 m (7.5 ft) in a disc-gap-band parachute configuration and weighs 3.4 kg (7.6 lbm). The parachute is exposed to dynamic pressures between 1707 and 2546 N/m^2 (35.7 to 53.0 psf) at approximately Mach 0.7 at deployment, depending upon the planet and the atmospheric model at entry. The descent probe after separation is decelerating at a rate of 3.9 to 6.6 g relative to the spent aeroshell, also dependent on the planet and the atmosphere.

The descent parachute is a circular parachute, selected to provide a ballistic coefficient of 110 kg/m^2 (0.7 slug/ft^2) to meet the atmospheric descent science requirements. The resulting parachute has a diameter of 0.73 m (2.4 ft) and a weight of 0.54 kg (1.2 lbm).

The main parachute is deployed by a pyrotechnic mortar which ejects the entire parachute canopy by means of a sabot. The parachute is released by a pyrotechnic pin puller in the parachute riser system and in being released, pulls out the descent parachute. Both parachutes are stowed in fiberglass canisters for RF transparency to the descent antenna.

Both parachutes are designed of Dacron fabric and are maintained at "room" temperature until deployment. It appears that the Dacron material, which has been tested to liquid nitrogen temperature (77°K), will suffice in spite of the extreme low temperature. However, sufficient doubt exists to warrant a test program of the material at some time in the future.

6. Heat Shield

The forebody heat shield is designed of ATJ graphite, and is based on the work performed by M Tauber of NASA/AMES for the Outer Planets studies. The heat shield mass fraction is established by entry of the atmosphere of the planet Saturn, which is more severe than the entry at Uranus. The heat shield mass fractions requirements for Saturn and Uranus were presented versus entry angle in Chapter VI, Section B.8.e of Volume II of this report. It can be seen from

this data that, for an entry angle of 30° plus a dispersion error of 5°, the heat shield mass fraction is 0.21. This results in a heat shield weight of 16.4 kg (36.2 lbm) for a probe having an entry weight of 89.0 kg (196 lbm), including heat shield.

In keeping with the heat shield design studies performed by M. Tauber, the heat shield mass fraction and initial thickness is based on maintaining a final ablator thickness of 4 mm (0.16 in.) after planetary entry and providing a low density carbon felt insulator between the hot backface and the aeroshell. In this concept, the heat shield must be rigidly supported to resist launch loads, and rigidly supported (but not restrained against thermal expansion) or released to rest against the carbon felt insulation during entry. In computing weights data for the probe, the released heat shield approach has been assumed. However, all the mechanical details of this approach have not been evaluated.

The afterbody heat shield is essentially the same as that described for the Saturn probe in Chapter VI, Section B.8.e of Volume II of this report. It is based on the analytical approach for afterbody heat shields described in Chapter V, Section A.8.c and tabulated data from Chapter B.8.3 of Volume II. This analysis assumes the amount of ablator to be used shall protect the understructure to a temperature of 422 °K (300°F). The resulting ablator weight is 1.37 kg/m² (0.28 lbm/ft²) using ESA 3560 ablator material.

The afterbody ablator is pre-split along the parting lines of the afterbody cover segments to facilitate opening of these segments after entry. This is not a new concept. A modified Gemini re-entry vehicle was launched by Martin Marietta Corporation in November 1966 as part of the MOL/HSQ (Manned Orbiting Laboratory/Heat Shield Qualification) program, in which the re-entry heat shield had an access door pre-cut through the heat shield.

7. Alternative Antenna Approach

Since two identical antennas are used for pre-entry and descent phases of the mission, it is logical to question whether one antenna could handle both jobs. As presently conceived, the probe design places one antenna external to the multilayer insulation blanket to transmit pre-entry data, and one antenna within the afterbody cover to transmit during atmospheric descent. This descent antenna is exposed for transmission after separation of the descent probe from the entry aeroshell. A comparison was made using a single antenna; the descent antenna on the probe was retained and the pre-entry antenna was eliminated.

For the single antenna configuration, it is necessary to provide RF transparency to the afterbody of the entry probe. If an RF transparent afterbody cover and ablator is used, then a portion of multilayer insulation approximately 0.37 cm^2 (4.0 ft^2), prior to data transmission. The time of separation of the insulation would be of the order of one hour prior to entry for late planetary arrival. If it is assumed that the RF transparent ablator on the afterbody has an emissivity of $\epsilon = 0.70$, which is probably conservative, then the heat loss from the afterbody by radiation is 165 watts, or approximately 165 w-hr for one hour. This value would be reduced to approximately 80 w-hr by use of a low-conductivity afterbody material.

The loss of heat could be accommodated by a decrease in temperature of the probe (undesirable), or by adding extra battery weight and using resistance heaters to compensate for the loss. To compensate for this heat loss using batteries and heaters would result in a weight penalty of approximately 1.4 kg (3.0 lbm). Thus, a first-cut comparison of the penalties of the two configuration options is as follows:

- 1) a weight increase of 1.4 kg (3.0 lbm) of batteries for the single antenna, compared to 0.7 kg (1.5 lbm) for the extra antenna and antenna switch of the two-antenna configuration;
- 2) an extra event for the single-antenna configuration (jettisoning of the insulation blanket);
- 3) a potential antenna interference problem for the single antenna due to the proximity of the undeployed dense-packed parachute;
- 4) RF transparency requirement for the base cover of the single-antenna configuration. (The weight comparison of RF transparent afterbody and ablator versus non RF transparent configurations has not been made.)

In keeping with the philosophy of maintaining the common Saturn/Uranus probe similar to the previous design approaches used in this study, the two-antenna configuration has been retained although it is recognized that the single-antenna warrants further study on future design activities.

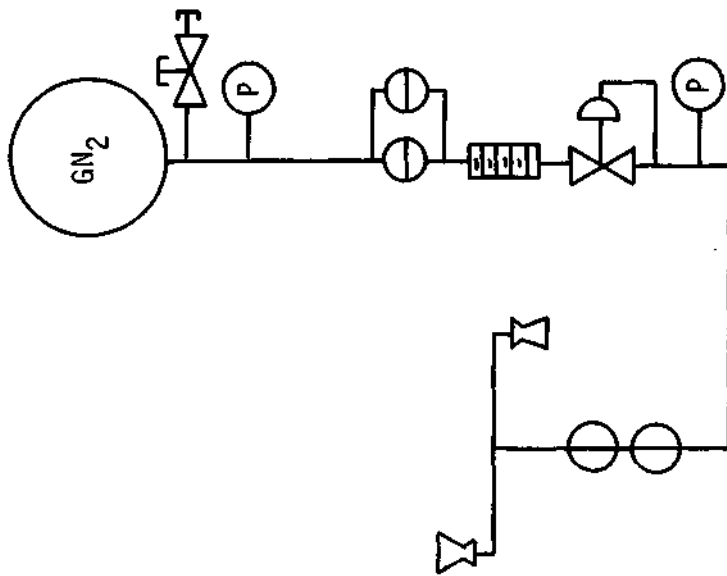
I. PROPULSION SUBSYSTEM

With deletion of the requirement for the probe deflection maneuver, the propulsion system becomes quite simple. The solid propellant deflection motor is deleted from the probe and with it, the need for a high rate of spin to stabilize the probe during motor burn. Thus, this common Saturn/Uranus probe needs only a small attitude-control spin-up system to provide the necessary probe attitude stabilization from probe/spacecraft separation until planetary entry. This system is small and light enough to be included in the entry probe. The propulsion system for probe attitude control is a cold gas (GN_2) system, basically the same as that reported in Volume II for the other planetary atmospheric probes. The spin rate to be imparted to the probes for attitude stabilization has been selected as 0.52 rad/sec (5 rpm). This spin rate is somewhat arbitrary, but will provide pointing attitude stability prior to entry, with minimum interference with dynamic forces of aerodynamic stabilization at entry.

The selected system, depicted in Figure IV-12, uses a stored high pressure gaseous nitrogen supply that is vented through a pair of spin nozzles to provide the desired spin torque. The system is activated by opening of a parallel pair of pyrotechnic valves that vent nitrogen through a pressure regulator to the spin nozzles. The spin-up torque is terminated by activating two series-connected pyrotechnic valves. This system provides a predictable spin rate even if some of the stored nitrogen gas leaks away.

For a probe having a moment of inertia about its spin axis of 5.02 kg-m^2 (3.7 slug-ft^2), the amount of gas required to spin the probe to 0.52 rad/sec (5 rpm) is approximately 0.015 kg (0.033 lbm) including 50% reserve. The pressure bottle weight is conservatively estimated to be 0.09 kg (0.2 lbm).

PROBE SPIN AXIS MOMENT OF INERTIA = 5.02 kg-m² (3.7 slug-ft²)
 PROBE COAST SPIN RATE = 5 rpm
 SPIN NOZZLE MOMENT ARM = 38.2 cm (1.25 ft)
 SPIN IMPULSE = 6.89 N-sec (1.55 lb_f-sec)
 PROPELLANT SPECIFIC IMPULSE = 707 N-sec/kg (72 sec)
 PROPELLANT REQUIRED (50% EXCESS) = 0.015 kg (0.033 lb_m)
 SYSTEM HARDWARE WEIGHT = 1.54 kg (3.4 lb_m)
 TOTAL SYSTEM WEIGHT = 1.63 kg (3.63 lb_m)



SPIN NOZZLES
 1.0 lb_f

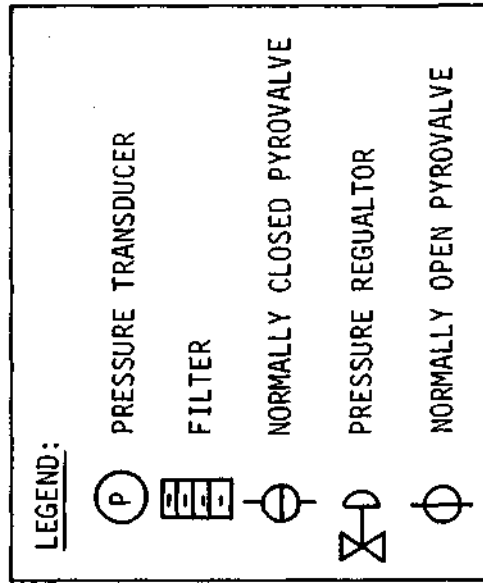


Fig. IV-12 Attitude Control Propulsion System

The characteristics of the system are depicted in Figure IV-12 and the components weights and quantities are listed.

Component	Weight	
	kg	lbm
GN ₂ bottle (1)	0.09	0.20
Fill valve (1)	0.09	0.20
Pressure transducers (2)	0.23	0.50
Squib valves (4)	0.45	1.00
Filter (1)	0.18	0.40
Pressure regulator (1)	0.18	0.40
Thrusters (2)	0.18	0.40
Lines	<u>0.23</u>	<u>0.50</u>
Total	1.63	3.60

J. THERMAL CONTROL SUBSYSTEM

The thermal control subsystem design outlined in Chapter III is used in Task I. To compensate for the cold atmospheres encountered, elevation of the probe coast temperature to a maximum before entry allows optimum leeway for internal temperature decrease during descent. For consistency of the common Saturn/Uranus probe design, the warm Saturn atmospheric encounter and the warm Uranus atmospheric encounter, both with late arrival uncertainty, were analyzed to determine a maximum probe equipment coast temperature for entry and descent. Because of the criticality of probe entry temperature, positive heating is achieved by radioisotope and a louver system design is recommended to control probe temperatures before entry. On the basis of the design for descent thermal control, a probe equilibrium arrival temperature of 302.0°K was chosen, and an uncertainty temperature band of $\pm 10^{\circ}\text{K}$ assumed. Calculations have shown that approximately 18 watts of radioisotope heater power supply with an Iridite 14-2 external finish would achieve the desired entry condition.

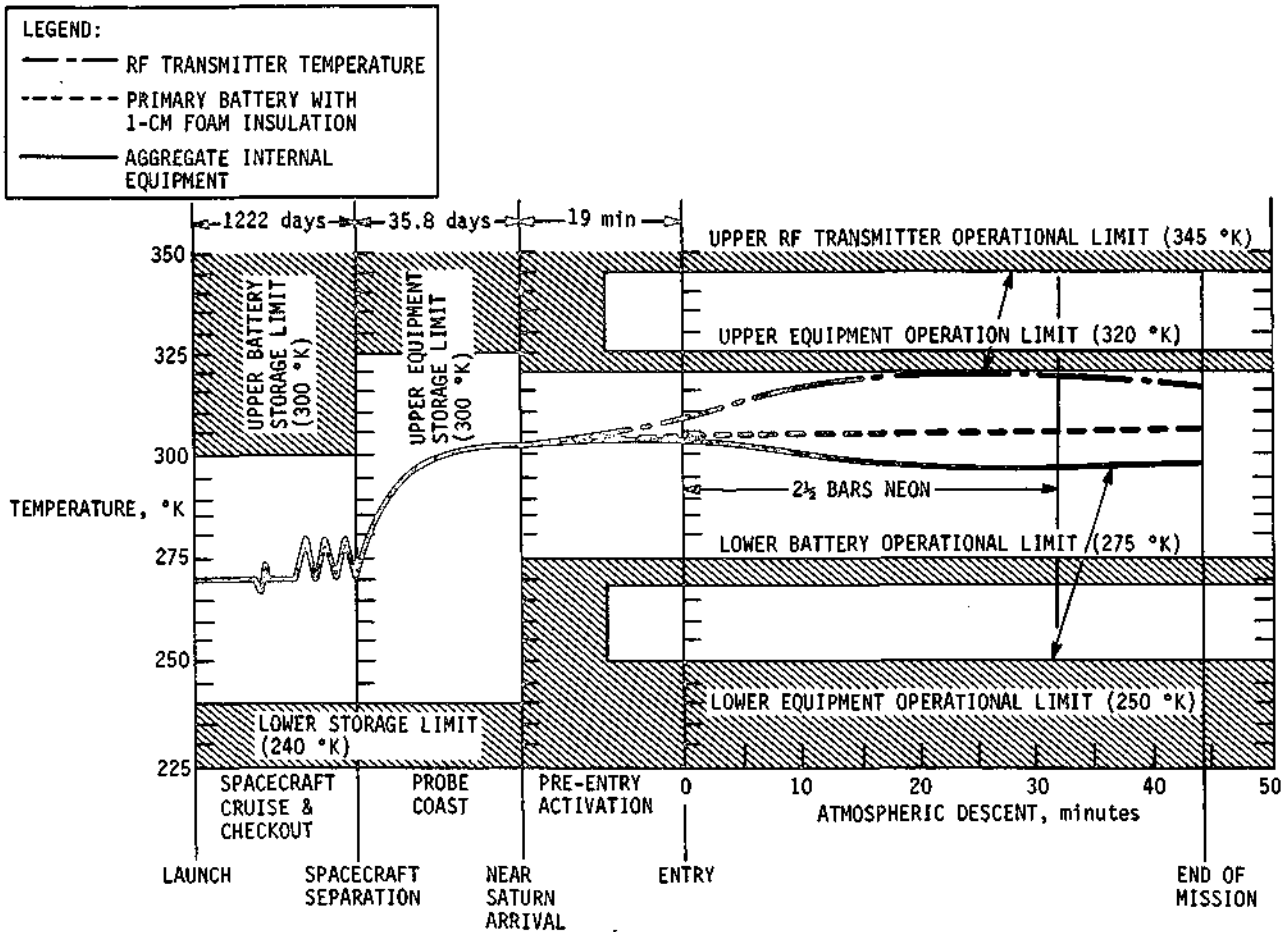
Thermal control for the atmospheric descent portion of the mission relies on the probe coast/entry temperature, internal probe foam insulation, and sufficient probe thermal inertia to survive the very cold descent environment encounter. On the basis of the thermal control design studies performed and previously outlined in Chapter III, results show that an environmental purge system using 2.5 bars (0.127 kg) of neon gas would be sufficient to offset electrical heating of the probe payload required for the nominal and cool Uranus atmospheres. For all Saturn atmosphere encounters anticipated, a totally passive system would be sufficient for descent thermal control requiring no gas purging or electrical heating.

The parametric results presented in Chapter III indicate the high probe heat losses accompanying vented probe design configurations. For the Uranus cool atmosphere encounter, a completely vented Task I probe design would experience a total heat loss of approximately 390 w-hr to the atmosphere, whereas the neon purged probe would experience a heat loss of only approximately 220 w-hr. Neon gas was chosen over previously identified nitrogen gas due to the cooler probe shell temperature anticipated in Uranus cool atmosphere encounters, and the increased probability of condensation and freezing of the nitrogen gas at the insulation/probe shell boundary.

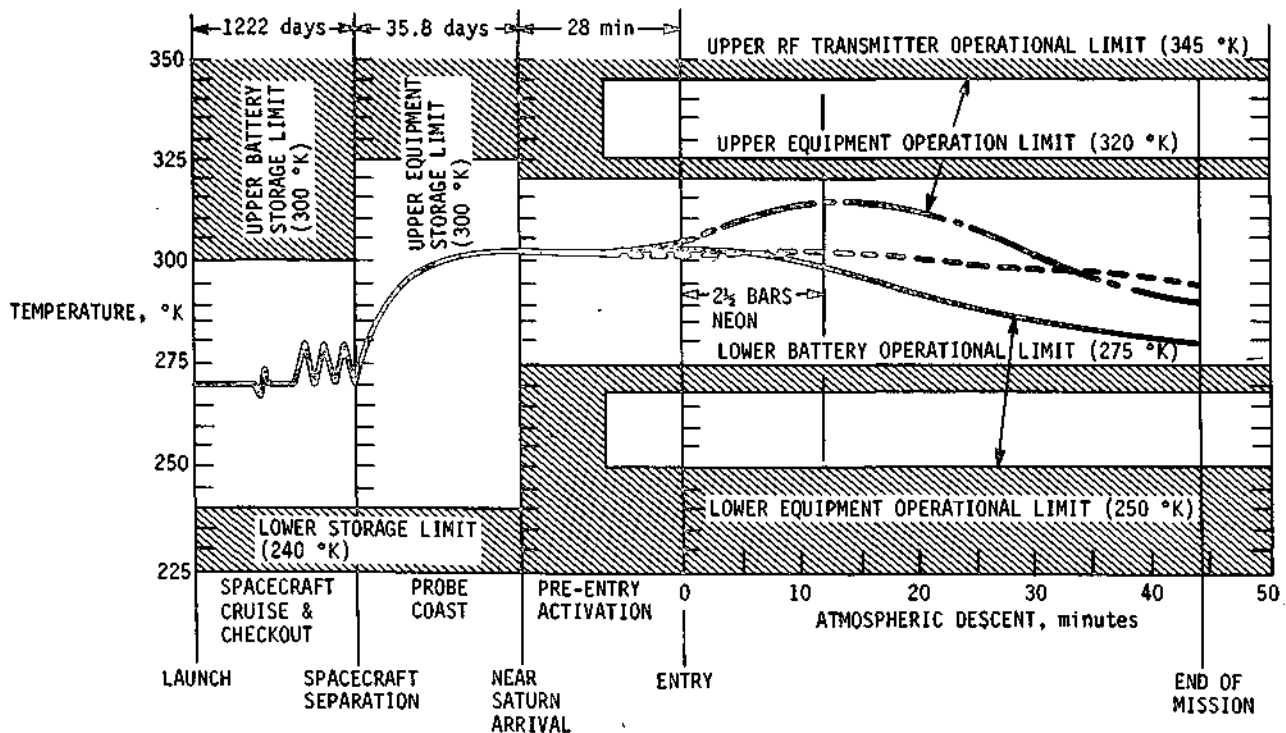
The worst-case atmospheric encounters and uncertainties were analyzed for the Science Advisory Group exploratory payload common probe design. The warm atmospheric encounters were analyzed with late arrival uncertainties and cool atmospheric encounters with early arrival uncertainties. Table IV-13 presents the minimum and maximum equipment temperatures experienced during the mission while figures IV-13 and IV-14 present plotted thermal analysis results. The worst-case conditions establish the probable operative temperature bands to be experienced at each planet. Assuming a 302°K probe arrival temperature, these bands are as follows:

	<u>Saturn, °K</u>	<u>Uranus, °K</u>
RF transmitter	291-319	274-327
Insulated primary batteries	294-307	290-310
Aggregate internal equipment	280-304	261-310

The baseline arrival temperature uncertainty of $\pm 10^\circ\text{K}$ was established as the required probe design margin and exists at all limits for the Task I design. Note that the large arrival uncertainty at Uranus establishes higher probe temperatures although Uranus atmospheres are cooler than Saturn's atmospheres. For this reason, the large Uranus arrival uncertainties became an important consideration for establishing acceptable pre-entry transmitter power levels. Although simpler design is afforded by using a constant power transmitter for pre-entry and descent, preliminary analyses indicate that over-temperature transmitter conditions would exist before atmosphere pressurization could occur. An additional item or probable constraint identified during the analyses was the effect of the cold atmosphere on the externally mounted RF antenna. Current intelligence indicates that potential thermal stress problems could exist at very low temperatures requiring possible radome protection with auxiliary heaters.

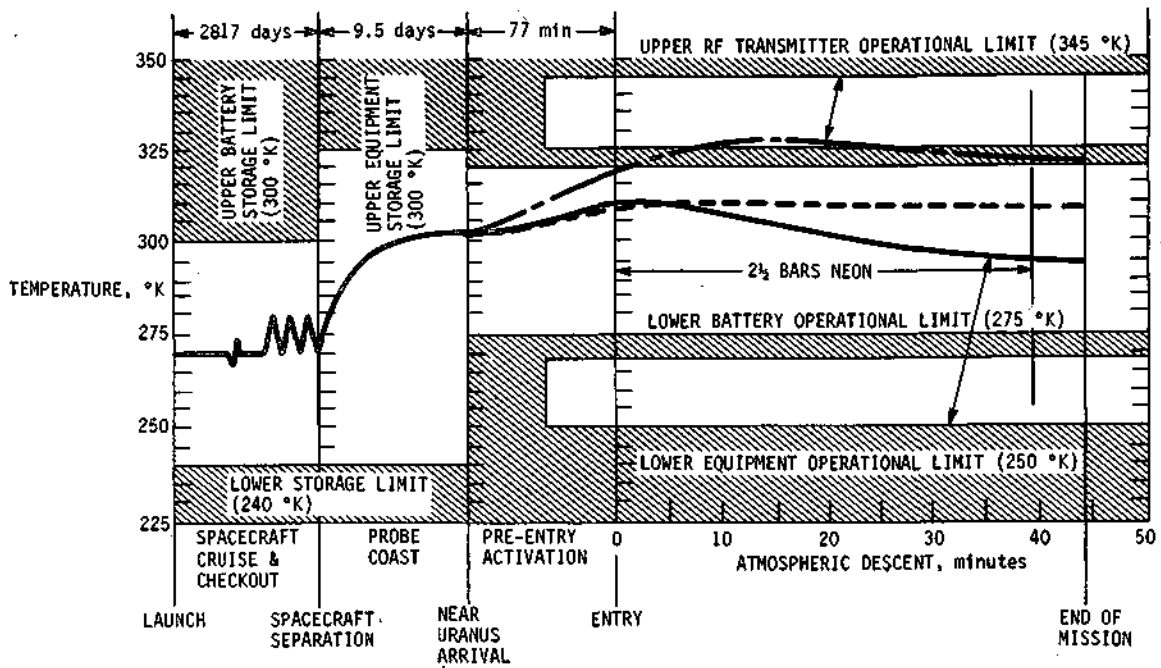


a. WARM ATMOSPHERE ENCOUNTER WITH LATE ARRIVAL UNCERTAINTY (MAXIMUM ANTICIPATED TEMPERATURES)

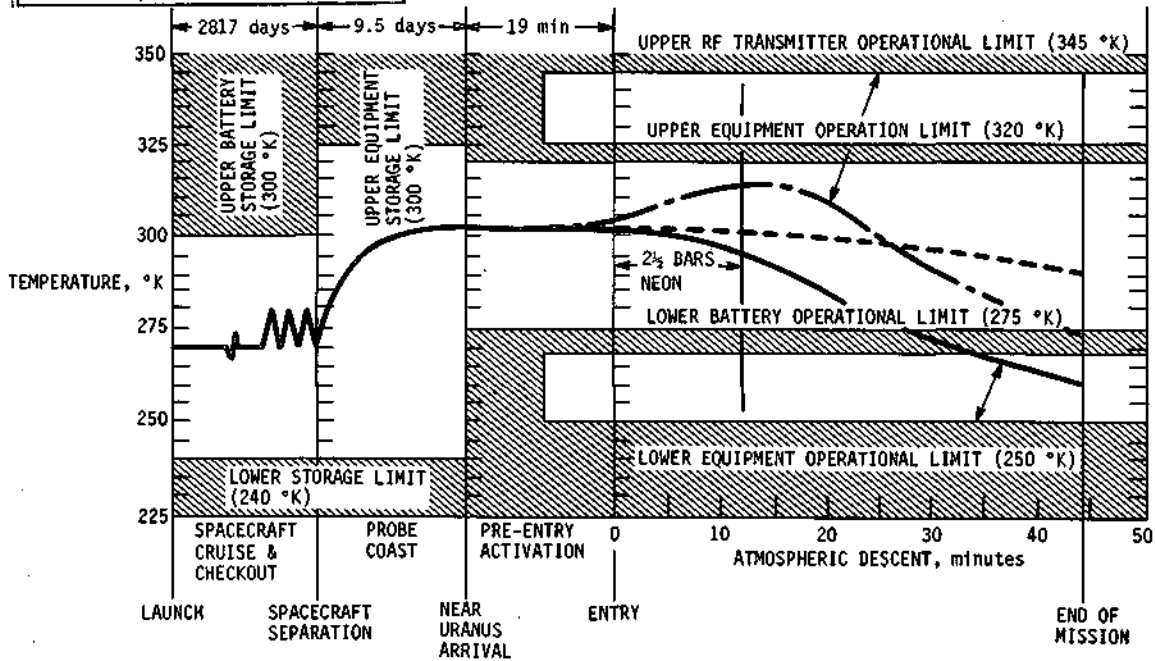
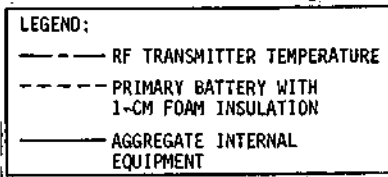


b. COOL ATMOSPHERE ENCOUNTER WITH EARLY ARRIVAL UNCERTAINTY (MINIMUM ANTICIPATED TEMPERATURES)

Figure IV-13 Saturn/Uranus Probe Thermal History for Saturn Mission (SAG Exploratory Payload)



a. WARM ATMOSPHERE ENCOUNTER WITH LATE ARRIVAL UNCERTAINTY
(MAXIMUM ANTICIPATED TEMPERATURES)



b. COOL ATMOSPHERE ENCOUNTER WITH EARLY ARRIVAL UNCERTAINTY
(MINIMUM ANTICIPATED TEMPERATURES)

Figure IV-14 Saturn/Uranus Probe Thermal History for Uranus Mission (SAG Exploratory Payload)

K. PROBE-TO-SPACECRAFT INTEGRATION

1. Mechanical

The Saturn/Uranus probe integration with the Mariner Spacecraft bus is very similar to that described in Volume II, Chapter VI, Section V.11 of the final report. The physical arrangement is depicted in Figure IV-15. From the figure, it can be seen that the probe is canted at an angle with respect to the spacecraft centerline to minimize interference with the spacecraft rocket engine. The probe is contained within an environmental enclosure to protect the probe from meteoroid impingement and other space environment during the cruise phase. The Mariner rocket engine is moved aft to minimize plume impingement of the engine on the probe enclosure. The engine must control the spacecraft with the probe attached and jettisoned. The line of action of the engine thrust is therefore nominally pointed 2° outboard such that the thrust vector is pointed halfway between the spacecraft-only and the spacecraft-plus-probe center of gravities.

The probe separation-spring thrust vector is directed to act through the center of gravity locations of both the probe and spacecraft to minimize imparted tumbling motions to each at probe separation.

2. Thermal

For thermal control, reduced probe equilibrium temperatures are required during cruise. The internal probe temperature is designed warm-biased to offset atmospheric heat losses during descent, but cooler probe equipment temperatures are desired for long-term equipment storage. Since probe heating is supplied exclusively by radioisotope heaters whose output cannot be changed during the mission, the design of the spacecraft mounts must be utilized to reject excessive heating during cruise. Preliminary calculations indicate that approximately 8 watts of excess heat must be dissipated and high conductance spacecraft/probe hard mounts should accommodate this load. Disconnect of these heat paths at separation will then allow the probe to attain its desired warm-biased temperature before planetary encounter.

3. Electrical/Electronic

All probe checkout commands will be channeled through the spacecraft command/control subsystem. Diagnostic data will return through the spacecraft flight data subsystem. Checkout and

Page intentionally left blank

diagnostic functions are transmitted to the probe by hardwire (in-flight disconnect umbilical) circuitry. Power will be supplied by the spacecraft for all probe activity before separation. Although launch and cruise functions have not been defined, it is expected that the probe data handling subsystem, and science and entry accelerometers will be powered during the launch phase; minor engineering instrumentation surveillance of temperature and pressure with occasional operation of low power heaters is expected during cruise. Pre-separation checkout will entail powering up the probe subsystems and performing tests under spacecraft control. The power required from the spacecraft during this period is determined by the probe DHS and subsystem under test. Operation of probe subsystems in reduced modes is indicated in order to reduce peak power demand on the spacecraft. Since there is probe capability for eliminating failed subsystems which are not essential to a reduced data return mission, pre-separation checkout should be started sufficiently early to allow several checkout cycles with ground station updating. The time for each cycle includes the loop delay of the spacecraft/ground station link which is approximately 5.3 hr at Uranus and 2.7 hr at Saturn. Probe checkout will take a relatively short time compared with the total cycle and the probe will be deactivated between cycles to reduce power drain on the spacecraft. Since the probe is deactivated between cycles, there is no requirement to confine checkout to the immediate period before separation. The only critical timing element during the pre-separation period is the initiation of the coast timer function, which must take place at a fixed time interval before planetary entry.

4. Communication Link

The spacecraft functions and requirements during probe planetary entry are essentially similar to the previous study. The details of the communication link are discussed in Section D of Chapters III, IV, and V of this volume.

V. SATURN/URANUS PROBE SYSTEM DEFINITION WITH EXPANDED SCIENCE COMPLEMENT

This section summarizes the common Saturn/Uranus probe system definition (Task II) which uses pre-entry science instruments such as the Langmuir Probe (LP), Ion Retarding Potential Analyzer (IRPA), and Neutral Particle Retarding Potential Analyzer (NRPA). The science package also includes a nephelometer for descent along with the SAG exploratory payload, discussed in Chapter IV. The definition uses concepts that were generated during the basic study and extended to be compatible with the three new missions, the "worst case" atmospheric models, and spacecraft deflection mode.

A. MISSION DEFINITION

The missions as defined in Chapter IV, Section A are not changed or altered by the expanded science complement. The primary impact of expanded science on mission design is that entry occurs on the sunlit side of the planet. Entry for the three missions (Saturn 79, Saturn/SU 80, and Uranus/SU 80) analyzed satisfies this requirement.

B. SCIENCE INSTRUMENTATION AND PERFORMANCE

The expanded science payload includes, in addition to the SAG exploratory payload instruments, a nephelometer for descent cloud location definition and a set of pre-entry instruments to investigate the upper atmosphere and ionosphere. The basic characteristics of these instruments are given in Table V-1 resolved into the primary components where possible. The expanded payload weighs 79% more than the exploratory payload and it occupies 104% more total volume, 93% of which is inside the probe body, the RPA sensors being mounted to the outside. The power increase is 72% more than for the exploratory payload. These percentages are for the instruments only; changes in the associated systems must also be accounted for. The exploratory payload instruments are discussed in detail in Chapter III, Section C.1 of Volume II and the expanded payload instruments in Chapter III, Section B of this volume.

Table V-1 Instrument Characteristics

INSTRUMENT/COMPONENT	WEIGHT, kg	POWER, w	VOLUME, cm ³
EXPLORATORY PAYLOAD			
TEMPERATURE GAGE	0.45	1.4	426
PRESSURE TRANSDUCERS (2)	0.68	1.3	246
ACCELEROMETER SYSTEM		2.8	
TRIAD SENSOR	0.60		262
PRC & ELECTRONICS	0.91		656
NEUTRAL MASS SPECTROMETER		14.0	
ANALYZER	1.83		935
ELECTRONICS	2.72		3,444
PUMP	0.44		443
INLET SYSTEM	0.45		492
EXPANDED PAYLOAD ADDITIONS			
NEPHELOMETER (DESCENT)	1.13	3.0	1,312
LANGMUIR PROBES (PRE-ENTRY)	1.36	3.0	1,200
ION RPA (PRE-ENTRY)		3.0	
SENSOR	0.23		400
ELECTRONICS	1.36		1,800
NEUTRAL RPA (PRE-ENTRY)		5.0	
SENSOR	0.44		400
ELECTRONICS	1.83		2,100
TOTALS	14.43	33.5	14,116

Pre-entry altitude profiles for both planets are given in Figure III-27 along with associated velocity time histories. The pressure descent profiles are given in Figure III-31 and are specified for the six model atmospheres. The descent ballistic coefficient is 110 kg/m² for all profiles. Values for descent parameters are given in Table III-14, showing that parachute deployment pressure varies from 41 to 102 millibars while the pressure at first descent measurement varies from 51 to 122 millibars. The final pressure for a descent designed for 44 minutes varies from 3.1 bars (-96 km alt) in the Uranus warm atmosphere to 19.2 bars (-60 km alt) in the Uranus cool atmosphere.

The pre-entry, entry, and descent times, instrument sampling times, and resulting bit rates are shown in Table V-2. The transmission bit rates for descent are slightly higher than the collection bit rates because the descent data collected during probe acquisition by the spacecraft must be stored and later interleaved with real-time data for transmission. The pre-entry transmission of 235 bps is real time; thus the collection equals the transmission.

Table V-2 Instrument Sampling Times and Data Rates for Common Saturn/Uranus Probe with Expanded Payload

PHASE	INSTRUMENT	SAMPLING TIMES, sec	COLLECTION BIT RATE, bps	TRANSMISSION BIT RATE, bps
PRE-ENTRY (200 sec)	LANGMUIR PROBES IRPA NRPA	0.5	60	60
		2.0	60	60
		3.0	93.3	93.3
				<u>213.3</u>
			ENGINEERING FORMATTING TOTAL	0.5 21.3 <u>235.1</u>
ENTRY (84.5 sec MAXIMUM)	ACCELEROMETERS AXIAL LATERAL (2)	0.2	50	0
		0.4	50	0
DESCENT (2640 sec)	TEMPERATURE GAGE PRESSURE GAGE NEPHELOMETER MASS SPECTROMETER ACCELEROMETERS TURBULENCE STORED STORED PRE-ENTRY	4	2.5	2.6
		4	2.5	2.6
		3	3.3	3.4
		50	8.0	8.3
		8	7.5	7.8
		0	0	3.4
		0	0	<u>16.8</u>
		SCIENCE TOTAL	44.9	
		ENGINEERING	1.0	
		FORMATTING	<u>4.6</u>	
		TOTAL	50.5	

The descent bit rate includes the nephelometer at 3.4 bps, which does not appear in Table IV-1 with the exploratory payload. Also included in the design is a capability for replaying the pre-entry data from storage, shown by the last full line in Table V-2. A rate of 16.8 bps is required to telemeter the stored pre-entry data. The redundancy mode for the pre-entry data is allowed by the fact that the total power requirements for the pre-entry real-time data transmission at 235 bps using PSK exceeds that for descent using FSK until the descent bit rate reaches about 53 bps. The use of the excess power during descent takes about 26 w-hr of energy at the bit rate of 50.5 bps. This is a minor penalty to pay for the extra data.

Other options are also available; one, of course, is not to utilize this excess power. In that case, the data rate would be 31.5 bps as shown in Table III-18. A more viable option is to use the excess to make more detailed descent measurements, for instance making the mass spectrometer sweeps more detailed. The present sampling is 400 bits/sample, which is one voltage setting and current reading per amu. For a total of only 48.8 bps, the sample size could be increased to 1200 bits which would be three readings per mass number, giving a more detailed mass spectrum. The excess power could also be used to obtain more sample points per kilometer with any instrument. Decreasing the sampling times on the simultaneous temperature and pressure measurements to one second would increase the amount of data by a factor of four at a total bit rate of about 48 bps.

The descent mission measurement performance is given in Table V-3 for Saturn and in Table V-4 for Uranus. The first column gives the instrument, its sampling interval, and the measurement to be made. The second column gives the criteria set forth in Volume II. The remaining columns give the performance numbers in the units specified by the criteria. The minimum values are those at the highest point in the atmosphere at which the measurement is to be evaluated, and are specified individually for each atmosphere to allow determination of worst-case atmospheres. The maximum value given in the last column is the maximum performance of all the atmospheres at the end of the design mission, which is 44 minutes from parachute deployment.

The primary difference from Tables IV-2 and IV-3 is the addition of the nephelometer performance. It exceeds the one measurement/kilometer criteria in all atmospheres and obtains a minimum of 34 measurements in all modeled clouds. The performance of all measurements is generally lowest in the warm atmospheres and improves in the cool.

Table V-3 Saturn Descent Measurement Performance - Expanded Payload

INSTRUMENT	SAMPLING TIME	MEASUREMENT	CRITERIA	MINIMUM PERFORMANCE			MAXIMUM PERFORMANCE	
				COOL ATMOSPHERE	NOMINAL ATMOSPHERE	WARM ATMOSPHERE		
MASS SPECTROMETER	50 sec	MINOR CONSTITUENTS	2 PER SCALE HEIGHT*	5.8	7.7	6.5	37	
		CLOUD COMPOSITION	2 INSIDE EACH CLOUD	10.4 IN NH ₃	4.0 IN NH ₃	3.0 IN NH ₃		
		H/He RATIO	4 MEASUREMENTS	52	16 IN H ₂ O	10.5 IN H ₂ O		52
		ISOTOPIC RATIO						
MOLECULAR WEIGHT								
TEMPERATURE GAGE	4 sec	TEMPERATURE PROFILE CLOUD STRUCTURE	1 PER °K 2 INSIDE EACH CLOUD	1.5 137 IN NH ₃	1.2 46 IN NH ₃ 196 IN H ₂ O	1.3 38 IN NH ₃ 47 IN H ₂ O	8.1	
PRESSURE GAGE	4 sec	PRESSURE PROFILE TURBULENCE CLOUD STRUCTURE	2 PER km } 1 PER km } * 2 INSIDE EACH CLOUD	2.7 137 IN NH ₃	2.0 46 IN NH ₃ 196 IN H ₂ O	1.5 38 IN NH ₃ 47 IN H ₂ O	7.8	
ACCELEROMETERS	8 sec	TURBULENCE	1 PER km*	1.3	1.0	0.7	3.9	
NEPHELOMETER	3 sec	CLOUD LOCATION CLOUD STRUCTURE	1 PER km† 2 INSIDE EACH CLOUD	1.4 183 IN NH ₃	1.3 66 IN NH ₃ 275 IN H ₂ O	1.4 50 IN NH ₃ 62 IN H ₂ O	10.4	
*BELOW CLOUD TOPS.								
†BELOW 100 mb.								

Table V-4 Uranus Descent Measurement Performance - Expanded Payload

INSTRUMENT	SAMPLING TIME	MEASUREMENT	CRITERIA	MINIMUM PERFORMANCE			MAXIMUM PERFORMANCE	
				COOL ATMOSPHERE	NOMINAL ATMOSPHERE	WARM ATMOSPHERE		
MASS SPECTROMETER	50 sec	MINOR CONSTITUENTS	2 PER SCALE HEIGHT*	5.6	6.1	4.6	38	
		CLOUD COMPOSITION	2 INSIDE EACH CLOUD	18.3 IN CH ₄	4.4 IN CH ₄	2.0 IN CH ₄		
		H/He RATIO	4 MEASUREMENTS	52	12 IN NH ₃	5 IN NH ₃		52
		ISOTOPIC RATIO						
MOLECULAR WEIGHT								
TEMPERATURE GAGE	4 sec	TEMPERATURE PROFILE CLOUD STRUCTURE	1 PER °K 2 INSIDE EACH CLOUD	3.0 230 IN CH ₄	3.0 48 IN CH ₄ 113 IN NH ₃	3.1 26 IN CH ₄ 63 IN NH ₃	10.9	
PRESSURE GAGE	4 sec	PRESSURE PROFILE TURBULENCE CLOUD STRUCTURE	2 PER km } 1 PER km } * 2 INSIDE EACH CLOUD	4.8 230 IN CH ₄	2.5 48 IN CH ₄ 113 IN NH ₃	1.6 26 IN CH ₄ 63 IN NH ₃	14.4	
ACCELEROMETERS	8 sec	TURBULENCE	1 PER km*	2.4	1.4	0.9	7.2	
NEPHELOMETER	3 sec	CLOUD LOCATION CLOUD STRUCTURE	1 PER km† 2 INSIDE EACH CLOUD	2.4 306 IN CH ₄	3.2 76 IN CH ₄ 174 IN NH ₃	1.8 34 IN CH ₄ 86 IN NH ₃	19.1	
*BELOW CLOUD TOPS.								
†BELOW 100 mb.								

Table V-5 Pre-Entry Measurement Performance

INSTRUMENT (Δt)	KILOMETERS PER MEASUREMENT			
	AT 5000 km		AT ENTRY	
	SATURN	URANUS	SATURN	URANUS
LANGMUIR PROBES (0.5 sec)	9.7	10.1	9.1	10.3
IRPA (2 sec)	38.8	40.2	36.4	41.3
NRPA (3 sec)	58.2	60.3	54.6	62.0

Table V-5 shows the performance during pre-entry in kilometers/measurement at the beginning and end of the pre-entry phase. As can be seen, the values change only a small amount during this period. The number of actual measurements was discussed together with the upper atmospheric models in Chapter III, Section B.3.c. According to the electron number density equation given in the Monograph (Ref III-1), the electron scale height is 250 km. This means that with the performance given in Table V-5, the Langmuir probes are making approximately 25 measurements per scale height. Since electrons are probably most abundant and other particles have a smaller scale height, this value is the largest number of measurement/scale height obtainable. The minimum number is an unknown based upon the number density profile of the heaviest neutral particle measurable.

C. SYSTEM DESIGN AND INTEGRATION

1. Functional Sequence

The functional sequence for the Saturn/Uranus probe with the expanded complement is similar to that for the SAG exploratory payload except for the added events required for the pre-entry science and the added descent nephelometer. During pre-entry, the science and engineering data is transmitted in real time and also stored for descent transmission as discussed in Subsection 3 herein. This dual pre-entry data mode was incorporated because the pre-entry and descent RF power requirements are almost identical as discussed in Chapter III, Section D.1 herein. Detailed sequences of events are shown in Tables V-6 and V-7 for Saturn and Uranus, respectively.

Table V-6 Saturn Sequence of Events (Task II)*

ITEM	TIME	EVENT	COMMENTS†
1.	L = 0	LAUNCH (DEC 3, 1980)	
2.	L + 2h	SEPARATE SPACECRAFT FROM LAUNCH VEHICLE	
3.	L + 2h TO L + 1221.8d	CRUISE	
4.	S - 7h, 30m, 0s	SPACECRAFT POWER TO PROBE; EJECT ENVIRONMENTAL COVER	
5.	S - 7h, 17m, 0s	START PROBE CHECKOUT	
6.	S - 0h, 17m, 0s	PROBE CHECKOUT COMPLETE; START SPACECRAFT ORIENTATION (10.6°)	
7.	S - 0h, 2m, 0s	SPACECRAFT ORIENTATION COMPLETE; ACTIVATE SEPARATION SUBSYSTEM	
8.	S = 0 (L + 1222.1d)	SEPARATE PROBE FROM SPACECRAFT	
9.	S + 0m, 0.5s	START PROBE SPINUP TO 5 rpm	
10.	S + 0m, 30s	START ORIENTATION FOR ΔV (59.1°)	
11.	S + 4m, 0s	PROBE SPINUP COMPLETE; DEACTIVATE PROBE SYSTEM	
12.	S + 15m, 30s	COMPLETE SPACECRAFT ORIENTATION FOR ΔV	
13.	S + 17m, 36s	APPLY SPACECRAFT ΔV (96 m/sec)	
14.	S + 18m, 0s	START SPACECRAFT ORIENTATION TO EARTH LOCK (69.7°)	
15.	S + 33m, 0s	SPACECRAFT ORIENTATION COMPLETE	
16.	L + 1222.12d TO L + 1257.9d	COAST	
17.	E - 40m, 14s	START BATTERY ACTIVATION PYRO CAPACITOR CHARGE	
18.	E - 20m, 14s	ACTIVATE BATTERY	
19.	E - 19m, 44s	POWER ON (DATA HANDLING & PYRO SYSTEMS); TURN LPS ON WARM-UP; START STORING ENGINEERING DATA	
20.	E - 9m, 54s	TRANSMITTER ON WARM-UP	
21.	E - 9m, 24s	START ACQUISITION; REMOVE NRPA COVERS	
22.	E - 8m, 14s	RPAs ON WARM-UP; CONTINUE STORING ENGINEERING DATA	RF POWER = 7 w (TRACKING TONE).
23.	E - 8m, 9.5s	DESCENT; SCIENCE ON WARM-UP	
24.	E - 7m, 44s	LPS & IRPAs READY TO MEASURE; ACQUISITION COMPLETE	
25.	E - 3m, 20s	LPS & IRPAs SENSE SIGNAL TO START STORING & TRANSMITTING DATA	4300 km ABOVE 1 atm.
26.	E = 0	ENTRY (536 km ABOVE 1 atm; 1×10^{-7} atm)	297 km (C); 968.5 km (W).
27.	E + 0m, 5s	RF POWER AMPLIFIER OFF (0.1-g SENSING); START DATA STORAGE; PRE-ENTRY SCIENCE OFF	1.7s (C); 12s (W).
28.	E + 0m, 17.5s	ENABLE PROBE DESCENT PROGRAM (100-g SENSING)	8.5s (C); 35s (W).
29.	E + 0m, 44.5s [5 g (REF)]	START DESCENT PROGRAM (5-g SENSING); OPERATE BASE COVER BAND CUTTERS	29s (C); 69.5s (W).
30.	E + 0m, 56.5s (5 g + 12s)	DEPLOY BASE COVER QUADRANTS	41s (C); 81.5s (W).
31.	E + 0m, 59.5s (5 g + 15s)	DEPLOY MAIN PARACHUTE (M = 0.7; ~65 mb); RF POWER AMPLIFIER ON; START ACQUISITION	44s (C); 84.5s (W); M = 0.56 (C); M = 0.88 (W); 102 mb (C); 44 mb (W).
32.	E + 1m, 9.5s (5 g + 25s)	EJECT AEROSHIELD	
33.	E + 1m, 14.5s (5 g + 30s)	RELEASE MAIN CHUTE; DEPLOY TEMPERATURE GAGE; UNCOVER NEUTRAL MASS SPECTROMETER & NEPHELOMETER	
34.	E + 2m, 39.5s (5 g + 115s)	PROBE ACQUISITION COMPLETE; START DATA TRANSMISSION	47.7 bps.
35.	E + 44m, 59.5s (5 g + 2655s)	END OF DESIGN MISSION (~8 bars)	145 m, 24.5s (W); 18 bars (C); 4 bars (W).
36.	E + 2h, 12m (L + 1258d)	SPACECRAFT PERIAPSIS (3.8 R _S); MAY 9, 1984	

*ASSUMES AN ENTRY ARRIVAL UNCERTAINTY OF 4.4 minutes, A DESCENT BALLISTIC COEFFICIENT OF 110 kg/m² (0.7 slug/ft²), AND A NOMINAL ATMOSPHERE.
†(C) = COOL ATMOSPHERE; (W) = WARM ATMOSPHERE.

Table V-7 Uranus Sequence of Events (Task II)*

ITEM	TIME	EVENT	COMMENTS†
1.	L = 0	LAUNCH (DEC 3, 1980)	
2.	L + 2h	SEPARATE SPACECRAFT FROM LAUNCH VEHICLE	
3.	L + 2h TO L + 2816.7d	CRUISE	
4.	S - 13h, 30m, 0s	SPACECRAFT POWER TO PROBE; EJECT ENVIRONMENTAL COVER	
5.	S - 13h, 17m, 0s	START PROBE CHECKOUT	
6.	S - 0h, 17m, 0s	PROBE CHECKOUT COMPLETE; START SPACECRAFT ORIENTATION (21.4°)	
7.	S - 0h, 2m, 0s	SPACECRAFT ORIENTATION COMPLETE; ACTIVATE SEPARATION SUBSYSTEM	
8.	S = 0 (L + 2817.3d)	SEPARATE PROBE FROM SPACECRAFT	
9.	S + 0m, 0.5s	START PROBE SPINUP TO 5 rpm	
10.	S + 0m, 30s	START SPACECRAFT ORIENTATION FOR ΔV (46°)	
11.	S + 4m, 0s	PROBE SPINUP COMPLETE; DEACTIVATE PROBE SYSTEM	
12.	S + 15m, 30s	COMPLETE SPACECRAFT ORIENTATION FOR ΔV	
13.	S + 17m, 36s	APPLY SPACECRAFT ΔV (85 m/sec)	
14.	S + 18m, 0s	START SPACECRAFT ORIENTATION TO EARTH LOCK (67.4°)	
15.	S + 33m, 0s	SPACECRAFT ORIENTATION COMPLETE	
16.	L + 2817.32d TO L + 2824.6d	COAST	
17.	E - 1h, 4m, 50s	START BATTERY ACTIVATION PYRO CAPACITOR CHARGE	
18.	E - 44m, 50s	ACTIVATE BATTERY	
19.	E - 44m, 20s	POWER ON (DATA HANDLING & PYRO SYSTEMS); START LP DECONTAMINATION; START STORING ENGINEERING DATA	
20.	E - 34m, 30s	TRANSMITTER ON WARM-UP	
21.	E - 34m, 0s	START ACQUISITION; REMOVE NRPA COVERS	RF POWER = 7 w (TRACKING TONE).
22.	E - 32m, 51.5s	DESCENT SCIENCE ON WARM-UP	
23.	E - 32m, 50s	RPA's ON WARM-UP; CONTINUE STORING ENGINEERING DATA	
24.	E - 32m, 20s	LPs & RPA's READY TO MEASURE; ACQUISITION COMPLETE	
25.	E - 3m, 20s	TRANSMIT AT HIGH POWER; STORE DATA (LPs & IRPA SENSING)	4300 km ABOVE 1 atm.
26.	E = 0	ENTRY (532 km ABOVE 1 atm; 1×10^{-7} atm)	200 km (C); 1074 km (W).
27.	E + 0m, 4s	RF POWER AMPLIFIER OFF (0.1-g SENSING); START DATA STORAGE; PRE-ENTRY SCIENCE OFF	0.5s (C); 14s (W).
28.	E + 0m, 15s	ENABLE PROBE DESCENT PROGRAM (100-g SENSING)	4.5s (C); 36s (W).
29.	E + 0m, 38.5s (5 g (REF))	START DESCENT PROGRAM (5-g SENSING); OPERATE BASE COVER BAND CUTTERS	18.5s (C); 65s (W).
30.	E + 0m, 50.5s (5 g + 12s)	DEPLOY BASE COVER QUADRANTS	30.5s (C); 77s (W).
31.	E + 0m, 53.5s (5 g + 15s)	DEPLOY MAIN PARACHUTE (M = 0.72; ~47 mb); RF POWER AMPLIFIER ON; START ACQUISITION	33.5s (C); 80s (W); M = 0.59 (C); M = 0.84 (W); 41 mb (C); 49 mb (W).
32.	E + 1m, 3.5s (5 g + 25s)	EJECT AEROSHELL	
33.	E + 1m, 8.5s (5 g + 30s)	RELEASE MAIN CHUTE; DEPLOY TEMPERATURE GAGE; UNCOVER NEUTRAL MASS SPECTROMETER & NEPHELOMETER	
34.	E + 2m, 33.5s (5 g + 115s)	PROBE ACQUISITION COMPLETE; START DATA TRANSMISSION	47.7 bps.
35.	E + 44m, 53.5s (5 g + 265s)	END OF DESIGN MISSION (~7.3 bars)	19 bars (C); 3.1 bars (W).
36.	E + 1h, 51m (L + 2826.9d)	SPACECRAFT PERIAPSIS (2 R _U); AUGUST 24, 1988	

*ASSUMES AN ENTRY ARRIVAL UNCERTAINTY OF 29 minutes, A DESCENT BALLISTIC COEFFICIENT OF 110 kg/m² (0.7 slug/ft²) AND A NOMINAL ATMOSPHERE.
†(C) = COOL ATMOSPHERE; (W) = WARM ATMOSPHERE.

2. Functional Block Diagram

The functional block diagrams for the Saturn/Uranus probe with the SAG exploratory payload and the probe with the expanded payload are the same except that the additional science instruments are added for the expanded configuration.

3. System Data Profile

Figure V-1 shows the data profile for the Saturn/Uranus probe with the expanded science complement. Included in the figure are the total data collected for Saturn and Uranus entries and the impact of the entry-arrival uncertainties. The entry and descent data profiles for each planet are the same. Compared with the basic Saturn/Uranus probe, discussed in Chapter IV, Section C.3, the descent data rate for this application is increased by 3.7 bps for the added nephelometer and approximately 18.5 bps for the stored pre-entry science data. The RF power requirement at pre-entry of 41 watts for transmission of 235 bps using PSK modulation, is almost the same as storing the pre-entry and entry data and transmitting at 50.5 bps.

The figure shows the total data storage requirement is 60,200 bits and the total data collected is 128,145 bits. See Sections B and D for further discussion of the science requirements and RF link analysis, respectively.

4. System Power Profile

Figure V-2 shows the "worst case" power profile for the Saturn/Uranus probe using the expanded science complement. The separation phase is identical to that for the earlier Saturn/Uranus probe. The pre-entry power profile is based upon the Uranus arrival uncertainty of 29 minutes, and the entry time is based upon Saturn warm atmosphere. The late arrival condition requires 191 w-hr of power to the equipment. Late arrival is described as the condition in which the probe has not yet arrived at the planet when the timer (preset before separation) runs out and starts the sequence before it is really needed.

5. System Weight Summary

The system weight summary is shown in Table V-8. The ejected weight is 103.22 kg (227.36 lb), entry weight is 103.21 kg (227.33 lb), and the final descent weight is 50.32 kg (110.82 lb). Compared to the basic Saturn/Uranus probe, this probe ejected weight is 13.36 kg heavier and its descent probe is 9.15 kg heavier.

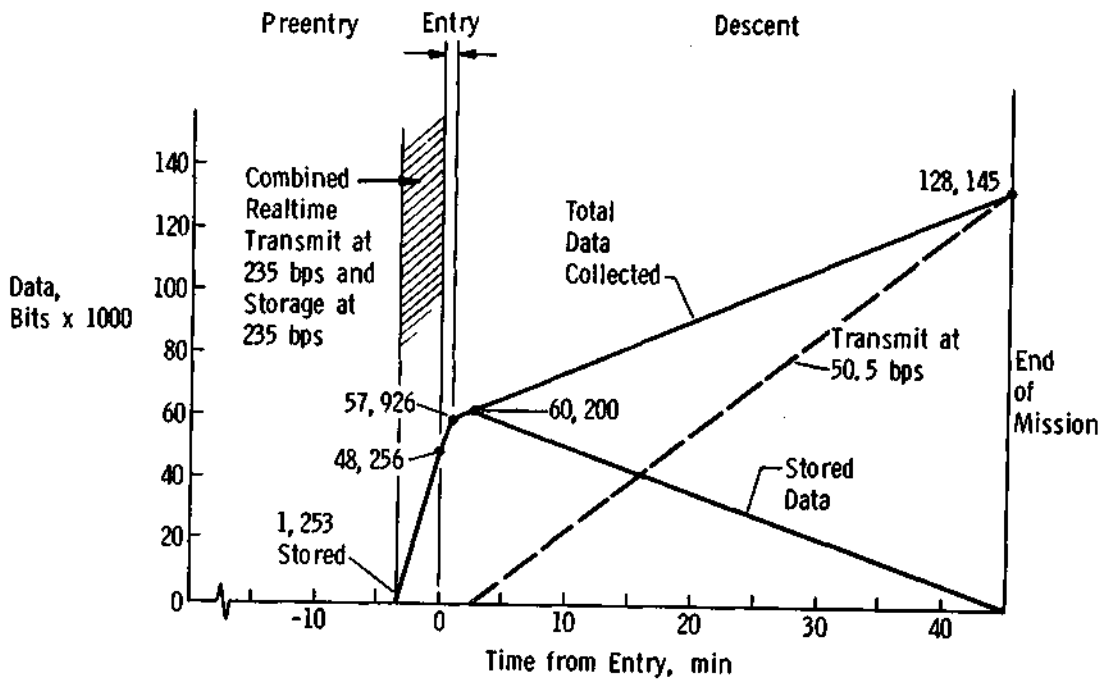


Fig. V-1 Data Profile for Saturn/Uranus Probe (Task II)

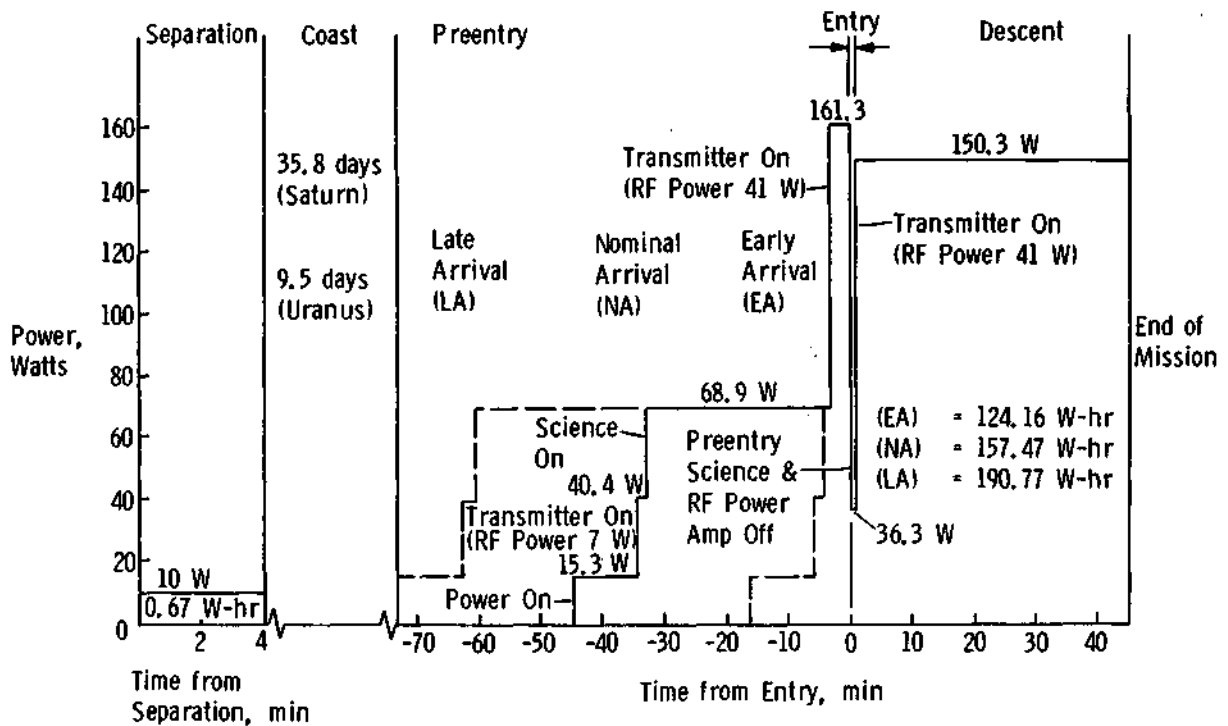


Fig. V-2 Power Profile for Saturn/Uranus Probe (Task II)

Table V-8 Weight Summary for Saturn/Uranus Probe with Expanded Science Complement

	WEIGHT	
	kg	lb
SCIENCE	14.44	31.60
POWER & POWER CONDITIONING	5.79	12.75
CABLING	4.50	9.92
DATA HANDLING	2.78	6.12
ATTITUDE CONTROL (DRY)	2.84	6.25
COMMUNICATIONS	3.95	8.70
PYROTECHNICS	6.44	14.19
STRUCTURES & HEAT SHIELD	37.12	81.76
MECHANISMS	6.67	14.68
THERMAL	5.22	11.50
PROPELLANT (ACS)	0.01	0.03
ENGINEERING INSTRUMENTATION	0.00	0.00
15% MARGIN	<u>13.46</u>	<u>29.66</u>
EJECTED WEIGHT	103.22	227.36
ENTRY WEIGHT	103.21	227.33
DESCENT WEIGHT (FINAL)	50.32	110.82

D. TELECOMMUNICATIONS SUBSYSTEM

The Task II expanded science payload impacts the telecommunications subsystem only from the standpoint of increased data bit rate. The three mission trajectories are unchanged from Task I. Table V-9 depicts the RF power required by the probe transmitter for Task II.

Table V-9 Task II Telecommunication Subsystem Comparisons for the Saturn/SU 80 Mission

MODULATION	DATA BIT RATE, bps	MISSION PERIOD	MAXIMUM PROBE RF POWER REQUIRED, w
FSK + TONE	235	Pre-Entry	116
PCM/PSK/PM	235	Pre-Entry	41
FSK + TONE	31.5	Descent	28.5
FSK + TONE	50.5	Descent	40

The expanded science package includes upper atmosphere instruments that increase the pre-entry data bit rate to 235 bps, which includes engineering data and formatting. RF power of 116 watts is required during pre-entry for the Saturn/SU 80 mission, using binary FSK modulation with a tracking tone. High power is required since a high E_b/N_o ratio of 8.9 dB is required for the noncoherent system (Vol II, Chapter V, Section A.4.e, p V-30).

PSK modulation is more efficient than FSK and was considered for the pre-entry portion of the mission. For a bit error rate of 5 parts in 10^5 , the required E_b/N_o ratio is 4 dB, as seen in Figure V-15 of Volume II, p V-31. With this improvement, the RF power required, using 235 bps, reduces to 41 watts, as indicated in Table V-9. Convolutional coding was selected as the preferred approach indicated in Chapter III, Section D.3. A half-rate, constraint-length 8 convolutional code was chosen with a Viterbi algorithm decoder using soft decision and 8-bit symbol quantization with the output delayed three constraint lengths.

The exploratory payload with an added nephelometer (Task II) increases the descent data rate to 31.5 bps and can be handled with maximum RF power of 28.5 watts. Since a 41-watt transmitter is already required to handle the high pre-entry bit rate, it was concluded that better use of the available RF power during descent could be achieved. It was found that data transmission reliability would be improved if the pre-entry data were transmitted to the spacecraft in real time and also stored on the probe. During descent, the pre-entry data will be interleaved with the real-time descent science and engineering data and transmitted to the spacecraft a second time to enhance the probability of pre-entry science data return to the spacecraft. This increases the descent data rate to 50.5 bps and RF power of 40 watts is required which fully utilizes the 41-watt probe descent transmitter capability.

Parameters of the RF link are depicted in Table V-10 for the Saturn/SU 80 mission with Task II science payload and PSK modulation for pre-entry transmission. Maximum RF power is required at entry with the high data rate. The probe RF power requirements for Task II are shown in Figure V-3. The probe is acquired for either planet from the tone only. The 7-watt probe transmitter level determined from Task I requirements during pre-entry is sufficient for Task II with a tone only.

Table V-10 Probe Pre-Entry Telemetry Link Design Table for the Task II Mission*

PARAMETER	NOMINAL VALUE	ADVERSE TOLERANCE	REMARKS
1. TOTAL TRANSMITTER POWER, dBw	16.1	0	40.5 w AT 0.86 GHz
2. TRANSMITTING CIRCUIT LOSS, dB	-1.1	0.1	CABLE & SWITCH
3. TRANSMITTING ANTENNA GAIN, dB	3.9	1.8	100° BEAMWIDTH
4. COMMUNICATIONS RANGE LOSS, dB	-197.0	0.3	1.97 x 10 ⁵ km
5. PLANETARY ATMOSPHERE & DEFOCUSING LOSS, dB	0	0	ENTRY
6. POLARIZATION LOSS, dB	-0.3	0	
7. ANTENNA PATTERN RIPPLE LOSS, dB	0	0.2	
8. RECEIVING ANTENNA GAIN, dB	17.9	1.2	20° BEAMWIDTH
9. RECEIVING CIRCUIT LOSS, dB	-1.0	0.1	
10. NET CIRCUIT LOSS, $\Sigma(2 \rightarrow 9)$, dB	-177.6	3.7	
11. TOTAL RECEIVED POWER (1 + 10), dBw	-161.5	3.7	
12. RECEIVER NOISE SPECTRAL DENSITY, dBw/H _Z	-196.2	0.4	T _s = 1750°K NF _s = 8.5 dB
CARRIER TRACKING			
13. CARRIER POWER/TOTAL POWER, dB	-8.0	0.2	P _c = 6.4 w
14. RECEIVED CARRIER POWER (11 + 13), dBw	-169.5	3.9	
15. CARRIER THRESHOLD LOOP NOISE BANDWIDTH, dBw/H _Z	12.4	0	17.5 Hz
16. THRESHOLD SIGNAL/NOISE RATIO, dB	10.0	0	
17. THRESHOLD CARRIER POWER (12 + 15 + 16), dBw	-173.8	0.4	
18. PERFORMANCE MARGIN (14 - 17), dB	4.3	4.3	
DATA CHANNEL			
19. DATA POWER/TOTAL POWER, dB	-0.7	0.2	P _d = 34.1 w, ϕ = 66.5°
20. RADIO SYSTEM & DOPPLER OFFSET LOSS, dB	-1.0	0	
21. SUBCARRIER DEMODULATION & BIT SYNC/DETECTION LOSS, dB	-1.0	0	
22. RECEIVED DATA POWER (11 + 19 + 20 + 21), dBw	-164.2	3.9	
23. DATA BIT RATE, dB	23.7	0	235 bps
24. THRESHOLD E _b /N ₀ FOR P _e = 5 x 10 ⁻⁵ , dB	4.0	0	
25. THRESHOLD DATA POWER (12 + 23 + 24), dBw	-168.5	0.4	
26. PERFORMANCE MARGIN (22 - 25), dB	4.3	4.3	
27. NOMINAL LESS ADVERSE VALUE (26 - 26 ADVERSE), dB	0		
<p>*CONDITIONS:</p> <ol style="list-style-type: none"> 1. S/SU 80 COMMON PROBE MISSION (WORST-CASE TRAJECTORY). 2. PRE-ENTRY TASK II SCIENCE PAYLOAD AT ENTRY CONDITIONS. 3. PCM/PSK/PM MODULATION WITH CONVOLUTIONAL ENCODER. 4. V = 2, Q = 8, K = 8. 5. DECODER - VITERBI ALGORITHM, BER = 5 x 10⁻⁵. 			

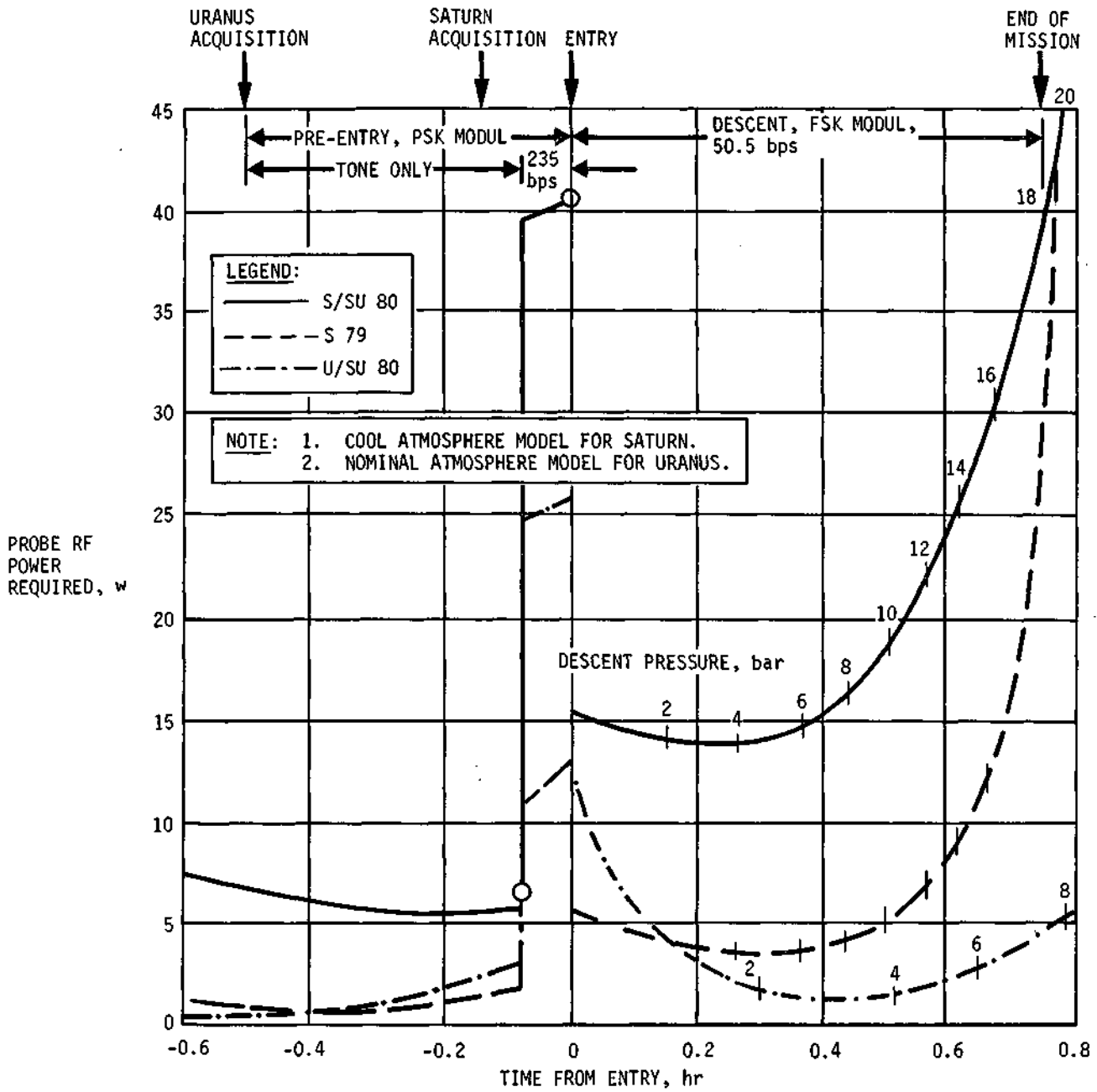


Fig. V-3 Task II Probe RF Power Requirements

At approximately E-3.5 minutes, when the Langmuir probe or IRPA senses the presence of the upper atmosphere, the data rate is increased to 235 bps and the maximum RF power requirement of 41 watts occurs at entry for the Saturn encounter from the SU 80 mission. During descent, the modulation is changed to FSK with a data rate of 50.5 bps. The worst-case trajectory is again the Saturn/SU 80 mission, as seen in the figure, and the maximum RF power required occurs at mission completion and is 40 watts. These values are also summarized in Table V-9. Also indicated on the curves are descent pressures for the two worst-case atmosphere models.

An RF link analysis for the worst-case descent condition for Task II is shown in Table V-11. FSK modulation is used with a data rate of 50.5 bps at 0.86 GHz. RF power of 40 watts is required at the end of mission in the cool atmosphere model for a Saturn encounter from the SU 80 trajectory.

Table V-12 depicts design details of the RF components that comprise the telecommunications subsystem for the common Saturn/Uranus probe with Task II science payload. The probe transmitter has two RF power levels of 7- and 41-watts available for the mission; 7-watts is sufficient for pre-entry during probe acquisition when only the tone is being transmitted; 41 watts is sufficient to handle the high pre-entry data rate for Task II using PSK modulation, and descent using FSK modulation with a lower data rate. Other components that comprise the subsystem remain unchanged from Task I as discussed in Chapter IV, Section D. For the increased transmitter RF power level, a mechanical antenna switch on the probe will most certainly be required to provide more reliable operation over a solid-state switch. A switch is necessary to connect the 41-watt transmitter output terminal from the pre-entry to descent antenna during planet entry. The transmitter output will be reduced to zero during the blackout period; only the oscillator and modulator will be energized during this time.

Design details of the spacecraft receiver are beyond the scope of the study. In general, a PSK receiver with two additional data filters for FSK could be used. Acquisition takes place with the logic technique described in Volume III, Appendix C. During pre-entry, the PSK receiver performs in a normal manner. During descent, the receiver provides the tracking function only, and the additional data channel filters demodulate the FSK data. The fact that PSK (235 bps) and FSK (50.5 bps) signals pass through different receiver channels simplifies the bit synchronization acquisition problem because each channel can be designed for an appropriate bit rate.

Table V-11 Probe Descent Telemetry Link Design Table for the Task II Mission*

PARAMETER	NOMINAL VALUE	ADVERSE TOLERANCE	REMARKS
1. TOTAL TRANSMITTER POWER, dBw	16.0	0	39.8 w AT 0.86 GHz.
2. TRANSMITTING CIRCUIT LOSS, dB	-1.1	0.1	CABLE & SWITCH
3. TRANSMITTING ANTENNA GAIN, dB	6.0	1.8	100° BEAMWIDTH.
4. COMMUNICATIONS RANGE LOSS, dB	-196.5	0.3	1.8 x 10 ⁵ km.
5. PLANETARY ATMOSPHERE & DEFOCUSING LOSS, dB	-4.1	0.2	COOL, 18 bar.
6. POLARIZATION LOSS, dB	-0.3	0	
7. ANTENNA PATTERN RIPPLE LOSS, dB	0	0.2	
8. RECEIVING ANTENNA GAIN, dB	17.9	1.0	20° BEAMWIDTH
9. RECEIVING CIRCUIT LOSS, dB	-1.0	0.1	CABLE.
10. NET CIRCUIT LOSS, $\Sigma(2 \rightarrow 9)$, dB	-179.1	3.7	
11. TOTAL RECEIVED POWER (1 + 10), dBw	-163.1	3.7	
12. RECEIVER NOISE SPECTRAL DENSITY, dBw/Hz	-196.2	0.4	$T_s = 1750^\circ K$ $NF_s = 8.5$ dB
TRACKING TONE			
13. TONE POWER/TOTAL POWER, dB	-6.6	0	$P_t = 8.8$ w
14. RECEIVED TONE POWER (11 + 13), dBw	-169.7	3.7	
15. TRACKING THRESHOLD BANDWIDTH, dB	12.4	0	17.5 Hz
16. THRESHOLD SIGNAL/NOISE RATIO, dB	10.0	0	
17. THRESHOLD TRACKING POWER (12 + 15 + 16), dBw	-173.8	0.4	
18. TRACKING PERFORMANCE MARGIN (14 - 17), dB	4.1	4.1	
DATA CHANNEL			
19. DATA POWER/TOTAL POWER, dB	-1.1	0	$P_d = 31$ w
20. RADIO SYSTEM PROCESSING LOSS, dB	-1.0	0	
21. FADING LOSS, dB	-1.0	0	
22. RECEIVED DATA POWER (11 + 19 + 20 + 21), dBw	-166.2	3.7	
23. DATA BIT RATE, dB	17.0	0	50.5 bps
24. THRESHOLD E_b/N_o , dB	8.9	0	
25. THRESHOLD DATA POWER (12 + 23 + 24), dBw	-170.3	0.4	
26. PERFORMANCE MARGIN (22 - 25), dB	4.1	4.1	
27. NOMINAL LESS ADVERSE VALUE (26 - 26 ADVERSE), dB	0		
*CONDITIONS: 1. S/SU 80 COMMON PROBE MISSION (WORST-CASE TRAJECTORY). 2. DESCENT TASK II SCIENCE PAYLOAD AT MISSION COMPLETION. 3. BINARY FSK MODULATION, CONVOLUTIONAL ENCODER. 4. $M = 2, V = 2, Q = 8$. 5. DECODER - VITERBI ALGORITHM, BER = 5×10^{-5} WITH $K = 8$ CODE.			

Table V-12 Telecommunications RF Subsystem for the Task II Mission*

COMPONENT	CHARACTERISTIC	VALUE
TRANSMITTER	RF POWER OUT	7 AND 41 w
	OVERALL EFFICIENCY	45%
	MAXIMUM DC POWER IN AT 28 vdc	91 w
	TOTAL WEIGHT OF DUAL-OUTPUT POWER & MODULATOR	2.82 kg (6.2 lb)
	VOLUME	3540 cm ³ (216 in. ³)
RF SWITCH	TYPE	MECHANICAL SPDT
	INSERTION LOSS	0.3 dB
	WEIGHT	0.23 kg (0.5 lb)
	VOLUME	443 cm ³ (27 in. ³)
PROBE PRE-ENTRY & DESCENT ANTENNAS	TYPE	TURNSTILE/CONE
	MAIN BEAM ANGLE	0 deg
	BEAMWIDTH	100 deg
	MAXIMUM GAIN	6.5 lb
	SIZE (DIAMETER x HEIGHT)	15.2 x 8.25 cm (6 x 3.25 in.)
	WEIGHT	0.45 kg (1.0 lb)
SPACECRAFT ANTENNA	TYPE	PARABOLIC DISH
	BEAMWIDTH	20 deg
	MAXIMUM GAIN	18.3 dB
	SIZE (DIAMETER)	128 cm (50.4 in.) (4.2 ft)
	WEIGHT	4.54 kg (10 lb)
	DESPIN	NO
	POSITION SEARCH	ONE
	FREQUENCY ACQUISITION	31 sec
	CLOCK ANGLE, θ	257 deg
	CONE ANGLE, ϕ	116 deg
SPACECRAFT RECEIVER	NOISE TEMPERATURE	300°K
	NOISE FIGURE	3.1 dB
	DC POWER IN AT 28 vdc	3.0 w
	WEIGHT	0.9 kg (2.0 lb)
<p>*CONDITIONS:</p> <ol style="list-style-type: none"> 1. PLANETS: SATURN & URANUS; 2. MARINER SPACECRAFT; 3. FREQUENCY = 0.86 GHz; 4. BIT RATE = 235 & 50.5 bps. 		

E. DATA HANDLING SUBSYSTEMS

The data processing electronics for Task II are essentially unchanged from the previous study (Chapter III, Section D.2). The modifications necessary to provide the inflight target planet selection consists of approximately 12 ROMs for the additional formats and a latching relay to implement the selection. As previously discussed, COS/MOS data storage design has been employed for this mission. The physical and electrical characteristics are approximated by the following equations:

$$V = \text{volume} = 443 + 16.0 M (10^{-3}) \text{ cm}^3$$

$$W = \text{weight} = 0.2 + 0.715 M (10^{-3}) \text{ kg}$$

$$\text{Power (standby)} = P_s = 0.2 + 11.0 M (10^{-6}) \text{ w}$$

$$\text{Power (operate)} = P_o = 1.0 + 5.50 M (10^{-6}) \text{ w}$$

M = memory = number of bits stored

The assumption is made that fifty-nine 1024-bit chips (M = 60,416 bits) will be required to store the blackout data. This results in the following values for physical and electrical interface characteristics of the memory electronics.

$$V = 1410 \text{ cm}^3 \quad W = 0.65 \text{ kg} \quad P_s = 0.88 \text{ w} \quad P_o = 4.4 \text{ w}$$

Similar characteristics of the data processing electronics are assumed the same as in the previous study (Volume I thru III).

$$V = 2330 \text{ cm}^3 \quad W = 2.13 \text{ kg} \quad P = 6.9 \text{ w}$$

The DHS begins the initial descent sequence shortly after the descent battery is energized. The initiation of the sequence and the initial state of the DHS will be established by a timing circuit working off battery voltage. This will ensure that the turn-on battery transient has subsided, and will eliminate the need of an additional event from the coast timer. The required sequence of events is illustrated in Table V-6 (*Saturn Sequence of Events Task II*). The pre-entry sequence occurs from Item 19 to Item 22 inclusive. The actual time with respect to entry of these events will vary (+4.4 min, Saturn; +29 min, Uranus) due to trajectory uncertainties. The control state established at Item 22 will remain fixed regardless of the actual time before entry until science data is detected (Item 27). The functions required of the DHS formats with respect to the Task II Saturn sequence are tabulated.

<u>From Item</u>	<u>To Item</u>	
19	25	Store engineering data
25	27	Interleave real-time pre-entry science and engineering data with stored engineering data
25	27	Store pre-entry science and engineering data
27	33	Store entry accelerometer and engineering data
33	34	Store descent science and engineering data
34	35	Interleave real-time descent science and engineering data with stored science and engineering data in this order: (a) Item 27 to 34, (b) Item 25 to 27.

The interleaved data (Item 25 to 27, and Item 34 to 35) is sequenced through the encoder to RF transmitter.

F. POWER AND PYROTECHNIC SUBSYSTEM

The configuration of the power and pyrotechnic subsystem for Task II is unchanged from the previous study (Volume I thru III), as indicated in Chapter III, Section D.3. The discussion on post-separation power, coast timer power, and initial entry/descent pyrotechnic power of Task I (Chapter IV, Section D.3) applies identically to Task II.

As in Task I, the entry and descent battery specification is based on the power required for subsystem components plus losses and margins and the sequence of events for a late arrival probe. The maximum transmitter power at Saturn and a late arrival probe at Uranus provides the worst-case requirements for the battery. The nominal power demands of the various subsystems are listed.

<u>Subsystem</u>	<u>Power (watt)</u>	<u>Subsystem</u>	<u>Power (watt)</u>
Transmitter	25/114	NMS	14.0
DHS	7.7/10.7	Pressure	1.3
		Temperature	1.4
Eng Hskpg	2.0	Accelerometer	2.8
Distribution			
Losses	15 (max)*	IRPA	3.0
Nephelometer	3.0	NRPA	5.0
Langmuir Probe	3.0		

*Assumes 5% of total power.

The margins that are applied consist of a +29-min trajectory uncertainty at Uranus, +5% uncertainty descent time, and 10% overall uncertainty in power levels. These calculations result in a total required energy storage of 227 w-hr and a peak demand of 169 watts at 28 volts. Using an energy density of 31 w-hr/lb and 0.138 w-hr/cm³, the entry/descent battery physical specification is 3.31 kg and 1640 cm³.

The physical specification of the power and pyrotechnic subsystem is based on a summation of the estimated required equipment as indicated in the following:

SCR - two per (dual bridgewire) event;

Relays - one per event;

Capacitor banks - six discharges allowed per bank; sufficient banks must be allowed to provide separate banks for simultaneous (less than 15 sec apart) discharges;

Electronics - engineering estimate.

The number of capacitor banks (8) is controlled by the number of simultaneous events (4) for these missions. The total of 16 events requires 32 SCRs and 16 relays. The increase in the number of events over Task I is due to the required removal of the NMS cover. The physical characteristics of the pyrotechnics are tabulated.

<u>Component</u>	<u>Size/Weight, cm³/g</u>	<u>Number Required</u>	<u>Total Size/Weight, cm³/g</u>
Capacitor bank	164/81.8	8	1310/0.66
Relays	14/34.1	16	224/0.55
SCR	13.6/14.1	32	360/0.45
Electronics	1230/0.91	1	1230/0.91

The size and weight of each element includes 10% to 15% for packaging.

G. ATTITUDE CONTROL

The attitude control dynamics are minimal for the design configuration considered for the Saturn/Uranus probe. The errors involved are:

- 1) initial error due to spacecraft pointing;
- 2) drift error accumulation during period between separation and spinup due to tip-off rate;
- 3) error due to tip-off rate combined with spinup;
- 4) error due to spin-up jet misalignment.

Only momentum vector errors are of significance in this analysis since nutation errors are damped out and the spin axis (principal moment of inertia) will align with the momentum vector. The momentum vector errors involved are discussed in the following paragraphs:

- 1) Initial error is a function of the spacecraft and will not be discussed.
- 2) Drift error - assuming an initial tip-off rate of 0.5 deg/sec about a nominal X-axis, the spin axis is displaced in the minus y direction.

$$\theta_T = W_T t_D \quad \theta_T = \text{drift error}$$

$$W_T = \text{tip-off rate} = 0.5 \text{ deg/sec} \quad t_p = \text{drift period} = 0.5 \text{ sec}$$

$$\theta_T = 0.25 \text{ deg}$$

- 3) As indicated in Chapter III, Section D.4, the error may be calculated from knowledge of the spin momentum torque, P, transverse moment of inertia, I_t and spin torque, m.

$$W = 0.52 \text{ rad/sec} \quad I_s = 6.9 \text{ kg-m}^2$$

$$m = 3.4 \text{ N-m} \quad I_t = 5.6 \text{ kg-m}^2$$

$$q = q^2/mI_t = 0.654 \quad P_x(0)/P = 0.795 \text{ (deg)}$$

$$\theta_x(P) \leq 0.81^\circ \quad \theta_y(P) \leq -0.26^\circ$$

Since the combination of the drift and spin-up/tip-off error is not random, the error due to (2) and (3) is,

$$\theta_x(P) \leq 0.81^\circ \quad \theta_y(P) \leq -0.51^\circ = -0.25^\circ - 0.26^\circ$$

- 4) The analysis of Chapter III, Section D.4 indicated the spin torque vector offset, $\theta_s = 0.136^\circ$. The total rss momentum vector error is then

$$\theta_E = 0.97^\circ$$

H. STRUCTURAL AND MECHANICAL SUBSYSTEM

The addition of the pre-entry science instruments of Task II to the Saturn/Uranus probe results in a general increase in its size and weight over that of the baseline probe. However, the design configuration is unchanged except for probe volume, and attachment provisions for the added science instruments and their support components. The changes to the probe are described briefly in this section.

1. Configuration and General Arrangement

The configuration of the entry and descent probes is shown in Figure V-4. The pre-entry science sensors require location on the forward (flight direction) face of the entry probe, such that they may sense undisturbed incoming particles from space. To accommodate this requirement, the NRPA and IRPA sensors are mounted directly on the forebody heat shield, projecting through the multilayer insulation so that the inlet to the sensors is actually ahead of the nose of the heat shield. In like manner, the Langmuir probe sensors are located on the forebody heat shield. The electronic black boxes associated with these sensors are mounted internal to the aeroshell and around its periphery so as to maximize the spin moment of inertia of the entry probe. Wiring joining the sensors to the electronic boxes is routed between the heat shield and the multilayer insulation blanket.

The physical attachment of the sensors to the heat shield is by means of a thermosensitive adhesive, such that the attachment will be severed by initial entry heating, permitting the sensors to separate. A high-thermally-conductive, low-mass attachment flange on the sensor will expedite separation of the sensors at entry prior to high heating.

An alternative approach for sensor separation would be the use of pyrotechnic devices to sever the structural connection. The final choice will involve a total system study of the heating, structural loading, and dynamic stability of the probe. However, for purposes of the system level definition, it appears that the bonded attachment is a practical approach.

The nephelometer is located inside the descent probe with a viewing window in the side. Although it is not shown in Figure V-4, a muff-type cover, attached to the descent-probe-retaining clamp band, protects the window from contamination until descent probe separation after entry. The window cover remains with the aeroshell structure at separation.

Page intentionally left blank

The nephelometer views horizontally through the side window of the descent probe. The remainder of the descent science instruments are located in the same relative orientation as the Task I instruments described in Chapter IV, Section H.1.

The Task II descent probe has a diameter of 48.9 cm (19.25 in.) and weighs 50.3 kg (110.8 lbm). The Task II entry probe has a diameter of 92.1 cm (36.2 in.) and weighs 103.2 kg (227.3 lbm). The configuration of the probe is the same as that for Task I except as noted herein.

2. Structural Design

The structural design of the Task II science probe is identical to that described in Chapter IV, Section H.2 for the Baseline (Task I) configuration except for physical size. The planetary entry decelerations are the same for either configuration, resulting in the same relative loads.

3. Mass Properties

The weights breakdown for the Task II configuration is presented in Table V-13. The weights are first presented by subsystem to arrive at a total cruise configuration weight, and are then presented at the end of the table for the various phases of flight.

The moment of inertia data for this probe has been computed about two axes. These data are as tabulated.

	<u>Descent Probe</u>	<u>Entry Probe</u>
I_{spin}	1.19 kg/m ² (0.88 slug/ft ²)	6.80 kg/m ² (5.00 slug/ft ²)
$I_{pitch/yaw}$	1.11 kg/m ² (0.82 slug/ft ²)	5.87 kg/m ² (4.32 slug/ft ²)

4. Parachute Subsystem

The added science complement of Task II results in an increased size and weight of both the descent and the entry probe configurations. Since the requirements imposed by science for entry and descent ballistic coefficients are the same as for Task I, the parachute sizes for Task II are increased. The separation parachute increases in size from 2.29 m (7.5 ft) to 2.50 m (8.2 ft),

Table V-13 Task II Saturn/Uranus Probe Weight Breakdown (Added Science)

	WEIGHT	
	kg	lb
SCIENCE		
TEMPERATURE GAGE	0.45	1.00
PRESSURE TRANSDUCER	0.68	1.50
ACCELEROMETER SENSOR	0.59	1.30
ELECTRONICS (CONVERTER)	0.91	2.00
NEUTRAL MASS SPECTROMETER ANALYZER	1.82	4.00
ELECTRONICS	2.72	6.00
PUMP	0.45	1.00
BALLAST TANK	0.45	1.00
NEPHELOMETER	1.14	2.50
IRPA SENSOR	0.23	0.50
IRPA ELECTRONICS	1.36	3.00
NRPA SENSOR	0.45	1.00
NRPA ELECTRONICS	1.82	4.00
LANGMUIR PROBES (2)		
LANGMUIR PROBE ELECTRONICS	1.36	3.0
	14.44	31.80
POWER & POWER CONDITIONING		
POWER CONDITIONER	0.23	0.50
POWER DISTRIBUTION BOX	0.68	1.50
POWER FILTERS	0.91	2.00
ENTRY BATTERIES	3.31	7.30
POST-SEPARATION BATTERIES	0.25	0.55
COAST BATTERIES	0.41	0.90
	5.79	12.75
CABLING		
INNER PROBE	2.77	6.10
EXTERNAL STRUCTURE	1.73	3.82
	4.50	9.92
DATA HANDLING		
DATA HANDLING SYSTEM	2.13	4.70
MEMORY BANKS	0.65	1.42
	2.78	6.12
ATTITUDE CONTROL SYSTEM (LESS PROPELLANT)		
ACS SYSTEM & TANKS	1.64	3.60
NUTATION DAMPER	1.09	2.40
COAST TIMER	0.11	0.25
	2.84	6.25
COMMUNICATIONS		
PRE-ENTRY ANTENNA	0.45	1.00
DESCENT ANTENNA	0.45	1.00
RF TRANSMITTER	2.82	6.20
RF ANTENNA SWITCH	0.23	0.50
	3.95	8.70
PYROTECHNIC SUBSYSTEM		
PYRO ELECTRONICS	0.91	2.00
PYRO CAPACITORS (PROBE)	0.33	0.72
PYRO CAPACITORS (EXTERNAL)	0.33	0.72
PYRO RELAYS (PROBE)	0.17	0.37
PYRO RELAYS (EXTERNAL)	0.38	0.83
PYRO SCR (PROBE)	0.14	0.32
PYRO SCR (EXTERNAL)	0.31	0.68
PYRO SQUIBS	0.26	0.60
PYRO THRUSTER	3.61	7.95
	6.44	14.19
STRUCTURES & HEAT SHIELDS		
DESCENT PROBE STRUCTURE	4.02	8.85
EQUIPMENT SUPPORT DECK	3.79	8.34
BASE COVER	4.04	8.9
AEROSHELL (2 lb FOR PAYLOAD RING)	5.08	11.20
FORWARD HEAT SHIELD (18.98 lb ABLATED DURING ENTRY)	19.07	42.01
AFT HEAT SHIELD	1.12	2.46
	37.12	81.76

	WEIGHT	
	kg	lb
MECHANISMS		
PIN PULLER	0.65	1.44
LATCHES & BANDS	0.91	2.00
MAIN PARACHUTE (3.51 lb IN CHUTE & RISER)	4.00	8.80
SECONDARY PARACHUTE	0.64	1.40
CLAMP SEPARATORS	0.47	1.04
	6.67	14.68
THERMAL		
EXTERNAL INSULATION BLANKET (FORWARD HEAT SHIELD)	1.27	2.80
EXTERNAL INSULATION BLANKET (BASE COVER)		
PROBE HULL INSULATION (INTERNAL)	1.59	3.50
ISOTOPE HEATERS	1.82	4.00
ENVIRONMENTAL TANK & N ₂	0.54	1.20
	5.22	11.50
PROPULSION		
ACS PROPELLANT	0.01	0.03
	0.01	0.03
TOTAL	89.76	197.70
15% CONTINGENCY	13.46	29.66
	103.22	227.36
1. PRE-ENTRY WEIGHT		
ACS PROPELLANT	0.01	0.03
	0.01	0.03
	$103.22 - 0.01 = 103.21 \text{ kg}$ $(227.36 - 0.03 = 227.33 \text{ lb})$	
2. POST-ENTRY WEIGHT		
FORWARD HEAT SHIELD (ABLATED)	8.62	18.98
FORWARD INSULATION BLANKET	1.27	2.80
AFT INSULATION BLANKET		
PRE-ENTRY ANTENNA	0.45	1.00
	10.34	22.78
15% CONTINGENCY	1.55	3.42
	11.89	26.20
	$103.21 - 11.89 = 91.32 \text{ kg}$ $(227.33 - 26.20 = 201.13 \text{ lb})$	
3. INITIAL WEIGHT ON PARACHUTE		
PARACHUTE (SEPARATION)	1.59	3.51
15% CONTINGENCY	0.24	0.53
	1.83	4.04
	$91.32 - 1.83 = 89.49 \text{ kg}$ $(201.13 - 4.04 = 197.09 \text{ lb})$	
4. FINAL WEIGHT ON PARACHUTE		
PYRO THRUSTERS	3.61	7.95
PYRO CAPACITORS	0.33	0.72
PYRO RELAYS	0.38	0.83
PYRO SCR	0.31	0.68
PYRO SQUIBS	0.18	0.40
AEROSHELL	5.08	11.20
FORWARD HEAT SHIELD (NOT ABLATED)	10.45	23.03
BASE COVER & AFT HEAT SHIELD	5.16	11.36
SEPARATION PIN PULLERS	0.85	1.84
LATCHES & BANDS	0.91	2.00
ISOTOPE HEATERS	1.82	4.00
EXTERNAL CABLING	1.73	3.82
NUTATION DAMPER	1.09	2.40
ACS SYSTEM	1.64	3.60
SEPARATION BATTERY	0.25	0.55
CLAMP SEPARATORS	0.47	1.04
	34.06	75.02
15% CONTINGENCY	5.11	11.25
	39.17	86.27
	$89.49 - 39.17 = 50.32 \text{ kg}$ $(197.09 - 86.27 = 110.82 \text{ lbs})$	

and weighs 4.00 kg (8.8 lbm); the descent parachute increases in size from 0.73 m (2.4 ft) to 0.89 m (2.9 ft) and weighs 0.64 kg (1.4 lbm). The remainder of the parachute description is the same as presented in Chapter IV, Section H.5.

5. Heat Shield

The planetary entry conditions are the same for the probe with Task II instrumentation as for Task I instrumentation, and consequently the forebody heat shield mass fraction is the same for both. The probe is heavier for Task II, however, resulting in a forebody heat shield weight of 19.07 kg (42.01 lbm). The afterbody ablator is ESA 3560, the same as in Task I, and is assumed to be evenly distributed over the afterbody at 1.37 kg/m² (0.28 lbm/ft²).

I. PROPULSION SUBSYSTEMS

As in Task I, a stored gas (nitrogen) propulsion system is used for probe spin at probe/spacecraft separation to stabilize its separation pointing attitude. The spin-axis moment of inertia for the Task II probe has increased to 6.80 kg/m² (5.00 slug/ft²) from 5.02 kg/m² (3.7 slug/ft²) for the Task I probe. The moment arm of the spin nozzles has increased to 41.9 cm (16.5 in.) from 38.6 cm (15.2 in.). Thus, the amount of gas required increases by 24%. However, since the weight of the gas is less than 1% of the total ACS spin-up system, the total weight is the same for both probes.

J. THERMAL CONTROL SUBSYSTEM

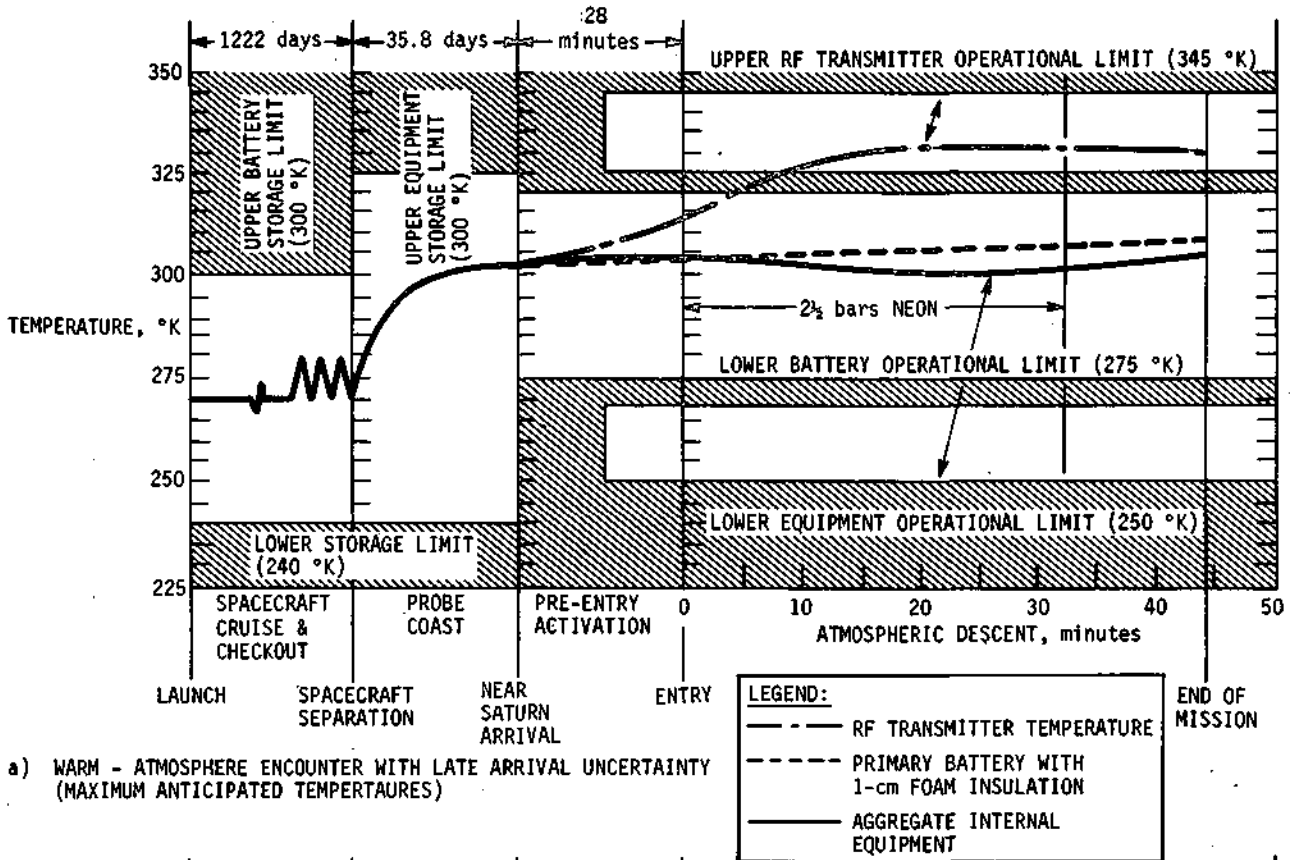
The thermal design developed and used for the SAG exploratory payload is directly applicable for the expanded science complement. The additional science results basically in only increased probe size, mass, and internal power, and the design trades and parametrics presented in Chapter III are, therefore, applicable for the probe design of Task II. Since the additional probe mass and power dissipation are desirable from the standpoint of thermal control; minor adjustment of the probe arrival temperature can be accomplished. Analysis showed, however, that only

a 2°K influence would result; therefore no adjustment in the probe coast temperature was considered. Perhaps the largest influence of the expanded science payload is on the probe coast thermal control. The increased penetrations in the multilayer blanket for the pre-entry science measurements result in more radioisotope heating to maintain positive probe heat balance. Again, due to the criticality of the probe entry temperature for descent thermal control, a louver system design is recommended to control probe coast temperatures prior to entry and reduce the thermal uncertainty.

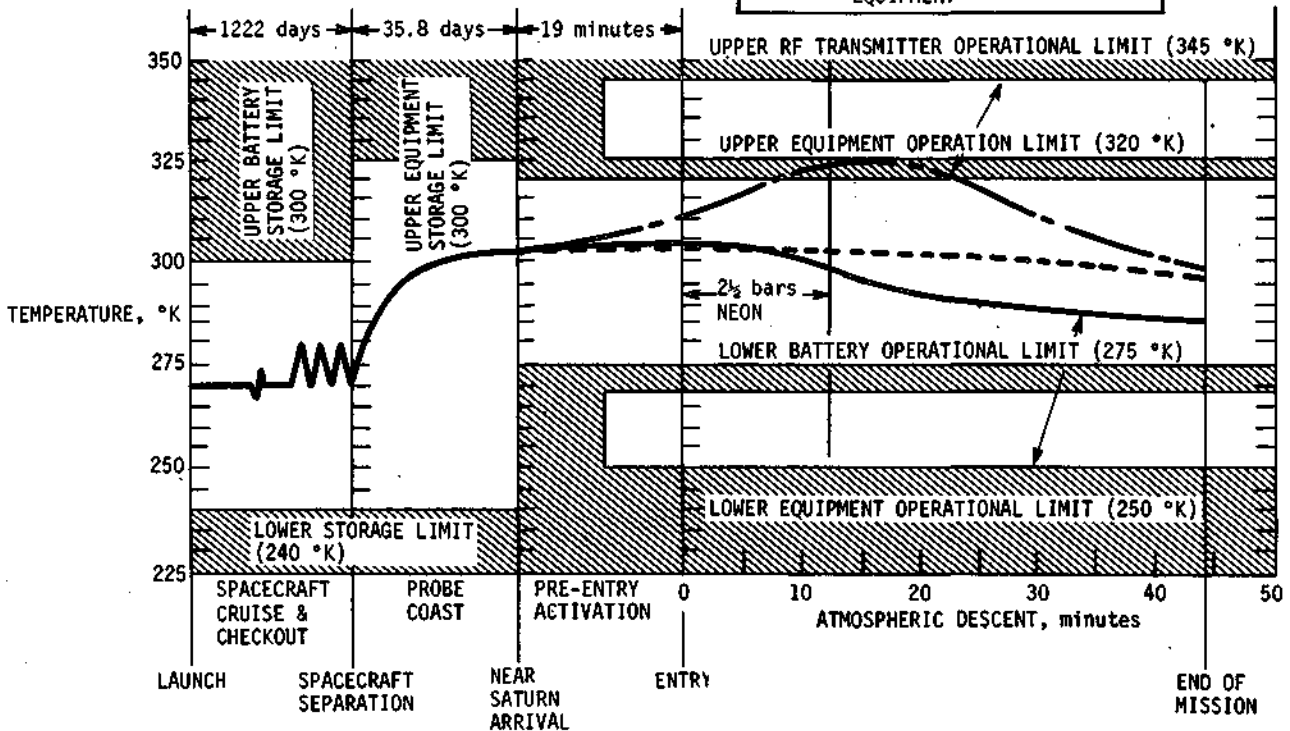
Using identical thermal subsystem design as outlined for the SAG exploratory payload (i.e., 2 cm internal foam insulation with 2.5 bars of neon gas environmental control), the expanded science complement probe design was analyzed for worst-case atmospheric encounters and arrival uncertainties. Table V-14 presents the minimum and maximum equipment temperatures experienced, and Figures V-5 and V-6 present plotted thermal analysis results. As before, the warm atmospheric encounters with late arrival uncertainty and the cool atmospheric encounters with early arrival uncertainty establish the probable operative temperature bands to be experienced at each planet. Assuming a 302°K probe arrival temperature, these bands are as listed:

	<u>Saturn, °K</u>	<u>Uranus, °K</u>
RF transmitter	297-331	291-341
Insulated primary batteries	295-307	281-309
Aggregate internal equipment	283-305	265-312

Again, the large Uranus arrival uncertainties are an important consideration for establishing acceptable pre-entry transmitter power levels. In addition, since the RF power requirement for Task II is 41 watts as compared to 25 watts for Task I, the RF transmitter becomes the pacing item that controls the allowable probe entry temperature. For Task II, therefore, the use of louvers to reduce the probe arrival temperature uncertainty, or the implementation of phase change material within the transmitter, presents a design trade to be carefully evaluated as a more detailed probe design evolves.

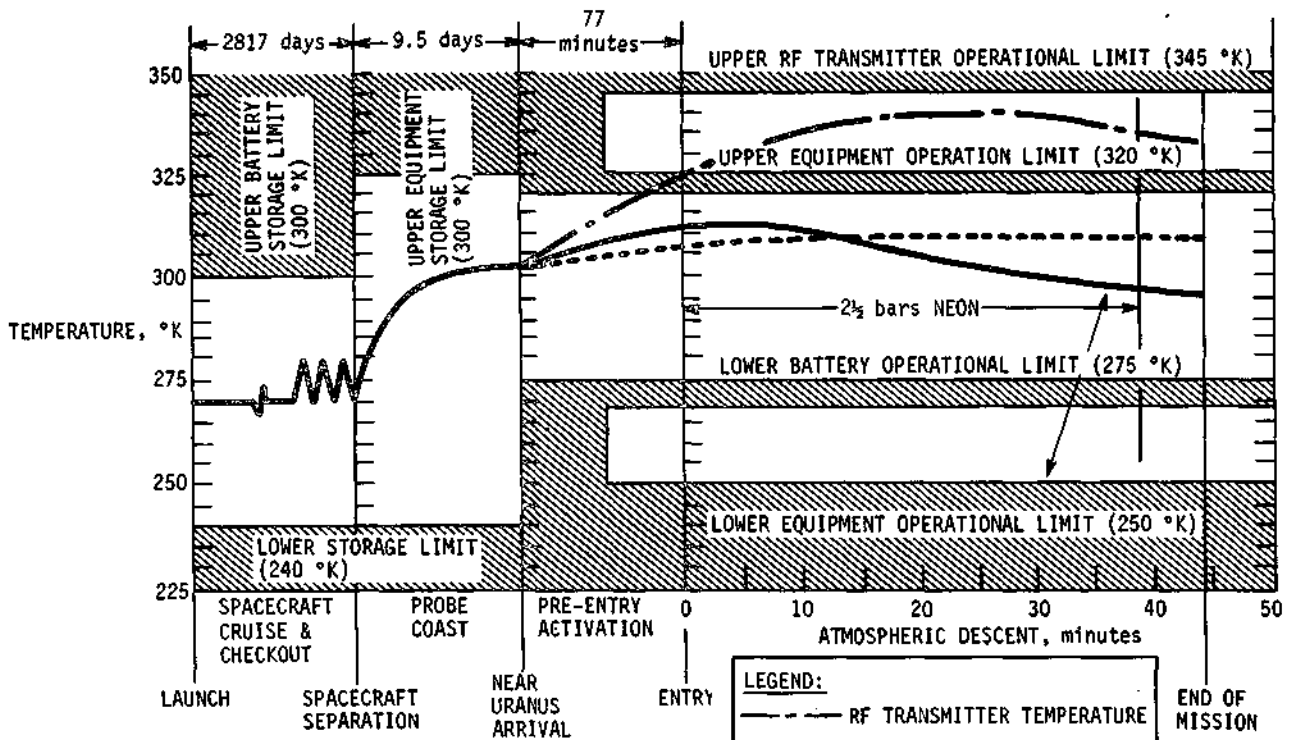


a) WARM - ATMOSPHERE ENCOUNTER WITH LATE ARRIVAL UNCERTAINTY (MAXIMUM ANTICIPATED TEMPERATURES)

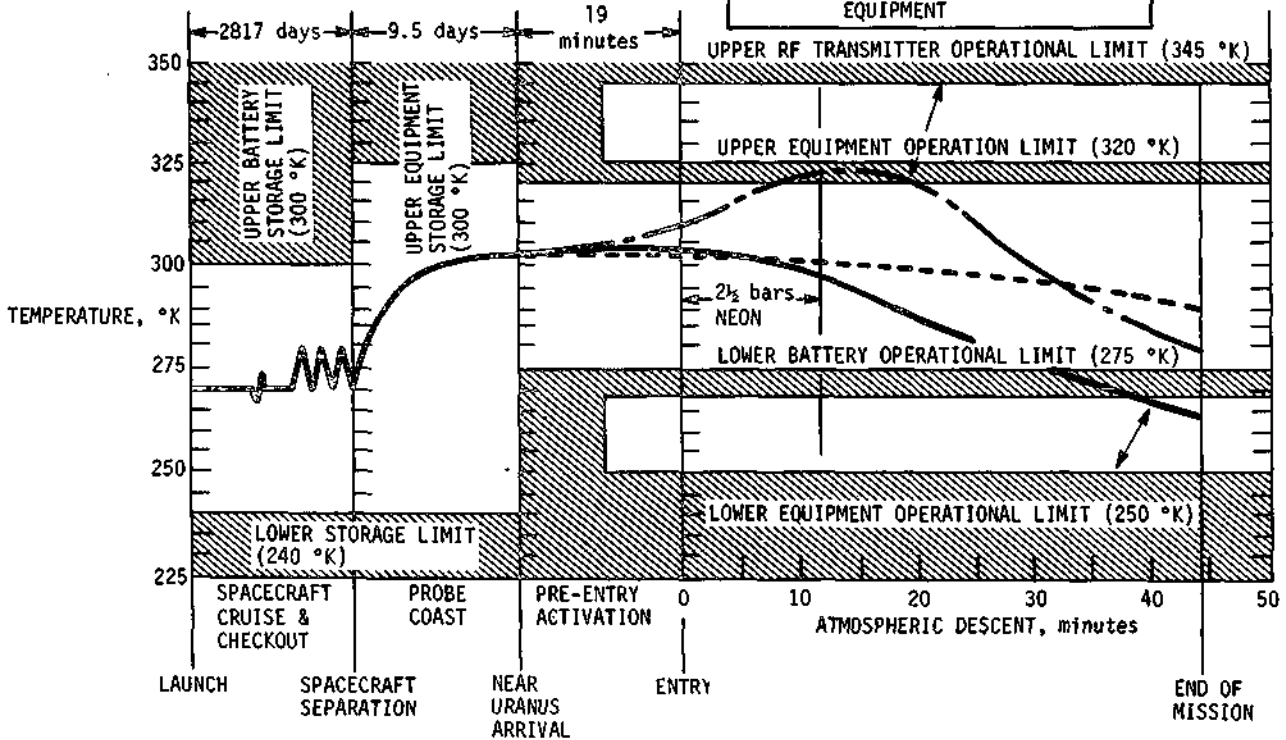


b) COOL-- ATMOSPHERE ENCOUNTER WITH EARLY ARRIVAL UNCERTAINTY (MINIMUM ANTICIPATED TEMPERATURES)

Fig. V-5 Saturn/Uranus Probe Thermal History for Saturn Mission (Expanded Science Payload)



a) WARM - ATMOSPHERE ENCOUNTER WITH LATE ARRIVAL UNCERTAINTY (MAXIMUM ANTICIPATED TEMPERATURES)



b) COOL - ATMOSPHERE ENCOUNTER WITH EARLY ARRIVAL UNCERTAINTY (MINIMUM ANTICIPATED TEMPERATURES)

Fig. V-6 Saturn/Uranus Probe Thermal History for Uranus Mission (Expanded Science Payload)

Table V-14

Table V-14 Minimum and Maximum Probe Temperatures for Worst-Case Atmospheric Encounters and Arrival Uncertainties, Expanded Science Payloads

	EQUIPMENT TEMPERATURE LIMIT, °K	SATURN		URANUS	
		WARM ATMOSPHERE (LATE ARRIVAL UNCERTAINTY)	COOL ATMOSPHERE (EARLY ARRIVAL UNCERTAINTY)	WARM ATMOSPHERE (LATE ARRIVAL UNCERTAINTY)	COOL ATMOSPHERE (EARLY ARRIVAL UNCERTAINTY)
PROBE COAST TEMPERATURE					
RF TRANSMITTER	225/350				
INSULATED PRIMARY BATTERIES	225/325	302°K	302°K	302°K	302°K
AGGREGATE INTERNAL EQUIPMENT	240/325				
PRE-ENTRY TEMPERATURES					
RF TRANSMITTER	250/345	314°K	310°K	322°K	310°K
INSULATED PRIMARY BATTERIES	275/325	304°K	302°K	308°K	302°K
AGGREGATED INTERNAL EQUIPMENT	255/320	305°K	304°K	312°K	304°K
MAXIMUM DESCENT TEMPERATURES					
RF TRANSMITTER	345	331°K	323°K	341°K	323°K
INSULATED PRIMARY BATTERIES	325	307°K	302°K	309°K	302°K
AGGREGATED INTERNAL EQUIPMENT	320	305°K	304°K	312°K	304°K
MINIMUM DESCENT TEMPERATURES					
RF TRANSMITTER	250	314°K	297°K	322°K	291°K
INSULATED PRIMARY BATTERIES	275	304°K	295°K	308°K	281°K
AGGREGATED INTERNAL EQUIPMENT	250	300°K	283°K	296°K	266°K

 MAXIMUM PROBE TEMPERATURES
 MINIMUM PROBE TEMPERATURES

K. PROBE-TO-SPACECRAFT INTEGRATIONS

Integration of the probe and spacecraft is the same for Tasks I and II, as reported in Chapter IV, Section K.